

FUNCTIONALISATION OF CLAY AEROGEL COMPOSITES FOR APPLICATIONS IN CONSTRUCTION

By

OMAR ABO MADYAN



College of Engineering, Design and Physical Science
Brunel University London

A thesis submitted for the degree of Doctor of Philosophy

October 2018

Abstract

Clay aerogels are relatively a new class of materials with number of merits suitable for many applications in various industrial sectors. With the current mandate to utilise environmentally friendly materials to produce functional materials, clay aerogels provide an attractive potential green solution to overcome thermal issues in construction. However for it to be effectively used as an insulation material, research work is required to address several critical issues and setbacks: the first of these is poor mechanical properties highlighted in the literature as its main weakness; the second is there extremely high hydrophilic and hygroscopic nature identified as the main research gap, which not only can cause a significant increase in thermal conductivity but also can disintegrate the aerogels. This thesis investigates and develops novel methodologies to overcome the associated setbacks through comprehensive characterisation and better understanding of mechanisms of formulation, architecture, behaviour and corresponding performance of clay aerogel constituents and composites: (I) The anisotropic structure of the aerogel was thoroughly investigated and its influence on properties was established; (II) By adjusting and tuning the mixing temperatures, the compressive modulus was enhanced by more than 7 folds; (III) Ultrasonic technologies were used to prepare organoclay- polyvinyl alcohol aerogel composites with 40% less moisture absorption in addition to lower thermal conductivity; (IV) Implementing organosilanes and isocyanates to prepare clay-PVA aerogels resulted in an effective method to reduce the moisture absorption by more than 40% with a 6 fold increase in compressive modulus; (VI) soluble water repellent was incorporated to prepare hydrophobic aerogel composites with contact angles of 140°; and (VII) Organosilanes and isocyanates are combined with a water repellent to generate highly functional clay aerogel composites. Overall this thesis paves the way for the industrialisation of functional clay-aerogel insulation materials for construction and other sectors.

Acknowledgement

I would like to express my great appreciation to Professor Mizi Fan. This thesis would not have been possible without his constant supervision, support and encouragement. I also thank him for pushing me to my true potential. I would also like to extend my thanks to the academic staff of the Civil and Environmental Engineering department for their engaging discussions and critique throughout the project as well as to the technicians of Joseph Lowe research centre for their help and support. Finally but not least I would like to express my deep gratitude to all my friends and colleagues who made my PhD journey much more enjoyable and enlightening throughout the years.

I dedicate this thesis to my beloved parents for their constant inspiration and support.

Declaration

The work in this thesis is based on research carried out at Brunel University London, United Kingdom. I hereby declare that the research presented in this thesis is my own work except where otherwise stated, and has not been submitted for any other degree.

Table of Contents

Abstract	I
Acknowledgement	II
Declaration	III
Table of Contents	IV
List of Figures	VIII
List of Tables.....	XIV
List of Abbreviations.....	XVI
Chapter One: Introduction	1
1.1 Introduction.....	1
1.2 Knowledge gap	3
1.3 Aim of the research project	4
1.4 Specific objectives of the project	4
1.5 Outline of Thesis.....	5
1.6 Novelty of research programme	9
1.6.1 Research significance	9
1.6.2 Contributions to the research community.....	10
Chapter Two: Literature review	12
2.1 Introduction.....	13
2.2 Clay minerals	13
2.2.1 Surface modification (Organoclay).....	15
2.3 Clay aerogels	16
2.3.1 Clay materials and concentrations.....	18
2.3.2 Freezing conditions	19
2.4 Factors affecting mechanical strength of clay aerogels composites.....	21
2.4.1 Enhancing mechanical strength of clay aerogel through natural polymers	23
2.4.2 Enhancing mechanical strength of clay aerogel through synthetic polymers	36
2.4.3 Enhancing clay-polymer aerogels through natural fibres	44
2.4.4 Enhancing clay-polymer aerogels through carbon nanotubes	47
2.4.5 Enhancing clay-polymer aerogels through laminating and dip coating.....	48
2.5 Physical properties of clay aerogels composites.....	50
2.5.1 Thermal conductivity of clay aerogels.....	51
2.5.2 Effect of clay aerogel structure on thermal conductivity.....	52
2.6 Combustion behaviour of aerogels	58

2.6.1 Combustion behaviour of PVA/clay Aerogels	59
2.6.2 Combustion behaviour of irradiated crosslinked clay-PVA aerogels	60
2.6.3 Combustion behaviour of alginate-clay aerogels.....	61
2.7 Thermogravimetric analysis (TGA) of clay aerogels composites.....	62
2.8 Liquid absorption of clay aerogel composites.....	64
2.9 Interim conclusions	68
Chapter Three: Materials, methodology and characterisation.....	70
3.1 Materials	71
3.1.1 Smectic clays (Inorganic fillers)	71
3.1.2 Polymers.....	71
3.1.3 Resins	72
3.1.4 Crosslinkers	72
3.1.5 Quaternary ammonium surfactant	73
3.1.6 Deionized water	73
3.2 Methodology.....	73
3.2.1 Clay-PVA aerogel production	74
3.2.2 Temperature induced clay-PVA aerogel production.....	79
3.2.3 Organoclay-PVA aerogel production.....	80
3.2.4 Crosslinked clay-PVA aerogel production	82
3.2.5 Water repellent clay-PVA aerogel production	83
3.2.6 Crosslinked-water repellent aerogel production	84
3.3 Characterisation and testing	85
3.3.1 Physical properties	85
3.3.2 Mechanical properties	89
3.3.3 Analytical techniques	90
3.3.4 Microstructure characterisation	92
3.3.5 Wettability.....	95
Chapter Four: Microstructure of clay-PVA aerogels and mechanisms formulating mechanical and physical properties.....	101
4.1 Introduction.....	103
4.2 Experimental work	103
4.3 Results and discussion.....	104
4.3.1 Factors influencing aerogel microstructure	104
4.3.2 Moisture absorption of clay-PVA aerogel	112
4.3.3 Influence of clay-PVA aerogel microstructure on the mechanical properties.....	117

4.3.4 Thermal conductivity of clay-PVA aerogels.....	118
4.4 Interim conclusions	121
Chapter Five: Temperature-induced nature and behaviour of clay-PVA colloidal suspension and its aerogel composites	122
5.1 Introduction.....	123
5.2 Experimental work	123
5.3 Results and discussion.....	123
5.3.1 Clay-PVA colloidal suspension at elevated temperatures.....	123
5.3.2 Clay-PVA colloidal suspension particle size vs temperature	126
5.3.3 Functional groups of temperature induced aerogels	129
5.3.4 Morphology of temperature induced aerogels.....	130
5.3.5 Mechanical properties of temperature induced aerogels	132
5.3.6 Thermal conductivity of temperature induced aerogels	133
5.4 Interim conclusions	134
Chapter Six: Functional clay aerogel composites through hydrophobic modification and architecture of layered clays.....	135
6.1 Introduction.....	136
6.2 Experimental work	136
6.3 Results and discussion.....	137
6.3.1 Morphology of organoclay-PVA aerogel composites.....	137
6.3.2 Functional groups of organoclay-PVA aerogels	140
6.3.3 Moisture absorption of organoclay-PVA aerogels	142
6.3.4 Compressive moduli of organoclay-PVA aerogels	144
6.3.5 Thermal conductivity of organoclay-PVA aerogels	146
6.4 Interim conclusions	148
Chapter Seven: Functionalising clay aerogel composites with water-soluble isocyanates and organosilanes	149
7.1 Introduction.....	150
7.2 Experimental work	150
7.3 Results and discussion.....	151
7.3.1 Morphology of crosslinked clay-PVA aerogels	151
7.3.2 Functional groups of crosslinked clay-PVA aerogels.....	154
7.3.3 Wettability of crosslinked clay-PVA aerogels.....	158
7.3.4 Compressive moduli of crosslinked clay-PVA aerogels.....	162
7.3.5 Thermal conductivity of crosslinked clay-PVA aerogels.....	164
7.4 Interim conclusions	165

Chapter Eight: Hydrophobic clay aerogel composites through the implantation of environmentally friendly water repellent agents.....	166
8.1 Introduction.....	167
8.2 Experimental work	167
8.3 Results and discussion.....	168
8.3.1 Morphology of water repellent clay-PVA aerogels	168
8.3.2 Functional groups of water repellent clay-PVA aerogels	169
8.3.3 Wettability of water repellent clay-PVA aerogels.....	172
8.4.4 Compressive modulus of water repellent clay-PVA aerogels	176
8.4.5 Thermal Conductivity of water repellent clay-PVA aerogels	178
8.4 Interim conclusions	179
Chapter Nine: Optimisation of highly functional hydrophobic clay aerogel composites for the construction industry	180
9.1 Introduction.....	181
9.2 Experimental work	181
9.3 Results and discussion.....	182
9.3.1 Wettability of crosslinked water repellent aerogels.....	182
9.3.2 Compressive modulus of crosslinked water repellent aerogels	190
9.3.3 Morphology crosslinked water repellent aerogels	192
9.3.4 Thermal Conductivity of crosslinked water repellent aerogels	197
9.3.5 Flammability of crosslinked/water repellent aerogels	198
9.4 Interim conclusions	200
Chapter Ten: Final appraisal and future work.....	202
10.1 Summary of the research	202
10.2 Major conclusions	202
10.3 Future work.....	207
References.....	210
Appendix A	227

List of Figures

Figure 1.1 Thesis layout.....	8
Figure 2.1 Illustration of Smectite clay structure.....	14
Figure 2.2 TEM images of Sodium Montmorillonite	15
Figure 2.3 Schematic illustration of the modification of clay layers by organic cations.....	16
Figure 2.4 Sodium clay montmorillonite before and after conversion to aerogel structure.....	17
Figure 2.5 (A) Layer thickness and spacing at different freezing temperatures and (B) Compressive moduli of clay aerogel frozen from different temperatures.....	20
Figure 2.6 Influence of freezing rate on clay aerogel microstructures: (A) Freezing at 2.5×10^{-2} ml/sec and (B) Freezing at 1×10^{-2} ml/sec.....	21
Figure 2.7 Reported moduli of various aerogel compositions with different parameters	22
Figure 2.8 Distribution of reported densities compiled for aerogel composites.....	23
Figure 2.9 SEM of the aerogels produced by freeze-drying dispersions of (A) 0.8 wt.% cellulose whiskers, (B) 2.5 wt.% clay +0.8 wt.% cellulose whiskers, (C) 2.5 wt.% clay + 2 wt.% cellulose whiskers and (D) 5 wt.% clay + 3 wt.% cellulose whiskers.....	27
Figure 2.10 Morphology of an HMW CHIT aerogel depicting uneven dispersion of CHIT within the clay matrix at (A) 2mm and (B) 100 μ m magnification	28
Figure 2.11 Compiled average compressive strength and density of lignin-clay aerogels	30
Figure 2.12 Schematic representation of the structure of the clay-PNR aerogel composites	32
Figure 2.13 Morphology of 2.5 wt. % NR aerogels cross-linked at different levels of S_2Cl_2 : (A) 0 (v/v %), (B) 0.25 (v/v %), (C) 0.5 (v/v %), (D) 1 (v/v %) and (E) 5 (v/v %). $T_{prep} = -18^\circ C$	33
Figure 2.14 Average compressive modulus of various clay-pectin aerogel compositions	34
Figure 2.15 Microstructure of pectin-clay aerogels with different compositions	35
Figure 2.16 Morphology of a 10 w/v% BDGE–TETA composite	37
Figure 2.17 Morphology of the clay-PEI structure: (A) Before solidification and (B) After solidification	38
Figure 2.18 Clay-PI aerogel mechanical and physical properties: (A) PI content relationship with density and (B) Modulus relationship with density	39
Figure 2.19 Compressive modulus of clay-PVA aerogels with variations of PVA molecular weight	41
Figure 2.20 Compressive strength and density of clay-PVA aerogels while using DVS as a crosslinker	43
Figure 2.21 Compressive strength and density of PVA-clay aerogel while using gamma irradiation....	44

Figure 2.22 Compressive moduli vs type of natural fibres.....	45
Figure 2.23 (A) Clay-PVA aerogel and (B) Clay-PVA aerogel that contains 1% hemp fibres	46
Figure 2.24 Aerogels with coatings applied: top= cube-shaped aerogel before and after coating and a bottom=cross section of the aerogel after coating.....	49
Figure 2.25 Schematic of glass fibre aerogel fabrication	50
Figure 2.26 Representation of heat flow within an aerogel	52
Figure 2.27 Structure of the aerogel (A) horizontally aligned and (B) vertically aligned	53
Figure 2.28 idealised heat flow through the samples prepared via directional freezing (A) vertical, (B) controlled nucleation points and (C) horizontal freezing	54
Figure 2.29 (A) House of cards structure and (B) Open cell structure	55
Figure 2.30 Thermal conductivity of coated/uncoated aerogel composites	57
Figure 2.31 Irradiated crosslinked clay-PVA aerogel residues after burning in cone calorimeter.....	61
Figure 2.32 Proposed water absorption mechanism (A) Capillary filling of the voids (B) Followed by absorption by the surrounding hydrophilic material.....	66
Figure 2.33 Water absorption of crosslinked clay aerogel composites	67
Figure 3.1 Chemical structure of polyvinyl alcohol (PVA)	71
Figure 3.2 Chemical structure of aliphatic polyisocyanate (Wcro1™)	72
Figure 3.3 Chemical structure of 3-glycidoxypropyltrimethoxysilane (Wcro2™)	73
Figure 3.4 Chemical structure of Hexadecyltrimethylammonium bromide	73
Figure 3.5 Illustration of the steps involved in preparing the stock clay suspension	74
Figure 3.6 Illustration of preparing the stock PVA solution	75
Figure 3.7 Illustration of chemical reaction between clay and PVA during the mixing process.....	76
Figure 3.8(A) Aerogel panels, (B) Aerogel prisms, (C) Aerogel frozen in one direction.....	77
Figure 3.9 (A) Aluminum foil mould (Vertical freezing) for aerogel panels ,(B) Polystyrene- aluminium foil mould (Vertical freezing) for aerogel prisms and (C) Hybrid mould for single horizontal freezing for aerogel panels,(D) Set up for vertical freezing and (C) Set up for horizontal freezing	77
Figure 3.10 Schematic illustration of the freezing process and set up (A) Horizontal freezing and (B) Vertical freezing	78
Figure 3.11 Schematic illustration of the freeze-drying process	78
Figure 3.12 Phase diagram of water	79
Figure 3.13 Schematic illustration of preheating the final aerogel suspension prior to freezing.....	80

Figure 3.14 Schematic illustration of clay modification using hexadecyltrimethylammonium bromide	81
Figure 3.15 Schematic illustration of dispersion of organoclay-PVA suspension using ultrasonic technology.....	82
Figure 3.16 (A) Advanced rheometric expansion system (ARES) and (B) schematic illustration of test set up.....	86
Figure 3.17 (A) Microscope fitted with NanoSight LM10 unit and (B) Schematic illustration of NanoSight LM10 operation.....	87
Figure 3.18 (A) Fox 200 unit and (B) Schematic illustration of the Fox 200 components.....	88
Figure 3.19 (A) UL94 flammability test and (B) Schematic illustration of UL94 test set up.....	89
Figure 3.20 (A) INSTRON 5900 and (B) Aerogel cuboid specimen for testing.....	90
Figure 3.21 (A) Diamond tipped ATR stage and (B) Schematic illustration of FTIR mechanism	91
Figure 3.22 (A) X-Ray Diffractometer D8 Advance and (B) Schematic illustration of Bragg's Law reflection.	92
Figure 3.23 (A) Polaron-SC7640, (B) Gold sheets and (C) Suptter coated aerogel samples mounted on a multi-holder	93
Figure 3.24 Leo® 1430VP SEM.....	93
Figure 3.25 rotation stage	94
Figure 3.26 (A) Raw processing, (B) Filtered processing and (C) Segmented processing	94
Figure 3.27 (A) Contact angle set-up (B) Contact angle classification	95
Figure 3.28 (A) Capillary water uptake test apparatus and set up and (B) Schematic illustration of capillary water uptake procedure	97
Figure 3.29 Clay-PVA aerogel composites being tested for moisture absorption	98
Figure 3.30 Long-term water absorption set up	99
Figure 3.31 Cup method test illustration	100
Figure 4.1 (A) Microstructure of clay aerogel (B) Microstructure of PVA aerogel.....	104
Figure 4.2 Cross-section of clay-PVA aerogel composites along the freezing direction.....	105
Figure 4.3 3D isotropic microstructure scan of clay-PVA aerogel composite (Gray parts represent empty space (Air), and bright/luminous part represent the solid phase).....	106
Figure 4.4 (A) Two main features of clay-PVA aerogel composite (B) Spacing between aerogel layers	107

Figure 4.5 (A) Porosity profile along each axis, (B) Porosity and pores model used for pores analysis (Dark blue represents solid phase, and lighter colours represent air pockets) and (C) Pore size distribution within an aerogel composite sample	108
Figure 4.6 Layers structured of clay-PVA aerogels: (A) perpendicular to the bottom and top surfaces of the aerogel and (B) parallel to the bottom and top surfaces of the aerogel.....	109
Figure 4.7 (A) Idealised orientation from horizontal freezing, (B) Realistic structure from horizontal freezing, (C) Idealized orientation from vertical freezing and (D) Realistic structure from vertical freezing.....	110
Figure 4.8 Weight increase of either clay or PVA aerogels	113
Figure 4.9 Weight and density increase of clay-PVA aerogel composites with a change in humidity	114
Figure 4.10 Water uptake of clay aerogel composite prisms: (A-C) through the base (Cross-section) , (D) from bottom face and along the lateral side, (E) from bottom face and (F) along the lateral side	116
Figure 4.11 Influence of freezing direction on the compressive modulus.....	118
Figure 4.12 Influence of freezing direction on the thermal conductivity	119
Figure 4.13 Influence of moisture absorption on the thermal conductivity.....	120
Figure 5.1 Loss and storage modules and their ratio of final aerogel suspension containing 2.5 wt. % Clay and 2 wt. % PVA.....	124
Figure 5.2 Illustration of the clay transition from large to smaller particle stacks or single unit layers	126
Figure 5.3 Size distribution and concentration of clay aerogel suspensions treated at (A) Room temperature (23°C) (B) 60°C (C) 70°C (D) 80°C (E) 90°C.....	128
Figure 5.4 FTIR analysis of clay-PVA aerogel composites prepared from different suspensions treated at various temperatures.....	129
Figure 5.5 Microstructure of clay-PVA aerogels with suspensions treated at various temperatures .	130
Figure 5.6 Web-like the structure of clay-PVA aerogel composites	131
Figure 5.7 Average compressive moduli (A) and density (B) versus mixing temperatures	132
Figure 6.1 SEM results of organoclay-PVA aerogels with different amount of surfactant	138
Figure 6.2 XRD spectrums of aerogel composites with different amount of cations exchanged.....	140
Figure 6.3 FTIR analyses of organoclay-PVA aerogel composites with different amount of surfactant added equivalent to CEC of clay.....	141

Figure 6.4 Moisture absorption of different organoclay-PVA aerogels at a different set of conditions	143
Figure 6.5 Representation of structural damage caused by moisture.....	144
Figure 6.6 Average compressive moduli of organoclay-PVA aerogels.....	145
Figure 6.7 Density of organoclay-PVA aerogels versus the amount of surfactant added	146
Figure 7.1 Illustration of crosslinking reaction with clay and PVA	152
Figure 7.2 (A) Clay-PVA aerogels (B) Clay / (PVA+Wcro1) aerogel (C) Clay / (PVA+Wcro2) aerogel ...	153
Figure 7.3 FTIR spectrum (A) PVA with/without crosslinks in solution (B) Cured PVA with/without crosslinks and (C) clay-PVA aerogel composite with/without crosslinks	157
Figure 7.4 Moisture absorption of clay-PVA aerogel composites with/without crosslinks.....	158
Figure 7.5 Water uptake of clay-PVA aerogels composites (A) Clay-PVA aerogel, (B) Clay-PVA-Wcro1™ aerogel and (C) Clay-PVA-Wcro2™ aerogel.....	160
Figure 7.6 Structural damage from water (A) Clay-PVA aerogel ,(B) Clay-PVA-Wcro1™ aerogel and (C) Clay-PVA-Wcro2™ aerogel	161
Figure 7.7 Contact angles of clay-PVA aerogel composites with/without crosslinks	162
Figure 7.8 Average compressive moduli of clay-PVA aerogels with/without crosslinks	163
Figure 8.1 SEM results of aerogel composites: (A) Clay-PVA, (B) Clay-PVA-WDisRep1™, (C) Clay-PVA-WDisRep3™ aerogel and (D) Clay-PVA-WDisRep4™	169
Figure 8.2 FTIR spectrum of water repellents and their aerogel composites: (A) WDisRep1™, (B) WDisRep3™ and (C) WDisRep4™	171
Figure 8.3 Moisture absorption of clay-PVA aerogels with/without water repellent components	173
Figure 8.4 Water uptake of aerogels composites: (A) Clay-PVA, (B) Clay-PVA-WDisRep1™, (C) Clay-PVA-WDisRep3™ and (D) Clay-PVA-WDisRep4™	175
Figure 8.5 Average compressive moduli of clay-PVA aerogels with/without water repellents	177
Figure 9.1 Aerogel exposure to varying moisture condition: Weigh change with (A) varying loading of WDisRep3™, (B) varying ratios of Wcro1™ to WDisRep3™ and (C) varying ratios of Wcro2™ to WDisRep3™	184
Figure 9.2 Water sorption of aerogels: Weight change with (A) varying loading of WDisRep3™, (B) varying ratios of Wcro1™ to WDisRep3™ and (C) varying ratios of Wcro2™ to WDisRep3™.....	185

Figure 9.3 Contact angle of aerogel with (A) varying loading of WDisRep 3™, (B) varying ratios of WCro1™ to WDisRep3 and (C) varying ratios of WCro2™ to WDisRep3 187

Figure 9.4 Shrinkage of aerogels after 30 days of water absorption: (A) varying loadings of WDisRep3™ and (B) varying ratios of Wcro1™/Wcro2™ to WDisRep3™ 189

Figure 9.5 Shrinkage of the sample after 30 days in water: Sample CR1/WR1:2 shrunken by 6 % (Left) and Sample 0.3WR shrunken by 92% (Right)..... 190

Figure 9.6 Compressive moduli of aerogel composites (A) with varying loading of WDisRep3™, (B) varying ratios of WCro1™ to WDisRep3™ and (C) varying ratios of WCro2™ to WDisRep3™ 192

Figure 9.7 Thermal conductivity of crosslinked water repellent aerogels composites vs relative humidity 198

Figure 9.8 (A) Samples CR1-WR 0.5:2 after UL94 test (B) Cross-section of burned aerogels 199

List of Tables

Table 2.1 Effect of concentration and composition on structure formation.....	19
Table 2.2 Composition, density and initial modulus of casein-clay aerogel	24
Table 2.3 Composition, density and modulus of cellulose-clay aerogel	26
Table 2.4 Composition, structure and mechanical properties of cellulose-clay aerogel	28
Table 2.5 Compression, density and void volume fraction of clay-PNR aerogel composites	32
Table 2.6 Modulus and density of clay-pectin aerogel cross-linked with various cations.....	36
Table 2.7 Compressive moduli of fibre reinforced aerogel with 5wt.% clay	47
Table 2.8 Modulus and density of SWNT reinforced aerogel	48
Table 2.9 Thermal conductivity, molecular weight and structure of PVA-clay aerogels	56
Table 2.10 Burning parameters of clay-PVA aerogels with/without flame retardant agents	59
Table 2.11 Burning Parameters of gamma-irradiated clay-PVA Aerogels	60
Table 2.12 Burning parameters of clay-alginate aerogels.....	62
Table 2.13 Physical characteristics of aerogel.....	65
Table 3.1 Formulations of crosslinked clay-PVA aerogels.....	83
Table 3.2 Formulations of water-replant clay-PVA aerogels	83
Table 3.3 Formulations of WDisRep3™ clay-PVA aerogels	84
Table 3.4 Formulations of WDisRep3™-crosslinked clay-PVA aerogels	84
Table 3.5 Composition and formulation codes for water-replant-crosslinked clay-PVA aerogels	85
Table 3.6 Flammability classification criteria	89
Table 4.1 Influence of moisture on the microstructure of clay-PVA aerogels.....	111
Table 4.2 Water vapor properties of clay-PVA aerogel composites	116
Table 4.3 Liquid water transport properties of clay aerogel composites	117
Table 5.1 pH of final aerogel suspensions in relation with temperature (°C).....	126
Table 5.2 Thermal conductivity and density of Clay-PVA aerogels.....	134
Table 7.1 Dimensional stability of clay-PVA aerogels with/without crosslinks after 30 days at 95% RH once removed to ambient condition	159
Table 7.2 Density of clay-PVA aerogels with/without crosslinks	164

Table 7.3 Thermal conductivity of clay-PVA aerogels with/without crosslinks	164
Table 8.1 Major functional groups of hydrophobic clay aerogel composites.....	172
Table 8.2 Dimensional stability of clay-PVA aerogels with/without water repellent components.....	174
Table 8.3 Water absorption of clay aerogel composite with/without water repellents	175
Table 8.4 Contact angle of clay-PVA aerogel composite with/without water repellent	176
Table 8.5 Thermal conductivity and density of clay-PVA aerogels with/ without water repellent	178
Table 9.1 Microstructures of control and WR samples before and after exposure to water.....	194
Table 9.2 Microstructures of CR1/WR samples before and after exposure to water	195
Table 9.3 Microstructures of CR2/WR samples before and after exposure to water	196
Table 9.4 UL94 test for WR samples	199
Table 9.5 UL94 test for CR1-WR samples.....	200

List of Abbreviations

(A)	Water absorption coefficient
Al(OH)_3	Aluminium hydroxide
(BDGE)	1,4-butanediol diglycidyl ether
(d)	Basal spacing (d)
(P)	Pectin
(R _f)	Fluoroalkane groups
(S ₂ Cl ₂)	Sulfur monochloride
(δ)	Water vapour permeability
$\text{Al}_2(\text{SO}_4)_3$	Aluminium sulfate
APP	Ammonium polyphosphate
AP-PAA	Poly (amic acid)
APTMS	3-Aminopropyltriethoxysilane
ARES	Advanced rheometric expansion system
CaCl_2	Calcium chloride
CEC	Cation exchange capacity
CHIT	Chitosan
CNT	Carbon nanotubes
D-values	Particle Size distribution
DVS	Divinyl sulfone
Ebecryl 860	Epoxidized soybean oil acrylate
EGDMA	Ethylene Glycol Dimethacrylate
EGDMA	Fire growth rate index
EHT	Electron high tension
FTIR	Fourier-transform infrared spectroscopy
g/cm^3	Gram per cubic centimetre
G'	Storage modulus
G''	Loss modulus

GC	DL-glyceraldehyde
HRR	Heat release rate
K_{app}	Apparent moisture diffusivity
kGy	Kilogray
LCST	Lower critical solution temperature
LSA	Lignosulfonic acid
Mpa	megapascal
MW	Molecular weight
MWCNTs	Multi-walled carbon nanotubes
Na ⁺ - MMT/MMT	Sodium Montmorillonite
NaCl	Sodium chloride
nm	Nanometer
PAA	Poly (acrylic acid)
PC	Potassium carbonate
PEG	Poly (ethylene glycol)
PEI	Polyethyleneimine
PEO	Poly (ethylene oxide)
PHRR	Peak of heat release rate
PI	Polyimide
PNIPAAm	Poly (N-isopropyl acrylamide)
PNR	Prevulcanized rubber ()
POSS	Methacryloxypropyl polysilsesquioxane
PVA	Poly (vinyl alcohol)
SDS	Sodium dodecyl sulfate
SG	silica gel
SWCNTs	single-walled carbon nanotubes
Tgase	Transglutaminase enzyme
THE	Total heat evolved as time to ignition

THR	Total heat release
TMOS	Tetramethyl orthosilicate
TTI	Time to ignition
TTPHRR	Time to peak of heat release rate
W	Water vapour permeance
W/(m.K)	Watts per meter-Kelvin
Wcro1™	Aliphatic polyisocyanate
Wcro2™	Glycidoxypropyltrimethoxysilane
WDisRep 3™	C6- Fluoroalkyl acrylate
WDisRep 4™	C2-C4 Fluorochemical
WDisRep1™	A combination of melamine resins with paraffin waxes
XRD	X-ray powder diffraction

Chapter One: Introduction

1.1 Introduction

Buildings all over the world, whether commercial or residential contribute significantly to the share of energy consumption. The bulk of this energy consumption is mostly as a consequence of either air-conditioning or heating systems required to obtain thermal comfort within a building envelope [1]. Heat transfer by conduction through walls and roofs represents a major component of the total thermal load of buildings, where a typical household can have significant heat loss without proper insulation systems, for instance, 40% of energy consumption and 36% CO₂ emissions in Europe are directly related mainly to inefficient insulation materials and systems. A typical household has a 35% heat loss due to un-insulated walls, 25% through the roof, 15% through doors, 10% through windows and 15% through the floor [2]. Therefore, using thermal insulation effectively could lead to a significant reduction in thermal loads and consequently reduction in the overall building energy needs.

An effective insulation material will retard the heat flow through conduction, convection and/or radiation (i.e. low thermal conductivity) [3]. However many different parameters have to be considered including cost, compressive strength, water vapour absorption and transmission, fire resistance, ease of application, and durability [4]. The most common insulation materials are mineral wool products but tend to contribute to a thick building envelope as result of the high thermal conductivity (0.04-0.06 W/(m.K)) [5], followed by petroleum-based materials which have high embodied energy due to the high energy cost associated with the petroleum extraction, manufacturing and shipping [6]. Many factors can influence the performance of insulation materials, such as the operating temperature. One of the major factors is the moisture content which can directly influence the thermal conductivity. It has been reported that the k-value

(thermal conductivity) of hydrophilic porous materials can increase by more than 50% for every 1 (v/v %) of moisture absorbed [7,8].

Increased energy concerns and the current mandate to utilise eco-friendly, harmless, and nano-scale minerals to prepare high-performance materials, has led to a new class of materials called “Aerogel”. Aerogels are classified as low density ($<0.1 \text{ g/cm}^3$), porous materials which are comprised of the interconnected three-dimensional solid network structures of more than 90% occupied air. The aerogel are produced by replacing a liquid in a gel with a gas usually through supercritical drying techniques where the liquid is removed by transforming it into a supercritical fluid [9]. The concept of supercritical drying consists of increasing the temperature of a gel in an autoclave until the pressure and temperature exceed that of the critical temperature T_c and pressure P_c of the liquid entrapped in the gel pores to transform it into a supercritical fluid without the collapse of the structure [10]. To date, most aerogel research are based on silica aerogels produced mostly as a consequence of their nanostructured layers, high porosity and lightweight ($0.003\text{-}0.5 \text{ g/cm}^3$), which leads to unique, and excellent, acoustic and thermal properties ($0.01\text{--}0.02 \text{ W/(m.k)}$) [11,12]. However, due to the fact that most aerogels are produced through supercritical drying methods, which create certain limitations especially when commercialisation is considered in terms of its cost efficiency, process continuity and safety because of high-temperatures and pressures which are needed to exceed the critical points of both the T_c and P_c [3], aerogel manufacturers shifted their focuses on cost reduction, performance enhancement and/or developing new types of aerogels that can be feasibly produced [13]. A relatively new family of low-density aerogel materials has recently been attempted to create a “house of cards” like structure by using clay suspension through an environmental friendly freeze-drying technique (lyophilisation) [14], the technology of which is commonly used in both the food and

pharmaceutical industries. This process can create clay aerogels with properties similar to or exceeded that of foamed polymers, with favourable properties, such as the increased compressive modulus, reduced gas permeability and enhanced fire resistance [15,16].

Smectite clays are one of the most common clay group used to produce aerogels; they have a layered structure formed by tetrahedral sheet(s) linked to an octahedral sheet through the sharing of oxygen ions which causes the layers to possess a partial negative charge on the face and partial positive charges on the edges [17]. Smectite clays have been used extensively as an inexpensive, widely available and an environmentally friendly material to produce nanocomposites due to their high cation exchange capacity, swelling ability and high surface area [18,19]. The clay aerogel is characterised with a lamellar structure with a layer thickness of 1-4 μm and distances between layers (intergallery) of 20-100 μm . This results in low densities (0.05-0.1 g/cm^3) and high porosity (void fraction of 95%) leading to extraordinary thermal and acoustic properties similar to those of silica aerogels [20]. The clay aerogel has gained much attention in the field of material science and is becoming an important class of materials due to its unusual properties as well as their potential use in many applications including automotive, electronics and food packaging. Use of clay aerogel can be considered a key solution in overcoming the thermal bridging issues in construction applications as an environmentally friendly insulation material [21].

1.2 Knowledge gap

Clay aerogel composites and their mechanical behaviour has been investigated in the literature. However for it to be implemented in the construction industry as an insulation material its wettability and moisture absorption mechanisms has to be investigated to allow for tailoring of these composites to address and overcome their high hydrophilicity and poor wettability that can significantly hinder their effectiveness and efficiency as an insulation material .

1.3 Aim of the research project

The project aims to create robust clay-aerogels by using harmless and inexpensive nano-scale minerals, water and eco-friendly or soluble/dispersible low-cost polymers, through an environmentally freeze-drying process, therefore making it more viable, and efficient for commercial applications. The project is to tackle and address the major setbacks and limitations of clay-polymer aerogels, which are its high hydrophilicity, high moisture absorbance and poor mechanical properties, while maintaining and retaining their physical properties such as low thermal conductivity and low density in order for them to effectively and efficiently be implemented in the construction industry as an insulation material as a replacement for petroleum-based thermal insulation and expensive insulation materials.

1.4 Specific objectives of the project

In order to achieve the main aims of the project, the following specific objectives have been set.

They include:

- Through an extensive review of the literature as the initial step, to determine critical information regarding both the mechanical and physical properties of clay aerogels.
- To Investigate and optimise the processing parameters of clay-PVA aerogel composites and their influence on the mechanical properties.
- To investigate and understand the mechanisms of moisture transportation and its interactions with clay aerogel composites in order to fully determine the weakness and limitations of both the mechanical and physical properties when the aerogel composites are subject to high moisture content
- To modify smectic clay (Organoclay) through an ion exchange process and implement it into clay-aerogel composites by using novel ultra-sonication technologies , without the use of any solvents in order to enhance the moisture resistivity of the aerogel composites.

- To identify water-soluble crosslinkers and investigate novel crosslinking techniques for clay aerogel composites, and investigate the mechanisms of performance enhancement relating to both the mechanical and physical properties.
- To implement water-soluble polymeric water repellents into clay aerogel composites and investigate their influence on the mechanical and physical properties.
- To develop the optimum formulation by using a hybrid system of both crosslinkers and water repellents to produce high functioning hydrophobic clay aerogel composites.

1.5 Outline of Thesis

This thesis consists of ten Chapters as illustrated in Figure 1.1 and the brief overview of the Chapters is outlined below:

Chapter one: Introduction

This Chapter gives an overview of aerogel materials and states the aims and objectives of the project, as well as the outlined structure of the thesis.

Chapter two: Literature review

This Chapter gives a critical review the state of the art of the clay-polymer aerogel materials. The aim of this Chapter is to create a comprehensive database and identify the limitations and potentials of such materials from the literatures. The review is comprised mainly of two parts: (I) Reviewing the mechanical properties of clay aerogel composites and how they are influenced by different polymers (Matrix) and other factors. (II) Reviewing the physical properties of clay aerogel composites and how they are influenced by different polymers (Matrix) and other factors.

Chapter three: Methodology

This Chapter describes the main methodologies used to prepare clay aerogel composites in the study, and gives a detailed description of the analytical methodologies and testing procedures carried out as well as all materials used in this study.

Chapter four: Microstructure of clay-PVA aerogels and the mechanisms formulating mechanical and physical properties

This Chapter presents an investigation of the clay-PVA aerogel structure and morphology, and how parameters, such as freezing direction and moisture absorption influence the structure and network systems of the developed clay aerogel composites. The sorption mechanism of clay-PVA aerogels is also investigated and how both the mechanical and physical properties may be influenced by moisture sorption is discussed. Physical properties, such as vapour transmission, water uptake, moisture absorbance and thermal conductivity are examined.

Chapter five: Temperature-induced nature and behaviour of clay-PVA colloidal suspension and its aerogel composites

This Chapter describes a novel technique by altering the processing parameters (Heat-induced) to enhance the compressive modulus of clay-PVA aerogels without any additives or increase in solid content. The Chapter investigates how the rheology and particle size are affected by heat, which in turn gives rise to an increase in the compressive modulus.

Chapter six: Functional clay aerogel composites through hydrophobic modification and architecture of layered clays

This Chapter describes and reports a surface modification technique for clay through an ion-exchange process and the application of the processed clay to prepare organoclay-PVA aerogel through a novel ultra-sonication technique without the use of any additives or organic solvents. The Chapter then discusses the mechanisms of an increase in the moisture resistance and reduction in thermal conductivity due to an increase in d-spacing.

Chapter seven: Functionalising clay aerogel composites with water-soluble isocyanates and organosilanes

This Chapter discusses the implementation of two different water-soluble crosslinking agents. Their functional groups were investigated and their compatibility for the production of clay-PVA aerogels assessed. The performance, both mechanical and physical properties of clay-PVA aerogel composites, was investigated.

Chapter eight: Hydrophobic clay aerogel composites through the implantation of environmentally friendly water repellent agents

This Chapter discusses the implementation of three different water soluble water repellent components that resulted in highly hydrophobic clay-PVA materials with superior mechanical and physical properties. Comprehensive characterisations of the developed aerogel composites have also been carried out.

Chapter nine: Optimisation of highly functional hydrophobic clay aerogel composites for the construction industry

This Chapter involves a hybrid system based on crosslinking agent from Chapter 7 and the most efficient water repellent from Chapter 8 in order to find the optimum formulation (crosslinker: water repellent ratio), in order to produce highly durable functional clay-PVA aerogel composites that can be implemented into the construction industry.

Chapter ten: Conclusions and future work

This Chapter contains the concise summary and conclusive statements established within this thesis. Future prospective and recommendations are also discussed.

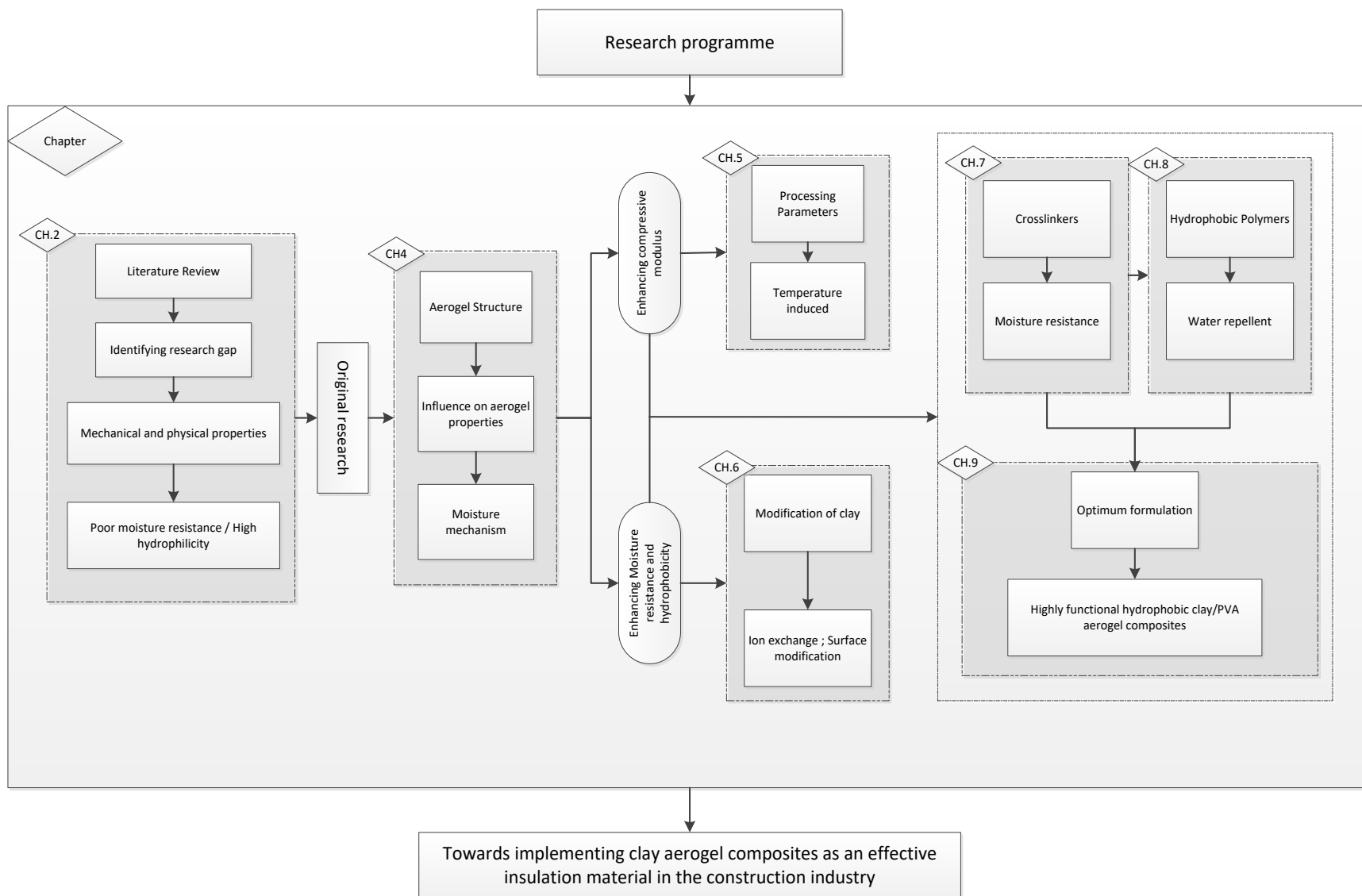


Figure 1.1 Thesis layout

1.6 Novelty of research programme

1.6.1 Research significance

This research presents an extensive study in developing clay-PVA aerogel composites and delivers solutions for overcoming main issues associated with clay aerogel composites, especially which are its poor compressive modulus and hydrophilicity. The development demonstrated and presented in this thesis allows for the implementation of clay-aerogel composites as an effective insulation material in the construction industry. The compressive modulus of the developed clay aerogel composites is equivalent to and even exceeds to the traditional foamed insulation materials. The durability of the aerogel composite has been critically addressed to ensure their functionality is not compromised when in contact with high moisture contents or direct water contact. With the developed hydrophobic clay aerogels composites and their processing techniques, the commercial viability of clay aerogel as an insulation material for the construction industry was demonstrated, reducing (the thickness of) building envelopes and thermal loss with natural and harmless materials.

The significance of this study can be summarised as follows:

- The thesis established an extensive database relating to clay aerogel composites and identifies the gaps and future perspectives in research fields of (I) enhancing the mechanical properties of clay aerogels by using different polymeric and fibrous materials, (II) enhancing the physical properties of clay aerogel composites and how they can be altered and modified and (III) highlighting the limitations of aerogel composites as an effective insulation material (Chapter 2).
- The study reveals the anisotropic structure of clay-PVA aerogel composites and how it can be influenced by processing parameters and moisture absorption, leading to a better understanding of the mechanisms formulating physical and mechanical characteristics of

clay-PVA aerogels. The effect of moisture absorption on the thermal conductivity as well as the water uptake and vapour transmission of clay-PVA aerogels were also investigated (Chapter 4).

- The study provides an in-depth analysis of nanoparticle size and rheological properties of clay-PVA colloidal suspension, and how they can be influenced by the mixing temperature (Environmentally friendly pre-treatment), resulting in a more interconnected/complex structure that is capable of effective transferring of load (Chapter 5).
- An Innovative methodology for using organoclay to prepare clay-PVA aerogels without the use of any solvents (Water only was used), though the use of ultrasonic technologies, was developed, resulting in 40% reduction in moisture absorption and 20% in thermal conductivity (Chapter 6).
- The study formulates highly functional hydrophobic clay-PVA aerogel composites through the combination of the crosslinker and water repellent component resulting in contact angles of 140° as well as high dimensional stability (6% shrinkage) after being submerged in water and a compressive modulus of 8 MPa while retaining low thermal conductivity (Chapter 7-9).

1.6.2 Contributions to the research community

1.6.2.1 Peer-reviewed journals (Appendix A)

1. **Omar Abo Madyan**, Mizi Fan, Luciano Feo, David Hui, Enhancing mechanical properties of clay aerogel composites: An overview, *Composites Part B Engineering* (May 2016).
<https://doi.org/10.1016/j.compositesb.2016.04.059>
2. **Omar Abo Madyan**, Mizi Fan, Luciano Feo, David Hui, Physical properties of clay aerogel composites: An overview, *Composites Part B Engineering* (July 2016).
<https://doi.org/10.1016/j.compositesb.2016.06.057>

3. **Omar Abo Madyan**, Mizi Fan, Zhaohui Huang, Functional clay aerogel composites through hydrophobic modification and architecture of layered clays, *Applied Clay Science* (June 2017). <https://doi.org/10.1016/j.clay.2017.01.013>
4. **Omar Abo Madyan**, Mizi Fan, Temperature-induced nature and behaviour of clay-PVA colloidal suspension and its aerogel composites, *Colloids and Surfaces A Physicochemical and Engineering Aspects* (June 2017). <https://doi.org/10.1016/j.colsurfa.2017.06.041>
5. **Omar Abo Madyan** , Mizi Fan , Organic functionalization of clay aerogel and its composites through in-situ crosslinking , *Applied Clay Science* (2018). <https://doi.org/10.1016/j.clay.2018.11.017>
6. **Omar Abo Madyan**, Mizi Fan, Hydrophobic clay-PVA aerogel composites using environmentally friendly water repellents, *Macromolecules* (2018). [10.0.3.253/acs.macromol.8b02218](https://doi.org/10.1021/acs.macromol.8b02218)

1.6.2.2 Publications in international conferences

1. Pei Huang, **Omar Abo Madyan** and Mizi Fan, Development of fracture-free clay aerogel, *23th INTERNATIONAL CONFERENCE ON COMPOSITES/NANO ENGINEERING* (March 2015).
2. **Omar Abo Madyan**, Mizi Fan, Development of moisture resistant clay aerogel for the construction industry, *International Conference of Biocomposites and Sustainable Developments in Construction* (Sept 2015).
3. **Omar Abo Madyan**, Mizi Fan, Development of clay aerogel composites, *Brunel graduate school research conference* (March 2015).
4. **Omar Abo Madyan**, Mizi Fan, Development of high insulated clay aerogel composites, *24th INTERNATIONAL CONFERENCE ON COMPOSITES/NANO ENGINEERING* (July 2016).
5. **Omar Abo Madyan**, Mizi Fan, Enhancement of mechanical properties of clay aerogel composites for construction, *24th INTERNATIONAL CONFERENCE ON COMPOSITES/NANO ENGINEERING* (July 2016).

Chapter Two: Literature review

Abstract

This Chapter presents a comprehensive review of clay aerogels, including the enhancement of clay aerogels with various natural and synthetic polymers, and the reinforcement of clay–polymer aerogel with carbon nanotubes, natural fibres, glass fibre lamination and dip coatings. Different physical properties of clay aerogel composites, including thermal conductivity, fire resistance, thermal stability and water absorption, and how these parameters are influenced by the microstructure, processing parameters and composition are also discussed. The results showed that many factors could contribute to the classification of clay aerogels, including processing parameters and methodologies, raw materials as well as minor additives.

Highlights:

- The incorporation of water-soluble polymers or fibrous materials has proven to be the most effective to achieve various levels of enhancements of clay-aerogels;
- Fire performance of clay aerogel composites can be significantly enhanced with different fire retardant additives without altering the aerogel structure and with the correct polymer and modification;
- The clay aerogels could act as excellent liquid absorbents in which they can absorb 300% their weight in liquid. On the other hand, highly moisture absorption hinders applications in many other sectors;
- Altering the molecular weight of Poly (vinyl alcohol) as well as controlling the processing parameters can create an open cell structure that could effectively lower the thermal conductivity.

2.1 Introduction

Many factors define the scope in which clay aerogels can be developed, as the nature of their structure results in a fragile neat clay aerogel that possesses poor mechanical strengths [22]. The reinforcement of clay structures is required even just for handling let alone for reaching a state where clay aerogels can be considered mechanically robust to be implemented in the construction industry as an effective insulation material [15,22]. Although a number of different publications have identified the boundaries and parameters of producing clay aerogels, the published data are varied, such making commercialisation the most challenging point for clay aerogels. Therefore, this Chapter carried out a comprehensive review, specifically focusing on the mechanical and physical performance of clay aerogels and its composites, aiming at providing a much useful concise database for the development, production and potential utilisation of clay aerogel composites for various industrial sectors.

2.2 Clay minerals

Clay is a natural and an abundant material formed through the erosion of feldspathic rocks into fine particles consisting primarily of hydrated aluminium silicates [23]. The definition of the term “Clay” is ambiguous. It can be used to define a “large group of microcrystalline secondary minerals based on hydrous aluminium or magnesium silicates that have sheet-like structures” [24], or defined as a “natural occurring material composed of fine-grained minerals, which is generally plastic at appropriate water contents and will harden when dried or fired. Clay usually contains phyllosilicates, but it may contain other materials that impart plasticity and harden when dried or fired” [25]. The use of clay has been a vital resource for many applications from antiquity to the current day [26]. As for centuries clay has been used in cosmetics, porcelain, and medical purposes and continues to gain interest in many applications, especially in nanotechnology applications [27-29]. Clay varies in

particle size, shape, distribution, surface chemistry and charge. Therefore the physical properties define the clay mineral and their application as they can affect the many properties such as viscosity, absorption, plasticity, dry and fired strength, casting rate, permeability and bond strength [30,31].

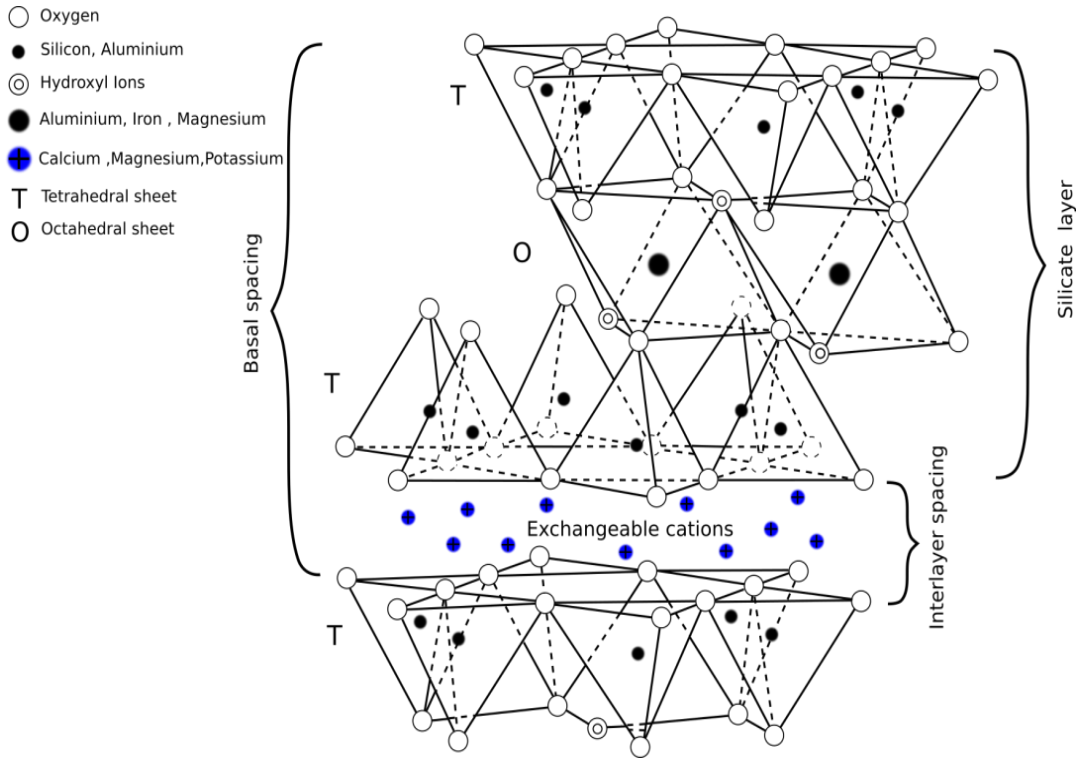


Figure 2.1 Illustration of Smectite clay structure [32]

Clay is characterised with a layered structure (Figure 2.1) formed by tetrahedral sheet(s) and linked to an octahedral sheet through the sharing of oxygen ions, this generates layers with a partial negative charge on the face and partial positive charges on the edges [17]. The clay layers can be formed from one tetrahedral sheet linked to one octahedral sheet known as a one to one (1:1) layer, such as kaolinite where they have cations in between each sheet to balance the surface charge on the layers. This structure requires no counter ions within the structure, as the octahedral sheets are able to balance the charge on the surface of the tetrahedral sheets. They can also be formed from one octahedral sheet between two tetrahedral sheets known as a two to one (2:1) layer such as,

smectites micas, vermiculite and chlorites. These minerals have cations in between each sheet to balance the surface charge on the layers. The best-known clay minerals of the 2:1 layer type are montmorillonite (smectic clays), as they are widely used in various branches of industry due to their high cation exchange capacity, swelling ability and high surface area [18,32,33]. Montmorillonite consists of about 1 nm thick aluminosilicate layers, the surface of which are surface-substituted with metal cations and stacked in about 10 μm -sized multilayer stacks (Figure 2.2) [34].

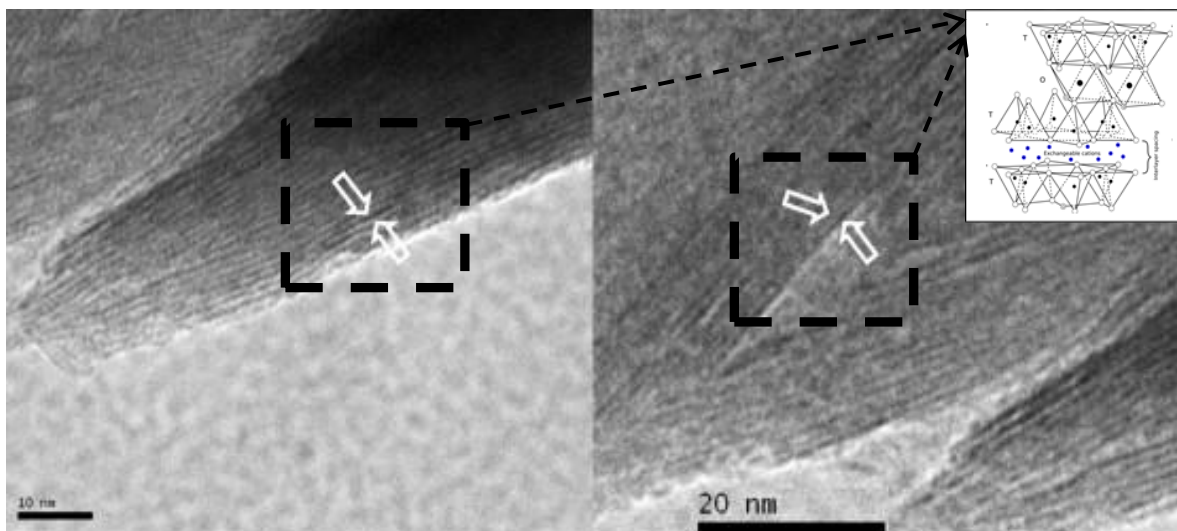


Figure 2.2 TEM images of Sodium Montmorillonite [34]

2.2.1 Surface modification (Organoclay)

Surface modification of clay has been considered vital in improving the practicality and performance of clay [35]. Several approaches can be utilised to modify clay, but mostly through chemical reactions such as adsorption, ion exchange, grafting of organic compounds, acid reactions, pillaring of poly(hydroxo metal) cations, interparticle polymerisation, dehydroxylation and calcination, delamination and reaggregation and also through physical treatments such as lyophilisation, ultrasound, and plasma [36]. However, the most well-known and investigated method is through ion exchange with alkylammonium ions (Figure 2.3). The modification process may be involved in

replacing the clay cations, such as Mg^{2+} , Ca^{2+} , Na^+ , K^+ , and Li^+ , with various organic cations, such as a nitrogen-based quaternary ammonium cation [37]. Alkylammonium salts may cause the interlayer space to expand and convert the initially hydrophilic silicate into hydrophobic organoclay as well as enhance the miscibility of the clay with polymers [38,39]. Organoclay has proven to be an effective tool for treating and filtrating water and more traditionally has been used as a thickening and gelling agent in paints and cosmetics [40,41]. Organically-modified nanoclays (organoclays) are also an attractive class of hybrid organic-inorganic nanomaterials with potential uses in polymer nanocomposites, as rheological modifiers, gas absorbents and drug delivery carriers [42-44].

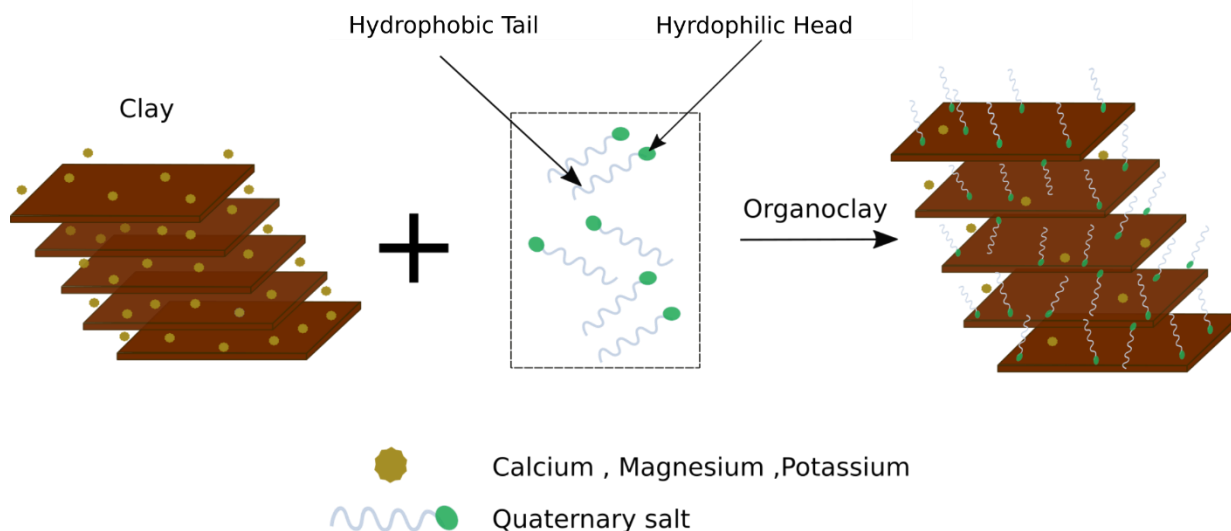


Figure 2.3 Schematic illustration of the modification of clay layers by organic cations.

2.3 Clay aerogels

The first clay aerogel was reported by Nakazawa in 1978 by freezing a clay suspension, followed by the lyophilisation of ice under vacuum [45]. Once the freeze-drying takes place, and the water is removed from the montmorillonite clay suspension, it was found that the gallery spacing decreased from greater than 0.003 to 0.001 μm during freezing, while upon thawing the originally layered morphology was restored, this can be related to ice crystal growth which is thought to be

responsible for the collapse of the swollen structure, which limits the structural transformation, although a monovalent cation, such as sodium, in montmorillonite (Na+MMT) allows for easy swelling and dispersion in aqueous solution, leading to high cation exchange capacity coupled with a high aspect ratio. Thus produces the most stable unreinforced clay structures [14]. It is apparent that the macroscopic clay particles of 5-50 μm diameters are comprised of multiple clay sheet aggregates (Figure 2.4), after the aqueous suspension/freeze-drying process, a sheet-like clay morphology is formed (Figure 2.4), which is much different from the powdery nature of the starting clay. The spaces between sheets are open galleries previously filled with ice (Ice negative). The high vacuum freeze-drying process maintains the clay orientation during sublimation and removes the liquid phase that could promote rearrangement and loss of the final aerogel structure [46]. The net clay “House of cards” structure (Figure 2.4) lacks any mechanical properties. In the cases in which the clay aerogel was considered workable to be tested (>5 wt.%), the highest compressive modulus was in order of at 9 kPa [47].

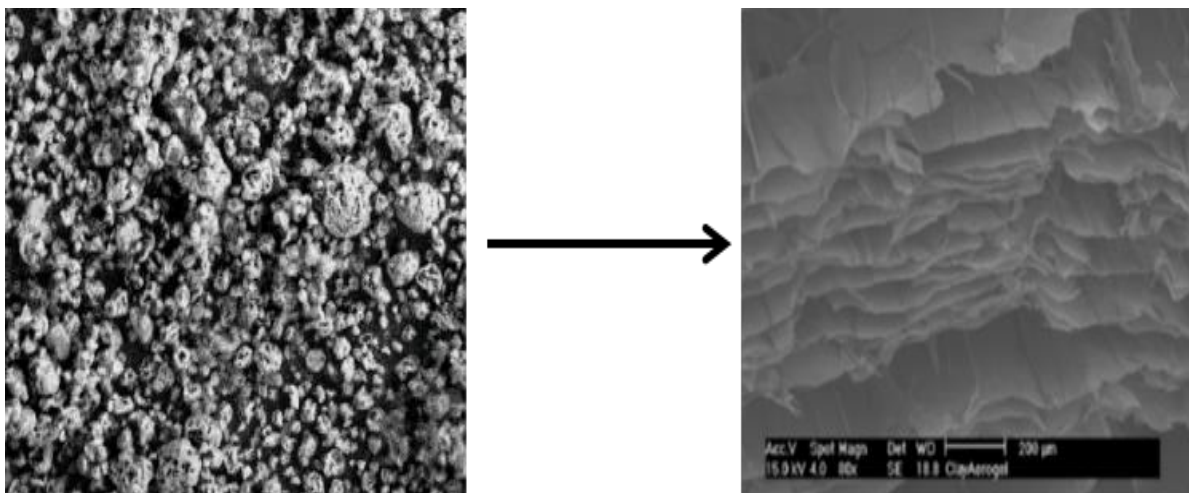


Figure 2.4 Sodium clay montmorillonite before and after conversion to aerogel structure [46]

2.3.1 Clay materials and concentrations

Many possibilities from a wide range of clay materials and concentrations can be used to produce aerogels (Table 2.1). An important factor for producing aerogel is the clay concentration and weight percentage (water to clay ratio), as it directly relates to the viscosity of the water-clay suspension which affects the crystallisation process and the end product morphology. The optimised (critical) concentration is different for most types of clay and even differs within a specific group depending on the physical aspects of a particular grade of clay. However a definite relationship exists between the particle shape distribution and the resulting viscosity of clay-water suspensions [48]. Hence a balance between suspension viscosity and the clay weight percentage (wt.%) is needed in order to produce a stable aerogel structure. Most of the literature focuses on smectite clays that have a 2:1 structure, such a sodium montmorillonite, PWG grade, which is extensively used as an inexpensive and nearly inexhaustible environmentally friendly material to produce nanocomposite [21,49]. It has been found that montmorillonite is an ideal source for making aerogel materials and the preferred fillers for ice-templated materials, because of their swelling abilities, high cation exchange capacity, high aspect ratios and large surface areas, and the ability of layers to interact with one another due to their negatively charged faces and positively charged edges. This produces thermodynamically stable suspensions that leads to a “house of cards” type structure dispersing in water at concentrations higher than 2 wt.% [50]. The concentration of clay in water is key in producing structured aerogels (Table 2.1) where clay concentrations of sodium montmorillonite of 1.4-2.9 wt.% produced stable aerogel structures, whereas less than or equal to 0.7 wt.% did not. Increasing the concentrations above 2.9 wt.% was viscous and difficult to be blended [46]. The use of clay with a one to one layer system (1:1) such as kaolin can be ice templated into aerogel only by increasing the concentration above 20 wt.%, thus leading to a very viscous solution and thick layers

after freeze-drying, this is due to the clay (1:1 kaolin) non-swelling properties, in contrast to using a two to one system that can produce clay aerogels from 2-5 wt. % clay suspensions.

Table 2.1 Effect of concentration and composition on structure formation [46]

Sample	Concentration	Outcome
Na+-MMT	< 2 wt.%	Expanded Powder
Na+-MMT	>2 wt.%	Layered Structure
Ca+-MMT	≤ 5wt.%	Expanded Powder
Fluoromica	5 wt.%	Layered Structure
Kaolin	≤ 5 wt.%	Expanded Powder
Kaolin	20 -50 wt.%	Layered Structure
Laponite RDS	5 wt.%	Layered Structure

2.3.2 Freezing conditions

When an aqueous solution is converted into a solid by freezing; which is the determinant step for producing layered structured clay aerogel, the freezing condition plays an important role as the precipitation and growth of ice-crystals may affect the end properties and texture of the clay aerogel. Once the ice begins to grow between the clay, it pushes the clay away into its grain boundaries, and only when ice growth wins over ice nucleation and becomes the predominant step, will the ice fronts begin to move at a constant rate, producing high aspect ratio, homogenous structured aerogel [14]. The pores in the clay-aerogel are the “negative” crystals of the ice when freeze-dried therefore by controlling the nucleation and growth processes of ice crystals; it is possible to alter the pores size and distributions, consequently defining the texture of the aerogel [14,45]. Two methods have been reviewed; one controlling the freezing temperatures and the second altering the freezing rate. The layer thicknesses and the interlayer spacing can be dependent on the freezing temperatures (Figure 2.5A). Such as lowering the freezing temperature from -23 to -77°C decreased the layer thicknesses from an average of 45 to 3 μm. Further reduction of the freezing temperature to a -172°C using liquid nitrogen/CO₂ resulted in an increase of layer thickness

to 37 μm . The decrease in the interlayer spacing exhibited a similar trend, as the freezing temperature was dropped. However at -172°C the spacing was at its lowest, and did not increase as in the case of the layer thickness. The reduction in both layer thickness and spacing can be related to the fact that ice nucleation will begin near the coldest surface, and the colder that surface is, the more heterogeneous the nuclei will be at the beginning [51].

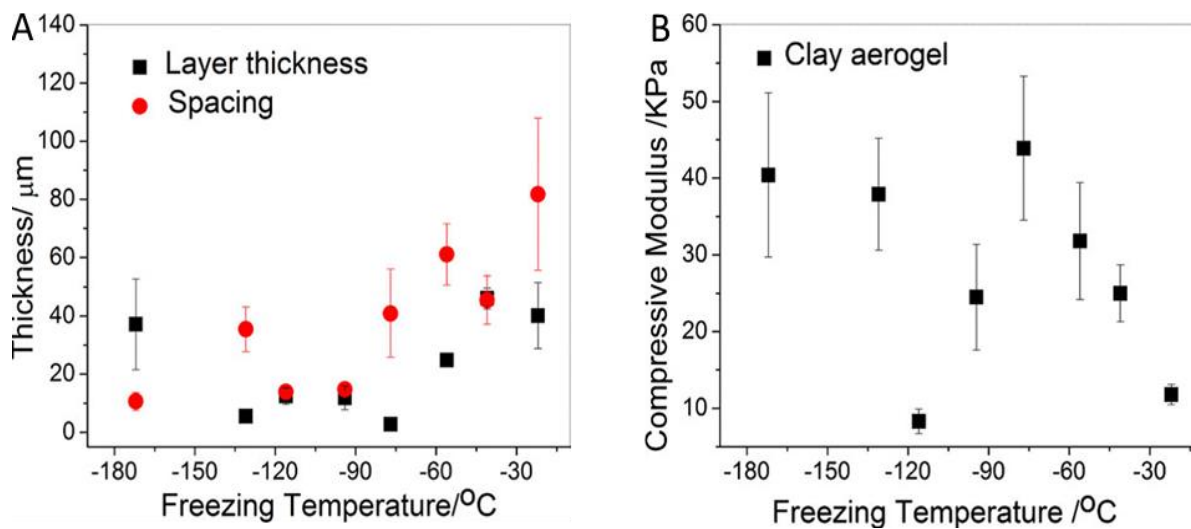


Figure 2.5 (A) Layer thickness and spacing at different freezing temperatures and (B) Compressive moduli of clay aerogel frozen from different temperatures [14]

Narrower interlayer spacing and thinner layer thicknesses translates into a more compacted structure, which should yield more rigid composites with higher compressive moduli, e.g. 45 kPa at -77°C (Figure 2.5B). The freezing rate is another important factor that can influence and control the size and the anisotropic distribution of the pores [14]. Freezing at a rate of 1×10^{-2} ml/sec resulted in a feather-like type structure (Figure 2.6B). When the freezing rate is slow enough, it allows the growth of extremely large ice crystals in the shape of thin lens where the clay fragments are condensed in the inter-crystalline boundaries and form rather thin films separated from each other rather than large pores. Increasing the freezing rate to 2.5×10^{-2} ml/sec resulted in an elongated pore type structure arranged in a parallel arrangement (Figure 2.6A) [45].

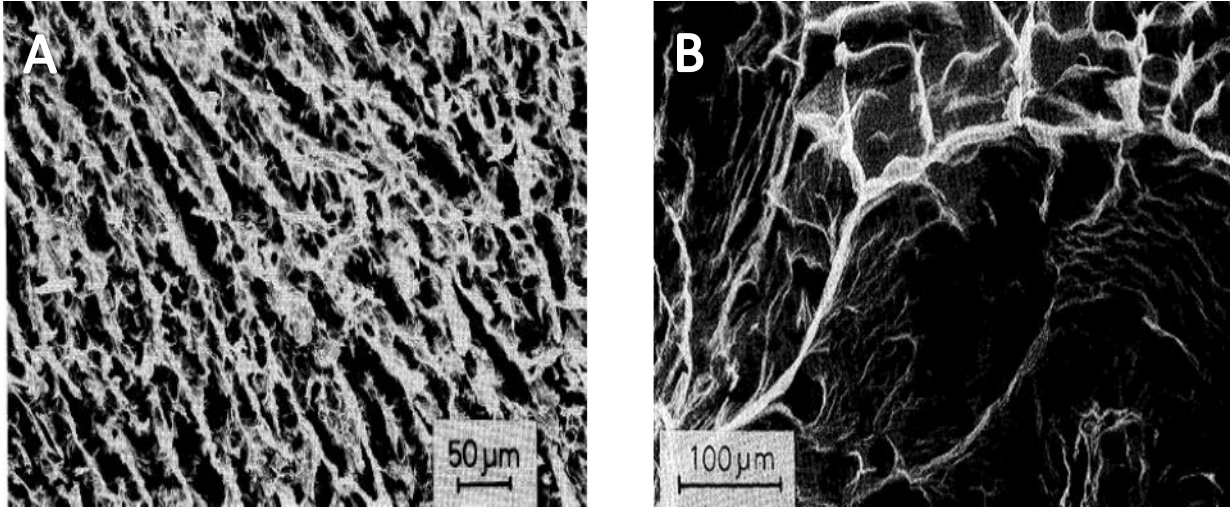


Figure 2.6 Influence of freezing rate on clay aerogel microstructures: (A) Freezing at 2.5×10^{-2} ml/sec and (B) Freezing at 1×10^{-2} ml/sec [45]

2.4 Factors affecting mechanical strength of clay aerogels composites

Most unreinforced clay aerogels are too weak to allow the measurement of compressive modulus unless the clay content is increased, which then sacrifices its low density [47]. Nanomaterials have gained significant attention as a reinforcement medium from those seeking to tailor and develop materials; where different components can significantly influence the final property of the composite [52]. Consequently, for the past several years, efforts have been made to improve the mechanical strength and toughness of clay aerogels, where successful attempts have been reported with the incorporation of either a natural or a synthetic component, including polymers and fibres into the framework of the clay aerogels. The addition of a reinforcing component may result in a significant increase in the compressive moduli of the reinforced clay aerogels as compiled in Figure 2.7. It is apparent that the compressive modulus of clay-PVA aerogel composites can reach to the values of 22000 kPa (22 MPa) for various clay aerogel composites, showing that these materials can be tailored for a wide range of applications including packaging and insulation materials [12,53-63].

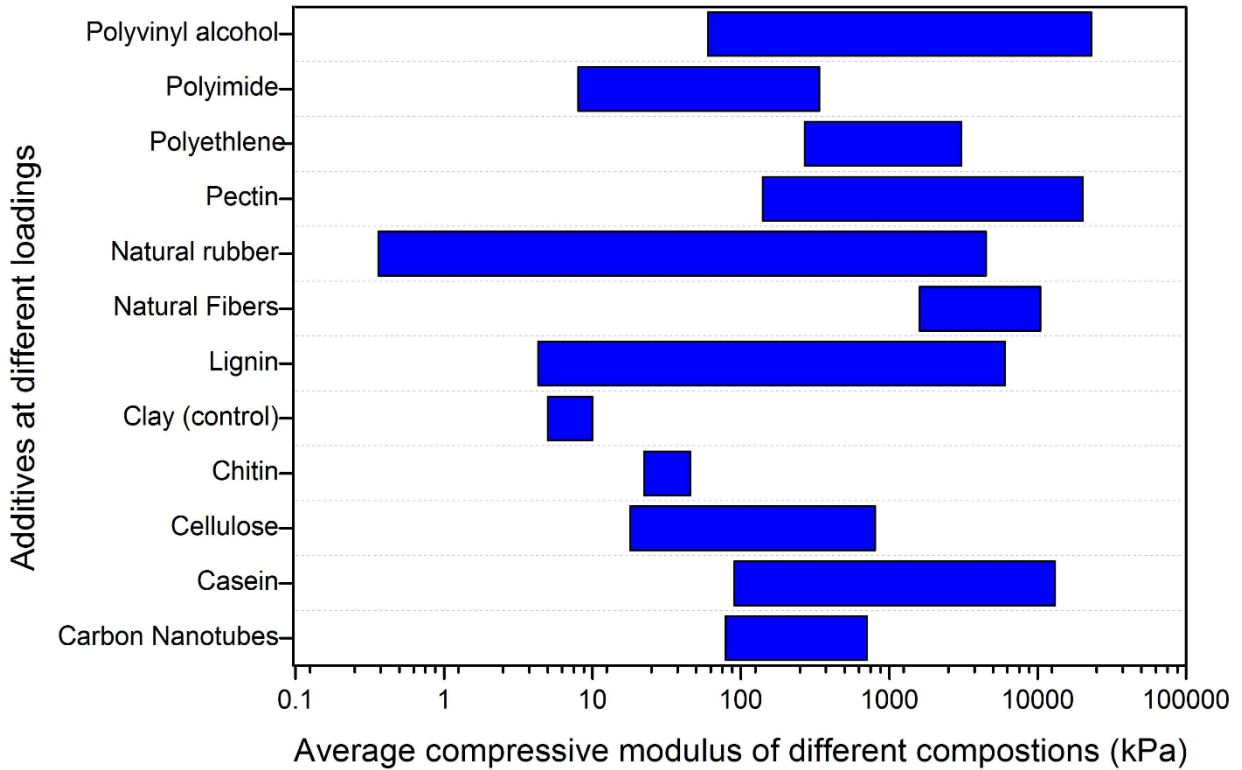


Figure 2.7 Reported moduli of various aerogel compositions with different parameters [12,53-63]

It would be expected that due to the porosity nature of the aerogel composites, an increase in the solid content is usually what to a certain extent, is responsible for any increase in strength according to basic intuition [12]. However, according to the histogram distribution compiled from literature (Figure 2.8), the density of aerogel mostly tends to cluster towards 0.1 g/cm^3 which is the preferred density for building applications [10,64]. The reported strength of these materials can compete with traditional foam materials [15], demonstrating that by altering the composition of the aerogel, it is possible to enhance the mechanical strength directly with minimal increase in density, which attributes to the most valuable properties of aerogel, such as their low thermal conductivity [14,65].

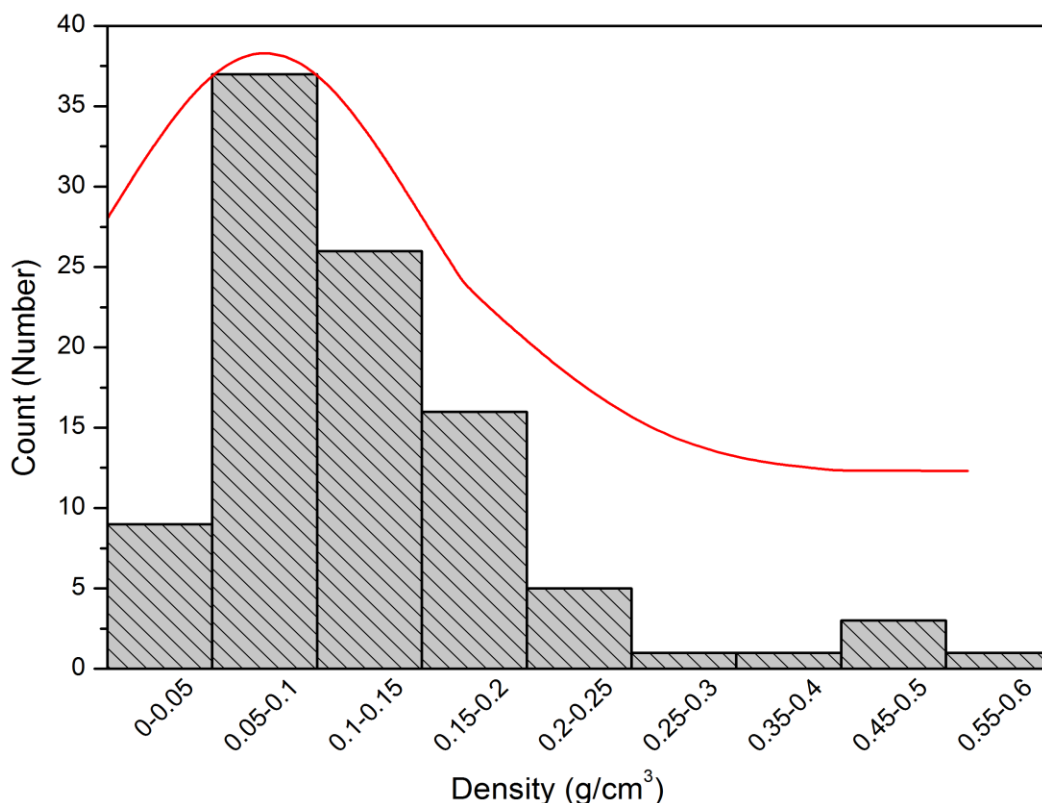


Figure 2.8 Distribution of reported densities compiled for aerogel composites [12,53-63]

2.4.1 Enhancing mechanical strength of clay aerogel through natural polymers

2.4.1.1 Casein reinforced clay aerogel

Casein is natural macromolecules, which makes up the majority of the protein in milk and is responsible for the milk-white and opaque appearance. Casein is part of the phosphorylated family (α S1-, α S2-, β - and κ -casein) and can exist in different forms depending on their structure, amino acid composition and molecular weight (19-24 kDa) [66]. It is vastly used in paper coating, wood adhesives, as well as food packaging due to their film-forming properties and barrier resistance to nonpolar substances such as oxygen, carbon dioxide and aromas. One of the biggest limitations of casein is its weak water resistance and stability due to the mass of polar groups, and hence it requires further modification to improve its performance for an effective application in aerogel and other composites [67,68].

One of the most controlled principles to enhance and stabilise proteins is by inducing crosslinks through enzyme-aided structural engineering [69]. Based on this mechanism, two approaches have been reported for implementing casein into aerogel composites using crosslinking agents to modify the functionality of the protein via an environmentally friendly freeze-drying process: one was to use the biocompatible DL-glyceraldehyde (GC) [70], which has proven to be effective in creating a tight cross-linked network [71], and the compressive modulus of the clay-casein aerogel increased from 3900 to 5600 kPa at high polymer contents and from 90 to 98 kPa at low polymer content (Table 2.2). It is apparent that the enhancement of the mechanical properties could be achieved by increasing the polymer content in suspension and in other words, it seems that the crosslinking agent (GC) had an insignificant role in increasing the modulus at low polymer content, this may be due to insufficient covalent bonds being formed between the polypeptide chains within the protein (intramolecular crosslinks) or between the proteins (intermolecular crosslinks) [72].

Table 2.2 Composition, density and initial modulus of casein-clay aerogel [70]

Samples	Density (g/cm ³)	Initial modulus (kPa)
CA10M5	0.113	3900
CA10G5M5	0.096	5600
CA2.5M5	0.071	90
CA2.5G5M5	0.078	98

Another approach was to use milk and the enzyme transglutaminase (Tgase) to produce milk-clay aerogels [73]. Tgase has been widely used in the food industry to alter the physical properties of proteins, such as their hydration, solubility and charge [74], by forming both inter- and intramolecular isopeptide bonds in and between various proteins [75]. The neat milk-clay aerogels can achieve a layered microstructure similar to that of other clay-polymer aerogels, with densities ranging from 0.14 to 0.23 g/cm³ and compressive moduli ranging from 1.4 to 13 MPa. The increase in the mechanical properties can be related to the effectiveness of the enzyme producing strong

covalent bonds between the protein molecules rather than an increase in density [76]. These new foam-like clay aerogel materials, which can be produced from off the shelf regular, skimmed as well as expired milk, are considered as an efficient means of using food waste for engineering useful materials such as bio-based packaging materials.

2.4.1.2 Cellulose reinforced clay Aerogel

Cellulose is one of the most abundant biopolymers, formed by the repeated connection of D-glucose building blocks associated with hydrogen bonds and is found in materials such as wood, cotton, hemp, and in a wide variety of living organisms including animals, plants and bacteria [77]. The cellulose is considered as an almost inexhaustible raw material with a wide range of application due to their high strength and stiffness, which makes them an excellent reinforcing agent for nanocomposites. The cellulose is also considered as highly functionalised, characterised by their hydrophobicity, chirality, biodegradability and broad chemical modifying capacity [78]. Cellulose can exist in many forms, for example, a semicrystalline nanofibre form known as whiskers, which have been studied intensively due to their high performance when used as reinforcement agent in polymer composites to produce “green” nanocomposites [56].

The manufacture of ultra-low density aerogel composites using different forms of cellulose and montmorillonite clay via the environmentally freeze-drying process has been tested, and the influence of cellulose on the properties of the end-product aerogels has been studied. Other parameters including solution composition and freezing direction vary considerably throughout the literature to determine their influence on cellulose-clay based aerogels [79-81]. The study on the addition of cellulose nanofibres to montmorillonite to create inorganic-organic hybrid aerogels [47] indicated that the addition of cellulose can improve the compressive modulus and is a more effective approach to enhance the compressive modulus than simply increasing the clay

concentration (Table 2.3). Usually, for foam materials, the increase in the modulus is strongly dependent on density [82], but the data suggest otherwise. For example, the sample which recorded a density of 0.031 g/cm³ performed better than that of a higher density of 0.069 g/cm³, where they recorded a modulus of 462 and 392 kPa, respectively. This indicates that the increase in the compressive modulus may be related to the effect of the whiskers on the microstructure of the aerogel, creating a three-dimensional network which can effectively transfer the stress applied (Figure 2.9). Also, it should be noted that the microstructure of the aerogels can be altered from a 3D network to a 2D sheet-like skeletons by controlling the solid content (Figure 2.9) [83].

Table 2.3 Composition, density and modulus of cellulose-clay aerogel [47]

Clay (wt. %)	Whisker (wt.%)	Modulus (kPa)	Density (g/cm ³)
0.8	0.0	N/a	0.010
0.8	0.8	20	0.014
0.8	2.0	462	0.031
2.5	0.0	N/a	0.024
2.5	0.8	125	0.038
2.5	2.0	438	0.059
5.0	0.0	9	0.040
5.0	0.8	392	0.069
5.0	3.0	439	0.055
7.5	3.0	788	0.101

A study to explore the relationship between freezing process and the structure of cellulose (NFC)-sodium montmorillonite (MMT) composite aerogels showed that the non-directional freezing (via liquid nitrogen) would produce foam-like, isotropic aerogels with high interconnectivity, while an anisotropic honeycomb-like aerogels of identical composition was witnessed from the directional freezing (freeze casting) which involved the freezing and drying under reduced pressure [81]. While the mechanical properties seem to be enhanced with increasing the solid content due to the increase in density, the structure architecture may have played a significant role in enhancing the

modulus which can be seen from those aerogels at identical compositions with a minor increase in density (Table 2.4).

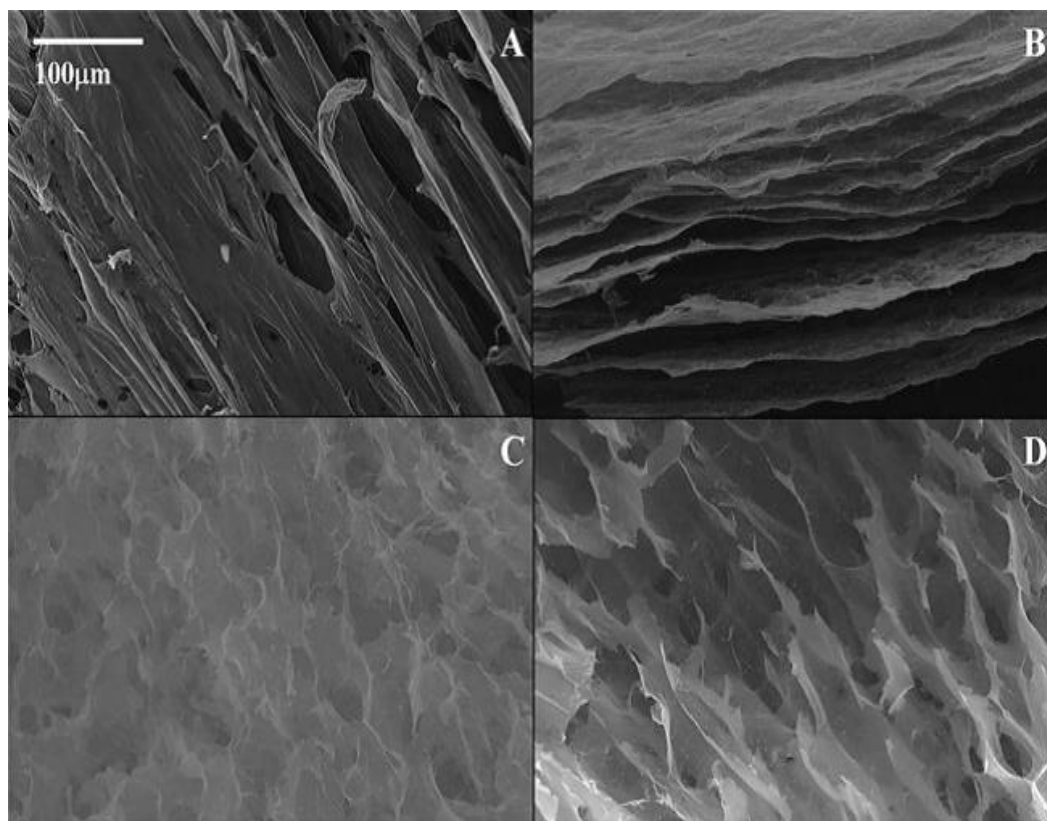


Figure 2.9 SEM of the aerogels produced by freeze-drying dispersions of (A) 0.8 wt.% cellulose whiskers, (B) 2.5 wt.% clay + 0.8 wt.% cellulose whiskers, (C) 2.5 wt.% clay + 2 wt.% cellulose whiskers and (D) 5 wt.% clay + 3 wt.% cellulose whiskers [83]

Therefore, the anisotropic aerogels produced from directional freezing provide better mechanical properties when tested in the perpendicular direction of the layered microstructure, where a vertically aligned structure with clay sheets spanning across the thickness [84] has the ability to resist load more effectively. In general, the reported mechanical properties of cellulose-based aerogels can possibly replace foamed polymer materials for food-packaging applications [85].

Table 2.4 Composition, structure and mechanical properties of cellulose-clay aerogel [85]

Composition	Structure	Young's modulus (kPa)	Yield Strength (kPa)	Work to failure (KJ/m ³)	Density (kg/m ³)
(3 wt.% MMT , 0.4 wt.% NFC)	Isotropic	25.8 ± 5.9	-	6.3 ± 0.4	29.8 ± 0.9
	Anisotropic ⊥	148.4 ± 13.9	3.30 ± 0.2	6.82 ± 0.22	31.0 ± 0.9
(3 wt.% MMT , 0.8 wt.% NFC)	Isotropic	160.5 ± 25.1	12.5±1.1	18.2. ± 1.1	47.1 ± 1.4
	Anisotropic ⊥	397.3 ± 34.5	6.90 ± 0.4	11.8 ± 0.19	33.0 ± 1.0
(3 wt.% MMT , 1.2 wt.% NFC)	Isotropic	386.4 ± 43.7	30.0 ± 4.1	24.1± 1.0	44.8 ± 1.3
	Anisotropic ⊥	1110.3 ± 109.4	18.0 ± 1.5	22.3 ± 0.06	37.0 ± 1.1

2.4.1.3 Chitin reinforced clay aerogel

Chitin is one of the most abundant polysaccharides and considered as an underutilised resource with high potential in many applications. It is present in high quantities in living organisms, such as in the shells of crustaceans and from crabs and shrimps [86,87]. The ability to incorporate such a naturally strong polymer into clay aerogels should allow for a synthesis of high strength, hard and tough aerogel composite, however, its reactivity and processability could limit its application as it is only soluble in an acidic media [88].

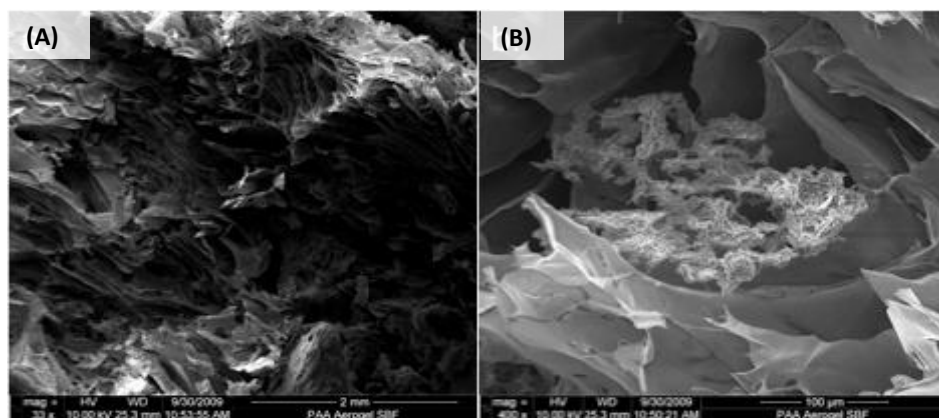


Figure 2.10 Morphology of an HMW CHIT aerogel depicting uneven dispersion of CHIT within the clay matrix at (A) 2mm and (B) 100 μm magnification [89]

The incorporation of chitosan (CHIT), a deacetylated derivative of chitin, and the effect of factoring parameters, such as the molarity of the CHIT solution, the molecular weight of the CHIT and the ratios of the solid content effects on the final aerogel composite were investigated [89]. Poly (acrylic

acid) (PAA) was also incorporated for a mineral nucleation, as it conveniently interacts with chitosan and enhances its bonding strength as the presence of acidic proteins, specifically carboxylic acid has proven to generate the nucleation of calcium carbonate and hydroxyapatite crystals. The primary minerals compose skeletal and shell structures [89,90].

Chitosan clay aerogel can effectively disperse within the clay platelets when the chitosan is in an acidic media as ammonium polyelectrolytes are formed, which intercalate with the galleries by exchanging sodium [91]. The miscibility (i.e. forming a homogenous solution) of CHIT and clay increased as the molecular weight decreased, this inverse relationship causes a heterogeneous dispersion when high molecular weight (HMW) CHIT was used, forming a heterogeneous aerogel structure with different properties at different cross-sections (Figure 2.10). However, a homogenous aerogel was also reported for low molecular weight (LWW) CHIT, because the latter resulted in a colloidal dispersion. While the addition of Poly (acrylic acid) PAA and/or CHIT to clay aerogels resulted in aerogels with increased structural integrity and increased moduli, the molecular weight of CHIT increased the density of the clay aerogel, with the enhanced mechanical properties generally coming at the expense of higher density [47]. On average, the modulus for clay-chitosan aerogels increased by about 0.0234 MPa, with the addition of CHIT at densities in the range of 0.04-0.08 g/cm³.

2.4.1.4 Lignin reinforced clay aerogel

Lignin is a natural amorphous polymeric material and considered as waste materials or by-product of pulping. Lignin is one of the most abundant and renewable materials, but its full potentials have not been fully utilised and currently mostly used to fuel the fire of the pulping boilers [92,93]. Current studies have been focused on exploring its value-added application, such as enhancing the mechanical properties of polymeric composites due to their phenolic base structure [94]. Lignin has

recently been exploited as a cheap raw material to produce organic aerogels [95,96]. The combination of lignin, both in its alkali and liginosulfonic forms, with sodium montmorillonite through a freeze-drying technique to form clay aerogels composites has been attempted [53]. The improvement of both physical and mechanical characteristics was found highly dependent on the reactive macromolecules functional groups of both the lignin alkaline and sodium liginosulfonate [97]. The functional groups of lignin and certain molecules can interact with the clay, leading to the formation of hydrogen bonds [98].

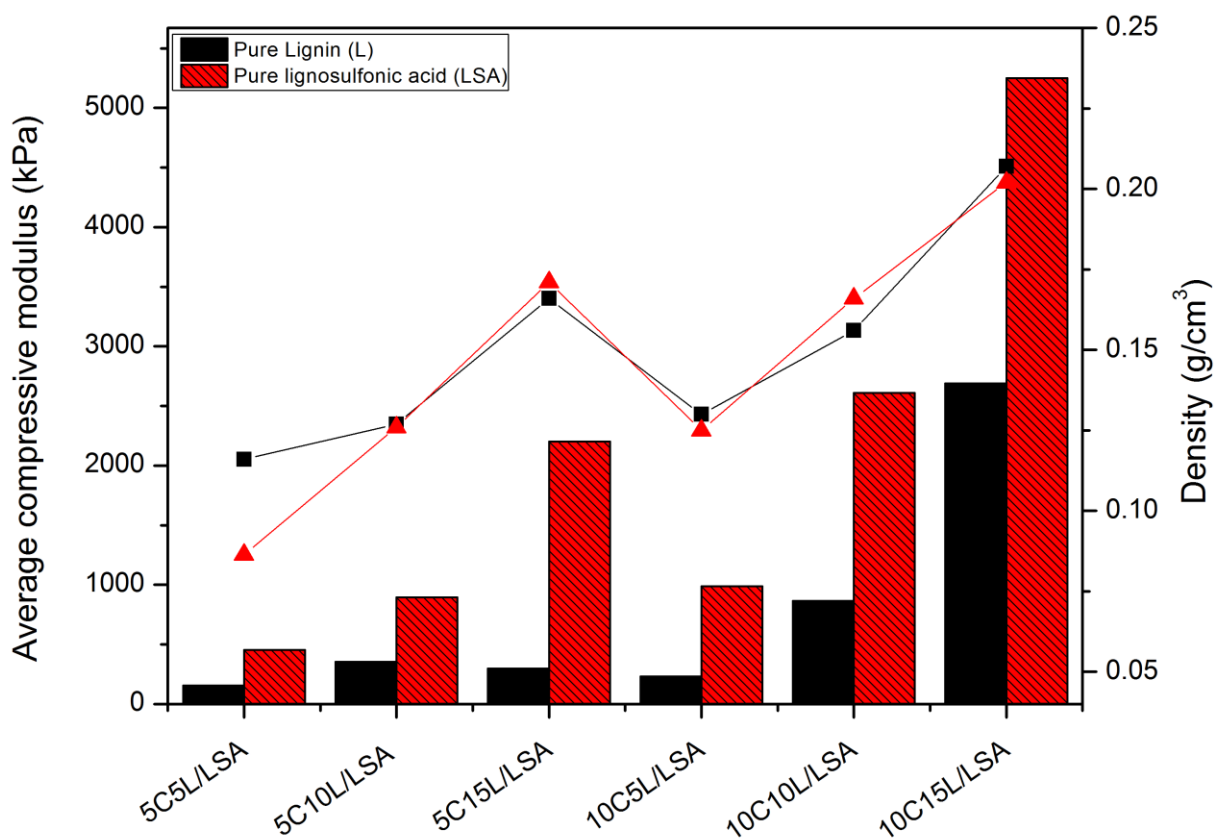


Figure 2.11 Compiled average compressive modulus and density of lignin-clay aerogels [53]

While the clay-lignin aerogel composites followed an expected trend of an improvement in mechanical properties with an increase in the solid content, the aerogels prepared from liginosulfonic acid showed a significant enhancement to the compressive modulus with no significant

change in density (Figure 2.11). This enhancement may be attributed to the fact that Lignosulfonic acid (LSA) contains sulfonic acid groups which makes it water-soluble [99], allowing a continuing formulation of 3D structures. The fact that lignosulfonic acid has a higher molecular weight than alkali lignin may also facilitate the formulation of a greater number of hydrogen bonds as well as chain entanglement. However, it should be noted that having a polymer with a high molecular weight is not a reliable method of reinforcement as this is only true to a certain extent where in some cases a moderate molecular weight is more effective [50].

2.4.1.5 Natural rubber reinforced clay aerogel

Natural rubber is another low-cost renewable resource extracted from a runny, white liquid called latex found in the sap of certain plants. It is an indispensable elastometric material because of its ability to crystallise at large deformation resulting in extraordinary toughness. The vulcanised natural rubber elongates on stretching and regains its original shape after the removal of the stress. Natural rubber is biocompatible and biodegradable and could be an ideal reinforcement medium for producing polymer-clay nanocomposites with low gas permeability [100-102]. Montmorillonite (Na⁺-MMT) aerogel-prevulcanised natural rubber (PNR) composites have been attempted with a single freeze-drying process [59].

Prevulcanised rubber (PNR) is non-crosslinked, and such molecules are able to freely pass each other at elevated temperatures [103]. The PNR-clay aerogel composites have densities in the range of 0.36-0.55 g/cm³ while typical montmorillonite converted aerogels in a range of 0.01-0.10 g/cm³ [104]. The higher density of PNR clay aerogel is a consequence of the high polymer content, a solid content of 30 wt.%, although the density might not play a significant role in increasing the initial modulus (Table 2.5), for example, PNR/M1 and PNR/ M2, which reported an initial modulus of 19.3 and 23 kPa respectively, have very similar density. Therefore, the mechanical enhancement may be

attributed to the strong rubber-clay interface, assigned to the electrostatic interaction between the clay and the rubber [105]. The schematic interaction of the dried natural rubber and clay may be represented as Figure 2.12, which is visible at higher clay loadings. The void volume fraction is crucial in understanding the properties of the aerogel, as it is directly related to the density of the samples.

Table 2.5 Compression, density and void volume fraction of clay-PNR aerogel composites [59]

Samples	Initial modulus(kPa)	Reinforcing efficiency (%)	Measured density (g/cm ³)	Void (%)
PNR ^a	17.3 ± 6.3	-	0.49 ± 0.03	48.6 ± 2.9
PNR/M1	19.3 ± 1.7	14.6	0.47 ± 0.01	50.7 ± 0.9
PNR/M3	23.0 ± 4.5	29.1	0.47 ± 0.02	51.4 ± 1.5
PNR/M5	22.5 ± 4.0	22.7	0.36 ± 0.03	63.1 ± 2.5
PNR/M7	35.4 ± 11.8	80.7	0.55 ± 0.05	43.5 ± 4.8

M represents the Na⁺-MMT, and the numbers 1, 3, 5 and 7 indicate the mass content of the Na⁺-MMT

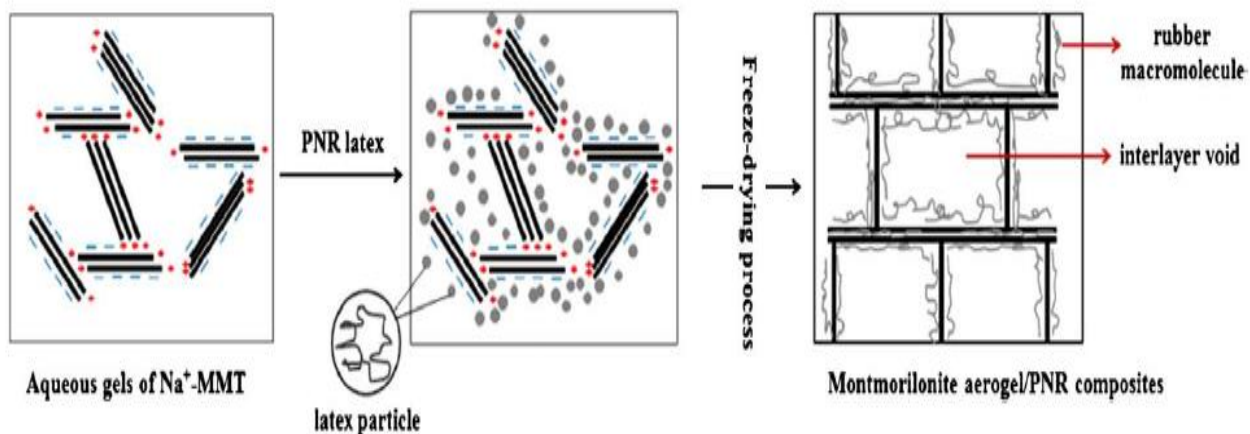


Figure 2.12 Schematic representation of the structure of the clay-PNR aerogel composites [59]

Clay-NR aerogels have been investigated through a simple freeze-drying process of the aqueous dispersions, with crosslinking in benzene using sulfur monochloride (S₂Cl₂) as a solution cross-linking agent, which has low reaction temperatures (~22°C) [106]. The results have demonstrated effectiveness in producing tough and responsive clay-NR composites [107,108]. The effects of the

concentration of (S_2Cl_2) and the reaction temperature on the clay-NR structure and properties were also investigated [109].

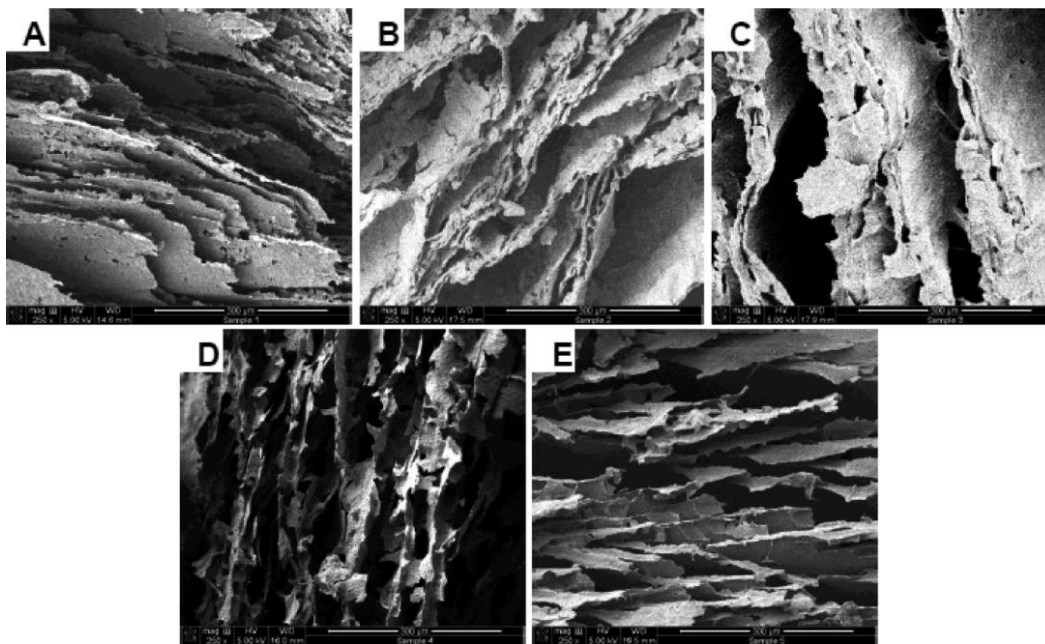


Figure 2.13 Morphology of 2.5 wt. % NR aerogels cross-linked at different levels of S_2Cl_2 : (A) 0 (v/v %), (B) 0.25 (v/v %), (C) 0.5 (v/v %), (D) 1 (v/v %) and (E) 5 (v/v %). $T_{prep} = -18^\circ C$ [109]

The concentration of (S_2Cl_2) was altered between 0.2 and 5% (v/v) and temperatures varied between 18 and $-18^\circ C$ for samples of 2.5 wt.% NR and 5 wt.% clay. It is apparent that as the (S_2Cl_2) concentration increased, the microstructure transitioned to a rough and coarse structure (Figure 2.13 A), which resulted in enhanced mechanical properties. Increasing the concentration above 1% (v/v) only resulted in an increase in density without further enhancement. Increasing the amount of crosslinker above a certain degree decreases the crosslink density and reduces the crosslinking efficiency [110]. The ideal combination was reported at a reaction temperature of $-18^\circ C$ with a 1% (v/v) (S_2Cl_2), which exhibited a compressive modulus and toughness of 1800 and 13 kPa, respectively, a significant improvement from 70 and 2 kPa and with a modest increase in density from 0.06 to 0.11 g/cm^3 . Increasing the NR content from 2.5 to 10 wt.% (with a constant 5 wt.% clay)

increased the compressive modulus from 70 to 300 kPa, which may be attributed to the increase in the solid content.

2.4.1.6 Pectin reinforced clay aerogel

Pectin is an important structural component found in the cell wall of plants, and its structure is made up from a heterogeneous group based on chains of linear regions of 1, 4- α -d-galacturonosyl units, which are natural carbohydrates that exist in fruit and vegetables. The macromolecule of pectin is known to bond with several organic and inorganic substances and can be easily found in the waste of sunflower oil and sugar manufactures [111].

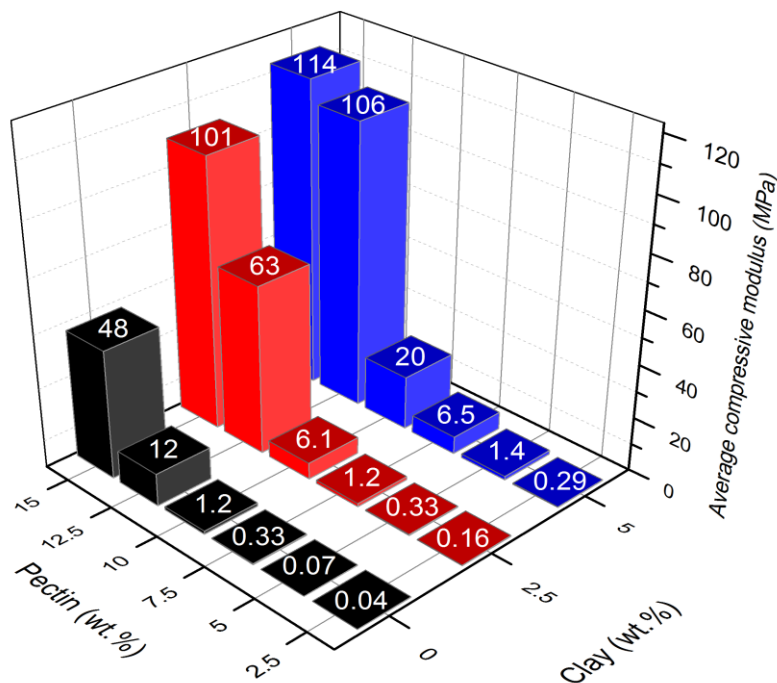


Figure 2.14 Average compressive modulus of various clay-pectin aerogel compositions [58]

Therefore, it is a very effective candidate for producing eco-friendly biodegradable materials to replace current petroleum-based materials [112,113]. Biodegradable aerogel composites were fabricated from pectin and sodium montmorillonite through a simple, environmentally friendly freeze-drying process [58]. The compressive moduli of the aerogel composites can be directly

related to the density of the composites, and the higher the solid content, the higher the compressive modulus (Figure 2.14). The highest recorded modulus of 114 MPa has been reported for a pectin clay aerogel with a density of 0.19 g/cm^3 , similar to the properties of petroleum-based closed cell foams [1]. The pectin (P)-clay (C) aerogels showed a “house of cards” microstructure similar to that of other polymer-clay aerogels at low polymer loading (5P5C) and low connectivity between the layers. However, increasing the solid content above 10% (P10C5 and P15C5) transformed the lamellar structure to a porous structure with a high connectivity (Figure 2.15), allowing for the load to be transferred more effectively within the material.

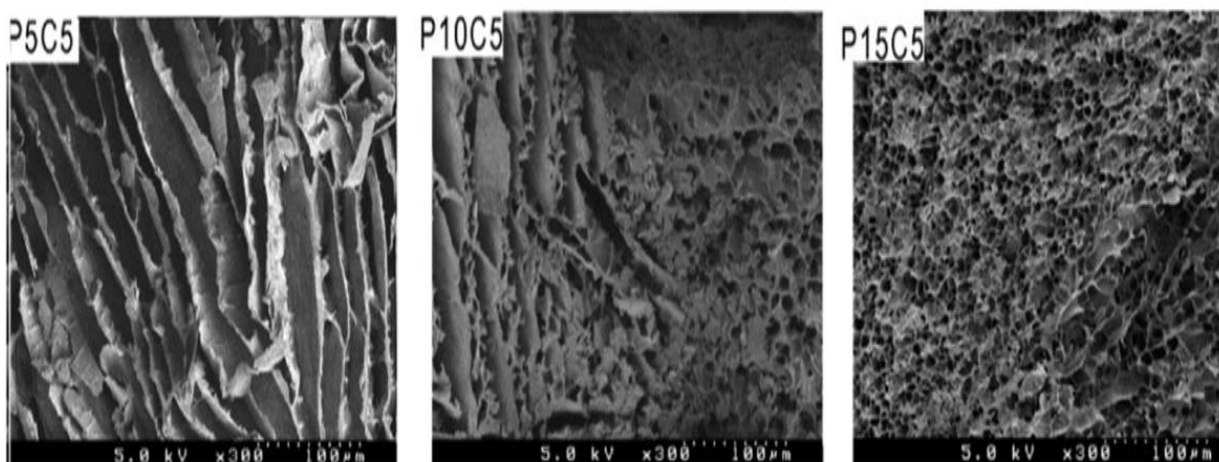


Figure 2.15 Microstructure of pectin-clay aerogels with different compositions [58]

The crosslinking of pectin has been vital for its implementation in many applications, where different cations have proven to influence its gelling and mechanical properties [114]. The influence of crosslinking pectin to produce clay aerogel composites was investigated [58]. Three cations, namely calcium chloride (CaCl_2), aluminium sulfate ($\text{Al}_2(\text{SO}_4)_3$) and sodium chloride (NaCl), were explored in the range of 0.001-0.004 mol/g pectin. The crosslinking had a negligible effect on the density of the clay-pectin aerogels, even when increasing the crosslinking concentration. The crosslinking significantly increased the compressive modulus, and the most effective system P5C5/ $\text{Al}_0.003$

showed a modulus of 6.8 MPa, which is a 3.8 fold increase compared to the neat clay-pectin aerogel of 1.4 MPa with the same composition (5P5C) (Table 2.6). The enchantment in performance can be related to the effect of the cation on the clay and its ability to exfoliate and improve the interaction between the clay platelets and the polymer. It is possible that the sodium at low concentrations had an effect on exfoliating the clay due to an increase in the surface charge of the clay, resulting in a more effective clay suspension with better surface chemistry [115,116].

Table 2.6 Modulus and density of clay-pectin aerogel cross-linked with various cations [58]

	pectin/clay/Cation	P5C5/0.001	P5C5/0.002	P5C5/0.003
NaCl	Modulus (MPa)	1.9 ± 0.2	4.1 ± 1.4	5.4 ± 0.6
	Density (g/cm ³)	0.10 ± <0.01	0.10 ± <0.01	0.10 ± <0.01
CaCl₂	Modulus (MPa)	2.7 ± 0.7	2.9 ± 0.6	5.5 ± 1.1
	Density (g/cm ³)	0.10 ± <0.01	0.11 ± <0.01	0.12 ± <0.01
Al₂(SO₄)₃	Modulus (MPa)	3.8 ± 0.3	3.9 ± 0.6	6.8 ± 1.1
	Density (g/cm ³)	0.10 ± <0.01	0.10 ± <0.01	0.12 ± <0.01

2.4.2 Enhancing mechanical strength of clay aerogel through synthetic polymers

2.4.2.1 Epoxy reinforced clay aerogel

High corrosion and chemical resistance, mechanical strength, thermal and electrical properties make epoxy resin highly attractive for many applications due to their ease of processing and high versatility. Altering the temperature, time the cure reaction and formulation could lead to different structures and mechanical properties [117,118]. Epoxy-clay aerogel can be produced by using a water-soluble crosslinking thermoset precursor 1,4-butanediol diglycidyl ether (BDGE) and triethylenetetramine (TETA) creating water-soluble epoxy monomers and producing aerogels through an environmentally freeze-drying process [119]. The polymer loading varied between 5, 10,

15, and 20 wt.% while maintaining the clay at a constant concentration of 5 wt.%. The density of the developed aerogel composites ranged from 0.05 to 0.28 g/cm³.

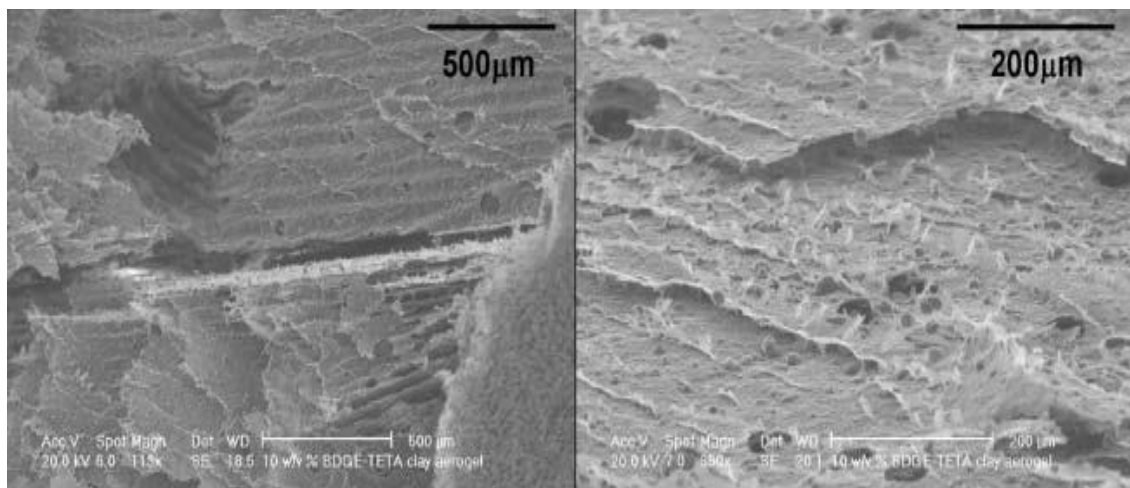


Figure 2.16 Morphology of a 10 w/v% BDGE-TETA composite [119]

Any increase in the mechanical properties of the clay-epoxy aerogel is directly related to the increase in polymer loading. However, it was considered that the main advantage and outcome from the incorporation of such polymers is elastomeric behaviour of clay-epoxy aerogel, which could be able to withstand large amounts of strain and recover its geometry with little permanent deformation [119]. Many reasons for achieving such property may be related to unique house of card structure where the clay surfaces were covered with BDGE-TETA polymer (Figure 2.16), and this provides clay-epoxy aerogel with elastomeric properties by the nature of the flexibility of the epoxy systems when cured [120,121].

2.4.2.2 Polyethylene reinforced clay aerogel

Polyethyleneimine (PEI) belongs to the synthetic polymer family and has a high cationic charge density that can exist with a linear or branched structure of different molecular weights (MWs) [122]. PEI is usually used in mineralised systems that consist of complex hierarchical structures with alternating layers of minerals surrounded by a polymer which acts as a binding agent [123]. PEI

composites have been extensively used for membrane fabrication [124]. PEI is a water-soluble polymer and has shown to effectively interact with smectic clays such as sodium montmorillonite due to the formation of covalent bonds [125,126], thus making it a suitable candidate to produce clay aerogel composites. The production of clay-PEI aerogel has been attempted through an environmentally freeze-drying process [127]. The interaction of PEI with clay platelets results in an initial modulus of the aerogel composite of 270 kPa while retaining low densities in the range of 0.075 g/cm^3 .

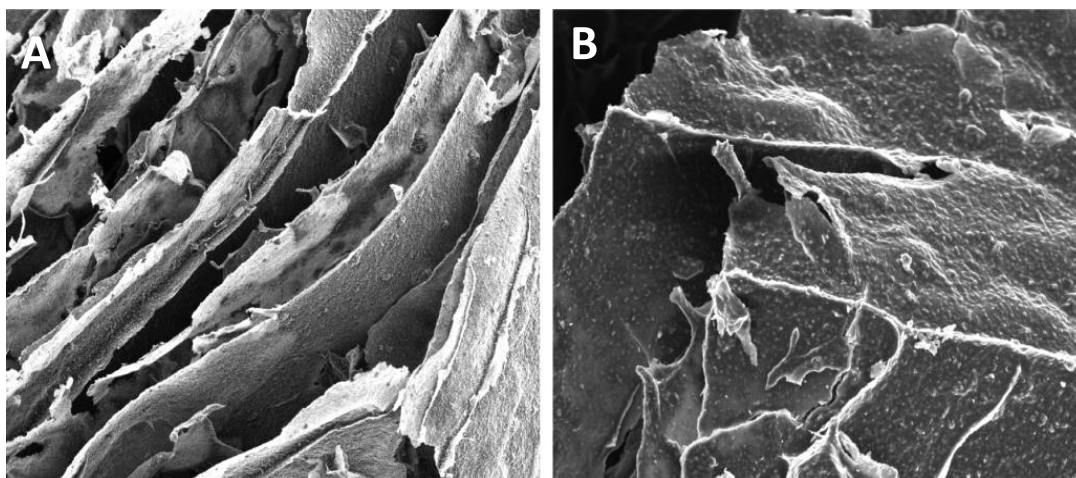


Figure 2.17 Morphology of the clay-PEI structure: (A) Before solidification and (B) After solidification [127]

Another approach for using PEI polymers for an aerogel production is through the solidification of the PEI using tetramethyl orthosilicate (TMOS), which involves acid hydrolysis [75]. The solidification of the aerogel clearly transitioned the structure from a lamellar to a rough surface (Figure 2.17). The property of the solidified aerogels is closely related to the solidification parameters, especially exposure humidity. For example, the initial modulus of the PEI aerogel composites treated at 60% RH increased from 270 kPa to 870 kPa, and the aerogel sample was found slightly deformed compared to its original dimension, while those treated at 80% RH demonstrated a significant increase in strength where the initial modulus was recorded at around 2.8 MPa, which is a 10 fold

increase compared to the untreated PEI aerogel and more than two times compared to the sample treated at 60% RH. The PEI aerogel also maintained its original dimensions without any deformation.

2.4.2.3 Polyimide reinforced clay aerogel

Polyimides (PI) are high-performance insoluble polymers used in many fields but are used largely for microelectronics due to their unique electrical, and heat and moisture resistance properties. PI is able to maintain its properties at a high temperature of up to 300°C [128,129]. Water-insoluble PI polymers can be integrated into clay aerogels [130], but this requires the use of solvent or surfactants to create a stable suspension. Polyimide aerogels have currently been produced through a supercritical CO₂ drying process.

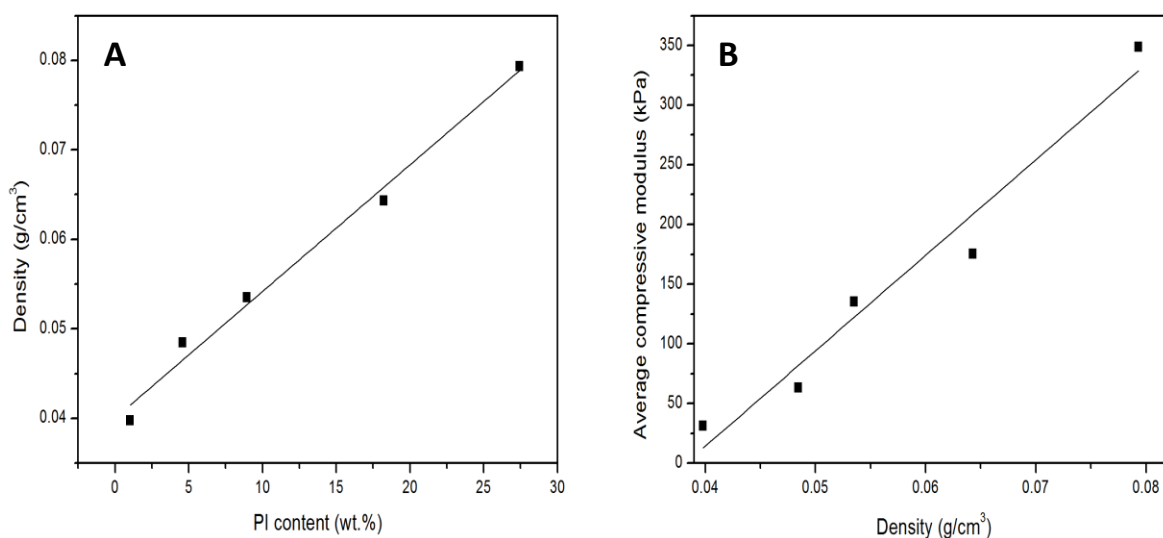


Figure 2.18 Clay-PI aerogel mechanical and physical properties: (A) PI content relationship with density and (B) Modulus relationship with density [12]

Polyimide has also been implemented into clay aerogels by using 3-Aminopropyltriethoxysilane (APTMOs)-capped poly (amic acid) (AP-PAA) and ammonium salt as a water-soluble precursor to blend with clay in water, followed by freeze-drying to produce PI-clay aerogel composites [12]. The APTMOs was used to promote and increase chemical and hydrogen bonding between polyimide and the substrate [131].

A number of different clay-PI aerogel composites with varying compositions of polyimide (PI) with a constant 5 wt.% of clay were produced. For most aerogel composites, the density is dependent on the polymer content (Figure 2.18B). The modulus is also related to the density (Figure 2.18A) with the compressive modulus increasing as the density increased. The unmodified clay aerogel had a compressive modulus of only about 7 kPa at a density of 0.039 g/cm^3 , but after the addition of 18.3% (w/w) PI, a significant increase in the compressive modulus to 201 kPa was achieved with a density of 0.071 g/cm^3 , which is still in the range of aerogel densities and similar to that of PVA reinforced aerogels [50].

2.4.2.4 Polyvinyl Alcohol reinforced clay aerogel

Polyvinyl alcohols (PVA) are synthetic water-soluble polymers produced through the hydrolysis of polyvinyl acetate. PVA is an excellent gas barrier. It is biodegradable and can provide excellent mechanical properties such as toughness and flexibility at a relatively low cost [132,133]. The properties of the PVA such as biodegradability and solubility are directly affected by the molecular weight (MW) and the amount of hydroxylation [134]. PVA is used in various commercial, medical and food applications due to their unique chemical and physical properties [135], and has been extensively used to prepare nanocomposites with layered silicate to enhance mechanical and barrier properties [136,137]. PVA is a suitable candidate for producing clay aerogels composites due to relatively low cost, non-toxicity, good mechanical properties, biocompatibility, solubility in water (highly hydrophilic), and strong attraction with clays, due to an ideal hydrogen bonding, that is, the hydrogen on the polymer is perfectly spaced to match the oxygen in the lattice of the Na^+ -MMT [138], PVA-clay aerogels could achieve a significant mechanical enhancement. The investigation of the mechanical properties of clay-PVA aerogels has shown that the addition of PVA may result in an increase in the clay aerogel compressive modulus by several orders of magnitude. However, the

degree of reinforcement is reliant on the molecular weight, which has a direct impact on the structure.

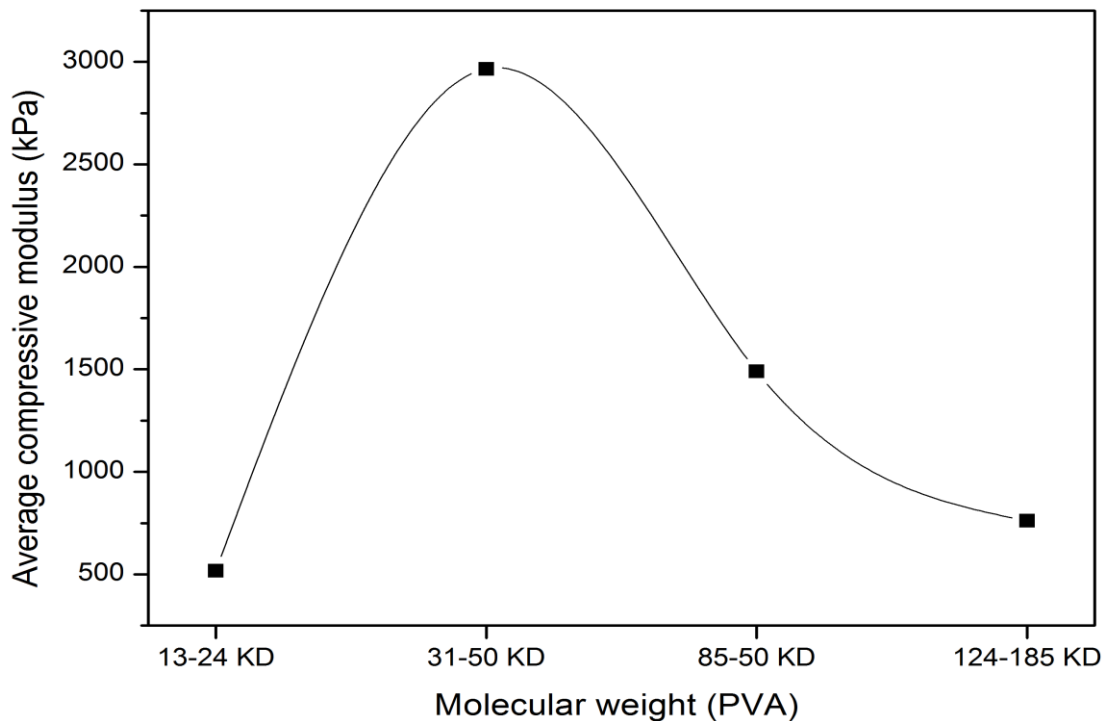


Figure 2.19 Compressive modulus of clay-PVA aerogels with variations of PVA molecular weight [50]

Using high molecular weight PVA to produce clay aerogels can result in a random and dendritic-type structure [139] as the polymer acts as a barrier preventing continuous ice growth but with a new ice crystal growing on the other side of the barrier (polymer) [140]. PVA of high molecular weights may not reinforce the structure as effectively as moderate molecular weight polymers [139], the change in the structure strongly affected the final properties of the aerogel. The structure with a lamellar and web-like structure obtained from low molecular weight could be stiffer due to the small web reinforcements that prevent layers from bending [50]. While on the other hand when the molecular weight increased a more random distributed structure was observed with thinner layers that can be easily broken. Figure 2.19 shows how the compressive modulus changes with molecular weight (N.B Constant PVA wt. %).

Cross-linking is widely used in material science to modify and enhance the performance of polymers to create new tailored materials [141]. Many crosslinkers in literature have been used to improve the properties of PVA, such as di-functional compounds, for instance, glutaraldehyde and glyoxal due to the reaction of the hydroxyl groups of PVA with aldehydes through the formation of acetal bonds [142]. However, limited literature is available regarding the implementation of crosslinked PVA in order to produce clay-polymer aerogel. The production of PVA-clay aerogels through an environmentally friendly freeze-drying process using water as a solvent and divinyl sulfone (DVS) as a crosslinking agent has been reported [60]. What makes Divinyl sulfone a suitable candidate to crosslink PVA and produce PVA-clay aerogels is the fact that it is a homobifunctional reagent where the vinyl groups can partake as electrophiles in the reaction of nucleophilic addition and can be reacted in a single chemical reaction [143]. The crosslinking method was confirmed to improve the mechanical properties of the clay-PVA aerogels (Figure 2.20). The total solid content was maintained at 10 wt.% and even the amount of DVS (Crosslinker) was fixed at 0.12 equivalents based on the free hydroxyl groups, the compressive moduli of aerogel composites increased by 2-30 MPa after crosslinking, compared to the control samples. It is apparent that the level of effect of the crosslinker is also related to the composition, i.e. clay-polymer ratio. It would be expected that the higher the polymer content, the more effective is the crosslinking. However, reinforcement effects are also evident at lower clay wt.% allowing for lower overall densities in structural materials [46]. The most effective system was witnessed for the P6C4 combination due to the higher interaction of the PVA with clay.

Another method for implementing cross-linked PVA in the fabrication of clay-polymer aerogels was to use gamma irradiation without chemical additives as a mean of crosslinking [63]. Chemical cross-linking can cause some setbacks, leading to a rise in viscosities which make it challenging to achieve

homogeneous blends of polymer-clay suspension and hence low efficiencies and residual of unreacted cross-linking agents as well as recyclability issues. The implementation of irradiation-induced cross-linking could enhance the production and the aerogel properties at a much quicker rate [144].

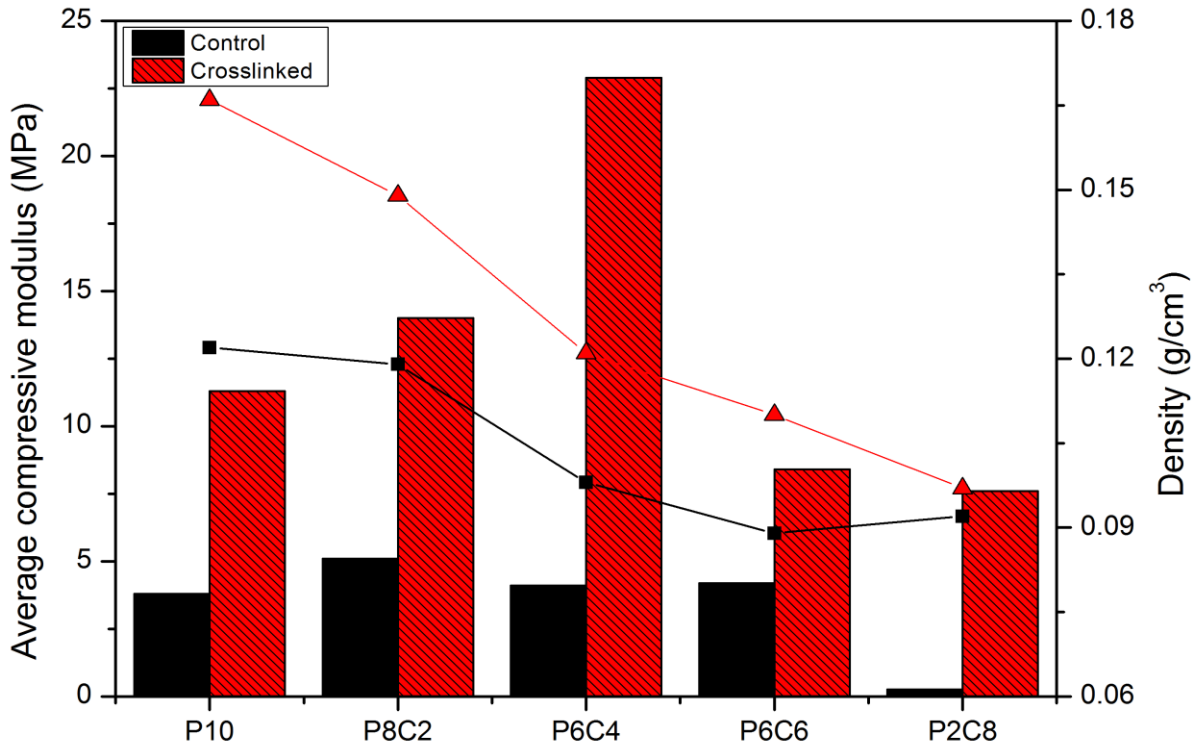


Figure 2.20 Compressive modulus and density of clay-PVA aerogels while using DVS as a crosslinker [60]

An experiment of using different dosages of gamma irradiation of 0, 10, 30, 50, and 100 kGy (Kilogray) indicated that the absorbed dose of 30 kGy was an optimum dose for fabricating strong PVA-Clay composites, while an increase of the absorbed dose could lead to a decreased porous size of network structures. The gamma radiation showed a significant increase in the compressive modulus at lower densities (Figure 2.21). The gamma radiation has also shown to be effective even at low polymer loadings, for example, the modulus of P1C9 aerogel indicated a 12-time increase.

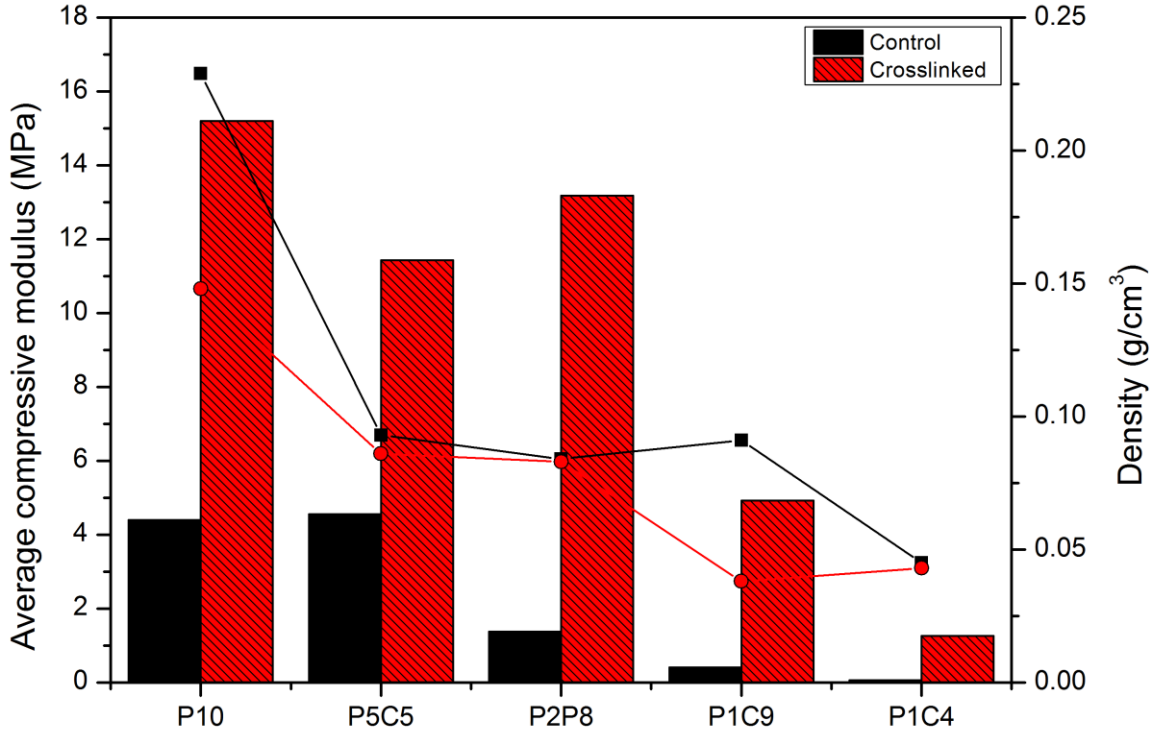


Figure 2.21 Compressive modulus and density of PVA-clay aerogel while using gamma irradiation [63]

2.4.3 Enhancing clay-polymer aerogels through natural fibres

Natural fibres have gained much attention recently to create natural reinforced composites due to their lightweight, non-toxic, low cost, biodegradable, nonabrasive and good mechanical properties, which makes them more attractive over other conventional reinforcement materials [145,146]. Many challenges arise when using natural fibres as a mean of reinforcements due to their large variation in properties and characteristics. The properties of a fibre reinforced composite can be directly influenced by the fibre type, source of fibre and processing method [147]. Many attempts have been reported to prepare natural fibre composites with a wide range of application [148]. However, the studies of implementing natural fibres to produce clay aerogels are limited even though that it could lead to environmentally robust and sustainable materials. Several fibres, such as silk, soy silk and hemp fibres have been attempted by using an environmentally freeze-drying process to create polymer-natural fibre-clay hybrid composites [62]. A composition of clay 5 wt.%,

PVA 2.5 wt.% and fibre content varying from 0 to 5 wt.% have been investigated. It was found that the fibres had a minimal effect on the “house of cards” structure where the fibres span across the laminar structure (Figure 2.23B) connecting the clay platelets together by creating long struts (2mm length of fibre used). The density of the hybrid aerogels ranged from 0.077 to 0.121 g/cm³. The fibres are capable of reinforcing the aerogels. At the highest fibre loading for silk, soy and hemp, the density were recorded at 0.012, 0.093 and 0.093 g/cm³, respectively, and the compressive modulus reached up to 8900 kPa (Figure 2.22), which is an almost 5 fold increase compared to the clay-PVA aerogels.

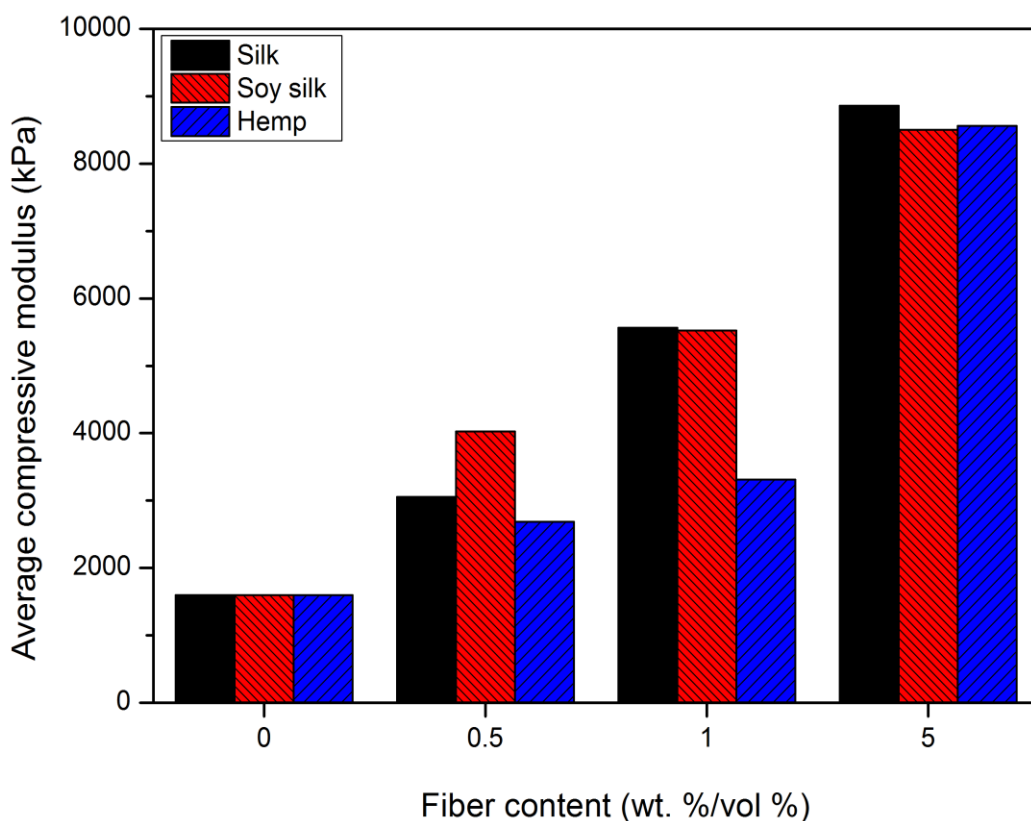


Figure 2.22 Compressive moduli vs type of natural fibres [62]

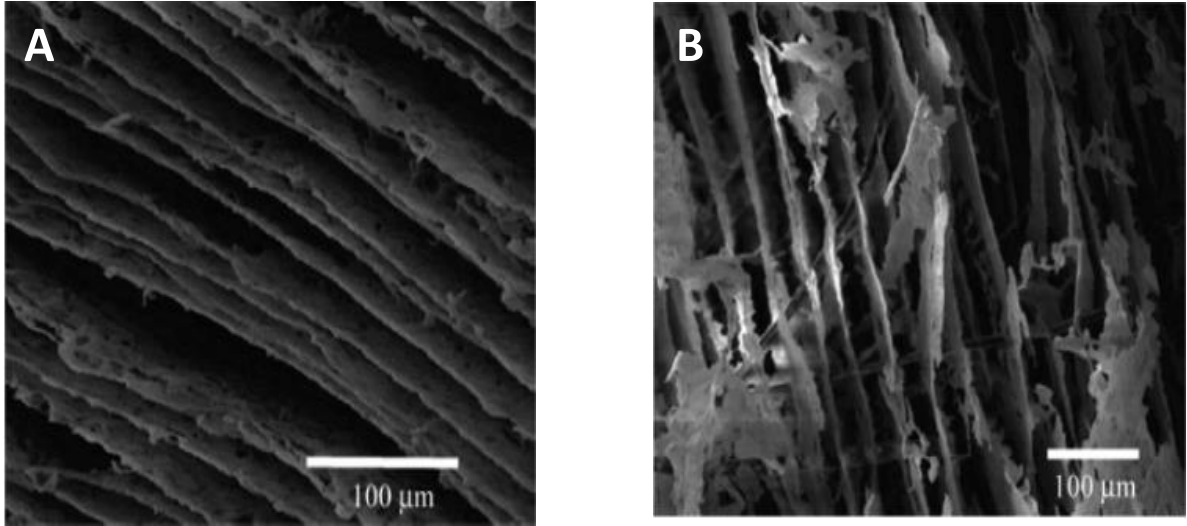


Figure 2.23 (A) Clay-PVA aerogel and (B) Clay-PVA aerogel that contains 1% hemp fibres [62]

It is apparent that the addition of the natural fibres did not significantly increase the density, and such the increase in the compressive modulus can be attributed to the fibre specific strength and stiffness [149], and the increased connectivity within the microstructure which is able to transfer the load more effectively. Average compressive moduli for fibre-reinforced clay aerogels without the addition of polymer are compiled (Table 2.7) in order to understand the effect of the fibre on the property of fibre reinforced aerogel. It can be seen that the addition of fibres even at low contents had a significant effect on the compressive modulus, although not as significant as PVA, did, while at 5 wt.% clay and 2.5 wt.% PVA had a compressive modulus of around 1600 kPa. This was almost what was recorded for the strongest composition of 5 wt.% silk and 5 wt.% clay. However, the addition of microcrystalline cellulose seems to have a negligible effect on the modulus, suggesting that the length of the fibres (2mm) is crucial in enhancing the mechanical performance, especially when dealing with clay fibre composites without the addition of polymer due to the non-existence of hydrogen bonding [150].

Table 2.7 Compressive moduli of fibre reinforced aerogel with 5 wt.% clay [62]

Fibre content	Compressive modulus (kPa)			
	Soy silk	Hemp	Silk	Microcrystalline cellulose
0	14 ± 8	14 ± 8	14 ± 8	14 ± 8
0.5	112 ± 14	65 ± 12	166 ± 20	7 ± 1
1	128 ± 18	179 ± 26	419 ± 46	-
5	473 ± 78	1292 ± 227	1771 ± 327	-

2.4.4 Enhancing clay-polymer aerogels through carbon nanotubes

Carbon nanotubes (CNT) exist in many forms and are of great interest for many applications due to their geometry and unique combination of mechanical, thermal, electrical and optical properties [151]. They have been considered as an ideal reinforcing candidate for preparing nanocomposites [152]. Carbon nanotubes can exist in two forms, either as single-walled carbon nanotubes (SWCNTs) or/and multi-walled carbon nanotubes (MWCNTs) [153]. Recent advancement in the development of CNT composites have mostly focused on multi-walled carbon nanotubes (MWCNT) [154]. One of the main drawbacks of using CNTs is that they are difficult to manipulate and process, and the market price remains considerably high [57,155]. Single-walled carbon nanotubes (SWCNT) can be combined with an aqueous gel of Na⁺-MMT, and poly (acrylic acid) PAA to produce low-density polymer–clay–nanotube aerogels composites [115], by dispersing SWNT into an aqueous solution with the aid of polyelectrolytes (i.e., pH-responsive) in order to control the aggregation and dispersion of the nanotubes [156]. The carbon nanotubes showed a significant increase in the modulus of the PAA-clay aerogels, without altering the composites densities (Table 2.8). The aerogel composites with 0.05 wt. %SWNT were characterised with a lamellar structure similar to that of most other clay aerogels composites, indicating that the increase in the compressive modulus is mostly independent of a structural change where the increase can be attributed to the mechanical properties of the carbon nanotubes. The pH contributed directly to the effectiveness of the carbon nanotubes reinforcement as its effect of aggregation and dispersion (Table 2.8). It is apparent that

increasing the pH leads to an increase in the compressive modulus. This phenomenon is likely a result of the aggregation of large bundles of SWNT that are strongly networked together due to strong van der Waals forces [157], consequently resulting in better resistance to bending, and hence an increase in the stiffness over long distances, enhancement of the compressive modulus and overall mechanical performance of the aerogel composites. Furthermore, the addition of SWNT to the aerogel composite provided a method of tailoring the electrical conductivity of aerogels, due to their electrical properties [158], which opens a wide range of applications for these aerogel composites.

Table 2.8 Modulus and density of SWNT reinforced aerogel [115]

Sample	Modulus kPa w/ SWNT	Density g/cm ³ w/ SWNT	Modulus kPa w/o SWNT	Density g/cm ³ w/o SWNT
2.5% Polymer 5% clay pH=3	462 ± 77	0.05	259 ± 56	0.05
2.5% Polymer 5% clay pH=9	628 ± 126	0.04	163 ± 34	0.05
0.5% Polymer 5% clay pH=3	79 ± 5	0.03	30 ± 3	0.03
0.5% Polymer 5% clay pH=9	373 ± 15	0.03	43 ± 9	0.04

2.4.5 Enhancing clay-polymer aerogels through laminating and dip coating

2.4.5.1 Dip coating

A commercially synthetic rubber coating (Liquid tape) has been attempted for clay-polymer aerogel composites [49]. The rubber coating not only meets the required performance but also has a rapid drying time, which is necessary to avoid the high absorption of the rubber by the pores of the aerogel and allows for ease of application. For example, epoxy-clay aerogel, as discussed in Section 2.4.2.1, was dip coated in the liquid rubber and dried overnight to produce a uniform rubber coat of about 0.38 mm (Figure 2.24). It was reported that visually the initial properties of the coated aerogels significantly improved compared with the plain uncoated original clay aerogels.

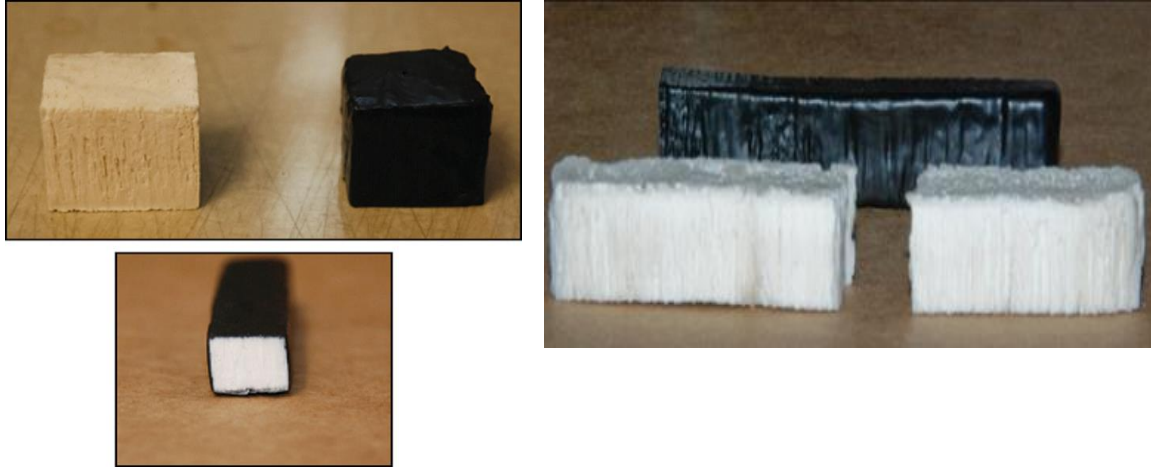


Figure 2.24 Aerogels with coatings applied: top= cube-shaped aerogel before and after coating and a bottom=cross section of the aerogel after coating [49]

Due to the fact that the samples had an average coat of only 0.38 mm, the coating had a direct effect on the density; the average density of the cube cut rose from 0.22 to 0.35 g/cm³, while the smaller rectangular samples rose from 0.24 to 0.39 g/cm³. The working modulus for the coated materials has almost doubled from 3.2 to 6.4 MPa and toughness almost increased by a factor of two from 5.2 to 9.2 MPa. Flexural testing (bending) of unreinforced clay aerogels is rather difficult and is usually unreported in the literature. Due to weak cohesion and bonding between the layers, samples tend to break at relatively low strain, which cannot be even recorded unless very sensitive equipment is used. However, the coated aerogel seems to significantly outperform the original aerogels, with an increase in the flexural modulus from 0.82 (uncoated) to 17 MPa. The yield strength raised from 0.95 to 15 N, reflecting it as an efficient method to increase the mechanical properties.

2.4.5.2 Glass fibre laminating

The process of laminating clay aerogels using glass fibres has been described as the most reliable reinforcing method for reinforcing composites [159,160]. The laminates could typically be fabricated by laying a sheet of glass fabric, following the addition of the suspension which is then subjected to

freezing. Different numbers of layers may be used (Figure 2.25). The polymer-clay aerogel-glass fibre laminates significantly increased the flexural moduli compared to polymer-clay aerogels; both epoxy and Poly(amide-imide) core clay-glass fibre laminates found more than a 10 fold increase in the flexural modulus [160]. An important factor in determining the strength was the epoxy system. The epoxy adhesive also played a role in influencing the peel strength with a direct relationship between the epoxy adhesive uptake and the peel strengths. Also, the compressive modulus seemed to decrease as the amount of epoxy increased.

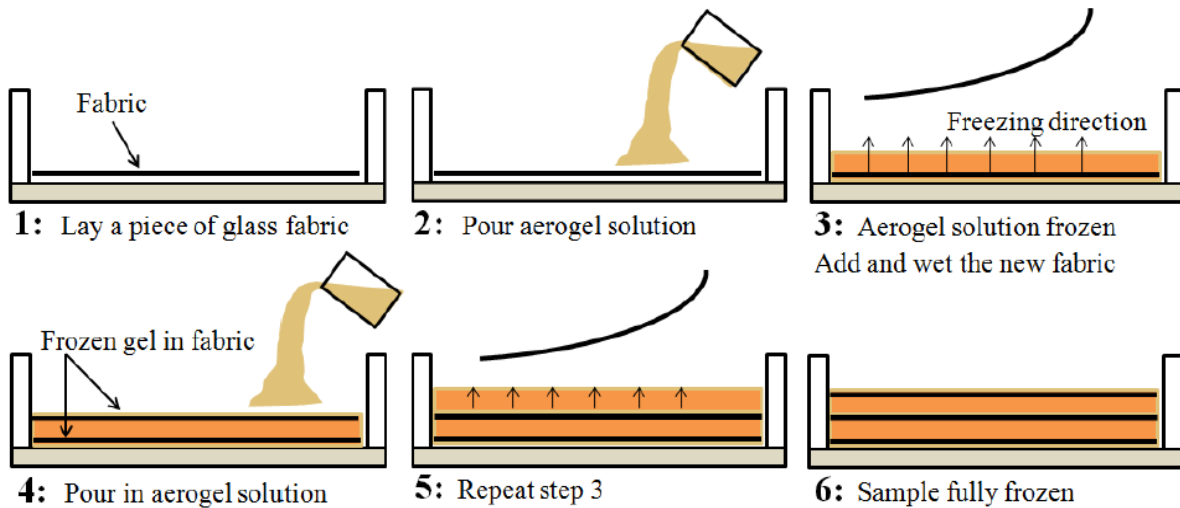


Figure 2.25 Schematic of glass fibre aerogel fabrication[160]

2.5 Physical properties of clay aerogels composites

In Section 2.4 it was established that one of the setbacks regarding clay aerogels is their poor mechanical strengths. However, it has been reported; that incorporating a reinforcing medium, such as polymers or other additives, is able to increase the mechanical strength comparable to that of petroleum-based foamed materials [15]. The process of producing clay aerogel has many variables, which once controlled or altered can have an impact on the final texture and properties of the aerogel composite. For example, the thermal and physical properties of the aerogel composite, to

a great extent, depends on the properties of the incorporated polymer which also gives rise to superior mechanical properties [15,54]. Clay aerogels are very versatile and can be manipulated suitable for many different industrial sectors. Therefore, the understanding and characterisation of the physical properties are critical for the classification of such materials for the intended uses. This Section (2.5) focuses on the different physical properties of clay aerogel composites and investigates how these properties are influenced by the microstructure, composition and processing parameters.

2.5.1 Thermal conductivity of clay aerogels

One of the most desirable properties for aerogels is their thermal property, which is seen as a pivotal characteristic in many applications, especially in the construction sector as an insulation material [10,21]. Heat flows between different objects and is an inevitable consequence at temperature gradient. Understanding how different materials emit and absorb heat is critical to identify efficient insulation materials for thermal comfort within a structure [1]. The heat flow within insulation materials is mainly governed by three components: conduction in the solid parts, conduction in gases and radiation through the pores [13], and the function of an efficient insulation material is to minimise the transport of heat through the three processes.

Clay aerogels have been proven to be effective thermal insulators, and are able to reduce heat flow due to their unique lamellar microstructures and achieve extremely low thermal conductivity, ranging between 0.015 and 0.05 W/(m.K) [20,119]. Figure 2.26 illustrates the heat flow within an aerogel where the solid conduction within the 3-dimensional network is limited due to high porosity and low densities, while the nature of the 3-dimensional network structure creates a tortuous path for gas molecules to pass through the material, thus limiting gas conduction. The least significant contribution of thermal conductivity within an aerogel, at low temperatures, involves radiation,

which is also influenced by the thickness of the material. However, this could become more dominant at higher temperatures [140,161,162]. Subsequently, the interaction of the three modes of heat transfer of convection, conduction and radiation determines the overall effectiveness of the aerogel as an insulation material.

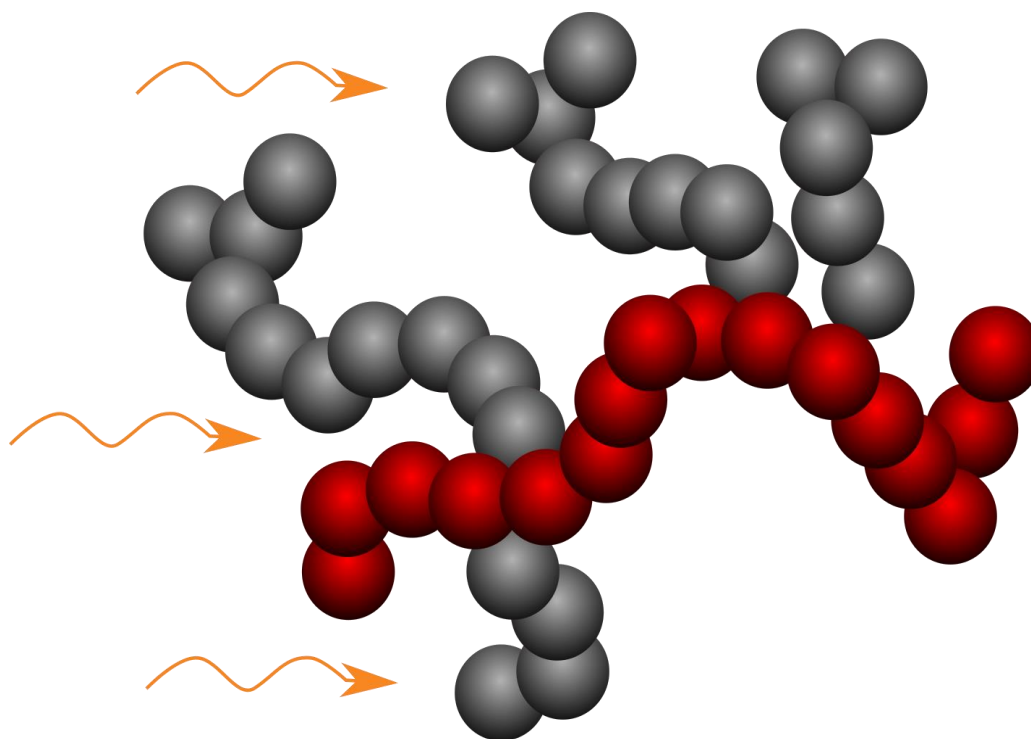


Figure 2.26 Representation of heat flow within an aerogel [10]

2.5.2 Effect of clay aerogel structure on thermal conductivity

The composition of the aerogel plays a direct role in influencing and controlling the morphology of the aerogel. A reliable method to effectively reinforce the clay aerogels has been through the addition of polymers, which has proven more effective than simply increasing the clay content, with an insignificant increase in density [14,82]. As discussed in Section 2.4.2.4, polyvinyl alcohol (PVA) is one of the most polymers used to prepare clay aerogel composites. The incorporation of PVA into clay aerogels was found to have an influence on the thermal conductivity of the clay aerogels and result in an increase in density from 0.050 to 0.068 g/cm³ [84]. It would be expected as with foamed

materials that increasing the density above a certain point can sacrifice the porosity and lead to a significant increase in thermal conductivity [82,163]; however, the thermal conductivity of the clay-PVA aerogel was unexpectedly lower than the specimens without polymer. This may be related to the structure architecture, in which the polymer created small struts between the clay layers resulting in a more complicated path for heat to flow through (Figure 2.27). Thus, the combination of clay and PVA is able to produce aerogels with a lower conductivity than either of its constituents (e.g. clay and PVA). In fact, the alignment of the aerogel structure may be one of the most decisive parameters that control the thermal conductivity [84]. The optimum structure of clay aerogel is in theory defined as parallel clay sheets connected through thin struts (Figure 2.27A). The orientation of the aerogel plays a vital role in its ability to conduct heat. Measuring the thermal conductivity perpendicular to the clay layers is more complicated with tortuous paths for the heat flow through both thin struts and air pockets. However, if the heat flows through an orientation where the clay layers are vertically aligned (Figure 2.27B), and the heat flow is perpendicular, the heat will flow uninterrupted along the entire sheets, with minimum effect from the thin struts between the layers.

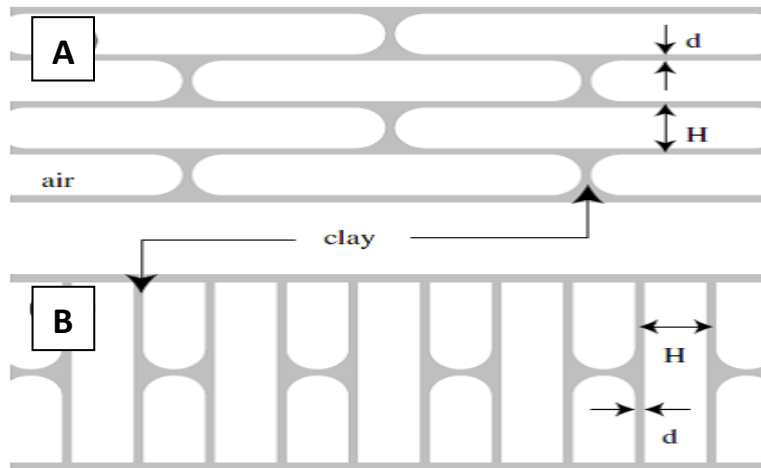


Figure 2.27 Structure of the aerogel (A) horizontally aligned and (B) vertically aligned [84]

The structure and morphology of the clay aerogel can be controlled via the freezing method. The frozen method may be altered between vertical frozen, horizontally frozen and controlled nucleation points [50]. The vertical frozen sample exhibited the highest thermal conductivity due to the continuous path (Figure 2.28A), the controlled nucleation had a lower thermal conductivity due to a more torturous architecture (Figure 2.28B) and the horizontally frozen aerogel did not show a significant reduction in thermal conductivity (Figure 2.28C). However, in all three scenarios, an ideal layered structure in which the layers are oriented normal to the heat flow direction as illustrated in Figure 2.28C (top) could not be achieved.

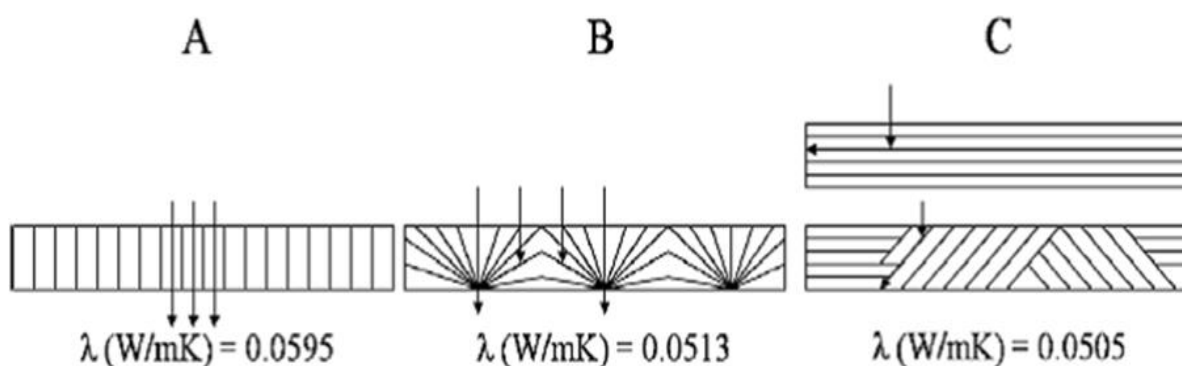


Figure 2.28 idealised heat flow through the samples prepared via directional freezing (A) vertical, (B) controlled nucleation points and (C) horizontal freezing [50]

Open cell foams in which the microstructure consists of interconnected cells have been widely used in many applications as they provide excellent energy absorption characteristics while retaining low densities [164]. The transformation of the well-known “house of cards” structure (Figure 2.29A) of clay aerogels composites into an open cell structure was attempted by the incorporation of air bubbles with the aim to lower thermal conductivity [65]. The air bubbles were induced via high-speed mixing and stabilised by controlling the viscosity. The addition of metal ions and xanthan gum has been proven effective to stabilise suspensions and emulsions and increase viscosity [165].

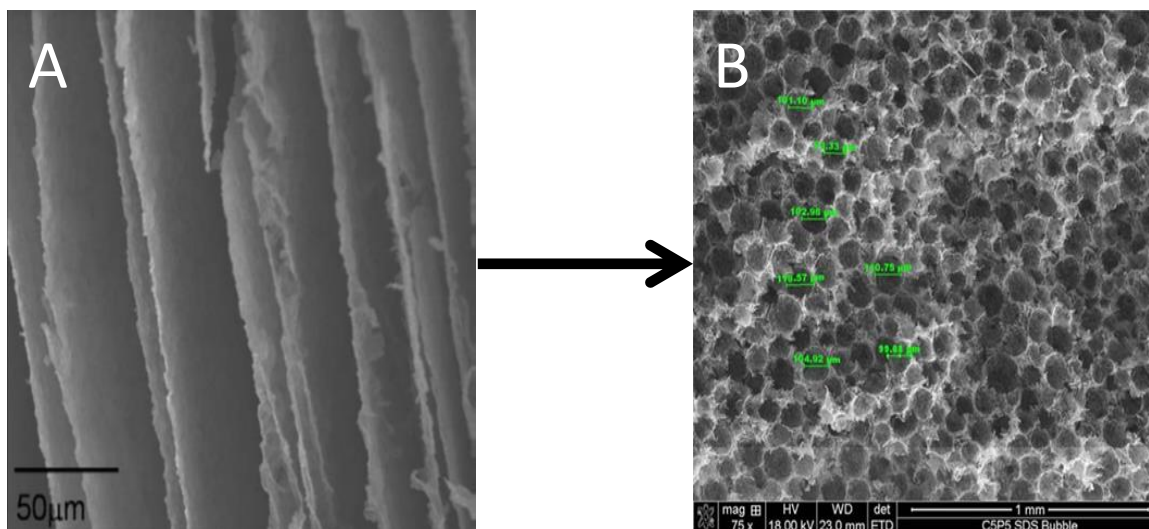


Figure 2.29 (A) House of cards structure and (B) Open cell structure [65]

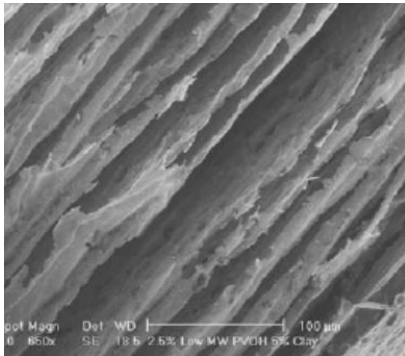
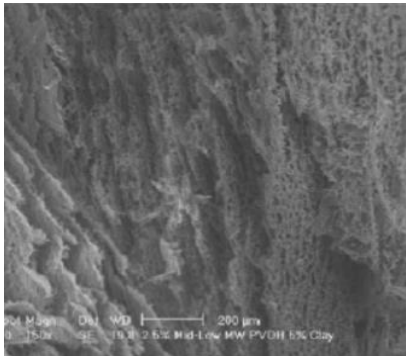
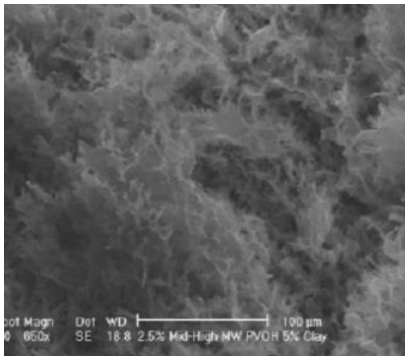
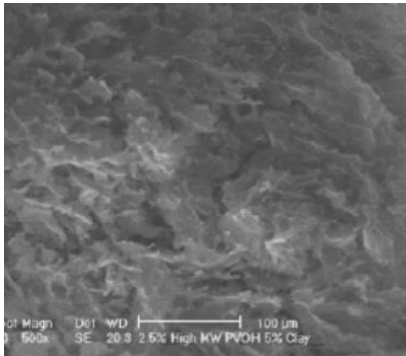
The transformation of clay-PVA “house of cards” structure to an open cell structure with uniform diameters of around 100 μm was achieved (Figure 2.29B). The stability and size of the induced bubbles were dependent on the viscosity, thereby increasing the viscosity by increasing the charge of the metal ions and the addition of xanthan gum, smaller air bubbles can be obtained due to higher shear stress [166].

To ensure a uniform distribution of the air bubbles across the aerogel composite and avoid agglomeration, the surfactant sodium dodecyl sulfate (SDS) was used, as it can lower surface tension and increase the frequency of the bubbles [167]. By inducing the air bubbles within the aerogel structure, the heat flow through the continuous phase may be limited (Figure 2.29B). The thermal conductivity was reduced by 22% from 0.052 to 0.042 $\text{W}/(\text{m}\cdot\text{K})$ for samples containing 5 wt.% clay and 5 wt.% PVA. It should be noted that although the overall bulk densities increased from 0.055 to 0.083 g/cm^3 when introducing the bubbles, as the extra additives are required to stabilise the bubbles, the most effective composition was reported at 5 wt.% clay 5 wt.% poly (vinyl alcohol), 0.5

wt.% xanthan gum, 0.5 wt.% sodium dodecyl sulfate (SDS) and 0.2 wt.% aluminium sulfate. This is an effective method able to reduce thermal conductivity by up to 20%.

2.5.2.1 Effect of polymer loadings on thermal conductivity

Table 2.9 Thermal conductivity, molecular weight and structure of PVA-clay aerogels [139]

Molecular Weight	13-24 KD	31-50 KD
Thermal conductivity (W/(m.K))	0.023	0.022
Structure		
Molecular Weight	85-124 KD	146-186 KD
Thermal conductivity (W/(m.K))	0.019	0.017
Structure		

The molecular weight of a polymer can influence the rheological properties, electrical conductivity, dielectric strength and surface tension [168]. The effect of the molecular weight on the thermal conductivity of clay-PVA aerogel composite was investigated [50,139]. It would be expected that increasing the molecular weight would increase the thermal conductivity due to an increase in density. However, it was observed that the thermal conductivity decreased as the molecular weight increased (Table 2.9). At low molecular weights (13-50 KD), the laminar structure was maintained,

while at higher molecular weights (85-186 KD) the structure transformed to a more distorted structure with a higher number of junctions. This means providing more paths for thermal energy to dissipate before travelling through the entire sample. Therefore, the heat flux density and recitative index are reduced. Meanwhile, complicating the path, in that the phonons velocity is reduced could result in a lower thermal conductivity [169].

2.5.2.2 Effect of coating and lamination on thermal conductivity

Rubber coating systems have been increasingly used to overcome the mechanical and physical properties of nanocomposites [170]. Rubber coating (Liquid tape) has also been attempted to enhance the mechanical properties of clay aerogels [49]. However, the increase in the mechanical strength can come at the expense of its thermal properties. Even though the coating thickness is small, approximately 0.38 mm (Figure 2.24, Section 2.2.5.1), it had an impact on the thermal conductivity where around 10% increase was witnessed (Figure 2.30).

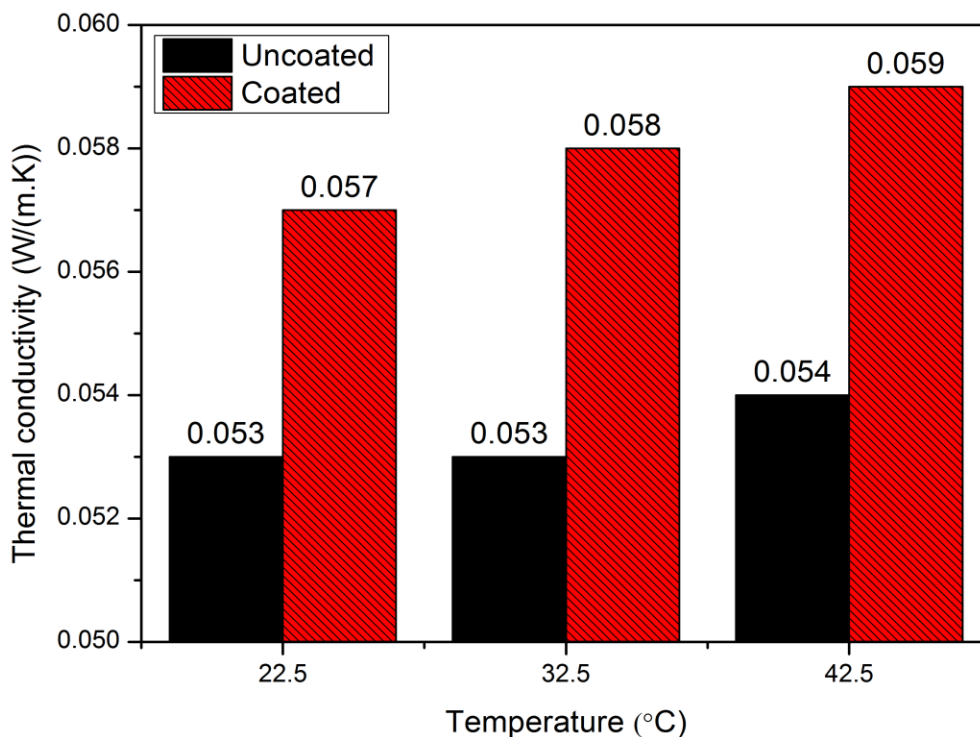


Figure 2.30 Thermal conductivity of coated/uncoated aerogel composites [49]

The increase could be attributed to the rubber filling the pores and gaps within the aerogel, thus creating a more connected structure for heat to flow through the aerogel uninterrupted. The use of a lamination system with fiberglass to reinforce the aerogel [160] has less impact on the thermal conductivity, although the values for glass fiber laminated aerogels was not reported, a conclusion can be drawn from the fact that the implementation of glass fiber into composite would show no significant increase in the thermal conductivity due to their low thermal conductivity and the resin may only be responsible for an increase in thermal conductivity [171].

2.6 Combustion behaviour of aerogels

Fire protection is one of the most important parameters for materials in construction. When designing and developing new materials such as clay aerogels, their fire performance has to be tested to determine how they would behave in a fire scenario and whether they meet specific standards of their intended applications. A cone calorimeter test is one of the most common methods used to understand how a material will behave under an actual fire scenario, especially when polymeric materials are being used [172]. The test consists of two parts: the test firstly covers the ignition of the material and followed by subsequent flaming combustion. The ignition measures the time required for ignition, which depends on several factors such as the critical heat flux, thermal inertia and critical mass loss for ignition, or the critical surface temperature for ignition [173]. The outcomes from the cone calorimeter generates a set of properties which include mass loss, HRR (heat release rate), THR (Total heat release), smoke production, CO₂ production, (FIGRA) fire growth rate index, (THE) total heat evolved as time to ignition (TTI), peak of heat release rate (PHRR), total heat release (THR), time to peak of heat release rate (TTPHRR) and fire growth [174,175].

2.6.1 Combustion behaviour of PVA/clay Aerogels

PVA is a highly flammable polymeric material and needs to be modified to meet the fire performance requirements of the intended application [176]. In order to overcome the flammability of PVA in clay aerogel composites, fire retardant agents, such as aluminium hydroxide ($\text{Al}(\text{OH})_3$), ammonium polyphosphate (APP), potassium carbonate (PC) and silica gel (SG), were used to prepare clay aerogel composites [177]. Flame retardants act either in the vapour phase or in the condensed phase through a chemical and/or physical mechanism which interferes with the combustion process during heating, pyrolysis, ignition and flame spread [178]. The burning parameters (Table 2.10) suggest that the addition of flame retardant agents can be an effective way to enhance fire performance. The additives are shown to be effective as FIGRA is reduced compared to the control sample. The most significant reduction is for samples containing aluminium hydroxide ($\text{Al}(\text{OH})_3$) (5P5C5Al(OH)₃), and ammonium polyphosphate (APP) (5P5C2APP) where (FIGRA) decreased to 0.5 and 0.4 respectively from an original value of 2.0 (W/s) (Table 2.10). It should also be noted that the clay aerogel composites performed better than traditional EPS foams which have a reported FIGRA value of around 5.7 [179].

Table 2.10 Burning parameters of clay-PVA aerogels with/without flame retardant agents [177]

Sample	PHRR(kW/m ²)	THR(MJ/m ²)	TTPHRR(s)	FIGRA(W/s)	Residue (%)
5P5C	182	9.0	9	2.0	61.9
5P5C5Al(OH) ₃	122	8.6	27	0.5	65.7
5P5C2APP	115	12.3	30	0.4	57.4
5P5C0.5SG	168	9.2	12	1.4	61.1
5P5C0.5SG0.3PC	174	9.3	24	0.7	59.1
5P5C1SG	179	6.8	15	1.2	65.7
5P5C1SG0.6PC	191	6.7	12	1.6	62.8

2.6.2 Combustion behaviour of irradiated crosslinked clay-PVA aerogels

The fabrication of PVA-clay aerogel composites by an environmentally friendly freeze-drying process followed by cross-linking induced by gamma irradiation without any chemical additives can result in aerogels with superior mechanical properties (Section 2.4.5.4), but can also influence the combustion behaviour of the composite [63,176]. The combustion behaviour reported for the crosslinked PVA-clay aerogels (Table 2.11) shows that the time to ignition (TTI) is considerably low (<5s), which is common when it comes to polymeric foamed materials [180], a longer TTI indicates slower flame spread and less flammable material. The gamma irradiation showed no significant enhancement to the combustion behaviour.

Table 2.11 Burning Parameters of gamma-irradiated clay-PVA Aerogels [63]

Sample	TTI(s)	PHRR(kW/m ²)	TTPHRR(s)	THR(MJ/m ²)	FIGRA(W/s)	TSR(m ² /m ²)	Residue (%)
P5C5-0	4	140.1	15	18.5	9.3	139.6	78.7
P5C5-30	5	137.1	20	16.3	6.9	182.3	76.4
P2C8-30	2	73.8	15	2.5	4.9	25.5	90.5
P1C9-30	No flame	10.7	15	0.26	0.7	15.0	94.1

The dominant parameter in determining the combustion behaviour could be the clay to PVA ratio, as PVA is the only fuel in the aerogel. Increasing the clay content and reducing the polymer content could lead to a significant decrease in the heat rate release value (HRR) and the heat fire growth index (FIGARA) (Table 2.11). No fire was observed during the entire testing period for sample of 1 wt. % PVA and 9 wt.% clay subject to 30 kilogray of gamma radiation (P1C9-30), while retaining a much higher weight residue (Figure 2.31).

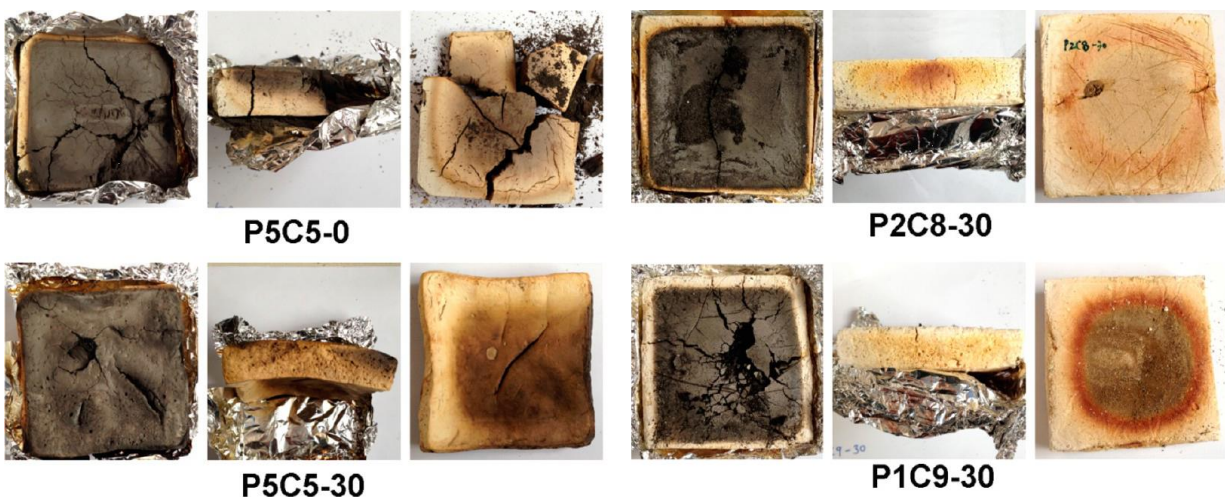


Figure 2.31 Irradiated crosslinked clay-PVA aerogel residues after burning in cone calorimeter [63]

The total smoke release (TSR) significantly decreases as the clay content increases (Table 2.11), which increases the safety aspect of the clay aerogel, because the smoke has been considered in the construction industry more lethal than the actual fire due to the release of toxins, such as hydrogen cyanide and inorganic acids [181].

2.6.3 Combustion behaviour of alginate-clay aerogels

Alginate is natural, renewable polysaccharide mostly extracted from seaweed and has gained attention due to its hydrophilicity, nontoxicity and biocompatibility [182]. It has been used to prepare hydrogels at mild temperatures and pH and is mostly used for the immobilisation of living cells such as yeasts and other gel-like products within the food industry [183,184]. Studies have shown that alginate fibre can effectively hinder smoke generation and provide good thermal properties [185]. The use of ammonium alginate to produce clay aerogel composite has been attempted, and the combustion performance of the developed aerogel was determined [179]. Based on the reported fire parameters (Table 2.12), the time to ignition (TTI) of alginate is around 10 times more than the EPS, which indicates that the alginate aerogel has a slower flame spread and is a less flammable material. The addition of clay to alginate resulted in no flames during the

entire test and further prolonged the burning time and time to peak of heat release rate (TTPHRR). This composition also resulted in a reduction in the flame spreading rate and prevented complete combustion. The residue of 5 wt. % alginate and 5 wt. % clay aerogel (5A5C) was 53.1% compared to 3.3 % that of pure alginate aerogel. Therefore, it can be concluded that the clay serves as heat and mass transport barriers and enhances the combustion behaviour of clay-alginate aerogels composites.

Table 2.12 Burning parameters of clay-alginate aerogels [179]

Sample	Mass(g)	TTI (s)	PHRR(kW/m ²)	THR(MJ/m ²)	AHR(MJ/kg)	TTPHRR(s)	FIGRA(W/s)	Residue (%)
EPS	2.5	9	256	9.1	36.0	45	5.7	8.6
A5	10.8	96	64	13.2	12.2	38	2.6	3.3
A5C5	21.8	No flame	32	12.0	5.5	45	0.7	53.3
A15	32.5	220	99	41.0	12.6	288	0.3	3.1

2.7 Thermogravimetric analysis (TGA) of clay aerogels composites

Thermogravimetric analysis (TGA) is an analytical technique used to investigate a material behaviour at elevated temperatures, in which the mass of the sample is recorded against time or temperature [186-188]. TGA can provide information concerning both physical and chemical properties of the aerogel composite, and be used to determine kinetic parameters, compositional behaviour and thermal stability. Knowing the ability of a material to maintain its properties as nearly unchanged as possible on heat is critical in determining the temperature ranges in which the material can be used [189,190]. Extensive studies have been carried out for clay nanocomposites, and the addition of clay as nanofiller has proven an effective method to enhance thermal properties [191,192]. Clay aerogel composite with different polymers including polyvinyl alcohol (PVA), casein, pectin and polyimide (PI) have been investigated through thermogravimetric analysis, which provides important numerical information such as the 5% weight loss temperatures (T5%), weight residues (WR), and

the maximum weight loss rates (dm/dT_{max}). It was consistent within the different clay aerogel composites that the decomposition occurred at two stages [109,119]. The first stage can be associated with the removal of absorbed or bond water, and this stage can be observed roughly at around 5% weight loss. The second stage is usually associated with the polymer degradation. However, the polymer functional groups can significantly influence the first stage, for instance, the free water from clay-cellulose aerogels could be removed from room temperature to 300°C [80], while clay-polyvinyl alcohol aerogels witnessed this phenomenon from room temperature to 150°C. This difference could be related to the high number of acetate groups in 98-98 hydrolysed PVA which results in a high hydrogen bonding, while the nature of the hydroxyl groups in unmodified cellulose results in lower hydrogen bonding (i.e. less hydrophilicity) [193]. The second stage of decomposition could be attributed to the thermal stability of the polymer incorporated in the aerogel, for instance polyimide clay aerogel composites recorded the highest 5% decomposition temperature and the highest weight loss temperature at 508 and 608°C respectively which can be related to nature of the insolubility of the polyimide as well as its excellent thermal and thermo oxidative stability [194]. Therefore, this composition has great potential in high-temperature applications. The addition of clay or increasing the clay content may make the first stage of decomposition of clay aerogel, which is associated with moisture loss, more evident and clear due to the highly hydrophilic nature of the clay [195]. A comparison of aerogel with and without the addition of clay shows a reduction in the temperature of the 5% weight loss but increase in the highest weight loss temperature and percentage of residue while decreasing the maximum weight loss rate. This may be due to the presence of the lamellae clay and such resulting in an increase in the diffusion path of oxygen [196]. This phenomenon has been consistent within clay aerogel composites, demonstrating that the addition of clay increases the thermal stability [12,58,60,70,197].

2.8 Liquid absorption of clay aerogel composites

Water soluble polymers and clay can be combined to create mechanically robust structures that have a great value in many applications. Clay aerogels can be produced through a freeze-drying process that can absorb both water and ionic solutions, but will not completely decompose or distort when saturated. The ability to modify the incorporated polymers in clay aerogels, such as Poly (vinyl alcohol) (PVA), poly (ethylene glycol) (PEG), poly (ethylene oxide) (PEO), enables the possibility of creating a wide variety of absorbent aerogels [198]. The process of producing clay aerogels usually involves the use of water-soluble polymers and hydrophilic sodium montmorillonite (Na⁺-MMT) to create an aqueous solution [199]. Therefore it can be expected that the dried structure will then also absorb water. Figure 2.32 is a representation of how the water flows within the aerogel structure, where it is believed that the liquid transports via capillary action into the space between each layer (capillary uptake) (Figure 2.32A) followed by absorption of the liquid into the hydrophilic materials, which make up the layers (Figure 2.32B). The absorption of the liquid can also be related to the structure. The more the lamellar the structure is, the easier it is for the liquid to flow. However, a less defined structure would create a more tortuous path for the liquid to pass through. The absorbed water can cause the polymeric structures to turn soft and lose its mechanical properties, as the dissolution of polymers and clay is typically held together by physical or chemical crosslinks.

Table 2.13 Physical characteristics of aerogel [198]

Sample	Structure	Density g/cm ³	Void Volume %	Void volume filled %
5% Clay 1% poly(acrylic acid)	random	0.054	97.37	31.84
Fired 5% Clay aerogel	lamellar	0.060	97.69	85.98
5%Clay 5% PEG 35K	lamellar	0.080	94.46	26.47
5%Clay 10% PEG 4600	lamellar	0.122	91.36	28.46
5% Clay 10% PVA	random	0.124	91.83	49.01
5% Soy-Silk 2.5% PVA 5% Clay	random	0.128	91.96	85.91
5% Clay 10% PEO	lamellar	0.134	90.48	28.73
10% Clay 20% PVA	random	0.340	77.64	70.84

While the absorption of aerogel is considered a disadvantage for its use in some industrial sectors, such as construction insulation, it is considered a great potential as absorbents. Materials which are biodegradable, porous and have a high uptake capacity are potential candidates for oil/water separation [200,201]. The voids and excellent network system play an important role in the clay aerogel to absorb water [103]. The void volume percentage could theoretically be equivalent to the maximum amount of liquid that can be absorbed by the aerogel without distortion (Table 2.13). However, this could also be related to other parameters, for example, Table 2.13 shows that the majority of the aerogels absorb less than 50% of the void volume, but the ceramic structured or fibre reinforced aerogel could absorb water more than 50% their void volume. This proves difficult to relate the structure to the absorption properties because of the different compositions used, which may result in different densities and shadow the impact of the structure.

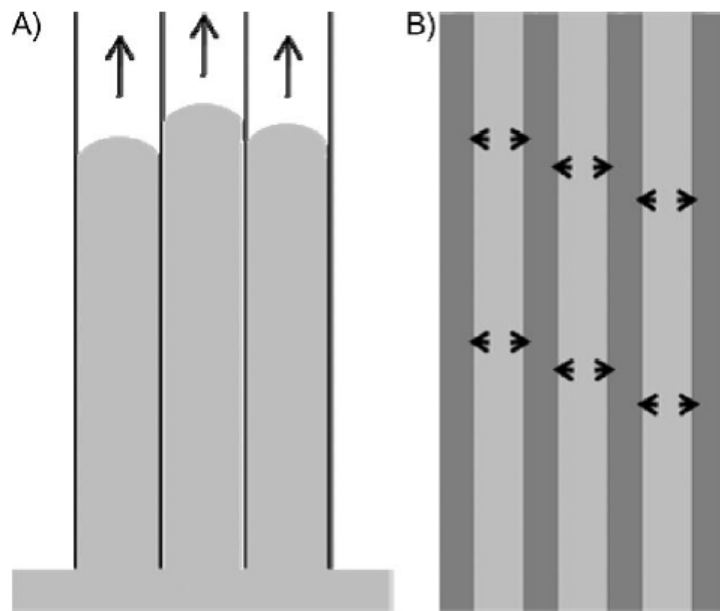


Figure 2.32 Proposed water absorption mechanism (A) Capillary filling of the voids (B) Followed by absorption by the surrounding hydrophilic material [198]

A more clear relationship could be established between the density and rate of absorption. It was witnessed that low-density aerogel absorbed liquids faster than high-density aerogel. However, it was found that both high density and low-density aerogel retained little structural integrity and lacked mechanical properties when saturated. In order to produce stable saturated structures that are able to absorb liquids rapidly, the clay aerogel could be combined with fibres or fired into ceramics.

Temperature-responsive polymers have also been reported as materials that could change their physical properties across a range of temperatures, such as their water vapour transmission rate [202]. The change in the physical properties is usually related to the crossing of the transition temperature in the material, such as the glass transition temperature [203]. Combing a thermo-responsive polymer Poly (N-isopropyl acrylamide) (PNIPAAm) with clay to prepare an aerogel composite has been attempted by using ethylene glycol dimethacrylate (EGDMA),

methacryloxypropyl polysilsesquioxane (POSS), and (Ebecryl 860) epoxidised soybean oil acrylate as crosslinking agents [104]. Thermo-responsive Poly (N-isopropyl acrylamide) (PNIPAAm) was chosen due to its swelling abilities and mechanical properties [204]. The phase change from hydrophilic to hydrophobic is usually witnessed around 31°C, mainly due to intermolecular interaction within the solute polymer molecule chain, resulting in a lower critical solution temperature (LCST) [205].

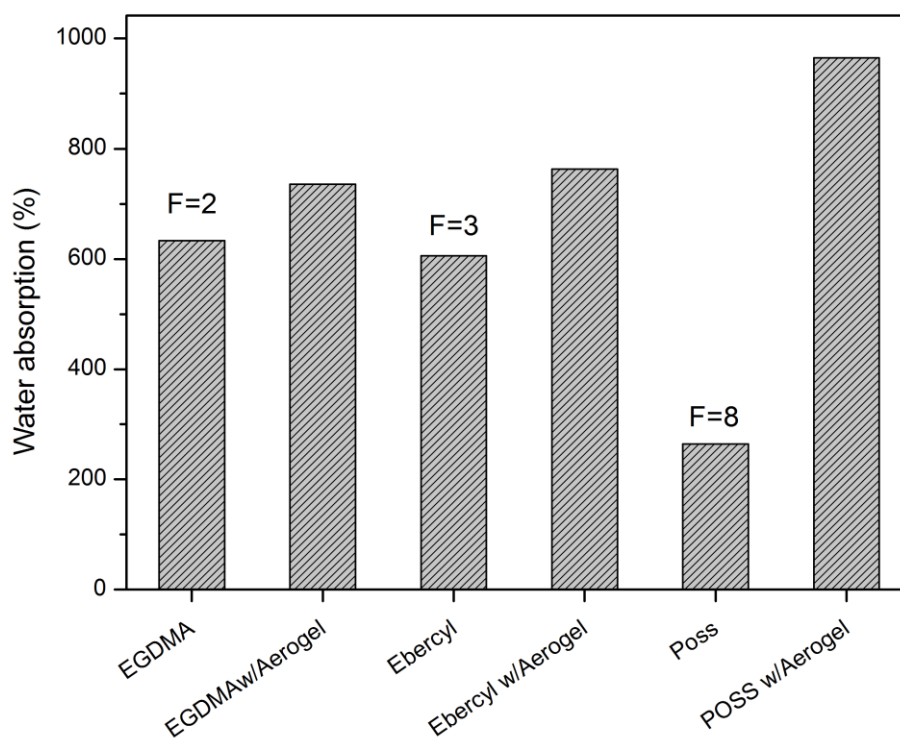


Figure 2.33 Water absorption of crosslinked clay aerogel composites [104]

The amount of water absorbed by the polymer seemed to be dependent on the functional groups (f) of the crosslinking agents, having higher functional groups resulted in a decrease in water absorption due to an increase in crosslinking density (Figure 2.33). Note the amount of crosslinker was kept constant at 10 wt.%. The final aerogel composite which incorporated the crosslinked PNIPAAm had little effect on the water uptake when using crosslinking agents of low functionality

($f=2$) and ($f=3$) the main water uptake can be related to the hydrophilicity of the clay and porosity of the aerogel composite, while when a crosslinker agent of higher function groups ($f= 8$) a 4-fold increase in water absorption is witnessed for the aerogel composite (Figure 2.33). Due to the biodegradability of such systems, absorbent compositions are useful for absorbing liquids, such as animal waste especially urine, chemicals such as gasoline, motor oil or other fluids [206].

2.9 Interim conclusions

A comprehensive review of clay-aerogels and its composites has been carried out. Many attempts, i.e. enhancing clay aerogel with various natural and synthetic polymers; reinforcement of clay-polymer aerogel with carbon nanotubes, natural fibres, glass fibre lamination and dip coatings, have been taken and/or proven to enhance the mechanical properties, especially the compressive modulus of clay aerogels while retaining very low densities. The most successful method demonstrated was the incorporation of a water-soluble polymers such as PVA to create a water-based suspension that can go through the freeze-drying process. Reinforcing aerogel composites with fibrous materials had also generated significant effects on the performance of clay aerogels. Clay aerogel composites have been characterised with good physical properties. Their physical properties could be influenced by processing parameters and with the addition of polymers or different additives. The aerogel structure showed to be the most decisive characteristic that influences the thermal conductivity whereby adding PVA; the structure became more capable of dissipating heat due to a more complicated path which could be further influenced by using PVA of a higher molecular weight. Controlling the processing parameters to induce air bubbles in the initial mixture to transform the “house of cards” structure to an open cell structure indicated the effectiveness in reducing thermal conductivity by up to 20%. The clay aerogel composites, in general, had good fire retardant properties due to the nature of clay and the only fuel content from

the integrated polymer, however, this could be further enhanced by the addition of various fire retardant additives. Increasing the clay content resulted in overall better thermal stability, and the integrated polymer within the aerogel could have an influence on the initial weight loss as well as the maximum weight loss rate. The hydrophilic nature of clay and the high porosity of the final aerogel composite nurtured these materials high ability to absorb liquids. Therefore, by implementing or modifying the correct polymer, these materials could be tailored to provide a rapid uptake of aqueous liquids, while maintaining structural integrity when saturated. An incorporation of thermo-responsive to produce clay aerogel composites could also result in an increase in water absorption. This Chapter indicates great potentials for possible development of this low cost, environmentally friendly aerogel material with many desired performance for many industrial sectors.

Chapter Three: Materials, methodology and characterisation

Abstract

This Chapter provides the specifications of the raw materials used throughout the study, including clay minerals, polymers, crosslinkers, and water-repellents. The methodologies of producing clay aerogel composites through an environmentally freeze-drying process are comprehensively explained and illustrated. Testing and characterisation procedures and standards are thoroughly reported.

Highlights:

- Temperature-induced aerogel composites;
- Organoclay aerogel composites;
- Crosslinked aerogel composites;
- Water repellent aerogel composites;
- Crosslinked-water repellent aerogel composites.

3.1 Materials

3.1.1 Smectic clays (Inorganic fillers)

Natural occurring and unprocessed clay, Sodium bentonite (50% SiO₂, 10.53% Al₂O₃, 3.21% Fe₂O₃, 0.43% TiO₂, 3.5% 2CaO, 13.44% MgO, 0.07% P₂O₅, 2.53% Na₂O, 1.21% K₂O) (75.2 meq/100g CEC, 90% of the dry particles < 28 μm, swell index = 23 ml/2g, and real density = 2.2 g/cm³) was obtained from Tubofuro, Portugal (Chapter 6).

Hydrophilic bentonite (Nanoclay) (9.98% Al³⁺, 20.78% Si⁴⁺, 4.10% H⁺, and 65.12% O²⁻)(145 meq/100g, montmorillonite ≤ 25 micron, swell index = 38 and real density = 0.85 g/cm³) was purchased from Sigma Aldrich (CAS number: 1302-78-9) (Chapters 4-5 and 7-9).

3.1.2 Polymers

3.1.2.1 Matrix

Polyvinyl alcohol (PVA) [-CH₂CHOH-]_n (Figure 3.1) 98+% hydrolyzed with a molecular of 146,000-186,000 and a density of 1.19-1.31 g/cm³ with a melting point of 200°C was purchased from Sigma Aldrich (CAS Number 9002-89-5).

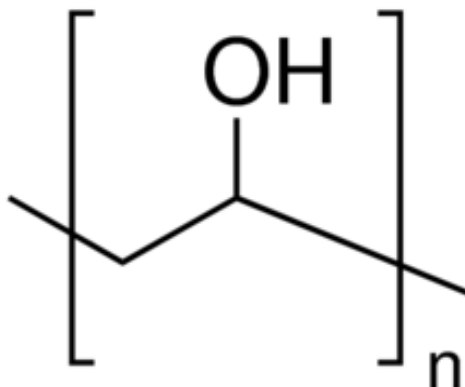


Figure 3.1 Chemical structure of polyvinyl alcohol (PVA)

3.1.2.2 Water repellants

Fluoropolymers

Water-dispersible C6- Fluoroalkyl acrylate (WDisRep 3™), solid content: 30%, cationic (pH 2.5-5) was supplied by a commercial chemicals company (Chapter 8-9).

Water-dispersible C2-C4 Fluorochemical (WDisRep 4™), solid content: 25%, cationic (pH 5-6) was supplied by a commercial chemicals company (Chapter 8).

3.1.3 Resins

A combination of melamine resins with paraffin waxes (Solid Content 25%) (WDisRep1™), solid content 30%, Cationic (pH 3.5 - 4.5) was supplied by a commercial chemicals company (Chapter 8).

3.1.4 Crosslinkers

Water-dispersible aliphatic polyisocyanate (Wcro1™) (Figure 3.2), solid content: 76% was supplied by a commercial chemicals company (Chapter 7 and 9).

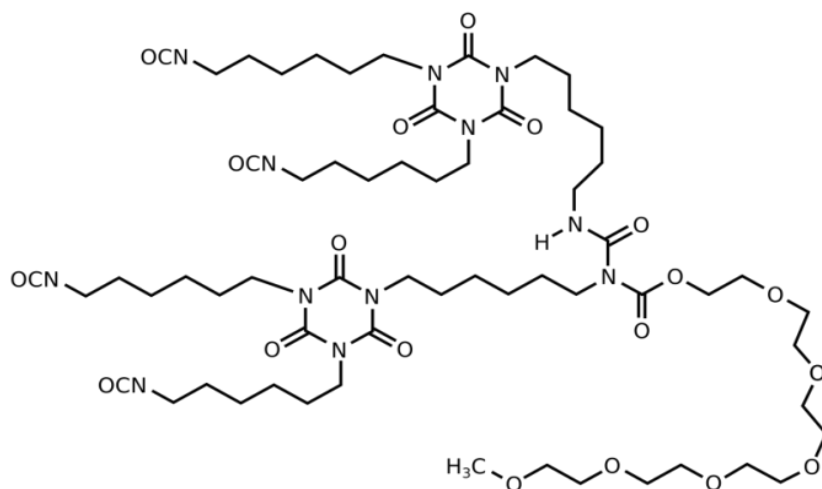


Figure 3.2 Chemical structure of aliphatic polyisocyanate (Wcro1™)

Water-dispersible 3-glycidoxypropyltrimethoxysilane (Wcro2™) (Figure 3.3), solid content: 100% was supplied by a commercial chemicals company (Chapter 7 and 9).

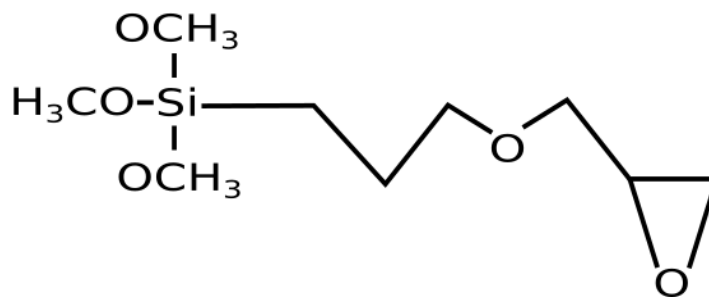


Figure 3.3 Chemical structure of 3-glycidoxypropyltrimethoxysilane (Wcro2™)

3.1.5 Quaternary ammonium surfactant

Hexadecyltrimethylammonium bromide $\geq 98\%$ ($\text{CH}_3(\text{CH}_2)_{15}\text{N}(\text{Br})(\text{CH}_3)_3$, solubility (100 mg/mL) (Mw 364.45), was purchased from Sigma Aldrich (CAS Number: 57-09-0)(Chapter 6).

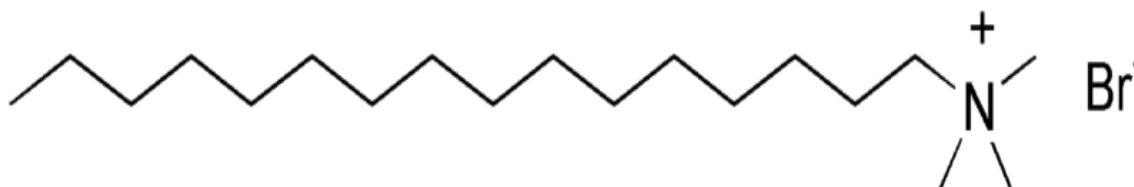


Figure 3.4 Chemical structure of Hexadecyltrimethylammonium bromide

3.1.6 Deionized water

Only water was used as a solvent in this study to prepare all solutions and suspensions. Deionized water was prepared through a Biopure 600 system (Veolia Water Technologies) unit.

3.2 Methodology

The process of making clay/Polymer aerogels involves three main steps: (Some specific details are given in the specific Chapters depending on the topics discussed in those Chapters.)

- I. Preparing solutions and suspensions
- II. Freezing via liquid nitrogen
- III. Freeze-drying (lyophilisation)

3.2.1 Clay-PVA aerogel production

3.2.1.1 Preparing stock solutions and suspensions

The method, which has been utilised for the purpose of this study, is preparing each of the clay and the polymer suspension separately in according with steps (I-III), and then mixing both the clay and PVA together to create a suspension with a final composition of 2.5 wt.% clay and 2 wt.% PVA. This base composition was constant throughout the study.

- I. The desired amount of clay and deionized water to achieve a 5 wt.% clay suspension are measured using an analytical balance and then mixed in a Warrant Blender (High shear) for 6 min in order to fully exfoliate the clay and then mixed using a magnetic stirrer (Low shear) for 24 hours (Figure 3.5).

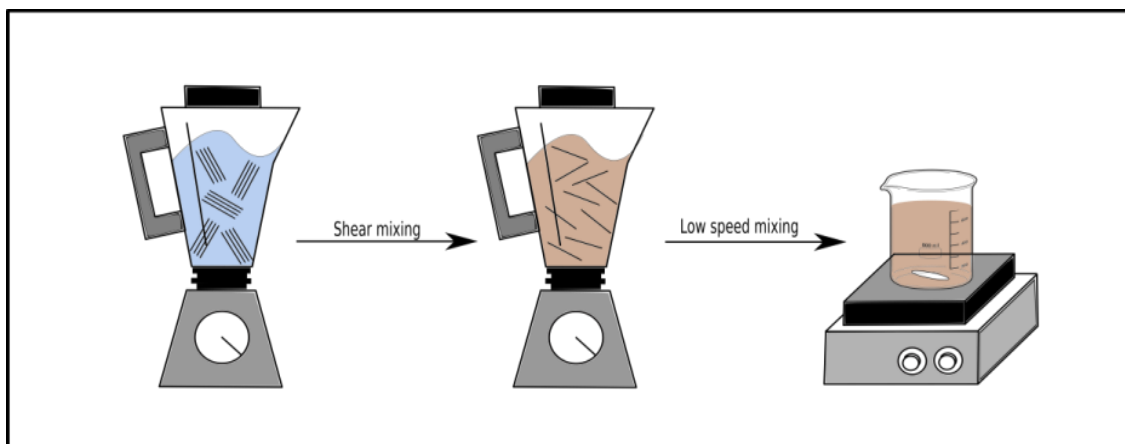


Figure 3.5 Illustration of the steps involved in preparing the stock clay suspension

- II. The desired amount of polyvinyl alcohol (PVA) and deionized water to achieve a 5 wt.% PVA solution are measured using an analytical balance and then added to a round-bottom flask, that is placed in a temperature controlled hot bath, mixed and stirred at 90°C for 3 hours (Figure 3.6) until it is clear with no inconsistency. The mixture was left to cool down at room temperature.

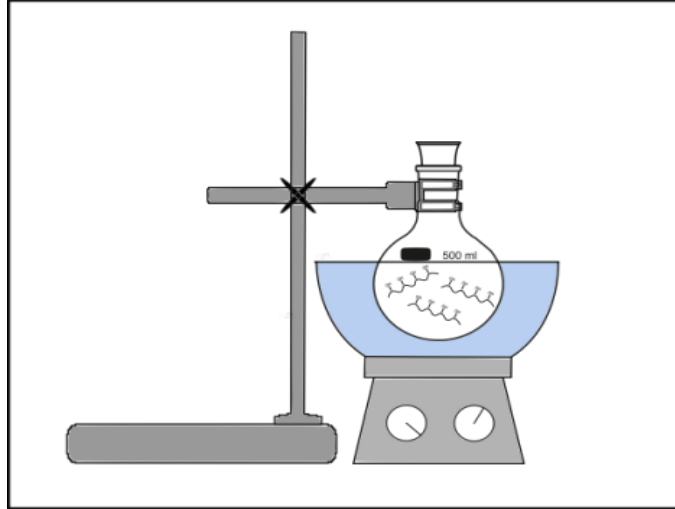


Figure 3.6 Illustration of preparing the stock PVA solution

III. Both clay and PVA stock solutions are diluted to produce a final composition of 2.5 wt.% clay and 2 wt.% PVA using Eq. (1) [207]. In this study, the composition was kept constant at 2.5 wt.% clay and 2 wt.% PVA (This composition was based on the outcome of the European project ICECLAY, ID: 315548) . The desired amount of clay and PVA are mixed using a magnetic stirrer (low shear) for 24 hours to make sure that the clay and PVA have fully interacted (Figure 3.7).

$$C_1M_1 = C_2M_2 \quad (1)$$

Where C is the concentration (wt.%) and M is the mass (g)

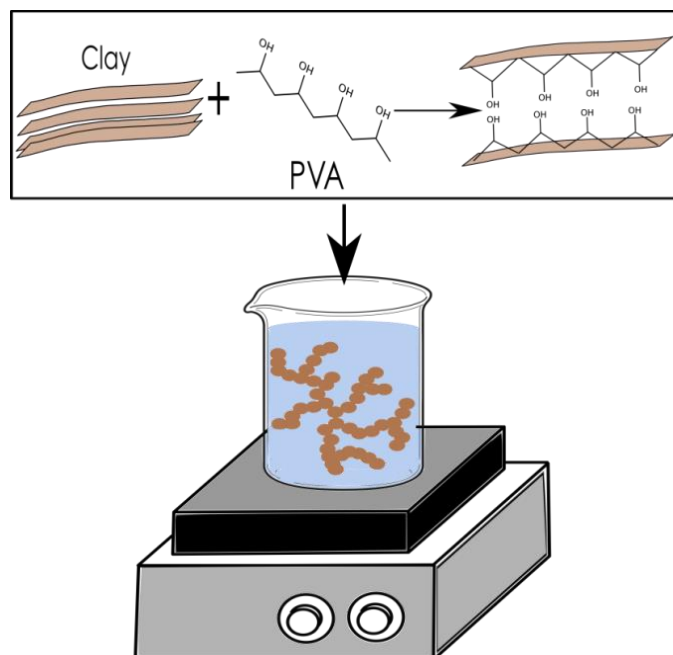


Figure 3.7 Illustration of chemical reaction between clay and PVA during the mixing process

3.2.1.2 Freezing

The final aerogel suspension is slowly poured into designated moulds to avoid the formations of bubbles on the surface, which can cause cracks (Weak points) during the freezing. If bubbles are formed, they are removed using a pipette. To prepare aerogel panels with dimensions of 100×100×10 mm (Figure 3.8A), or aerogel prisms with the dimensions of 150×50×50 mm (Figure 3.8B), the suspension is poured into aluminium foil moulds (Figure 3.9A) or polystyrene- foil moulds (Figure 3.9B), respectively. The moulds are then placed on an aluminium tray with a thickness of 3mm (Figure 3.9D) that rests on four legs. The whole pack is then set into a polystyrene box that is filled with liquid nitrogen to allow vertical freezing of the sample from bottom to top as illustrated in Figure 3.10A. To prepare samples aerogels panels that are horizontally frozen from edge to edge, the final aerogel suspension is poured into a hybrid mould with insulating sides made from wood, the bottom made from release film and the freezing side from aluminium foil (Figure 3.8C and Figure 3.9C).

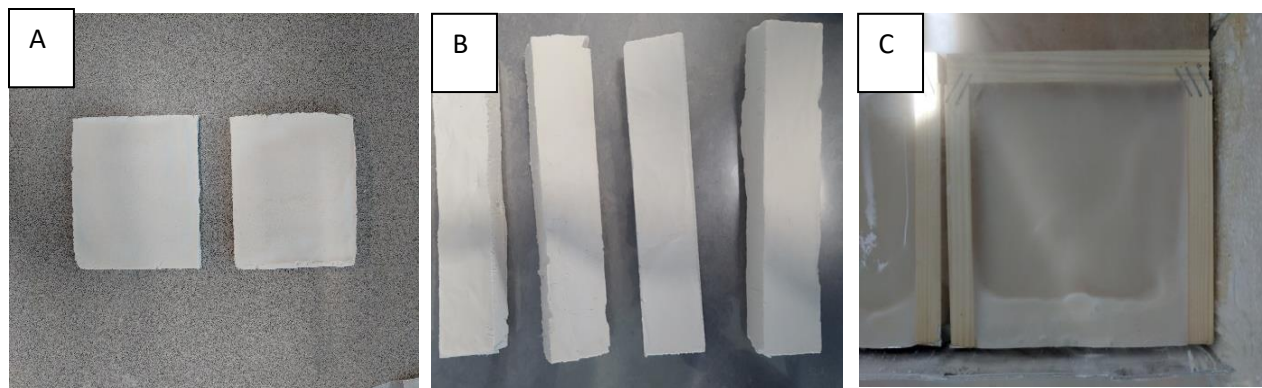


Figure 3.8 (A) Aerogel panels, (B) Aerogel prisms, (C) Aerogel frozen in one direction

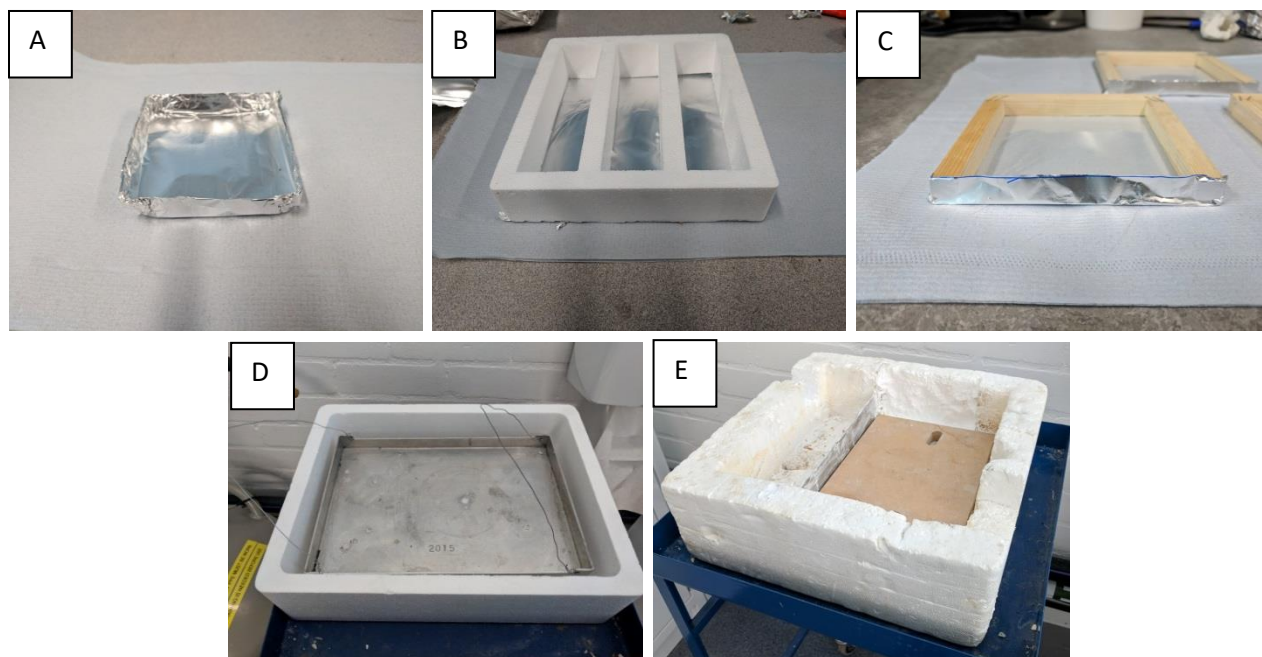


Figure 3.9 (A) Aluminum foil mould (Vertical freezing) for aerogel panels ,(B) Polystyrene- aluminium foil mould (Vertical freezing) for aerogel prisms and (C) Hybrid mould for single horizontal freezing for aerogel panels,(D) Set up for vertical freezing and (E) Set up for horizontal freezing

The mould is then placed next to an aluminium sheet with a thickness of 3 mm that partitions a polystyrene box into 2 Sections (Figure 3.9E). The part behind the aluminium sheet is filled with liquid nitrogen as illustrated in Figure 3.10B. The samples are left to freeze until they are completely solid. The frozen samples are then placed in a freezer until the entire designed batch is frozen (N.B the freeze-dryer can fit 21 samples).

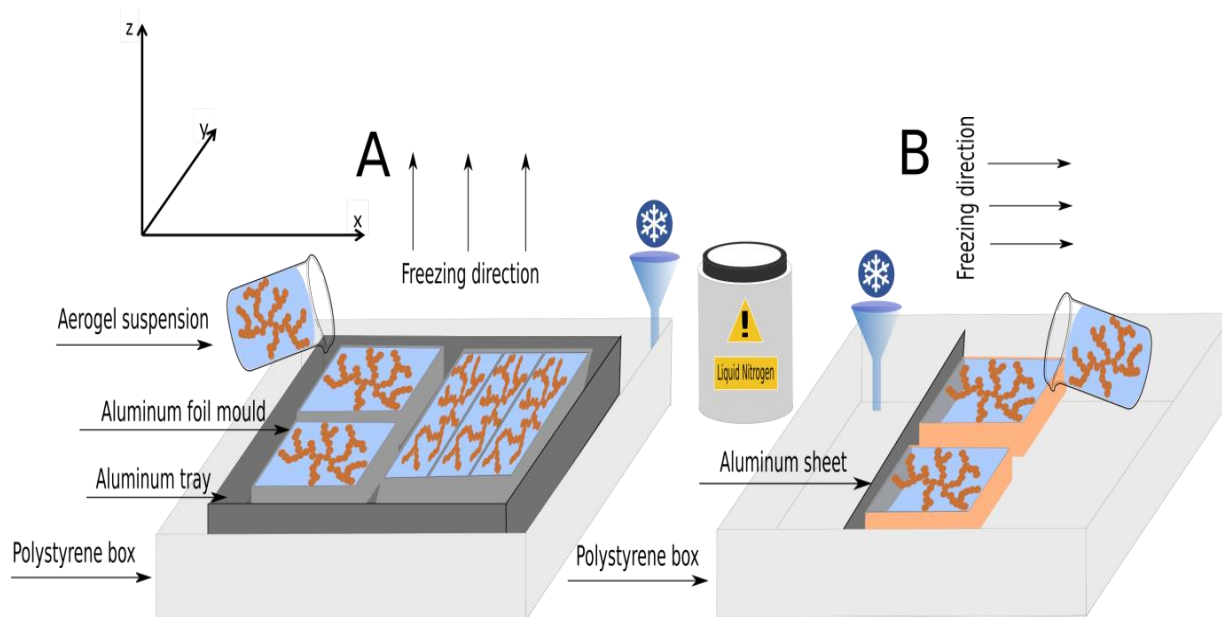


Figure 3.8 Schematic illustration of the freezing process and set up (A) Horizontal freezing and (B) Vertical freezing

3.2.1.3 Freeze-drying (Sublimation)

Alpha 1-2 LD chamber was used throughout the experiments to sublime the ice. The Alpha 1-2 LD has a max ice condenser of 2kg/24hr and an ice condenser temperature of -55°C . The freeze-dryer is set to pre-freezing an hour prior to the main drying to reach -55°C .

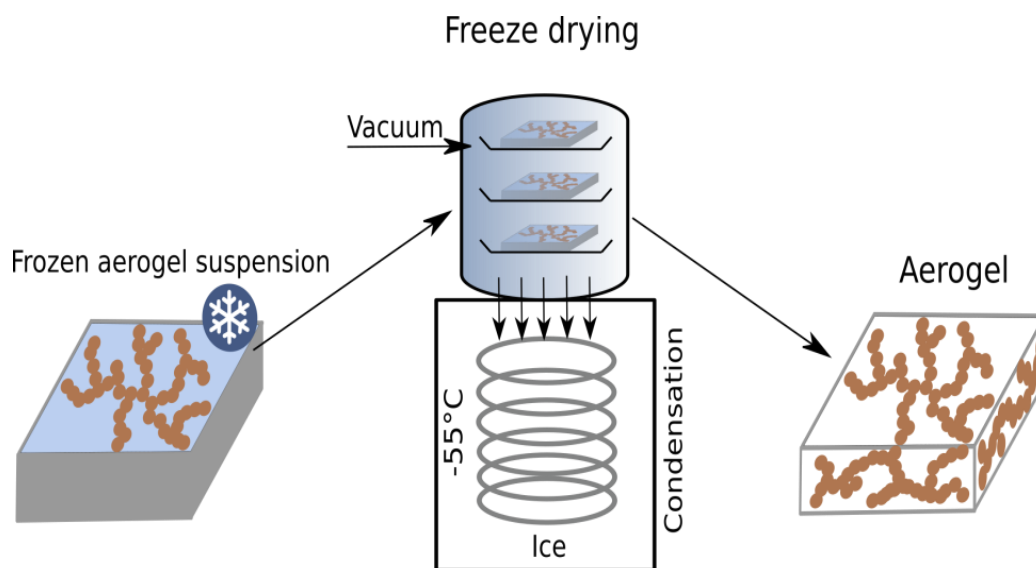


Figure 3.9 Schematic illustration of the freeze-drying process

Once all the samples are frozen, the freeze-dryer is loaded with the samples and the vacuum pump is turned on. The frozen sample is then subjected to high vacuum and progressively increasing heat, bringing about sublimation at an optimised rate (Figure 3.12). The drying process leaves a residual structure of the ice-crystals grain boundaries as the solid matter in the finished aerogel composite as illustrated in Figure 3.11. Once the samples are removed from the freeze-dryer, the samples are placed in resealable plastic sample bags and then either directly tested or characterised or stored in a desiccator until needed.

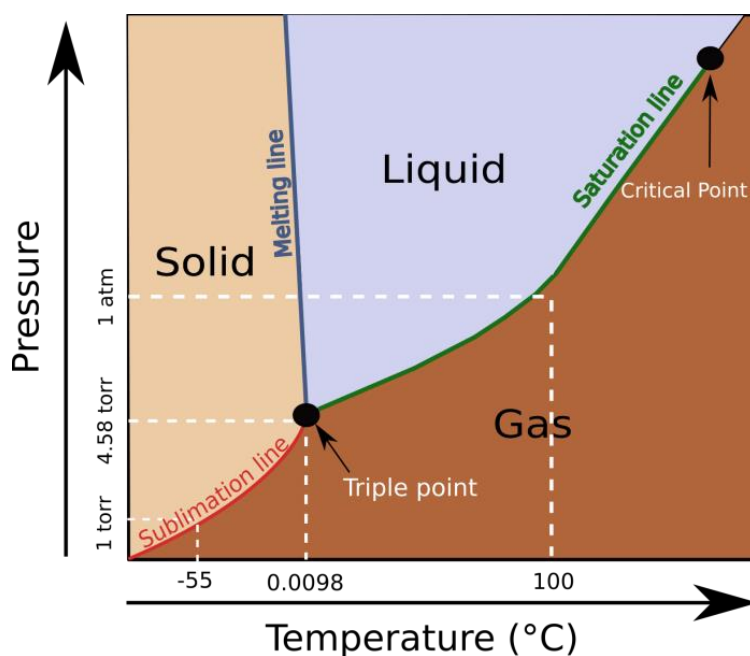


Figure 3.10 Phase diagram of water

3.2.2 Temperature induced clay-PVA aerogel production

Temperature-induced aerogel was prepared by preparing the final aerogel suspension (2.5 wt.% bentonite (Nanoclay) and 2 wt.% PVA) as described in Section 3.2.1.1. An additional step prior to freezing is then added; the final suspension is added to a round bottom flask and then placed in a hot bath for two hours (Based on trial and error) under mechanical stirring at various temperatures,

including room temperature (RT), 60, 70, 80 or 90°C as illustrated in figure 3.13. The final temperature induced suspension is left to cool down to room temperature prior to freezing to prepare aerogel panels, that are vertically frozen as described in Section 3.2.1.2.

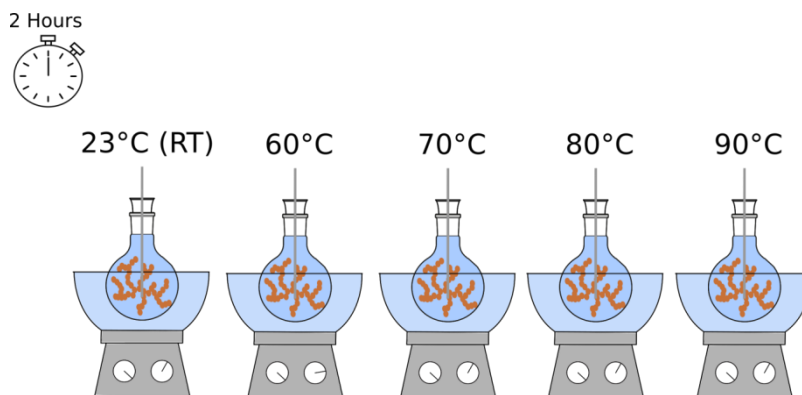


Figure 3.11 Schematic illustration of preheating the final aerogel suspension prior to freezing

3.2.3 Organoclay-PVA aerogel production

3.2.3.1 Clay modification

The first step that goes into preparing organoclay-PVA aerogels is modifying the natural bentonite using the surfactant hexadecyltrimethylammonium bromide, which is water-soluble (Section 3.5.1). The amount of surfactant is dependent on the CEC (Cation Exchange Capacity) (75.2 meq/100g) of the sodium bentonite and is calculated using Eq. (2) [208].

$$\text{Weight of surfactant (g)} = n \times \text{CEC} \left(\frac{\text{meq}}{\text{g}} \right) \times A(\text{g}) \times B \left(\frac{\text{g}}{\text{mol}} \right) \quad (2)$$

Where n is the percentage of surfactant for ion exchange with metal cation in clay layers, A is the amount of required output of clay in (g) and B is the molecular weight of hexadecyltrimethylammonium bromide (Mw 364.45 g/mol).

The percentage of concertation (n) varied between 0.3, 0.4, 0.5, 0.6, 0.7 and 1 of the CEC of the bentonite montmorillonite. A suspension of 1 wt. % of natural clay is prepared as described in Section 3.2.1.1. Depending on the percentage of concentration (n), the required amount of surfactant hexadecyltrimethylammonium bromide was dispersed into an aqueous solution and mixed using a

magnetic stirrer (100 mg/mL). This is then added to the 1 wt.% clay solution and mixed using a magnetic stirrer for eight hours to complete the reaction as illustrated in Figure 3.14.

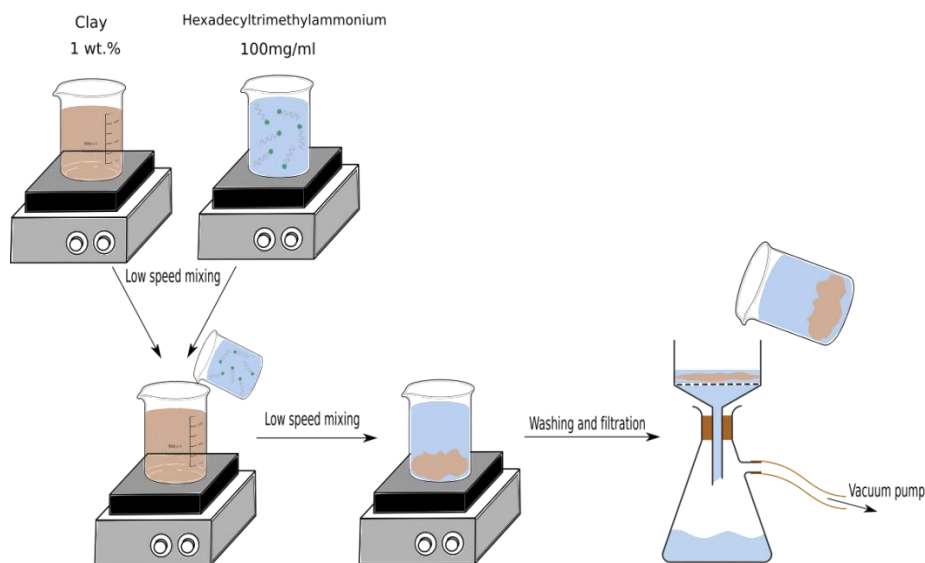


Figure 3.12 Schematic illustration of clay modification using hexadecyltrimethylammonium bromide

The resulting organoclay was filtered under vacuum, washed with deionized water three times, and then dried in a vacuum oven at 60°C. The oven dried organoclay was finally ground into a fine powder using a pestle mortar.

3.2.3.2 Organoclay-PVA aerogel

Using a homogenizer (UP400), which creates high-speed liquid jets of up to 1000 km/h (approx. 600mph), a 5 wt.% stock suspension of organology ($n= 0.3, 0.4, 0.5, 0.6, 0.7$ and 1) is prepared by adding the desired amount of organoclay and water into a beaker, and subjected to ultrasonic energy for 3 minutes to disperse the particles, where mechanical stress are applied on attracting electrostatic forces (e.g. van der Waals forces) causing deagglomeration. In parallel a 5 wt.% stock solution is prepared as described in Section 3.2.1. Using Eq. (1) a final suspension of (2.5 wt.% clay and 2 wt.% PVA) is prepared, homogenized and dispersed for 2 minutes using the UP400 as illustrated in Figure 3.15.

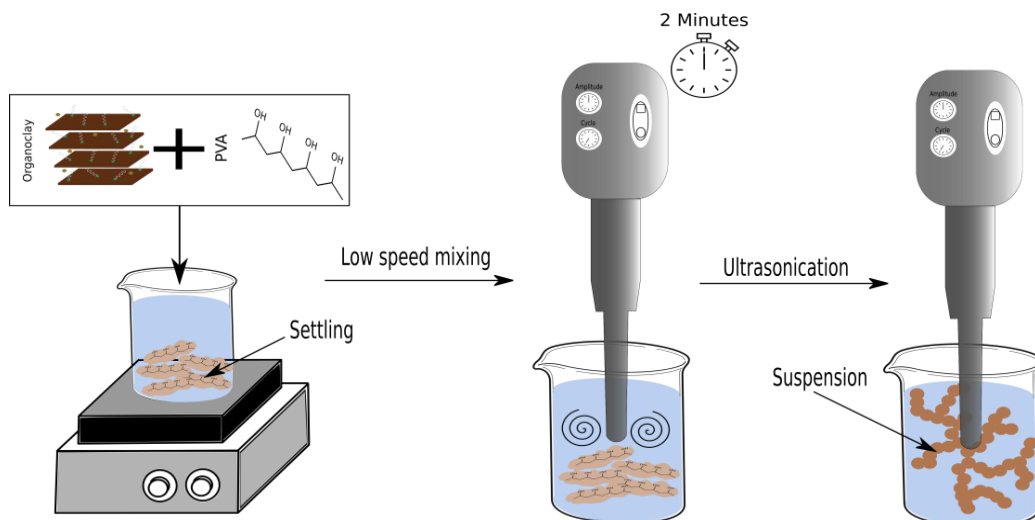


Figure 3.13 Schematic illustration of dispersion of organoclay-PVA suspension using ultrasonic technology

After being homogenized, the samples are quickly poured into aluminium moulds for vertical freezing to prepare aerogel panels as described in Section 3.2.1. Samples were coded according to the percentage of concentration of the surfactant, for example the sample (0.3 CEC) was prepared from organoclay with 0.3 of the cation exchanged and a final formulation of 2.5 wt.% clay and 2 wt.% PVA.

3.2.4 Crosslinked clay-PVA aerogel production

Three stock solutions were used to prepare cross-linked clay-PVA aerogels. A 5 wt.% bentonite (Nanoclay) stock suspension and a 5 wt.% PVA solution were prepared as described in Section 3.2.1. Either a stock solution of a 76 wt.% of Aliphatic polyisocyanate (Wcro1™) or a 100 wt.% stock solution of 3-glycidoxypropyltrimethoxysilane (Wcro2™) were used. Using Eq. (1) the amount of each solution in (g) is added to the beaker to achieve a final suspension of 2.5 wt.% clay, 2 wt.% PVA and 2 wt.% of either Aliphatic polyisocyanate (Wcro1™) or 3-glycidoxypropyltrimethoxysilane (Wcro2™) (Table 3.1). The final suspension was mixed using a magnetic stirrer for 24 hours and then poured into aluminium moulds for vertical freezing to prepare aerogel panels as described in Section 3.2.1.

Table 3.1 Formulations of crosslinked clay-PVA aerogels

	Clay	PVA	(WCro1™)	(Wcro2™)
Weight percentage (wt. %)	2.5	2	2	-
			-	2

3.2.5 Water repellent clay-PVA aerogel production

Three stock solutions were used to prepare water repellent clay-PVA aerogels. A 5 wt. % bentonite (Nanoclay) stock suspension and a 5 wt.% PVA solution were prepared as described in Section 3.2.1. Either a stock solution of a 30 wt.% a combination of melamine resins with paraffin waxes (WDisRep1™), a 30 wt.% stock solution of C6- Fluoroalkyl acrylate (WDisRep3™), or a 25 wt.% stock solution C2-C4 Fluorochemical (WDisRep 4™) were used. Using Eq. (1) the amount of each solution in (g) was added to the beaker to achieve a final suspension of 2.5 wt.% clay, 2 wt.% PVA and 2 wt.% of either the water repellents (Table 3.2).

Table 3.2 Formulations of water-replant clay-PVA aerogels

	Clay	PVA	(WDisRep1™)	(WDisRep3™)	(WDisRep4™)
Weight percentage	2.5	2	2	-	-
(wt. %)	2.5	2	-	2	-
	2.5	2	-	-	2

The final suspension was mixed using a magnetic stirrer for 24 hours and then poured into aluminium moulds for vertical freezing to prepare aerogel panels as described in Section 3.2.1. The most efficient water repellent (WDisRep3™) was further investigated in another set of experiments, where the amount of C6- Fluoroalkyl acrylate (WDisRep3™) was varied between 0.3, 0.5, 0.8, 1, 1.2, 1.5, and 2 wt.%. The samples are coded according to the content of WDisRep3™ (Table 3.3). For instance, the sample 0.8WR has a composition of 2.5 wt.% clay, 2 wt.% PVA and 0.8 wt.% C6- Fluoroalkyl acrylate (WDisRep3™).

Table 3.3 Formulations of WDisRep3™ clay-PVA aerogels

WDisRIP3 (wt. %)	Code
0.3	0.3WR
0.5	0.5WR
0.8	0.8WR
1.0	1.0WR
1.2	1.2WR
1.5	1.5WR
2.0	2.0WR

3.2.6 Crosslinked-water repellent aerogel production

Four stock solutions were used to prepare aerogels that combine both crosslinkers and water repellents. A 5 wt.% bentonite (Nanoclay) stock suspension and a 5 wt.% PVA solution were prepared as described in Section 3.2.1. Stock solutions were either a 76 wt.% of aliphatic polyisocyanate (Wcro1™) or a 100 wt.% of 3-glycidoxypropyltrimethoxysilane (Wcro2™) with a 30 wt.% stock solution of C6- Fluoroalkyl acrylate (WDisRep3™). Using Eq. (1) the amount of each solution in (g) was added to a beaker to achieve the compositions as proposed in Table 3.4 and mixed using a mechanical stirrer for 24 hours. The final suspensions were poured into aluminium moulds for vertical freezing to prepare aerogel panels as described in Section 3.2.1.

Table 3.4 Formulations of WDisRep3™-crosslinked clay-PVA aerogels

	Clay	PVA	(WDisRep3™)	(Wcro1™)	(Wcro2™)	
Weight percentage (wt. %)			0.5	0.5	-	
			0.5	-	0.5	
	2.5	2		1	1	-
				1	-	1
				2	1	-
				2	-	1
				1	2	-
				1	-	2

Samples are coded to ease their description in the thesis according to the ratio of WDisRep3™ to either Aliphatic polyisocyanate (Wcro1™) or of 3-glycidoxypropyltrimethoxysilane (Wcro2™) (Table 3.5). For instance, the sample CR1/WR1:2 has a composition of 2.5 wt.% clay, 2 wt.% PVA, 1 wt.%

Aliphatic polyisocyanate (Wcro1™) and 2 wt.% C6- Fluoroalkyl acrylate (WDisRep3™). Sample CR2/WR1:2 has a composition of 2.5 wt.% clay, 2 wt.% PVA, 1 wt.% glycidoxypropyltrimethoxysilane and 2 wt.% C6- Fluoroalkyl acrylate (WDisRep3™).

Table 3.5 Composition and formulation codes for water-replant-crosslinked clay-PVA aerogels

WCro1™:WDisRep3™ (wt.%)	Code	WCro2™:WDisRep3™ (wt.%)	Code
0.5:0.5	CR1/WR0.5:0.5	0.5:0.5	CR2/WR0.5:0.5
1:1	CR1/WR1:1	1:1	CR2/WR1:1
1:2	CR1/WR1:2	1:2	CR2/WR1:2
2:1	CR1/WR2:1	2:1	CR2/WR2:1

3.3 Characterisation and testing

3.3.1 Physical properties

3.3.1.1 Apparent density

The density was calculated by dividing the dry mass over the volume using Eq. (3) in accordance with ASTM D 1622-98 [209]. The volume was measured using a digital calliper with an accuracy of 0.02 mm, and the dry mass was measured using an analytical balance with an accuracy of 0.01 mg (4 digits). The average density reported in the thesis for each aerogel composition was calculated from six samples cut from the monolithic aerogel tile.

$$\rho = \frac{m}{v} \quad (3)$$

Where ρ is the density in (g/cm^3), m is the mass in (g), and v is the volume in (cm^3).

3.3.1.2 Dynamic rheometry and pH

Rheological properties of the final aerogel suspension prepared as described in Section 3.2.1.1, were investigated using an advanced rheometric expansion system (ARES) rheometer (Figure 3.16) with dynamic shear deformation. The final aerogel suspension is loaded between a flat plate and a cone-plate of 50 mm with a contact angle of 0.04 (radians) with an overall 0.6 mm gap as illustrated in

Figure 3.16. A temperature sweep was carried out in which at each temperature step, a frequency sweep is run (while the temperature is held constant). The temperature is then changed to the next step, allowed to equilibrate, and the frequency sweep is run again. The temperature sweep was carried out from 23 to 90°C with a heating rate of 2°C/min and a frequency of 6 (rad/s) with auto-tension on. TA Orchestrator software was used to analyse and record the data. The suspensions prepared as described in Section 3.2.2 were left to cool down overnight before measuring the pH using an electronic pH metre with a resolution of 0.01 pH \pm 0.01.

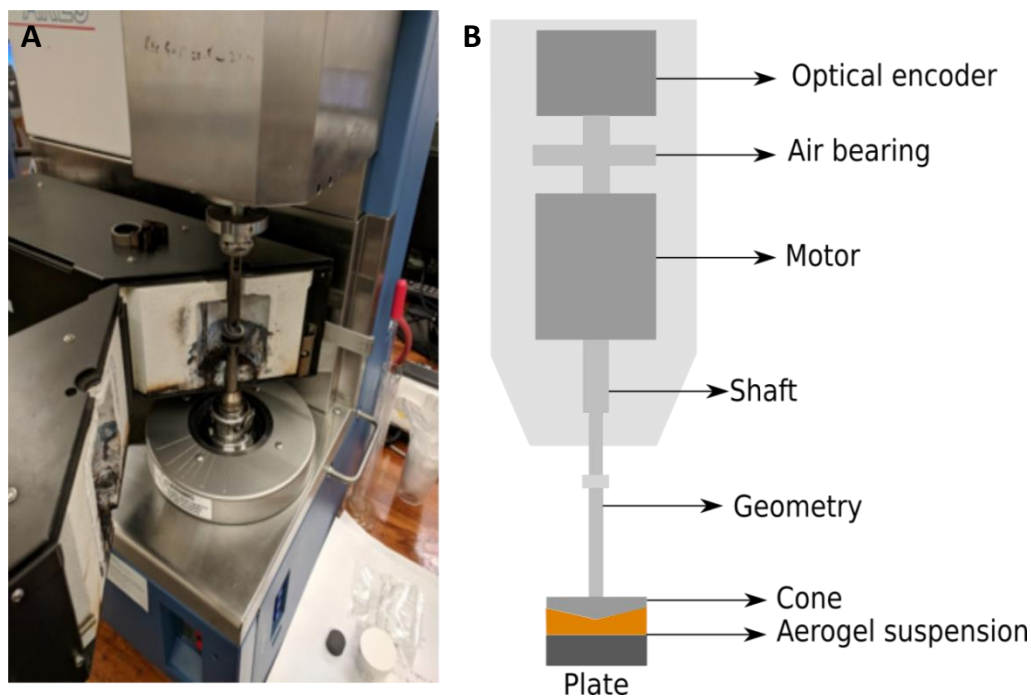


Figure 3.14 (A) Advanced rheometric expansion system (ARES) and (B) schematic illustration of test set up

3.3.1.3 Particle size analysis

The particle size was measured using a light scattering based system (NanoSight LM10) (Figure 3.17A) which relies on capturing the paths of the suspended particles under Brownian motion (Figure 3.17B). The final aerogel suspensions prepared as described in Section 3.2.2 were left to cool down for 24 hours before loading the LM10 unit via a syringe. The samples are injected into the unit slowly and at a tilted angle to avoid the formation of bubbles which can cause unwanted reflection of the beam.

The suspension is allowed to equilibrate to unit temperature for a few minutes. The final aerogel suspensions were diluted to 0.001 wt.%, before loading and 5 recordings of 90 seconds each were carried out for each temperature set as described in Section 3.2.2. The video images of the particle's movement under Brownian motion were analysed by a single particle tracking programme (Nanoparticle Tracking Analysis [NTA] software).

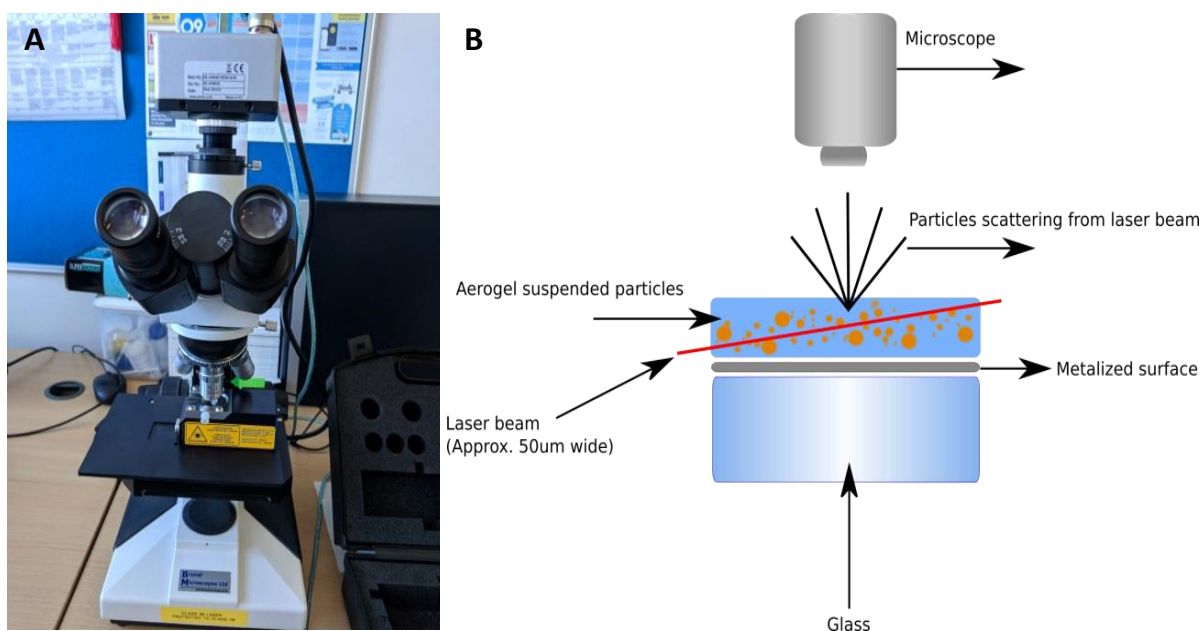


Figure 3.15 (A) Microscope fitted with NanoSight LM10 unit and (B) Schematic illustration of NanoSight LM10 operation

3.3.1.4 Thermal conductivity

Aerogel panels were prepared as described in Section 3.2.1.2. Their thermal conductivity was measured using a Fox200 system (Figure 3.18A). The aerogel panels are placed between a cold and a hot plate in the test stack, and a temperature gradient is established over the thickness of the material as illustrated in Figure 3.18B. The hot plate is set to 20°C and the cold plate to 0°C to measure the thermal conductivity across a mean temperature of 10°C (ASTM C518 and ISO 8301). The plates are then positioned using auto-thickness to establish a tight contact with samples and eliminate any

thermal bridges that might arise from air pockets. The Heat Flux Transducer integrates over an entire active area 75 x 75 mm and measures the thermal conductivity according to ASTM C518 and ISO 8301. The thermal conductivity reported in the thesis is an average of three samples.

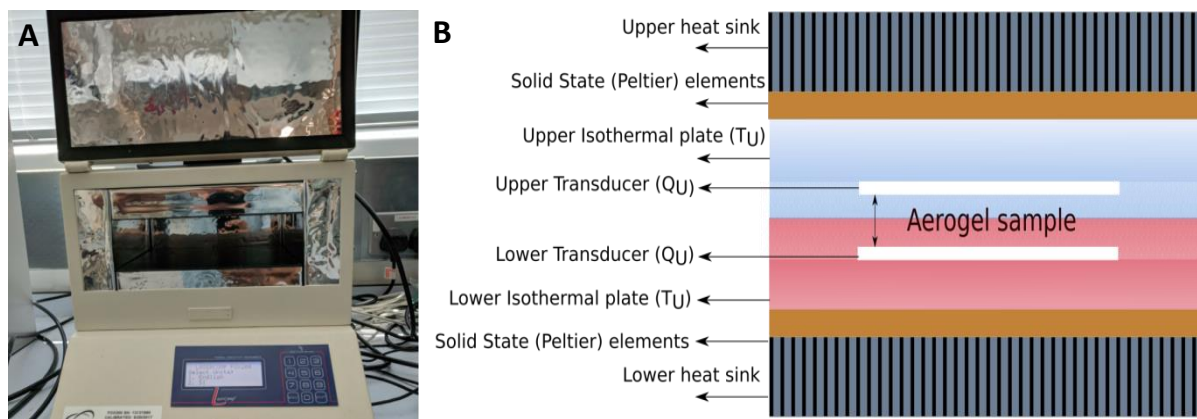


Figure 3.16 (A) Fox 200 unit and (B) Schematic illustration of the Fox 200 components

3.3.1.5 Flammability (UL94 test)

A vertical UL94 test was carried out to determine the flammability of aerogel composites. The test was carried out according to Underwriters laboratories test standards [210]. The test begins by mounting an aerogel composite vertically on a stand. A butane burner was used as the flame source (Figure 3.19A). A gap of 10mm is set between the top of the burner and the aerogel composite. The flame is adjusted so that a blue flame is present with a 20mm high central cone (Figure 3.19B). The flame is applied for 10 seconds and the time for the flame or combustion to distinguish is noted as t_1 . Then the flame is applied for another 10 seconds and the time for the second flame or combustion to distinguish is noted as t_2 . If the sample drips due to combustion and the cotton indicator are ignited, a note is recorded.

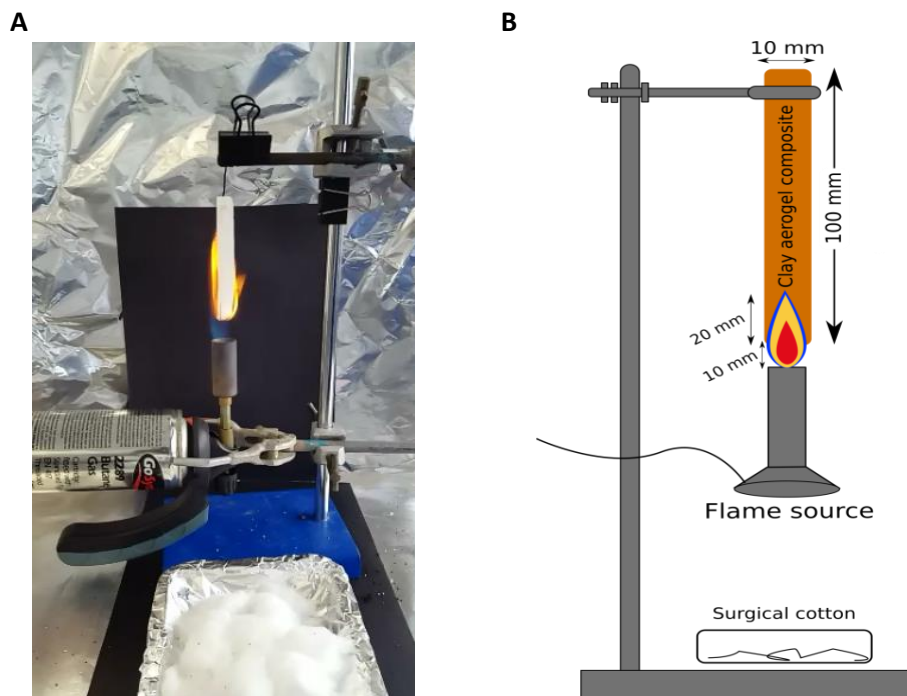


Figure 3.17 (A) UL94 flammability test and (B) Schematic illustration of UL94 test set up

Several criteria exist to specify the flammability of the aerogel (Table 3.6). The classification is V-0 (Lowest flammability), V-1 and V-2 (Highest flammability) depending on the time after flame 1, time after flame 2 and whether the cotton indicator is ignited. According to the standard, the classification was determined from five specimens.

Table 3.6 Flammability classification criteria

Criteria	V-0 (low flammability)	V-1	V-2 (High flammability)
After flame 1	<10 seconds	< 30 seconds	< 30 seconds
After flame 2	<10 seconds	< 30 seconds	< 30 seconds
Cotton Indicator ignited?	No	No	Yes

3.3.2 Mechanical properties

3.3.2.1 Compressive modulus

The aerogel composite panels were cut into cuboids (20×20×10mm) (Figure 3.20B) using a diamond band saw. The compressive test was carried out by an INSTRON 5900 fitted with a 50 KN load cell. The load was applied at a speed of 1 mm/min with an end of test condition at 30% strain. The test

was carried out in a controlled environment of 45% RH and at 23°C in accordance with BS EN ISO 604. As the samples do not fracture (Soft foamed materials), the compressive modulus is calculated from the most linear region of the stress-strain curves using Eq. (4), which typically occurred at $3 \pm 2\%$ strain [211]

$$E_c = \frac{\sigma_2 - \sigma_1}{\epsilon_2 - \epsilon_1} \quad (4)$$

where, E_c is the modulus in (MPa)/(N/mm²), σ is the stress in (N/mm²), and ϵ is the strain which is dimensionless

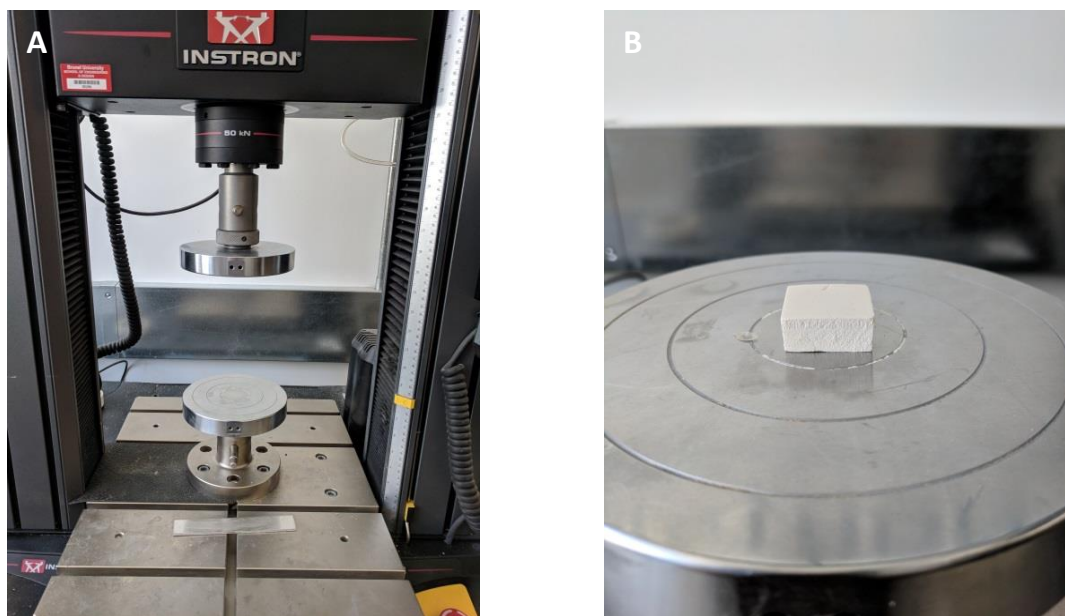


Figure 3.18 (A) INSTRON 5900 and (B) Aerogel cuboid specimen for testing.

3.3.3 Analytical techniques

3.3.3.1 Attenuated total reflectance -Fourier transform infrared spectroscopy (ATR-FTIR)

The functional groups of aerogel composites were analysed through Fourier transform infrared (FTIR) analyses using a Perkin Elmer Spectrum One. The aerogel samples were cut into thin strips of 3 mm using a diamond saw. Aerogel samples were stored in a desiccator prior to testing to avoid excess

moisture absorbance. The required sample is then taken out of the desiccator and placed on the ATR equipped with 3× bounce diamond crystal detector (Figure 3.21A). The IR beam passes through the sample, and the transmitted energy is measured. A spectrum is generated using Perkin Elmer Spectrum One (Figure 3.21B). The spectra were recorded over a wavenumber range of 4000 - 600 cm^{-1} with a resolution of 16 cm^{-1} from 16 scans.

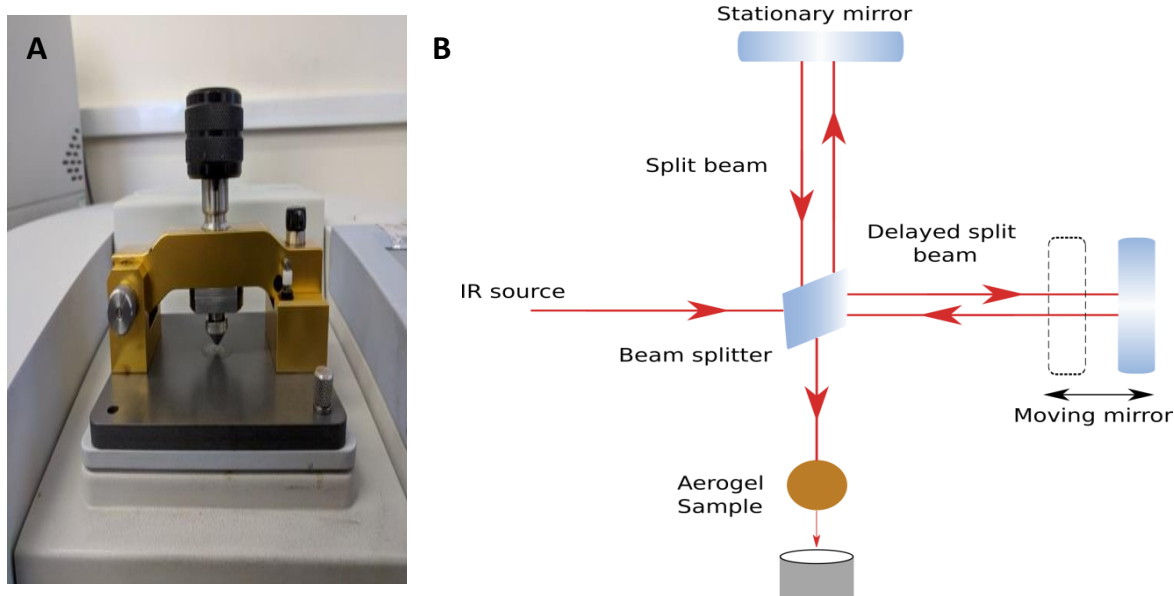


Figure 3.19 (A) Diamond tipped ATR stage and (B) Schematic illustration of FTIR mechanism

3.3.3.2 X-ray powder diffraction (XRD)

X-ray diffraction method analysis (XRD) was used to identify the intercalated and exfoliated structures of aerogel composites and calculate the d-value (Interlayer space) using Bragg's law (Eq. 5) [212]. Solving Bragg's Equation gives the d-spacing between the crystal lattice planes of atoms that produce the constructive interference (Figure 3.22B). XRD patterns were recorded using an X'Pert ray D8 advanced Bruker AXS diffractometer with a $\text{CuK}\alpha$ radiation source ($\lambda=0.15406 \text{ nm}$), graphite monochromator and a 2D-area detector GADDS system (Figure 3.22A). 2θ was scanned from 1° to 10° with a resolution of 0.02° at a rate of $1^\circ/\text{min}$.

$$n\lambda = 2d\sin\theta \quad (5)$$

where n is an integer ($=1$), λ is the x-ray wavelength in angstroms (\AA), d is the interatomic spacing in angstroms (\AA), and θ is the diffraction angle in degrees ($^\circ$).

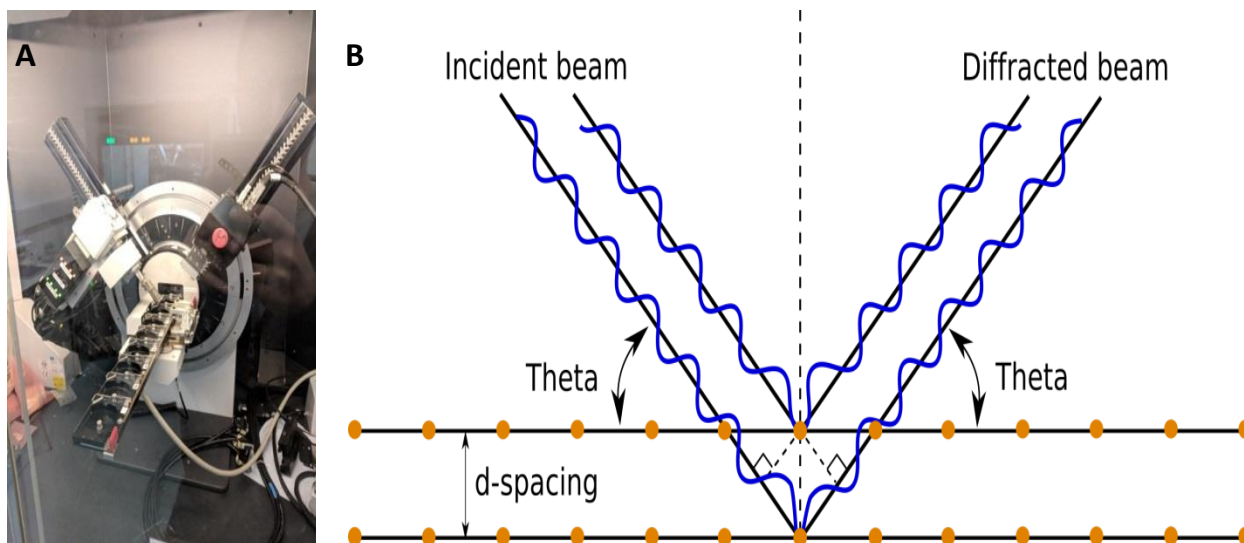


Figure 3.20 (A) X-Ray Diffractometer D8 Advance and (B) Schematic illustration of Bragg's Law reflection.

3.3.4 Microstructure characterisation

3.3.4.1 Scanning electron microscope (SEM)

The developed microstructures were characterised through Field emission gun-scanning electron microscopy using a Leo[®] 1430VP SEM (Figure 3.23). Due to the uncondutive nature of the aerogel composites, they were first sputter-coated with a thin layer of gold prior to imaging using a Polaron-SC7640 for 120 seconds (Figure 3.24A and B). The samples were then placed on a holder by using carbon tape (Figure 3.24C).

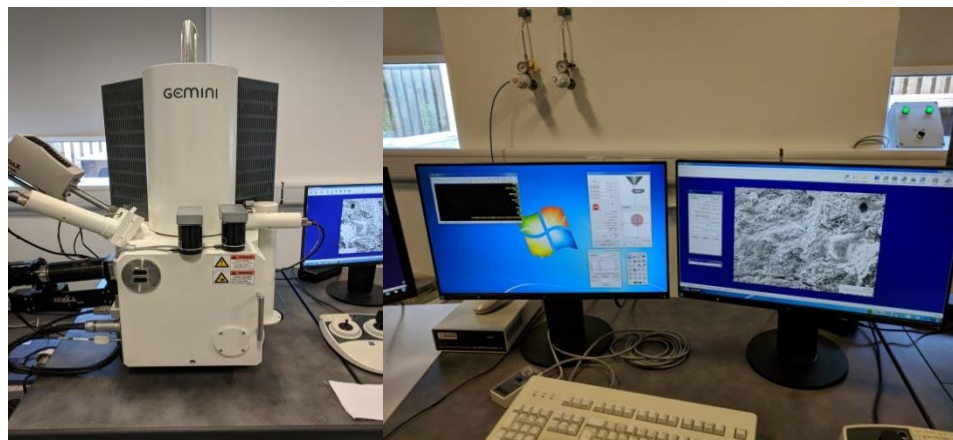


Figure 3.21 Leo® 1430VP SEM

The samples are placed in the SEM chamber and vacuumed. The electron high tension (EHT) was set at 10 kV, and imaging was carried out using the SE2 detector at a scanning speed of 9 ± 2 . The working distance, brightness, contrast and stigmatisms are adjusted as required to produce a high-resolution image. Each sample is imaged at several different locations and the dominant structure is reported in this study.

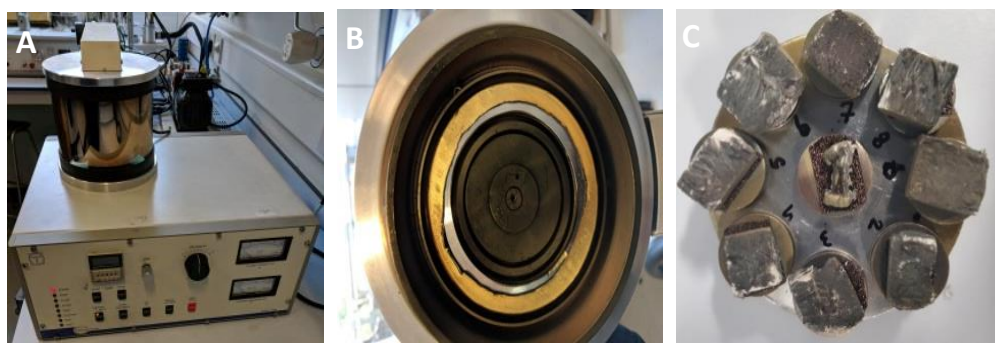


Figure 3.22 (A) Polaron-SC7640, (B) Gold sheets and (C) Suptter coated aerogel samples mounted on a multi-holder

3.3.4.2 X-ray 3D scanning

X-ray imaging was conducted using a Zeiss Xradia 500 scanner. A small piece of aerogel, prepared as described in Section 3.2.1.1, was mounted on a metallic assembly that was fitted on a rotation stage (Figure 3.25). The voltage was set to 80 kV and the power to 7 W. A total of 3000 projections were acquired at a pixel size of 1 micrometre, with a 2x binning mode, using 4x optics. The projection data

were reconstructed using proprietary software provided by Zeiss and image processing, and analysis was performed using Avizo 9.3 software.

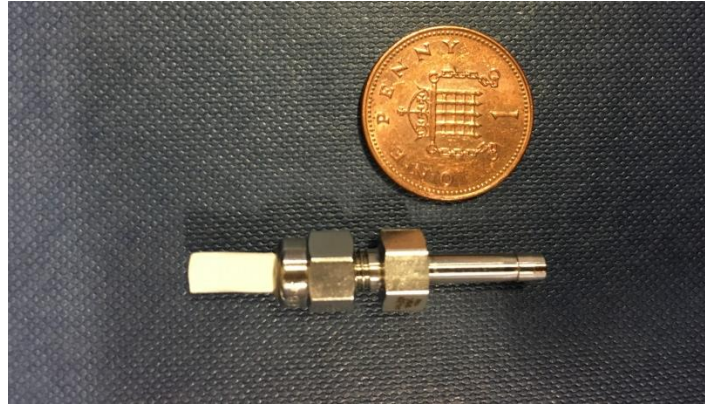


Figure 3.23 rotation stage

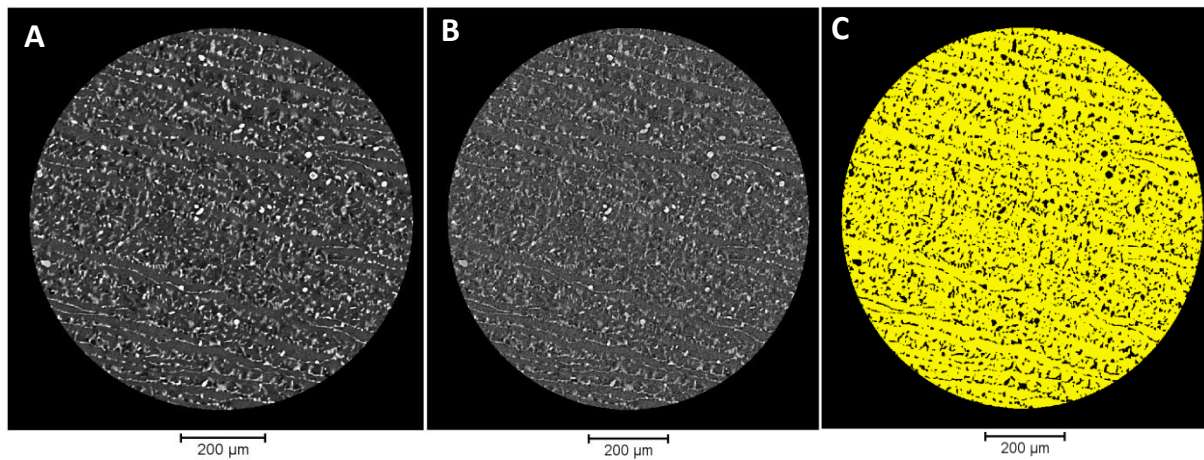


Figure 3.24 (A) Raw processing, (B) Filtered processing and (C) Segmented processing

The raw image was filtered using an edge-preserving Non-local Means Filter. The 3D image was pre-processed to remove the distorted outer regions at the top and the base of the sample (Figure 3.26A). The filtered image was then segmented (or binarized) using a seeded Watershed algorithm based on the grey-scale gradient and grey-scale intensity of each voxel (Figure 3.22C). This final segmented image (Figure 3.26C) was used for visualisation and quantifications. Finally, the pore-size distribution

was obtained by using “Thickness” module on Avizo, which results in a map of maximum radii as spheres in the aerogel open pore spaces.

3.3.5 Wettability

3.3.5.1 Contact angle

Drop shape analysis was used to determine the contact angle from the shadow of a sessile drop using a ten Angstroms FTA 1000 Analyzer System (Figure 3.27A). The static contact angle was obtained from a 3.5 μL drop of distilled water. The contact angle is given by the angle between the calculated drop function and the surface of the aerogel (Baseline). The contact angle was calculated from 3 minutes of video footages. The experiment was conducted in a controlled environment of $18 \pm 2^\circ\text{C}$ to try and restrict evaporation of the water droplet. Three measurements were conducted on three different sides of the aerogel surface (Top, bottom and cross-section) and the average contact angle was reported. The contact angle is then classified according to the measurement as illustrated in Figure 3.27B.

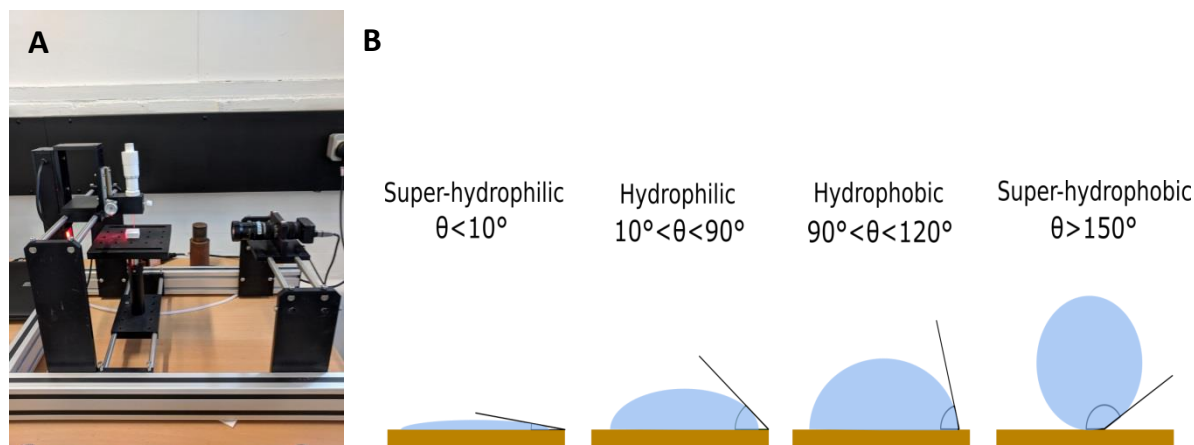


Figure 3.25 (A) Contact angle set-up (B) Contact angle classification

3.3.5.2 Capillary water uptake

Prism aerogel samples (50×50×150mm) were prepared as described in Section 3.2.1.2. The water uptake was measured across three sides of the prism; lateral side, base (cross-section) and bottom

faces. The specimens are dried for 24 hours at $110\pm 2^\circ\text{C}$ and then placed in a desiccator for three hours to allow the samples to cool down before recording their dry weight. The sample is then placed on a perforated stand in a water tray and filled with water so that the water level is no more than 5mm above the base of the specimen as illustrated in Figure 3.28B. The specimens were water- and vapour-proof insulated on all lateral sides (i.e., the sides parallel to the main direction of water transport) using paraffin wax. The quantity of water absorbed is measured at intervals until the water reached the top of the sample. The samples were monitored using a FLIR thermal camera to check whether the water reached the top. The water absorption coefficient (A) ($\text{kg m}^{-2}\text{s}^{-1/2}$) was then calculated as defined by Hull (Eq. 5) [213].

$$i = A \cdot \sqrt{t} \quad (5)$$

where i is the cumulative water absorption in (kg m^{-2}), t is the time from the beginning of the experiment in seconds (s), and (A) is the water absorption coefficient in $\text{kg m}^{-2}\text{s}^{-1/2}$.

The water absorption coefficient was then used to calculate the apparent moisture diffusivity Eq. (6).

$$k_{app} \approx \left(\frac{A}{w_{sat} - w_o} \right)^2 \quad (6)$$

where w_{sat} is the saturated moisture content in (kg m^{-3}) and w_o the initial moisture content in (kg m^{-3}).

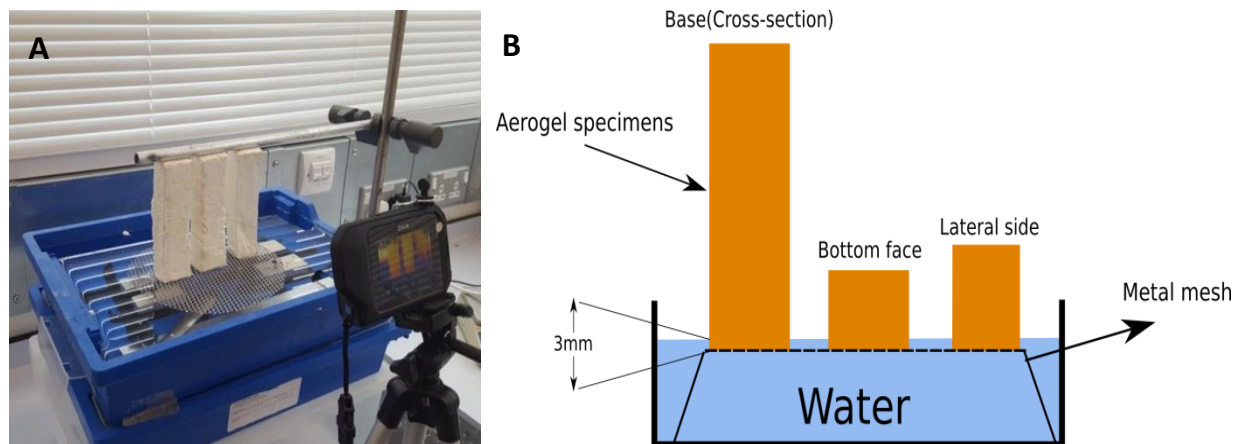


Figure 3.26 (A) Capillary water uptake test apparatus and set up and (B) Schematic illustration of capillary water uptake procedure

3.5.5.3 Moisture absorption

Clay aerogels were prepared as described in Section 3.2. The aerogel panels were then cut into cuboids (20×20×10 mm). The samples were then placed on aluminium trays and dried in an oven for 24 hours at 110±2°C (Figure 3.29B). The mass was then measured using an analytical balance with an accuracy of 0.01 mg (4 digits). The samples were then placed in a controlled environmental chamber at elevated humidity (Figure 3.29A). Different humidity conditions were used as the thesis progressed.

The following are the conditions of humidity used and their intended Chapters:

- Chapter 6: Samples were either subjected to 35%, 65% or 85% relative humidity (RH) for 24 hours. A long-term test was carried out for 30 days at 85% relative humidity. The temperature fixed at 23°C for all sets of humidity.
- Chapters (4-5, 7-8): Samples were either subjected to 45, 65, 85 or 95 % relative humidity (RH) for 24 hours. A long-term test was carried out for 30 days at 95% relative humidity. The temperature was fixed at 23°C for all sets of humidity.
- Chapter 9: Samples were either subjected to 45, 65, 85 or 95 % relative humidity (RH) for 24 hours. A cyclic test was carried out for four weeks; one week at 95 % RH, one week 45% RH, one week at 85% RH and one week 65% RH. The temperature was fixed at 23°C for all sets of humidity.

The moisture absorption was calculated from the difference between the wet and dry mass using Eq. (7) [214]. The reported moisture absorbance is an average of six samples.

$$\text{Weight increase (\%)} = \frac{W_w - W_d}{W_d} \times 100 \quad (7)$$

where W_w is the wet mass in grams (g), and W_d is the dry mass in grams (g)

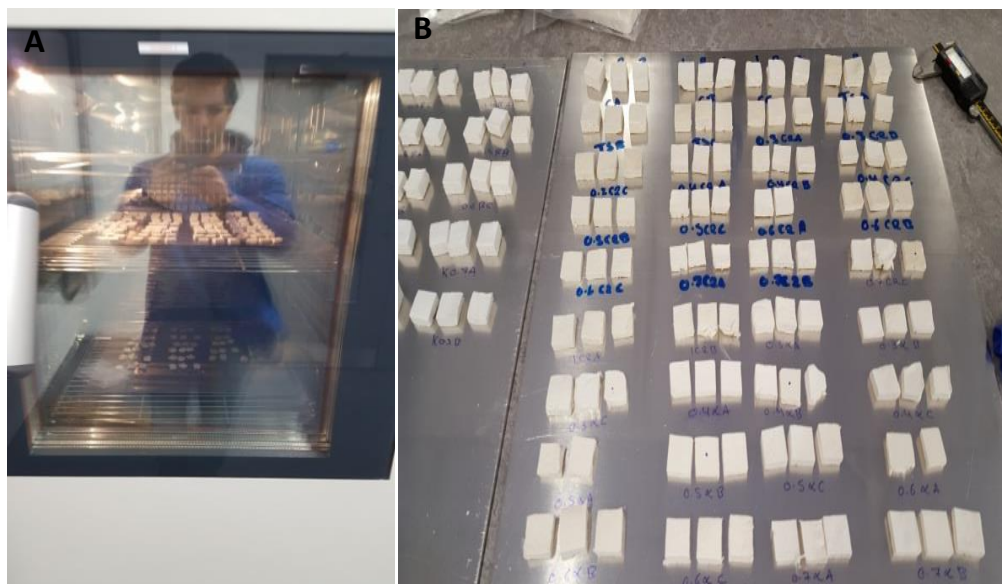


Figure 3.27 Clay-PVA aerogel composites being tested for moisture absorption

3.5.5.4 Water absorption

Clay aerogels were prepared as described in Section 3.2. The aerogel panels were cut into cuboids (20×20×10 mm). Each sample is then placed in a beaker filled with distilled water (Figure 3.30). Consecutive weight measurements were carried out at the 60s, 1, 7, 10, 15, and 30 days. Samples were wiped with a dry cloth before measuring the mass to remove any excess water bonded to the surface of the aerogels. The beakers were topped up with water as necessary. The water absorption was calculated from the difference between the wet and dry weights using Eq. 7 [214]. The weight increase reported is an average of the water absorption of three samples.



Figure 3.28 Long-term water absorption set up

3.5.5.5 Water vapour transmission

The determination of water vapour transmission (cup method) properties was carried out according to the British standard (EN ISO 12572:2001) [215]. Using a carbon steel scalpel, the aerogel panels were cut into samples with a diameter of 40mm and a thickness of 12mm. The aerogel test specimen is used to seal an open side of a test cup (Figure 3.31), the edges are masked with silicon to create a tight seal. The cups are filled with either a desiccant (Calcium chloride, CaCl₂ - particle size < 3mm) (dry cup) or an aqueous saturated solution (Potassium chloride, KCl) (wet cup) (Figure 3.31). The assembly is then placed in an environmental chamber at 50 and 85% relative humidity for the dry cup and wet cup respectively, while monitoring mass change and time as illustrated in Figure 3.31. Periodic weighings of the assembly are made every hour for 72 hours. The water vapour resistance (u-value) was calculated according to EN ISO 12572:2001[215] using Eq. (10).

The water vapour permeance (W) (Kg/m².s.Pa), is calculated using Eq. (8)

$$W_c = \frac{1}{\frac{A \cdot \Delta P_v}{G} - \frac{d_a}{\delta_a}} \quad (8)$$

where A is the area of the specimen in m², ΔP_v is the water vapor pressure difference across the specimen according to the psychometric chart ([216]), G is the slope of the line of the change in

mass per time in (kg/s), d_a is thickness of the air layer in (m), and δ_a is the water vapour Permeability of air as a function of barometric pressure at 23°C ($=2 \times 10^{-10}$ kg/(m.s.Pa))

Using the water vapour permeance (W), the water vapour permeability (δ) (kg/(m.s.Pa) is calculated using Eq. (9)

$$\delta = W \times d \quad (9)$$

where W is the water vapour permeance in (Kg/m².s.Pa), and d is the thickness of the specimen in (m).

Finally using the water vapour permeability (δ), the water vapour resistance (u-value) can be calculated using Eq. (10):

$$\mu = \frac{\delta_a}{\delta} \quad (10)$$

where δ_a is the water vapour Permeability of air as a function of barometric pressure at 23°C ($=2 \times 10^{-10}$ kg/(m.s.Pa)), and (δ) is the water vapour permeability (δ) in (kg/(m.s.Pa))

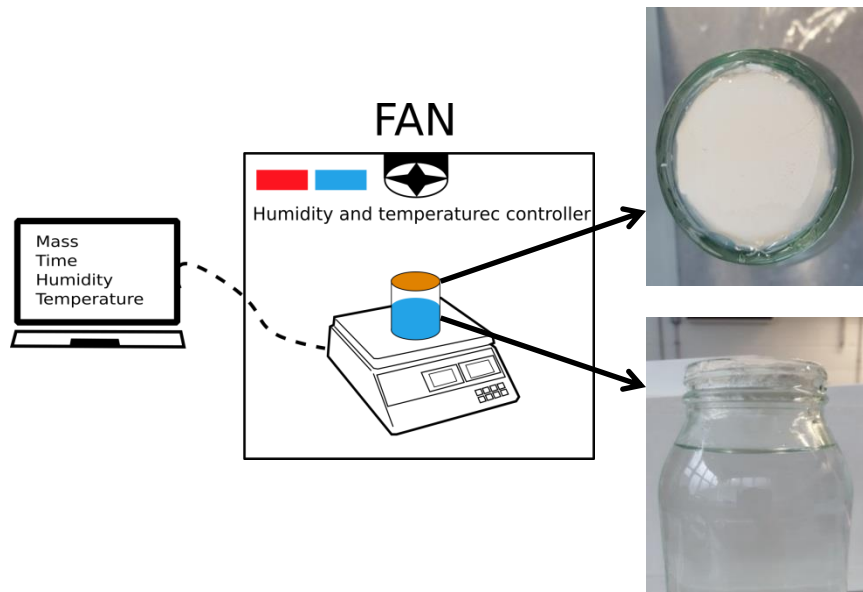


Figure 3.29 Cup method test illustration

Chapter Four: Microstructure of clay-PVA aerogels and mechanisms formulating mechanical and physical properties

Abstract

This Chapter examines the behaviour of clay aerogel and its composites under controlled conditions, and their morphology and microstructure are extensively investigated to understand the contribution of constituents to the characteristics of clay aerogel composites and mechanisms of formulation and interactions. Their limitations examined and inspected. The clay and poly (vinyl alcohol) (PVA) aerogel composites presented an anisotropic layered morphology that can be tailored by freezing directions. The layers are structured depending on the freezing direction (Horizontal or Vertical), leading to different physical and mechanical properties. The aerogels exhibited high moisture absorption mostly through the solid hydrophilic solid content and only partially through the capillary voids. High moisture absorption resulted in significant damage and shrinkage due to the disintegration of the microstructure. The aerogel composites exhibited extremely low vapour resistivity (7.9 MNs/gm) comparable to the resistivity of air, while the anisotropic structure resulted in different absorption coefficients across the faces of the prism. The results showed that the thermal conductivity of the aerogel composites is highly sensitive to the freezing direction as well as moisture absorption in which for every 0.1 g of moisture absorbed the thermal conductivity increased by 2.5%.

Highlights:

- Clay-PVA aerogels have an anisotropic microstructure that influences the physical and mechanical properties;
- Mechanisms of clay aerogel formulation and behaviour and performance;
- Mass of clay aerogel composites can increase by more than 33% in high humidity conditions leading to the disintegration of the hydrophilic solid content;

- Vertical freezing can result in stronger aerogels with higher thermal conductivity, while horizontal freezing resulted in, weaker aerogels with lower thermal conductivity;
- The thermal conductivity is significantly hindered by high moisture absorbance and can result in a 30% increase in thermal conductivity.

4.1 Introduction

An effective porous insulation material is characterised with having low cost, good compression strength, good water vapour absorption and transmission, and most crucial having low thermal conductivity (K-value) [217]. Therefore it is critical to understand the morphology and microstructure of such materials and their influence on these properties. The durability and performances of all building insulations especially porous materials, are highly affected by the moisture content and sorption properties [218]. Several durability issues can arise with high moisture absorption into an insulation material, causing a significant increase in the thermal conductivity by more than more than 50% for every 1 (v/v%) of moisture absorbed and hence remarkably decrease the thermal resistance [7,8]. High moisture content can also create an ideal environment to boost mould and mildew growth, causing physical damage to the material. Due to the highly hydrophilic nature of the components of the aerogel (i.e. sodium montmorillonite and PVA), it would be expected that final aerogel composite would tend to absorb a high amount of moisture and water [198].

The objective of this Chapter is to investigate the morphology of clay-PVA aerogels and its influence on the physical and mechanical properties, such as the mechanisms resulting in water and moisture absorption, and change in compressive modulus in order to create a better understanding of how these materials would perform as an insulation material, when used as in a building envelope of various geographic locations, i.e. they may be exposed to different humidity conditions, and to fully address the limitations and behaviour of the clay-aerogel composites in the next five Chapters.

4.2 Experimental work

Clay-PVA aerogel composites were developed as described in Section 3.2.1. Stock solutions of clay and PVA are prepared and the required amount of each are mixed together at low shear for 24 hours to prepare a precursor aerogel suspension of of 2.5 wt.% clay and 2 wt.% PVA (Chapter 3,

Section 3.2.3.2) without any additives or chemicals. The final aerogel suspension is either poured into aluminium foil moulds for vertical freezing or poured into hybrid moulds for horizontal freezing (Chapter 3, 3.2.1.2). The frozen samples are finally freeze-dried (Chapter 3, 3.2.1.3). Testing and characterisation is carried out according to Chapter 3, Section 3.3.

4.3 Results and discussion

4.3.1 Factors influencing aerogel microstructure

4.3.1.1 Microstructure of clay and PVA aerogels

Figure 4.1 shows the morphology of either clay or PVA aerogels. It is apparent that the freezing process is the dominant factor in influencing the morphology of aerogel and its composites prepared.

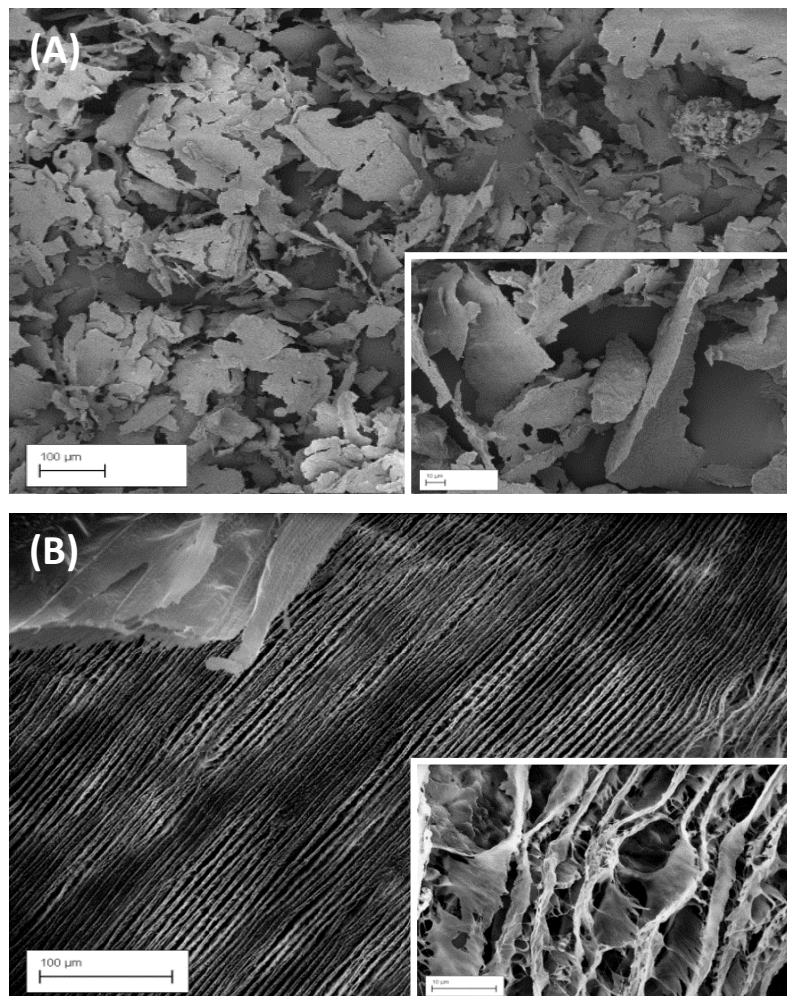


Figure 4.1 (A) Microstructure of clay aerogel (B) Microstructure of PVA aerogel

The sublimation process of water results in a structure that is a representation of the grain boundaries filled with air. During the freezing process of the clay suspension, the ice-growth will assemble and trap the silicate sheets lateral to the direction of growth, creating a laminar structure. The transition of clay particles to a sheet-like architecture associated with clay aerogels can be seen in Figure 4.1A. Due to the weak, Van der Waals forces between the silicate sheets, the structure collapsed on itself when handled and lost its dimensional stability, transitioning into a powder-like material. The PVA aerogel showed a highly layered architecture (Figure 4.1B) with high connectivity between the layers (Figure 4.1B inset). The sample was rigid enough to be handled without distorting the structure due to the strong covalent bonds formed between individual PVA chains. However one of the greatest setbacks of PVA aerogels as an insulation material is their high thermal conductivity and extremely poor dimensional stability.

4.3.1.2 Clay-PVA aerogel microstructure

As discussed the freezing is the dominant step in influencing the microstructure. However, from the SEM of the raw materials (Figure 4.1), it seems that PVA as a raw material is more significant in influencing the final aerogel composite layered morphology (Figure 4.2) as it produced a highly layered architecture.

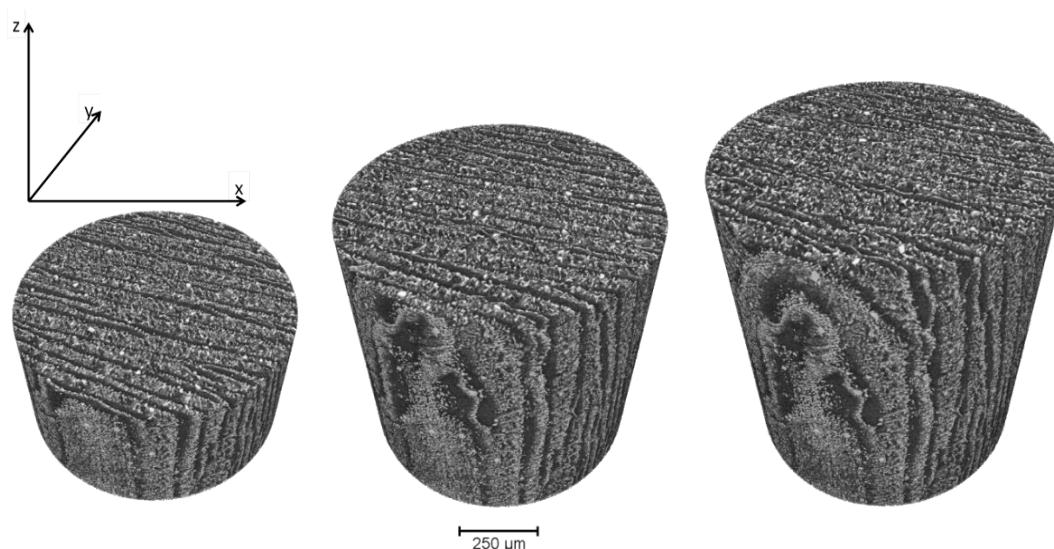


Figure 4.2 Cross-section of clay-PVA aerogel composites along the freezing direction

This is expected as the purpose of the PVA is to hold or “glue” all the clay together to form the bulk aerogel. This is part of reason that PVA is selected for the production of clay aerogel. While the clay acts as the filler which is responsible for enhancing the overall properties to overcome high thermal conductivity and extremely poor dimensional stability. The morphology of the clay-PVA aerogel composites is characterised by an anisotropic lamellar architecture (Figure 4.3). Therefore their properties are direction-dependent and can vary largely accordingly. Two main features exist within the morphology of clay-PVA aerogel composites: One is the texture and morphology of the individual layer surface (Figure 4.4A), and the other is the morphology of the layers edges and their connectivity (Figure 4.4B). The layers are aligned in the direction of the freezing direction along the z-axis travelling from the bottom to the top of the samples during vertical freezing (Figure 4.2). The aerogel composite is characterised with open pores that are the negative of the ice grain boundaries along the freezing direction (Figure 4.5B).

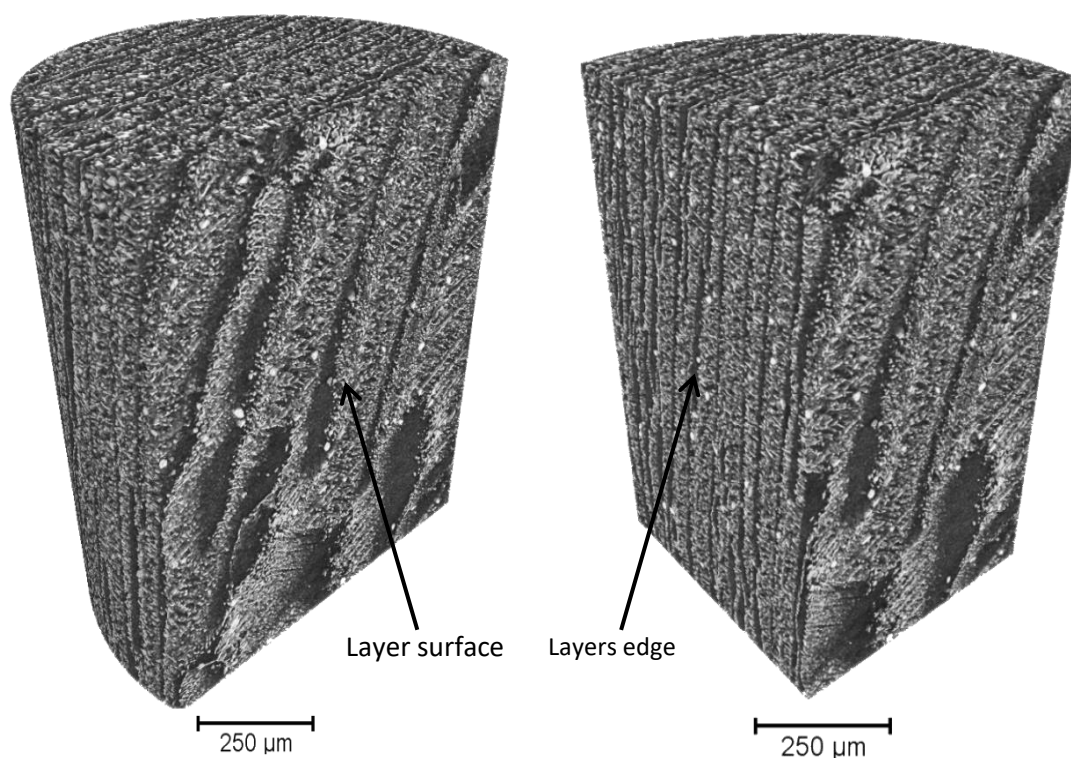


Figure 4.3 3D isotropic microstructure scan of clay-PVA aerogel composite (Gray parts represent empty space (Air), and bright/luminous part represent the solid phase)

Although an anisotropic structure is observed the porosity along each axis are almost identical, having $85.70\pm 0.25\%$, $85.71\pm 61\%$, and $85.66\pm 0.23\%$, porosity across the X, Y and Z- axis, respectively (Figure 4.5A). The overall porosity of the clay-PVA aerogels is $85.69\pm 0.36\%$. This high porosity is responsible for the bulk properties of the clay-PVA aerogel composites, such as its low thermal conductivity and low density. The pore size distribution for an aerogel sample (Figure 4.5C), ranges greatly, ranging from 1 to 35 micrometres. The highest number of pores clusters between 10 to 6 micrometres. Due to the open pore nature of the aerogel composite, the reported average pore size is actually the distance between the aerogel layers (Figure 4. 4B).

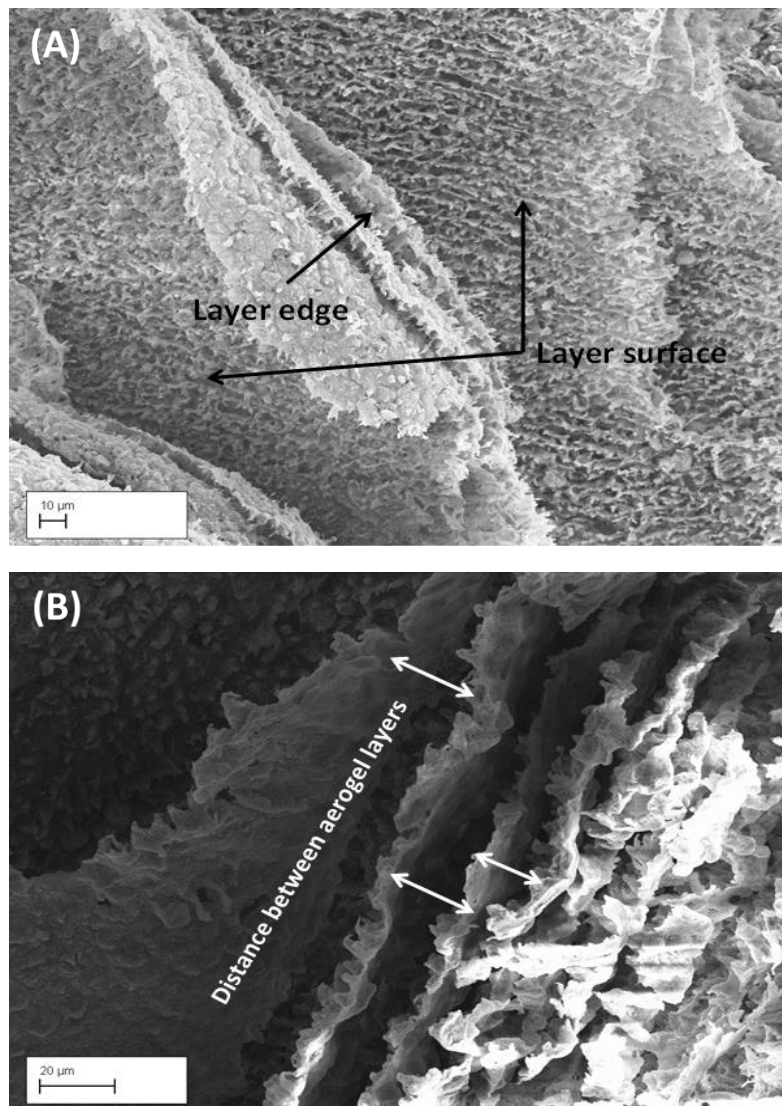


Figure 4.4 (A) Two main features of clay-PVA aerogel composite (B) Spacing between aerogel layers

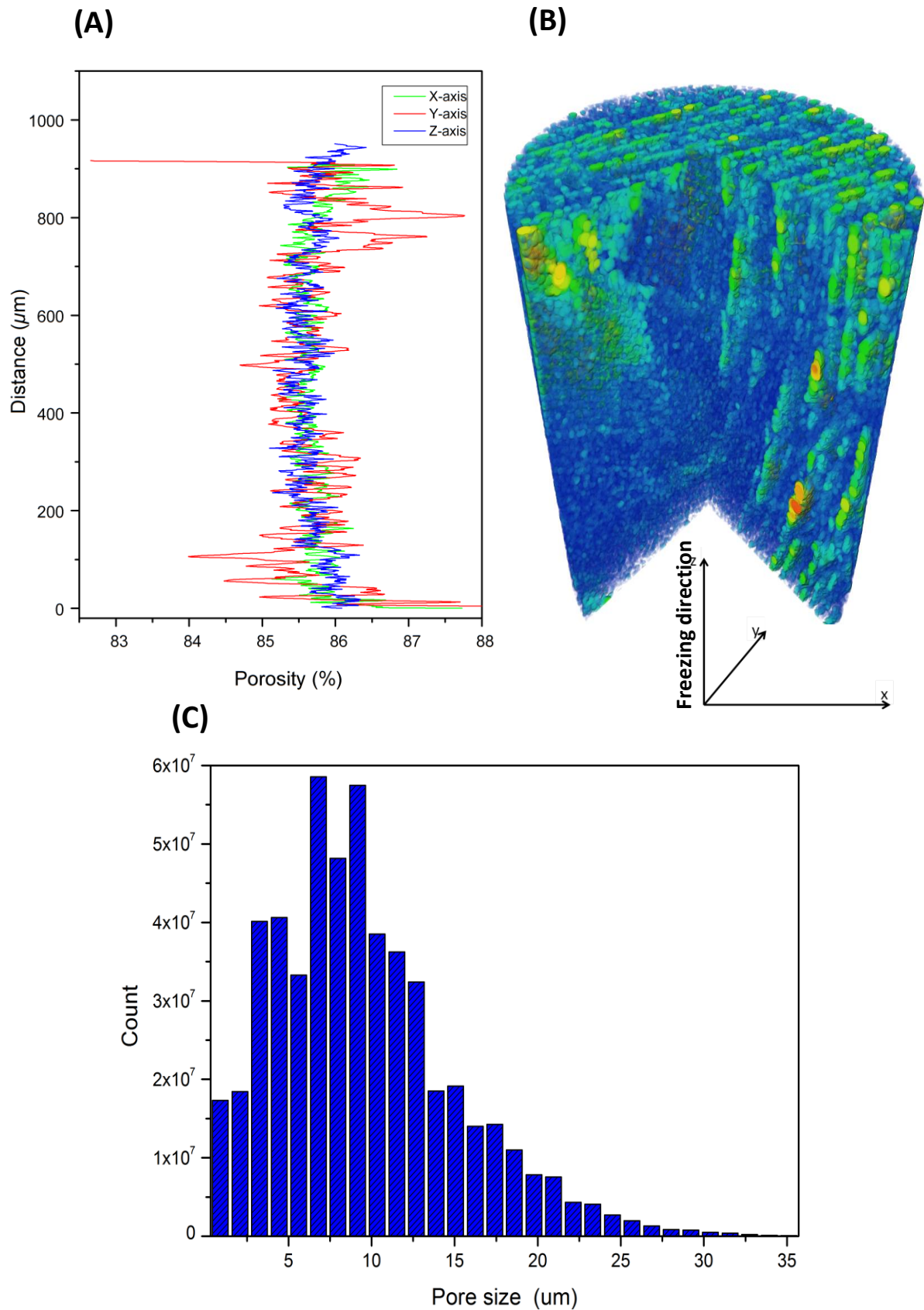


Figure 4.5 (A) Porosity profile along each axis, (B) Porosity and pores model used for pores analysis (Dark blue represents solid phase, and lighter colours represent air pockets) and (C) Pore size distribution within an aerogel composite sample

4.3.1.3 Influence of freezing direction on clay-PVA aerogel microstructure

The orientation of the aerogel layers is a consequence of the freezing process. Depending on the freezing direction, the orientation or the direction of the layers can be tailored. This can influence the mechanical and physical properties of the clay aerogel composites. Freezing the sample horizontally will structure the layers parallel to the top and bottom surface of the aerogel sample (Figure 4.6A). Vertical freezing will structure the layers perpendicular to the bottom and top surface of the aerogel (Figure 4.6B). The randomness nature of the formation of ice crystals and random nucleation points at impurities, will result in distribution to the orientation as illustrated in Figure 4.7B and D compared to a theoretical structure in figure 4.7A and C. By altering the orientation, the ability of the aerogel to respond or react to physical and mechanical inducements is altered as illustrated in Figure 4.7. Horizontal freezing can result in a more tortuous path for heat to pass through the samples due to higher resistance from the solid phase. This orientation will, however, have lower mechanical properties due to less resistance from axial loadings.

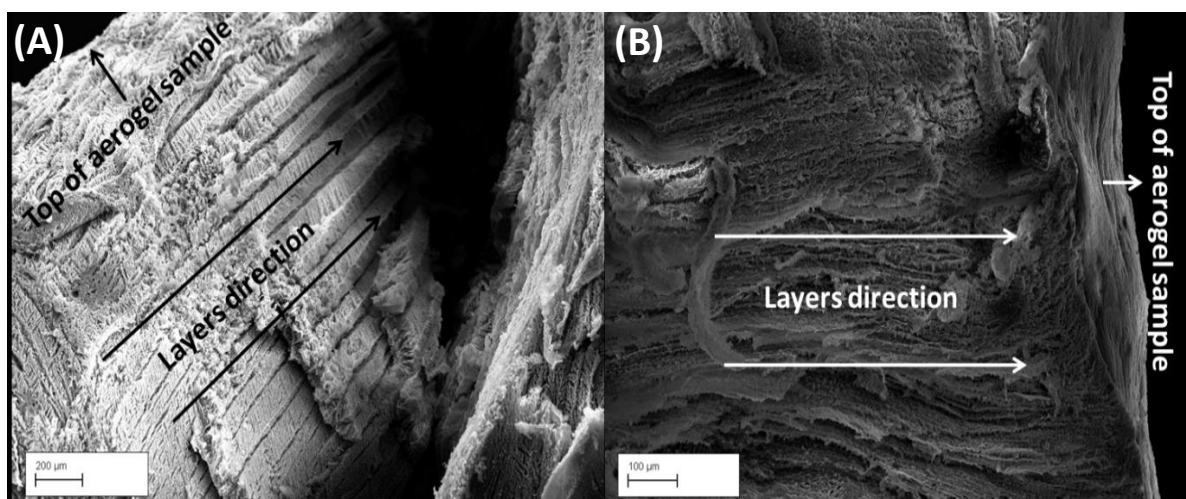


Figure 4.6 Layers structured of clay-PVA aerogels: (A) parallel to the bottom and top surfaces of the aerogel and (B) perpendicular to the bottom and top surfaces of the aerogel

Vertical freezing will result in structure and networks easier for heat to flow across the sample through the path of least resistance between the layers and thus less heat travelled through the

solid content. This orientation is capable of transferring the axial load more efficiently as the layers are parallel to the direction of the load.

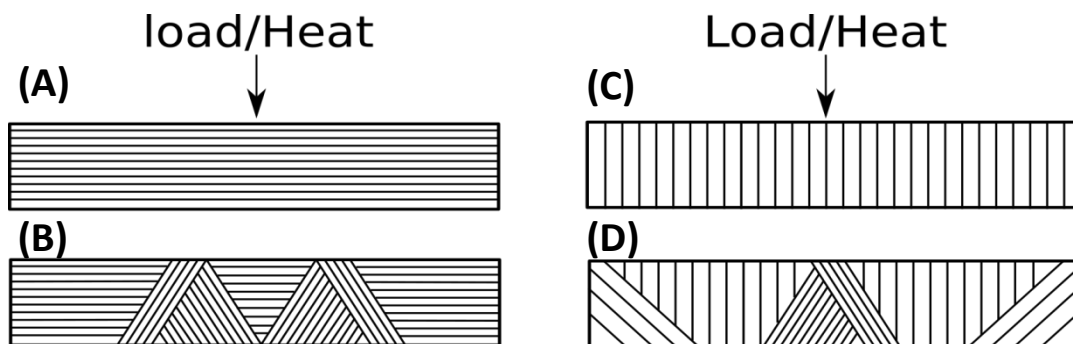
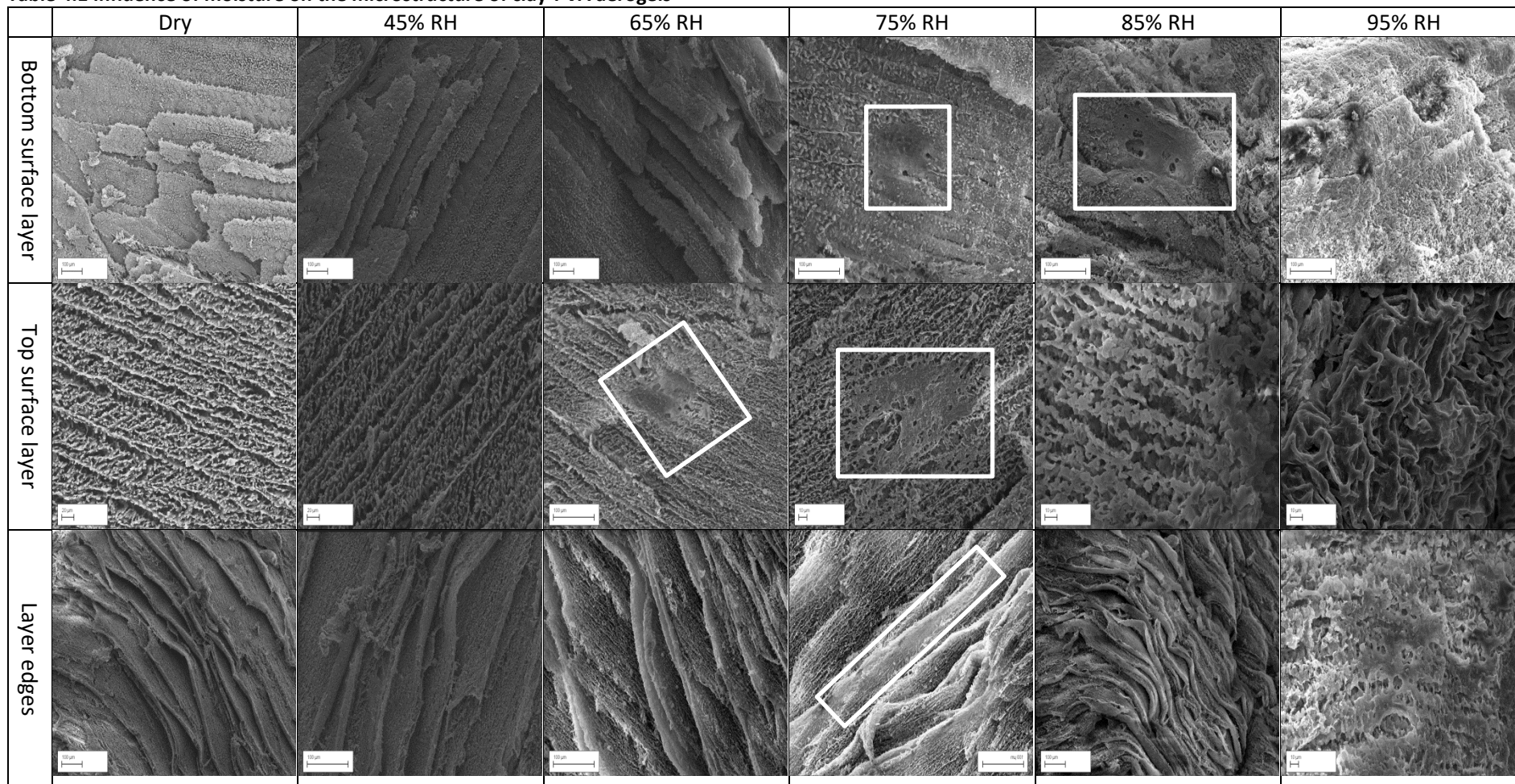


Figure 4.7 (A) Idealised orientation from horizontal freezing, (B) Realistic structure from horizontal freezing, (C) Idealized orientation from vertical freezing and (D) Realistic structure from vertical freezing

4.3.1.4 Influence of moisture absorption on clay-PVA aerogel microstructure

The morphology of clay aerogel composites are highly influenced by moisture. Absorption of high moisture through the solid phase can cause the clay and PVA to disintegrate. This is expected due to the hydrophilic nature of the components. Due to the anisotropic nature of the aerogel structure, the moisture transfusion into the aerogel pores is influenced by the morphology (Table 4.1). The dry structure and its lamellar characteristics have been discussed in Section 4.3.1.2. Exposing the samples to 45%RH resulted in no change to morphology, suggesting that the moisture at 45%RH is only filling the open pores through capillary absorption and no saturation occurs for the solid content to absorb the moisture. At 65%RH, disintegration begins to be on the top surface layers, while the bottom layer and the layer edges showed almost no damage. This might be due to the fact that the layer surface has the highest roughness and surface area within the aerogel (Figure 4.4A), thus trapping the moisture on the layer surface's open pores and eventually, the hydroxyl groups of solid phase will begin to absorb the moisture. At 75%RH, the damage becomes more evident, resulting in damage at the bottom of the layer, however, this is most likely the damage from the surface travelling through.

Table 4.1 Influence of moisture on the microstructure of clay-PVA aerogels



The layer edges at 75%RH begin to disintegrate from the edges towards the inner of the aerogel. At 85%RH severe disintegration takes place (Table 4.1). The bottoms of layers begin to curl up together, causing shrinkage. The top of the layer surface begins to fuse together into an almost solid structure, and the layers distance between the aerogel layers begin to shrink and get closer together. This might be a result of the layers getting curled up. At 95%RH almost nothing resembling a layered architecture remains. The bottom layers completely fuse together into a solid structure, and all the pores and surface roughness on the top of the layer are diminished. The layers edges begin to join together to form one single layer. Overall it can be understood that moisture absorption through the solid content begins at the surface of the top layer, in which the open pores begin to trap the moisture, inducing absorption through the solid phase followed by shrinkage due to curling up of the layer.

4.3.2 Moisture absorption of clay-PVA aerogel

4.3.2.1 Moisture absorption of clay/PVA aerogels

Either clay or PVA aerogels with a composition of 2.5 and 2 wt.% respectively have been prepared to investigate the contribution of constituents to the moisture absorption of aerogels. PVA is known to be highly hydrophilic due to their hydroxyl groups that allow for hydrogen bonds to be created with water, while the naturally occurring inorganic cations that exist within the layers of the clay is responsible for the hydrophilic clay surface. Figure 4.8 shows the increase in the mass of either clay or PVA aerogels at various humidity conditions. On average the clay aerogel absorbed 24.5% more than the PVA across all humidity conditions. This might due to the fact that clay aerogels did not form any coherent structure resembling aerogels (Figure 4.1A), such allowing moisture to cover most of the materials while the PVA aerogel structure (Figure 4.1B) would create a more tortuous path for moisture to diffuse into the structure. The combinations of both clay and PVA to produce aerogel

composites resulted in a reduction of the mass increase (Figure 4.8) even though the solid is increased to almost the double (2.5 wt.% clay and 2wt.% PVA).

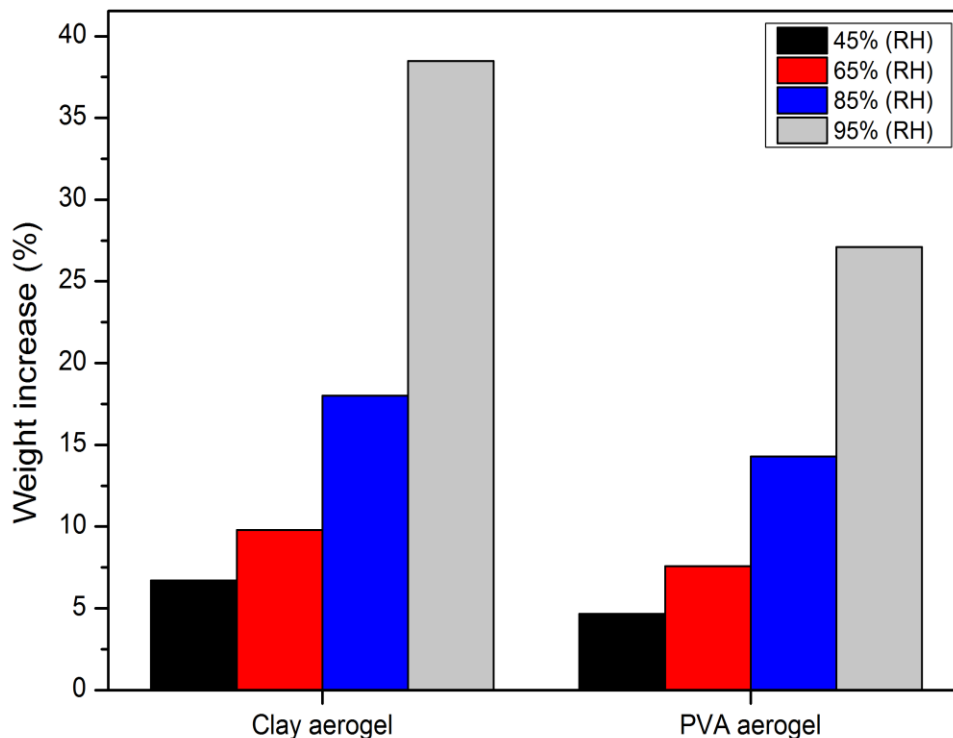


Figure 4.8 Weight increase of either clay or PVA aerogels

This may be considered counterintuitive but can be explained by the formation hydrogen bonds between the inorganic cations clay and the hydroxyl groups of PVA, which would limit the interactions with the water molecules. The incorporation of clay as a filler would create more barriers and tortuous paths in the solid phase and generate a microstructure with high surface area and roughness (Figure 4.4). This may create more difficulties in diffusion through the composite as a whole. A comparison of the roughness of the microstructure of clay-PVA aerogel composites (Figure 4.4) to either counterparts, shows that either PVA or clay aerogels have less surface roughness (Figure 4.1A and B). More details in the behaviour of clay-aerogel composites are given in next Section.

4.3.2.2 Moisture absorption of clay-PVA aerogels

The clay-PVA aerogel composites are expected to absorb high amount of moisture due to their hydrophilic nature and high porosity ($\rho_{\text{dry}} = 0.048 \text{ g/cm}^3$). The aerogel composites absorbed only 2% of their weight at 45% RH (Figure 4.8), resulting in an increase in density ($\rho_{\text{wet}} = 0.049 \text{ g/cm}^3$); at this point the moisture is mostly absorbed through the capillary and fill the pores of the aerogel composites. It can be calculated that the 2% moisture absorbed by a (4 cm^3) sample would be equivalent to 0.0038 g of moisture, which is almost the value (90%) of the weight of moist air (0.0045 g) that would fill the voids of the aerogel (86% porosity $\approx 3.44 \text{ cm}^3$ and taking that the density of moist air at 23°C and 45%RH as 0.00125 g/cm^3). At 65 %RH, the weight increased by 9% (Figure 4.8) which is a 6% increase from 2% resulting in an increased density of 0.052 g/cm^3 . At this point, the moisture may completely fill the capillary pores, and 64% of the weight increase can be attributed to the absorption of the solid content (0.0038 g through the pores and 0.012g through the solid phase).

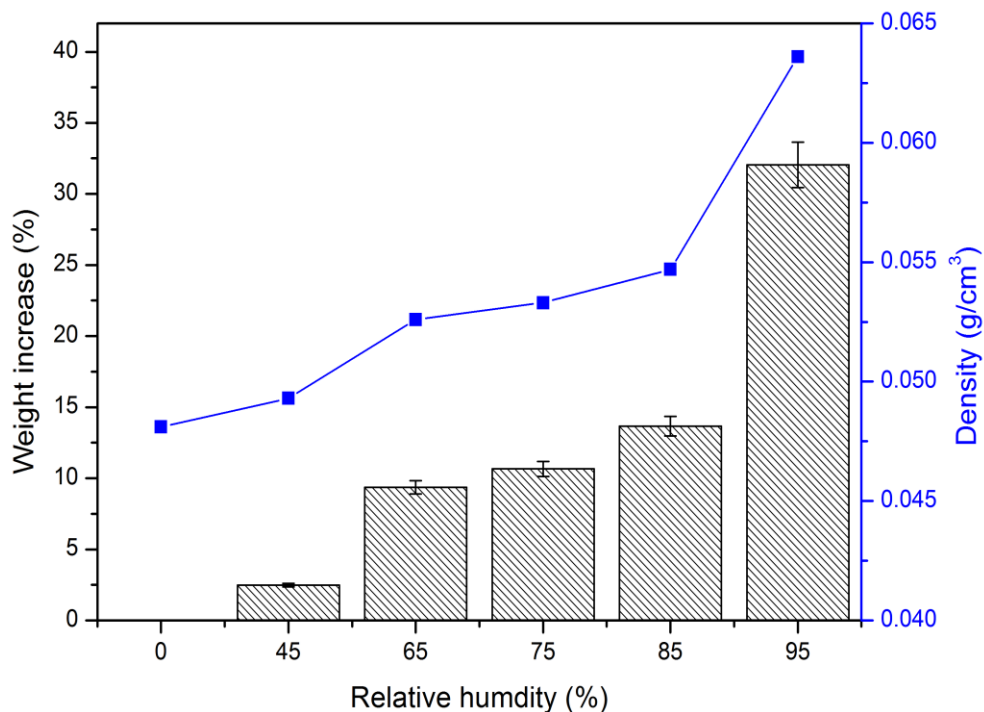


Figure 4.9 Weight and density increase of clay-PVA aerogel composites with a change in humidity

At 75 and 85% RH the weight increased by 11 and 14% respectively, an average increase by 80%. The solid content was responsible for 80.8% of the weight increase at 75% RH and 84% at 85% RH, resulting in an increase in density to 0.053 and 0.054 g/cm³ respectively. At 95%RH, the mass witnessed the highest weight increase by 32% and the steepest increase by 93% from a 2% weight increase. At 95% RH the solid content was responsible for 94% of the weight increase and only 8% of the weight increase was due to the capillary of filling of the pores. The steep increase in density (0.064 g/cm³) can also be attributed to the shrinkage (i.e. < volume) and not just increase in weight as a result of the microstructure disintegrating (Table 4.1).

4.3.2.2 Vapour resistance of clay-PVA aerogels

Table 4.2 shows both the vapour resistance and water vapour resistance factor “u-value” of the vertically frozen aerogel composites. The aerogels had a very low vapor resistance factor of only 1.58 (7.9 MNs/gm) using the dry cup arrangement, which is only slightly higher than u-value of air, 1 (5 MNs/gm). This is expected due to high porosity of the aerogel and the parallel layer alignment to the direction of the diffusion. In the wet cup arrangement, the aerogel exhibited a vapour resistance comparable to the closed cell expanded polystyrene, which is an effective vapour barrier. The contradictory in the results between the dry and wet cup arrangement may be attributed to the fact that the wet cup is exposed to 85% RH and as discussed earlier at 85% RH the moisture will be absorbed through the capillaries which in turn result in a collapse of the pores and the layered architecture (Table 4.1) of the aerogel composites, thus creating a barrier preventing vapor to pass through the open pores of the aerogel.

Table 4.2 Water vapor properties of clay-PVA aerogel composites

	Dry Cup	Wet Cup
Water vapour resistance factor (u-value)	1.58	22.31
Vapour resistivity (MNs/gm)	7.90	111.57

4.3.2.3 Water uptake of clay-PVA aerogels

The aerogel composites exhibited very high water absorption coefficients across the different faces of the prism (Table 4.3). The water absorption coefficient was measured across the different faces of the aerogel composite prism (Base, lateral side and bottom side), resulting in different values depending on the orientation (Table 4.3) with, the highest value up to $2.16 \text{ kg m}^{-2}\text{s}^{-1/2}$, which is significantly higher than values of EPS for instance which have a typical value of $\pm 0.0025 \text{ kg m}^{-2}\text{s}^{-1/2}$.

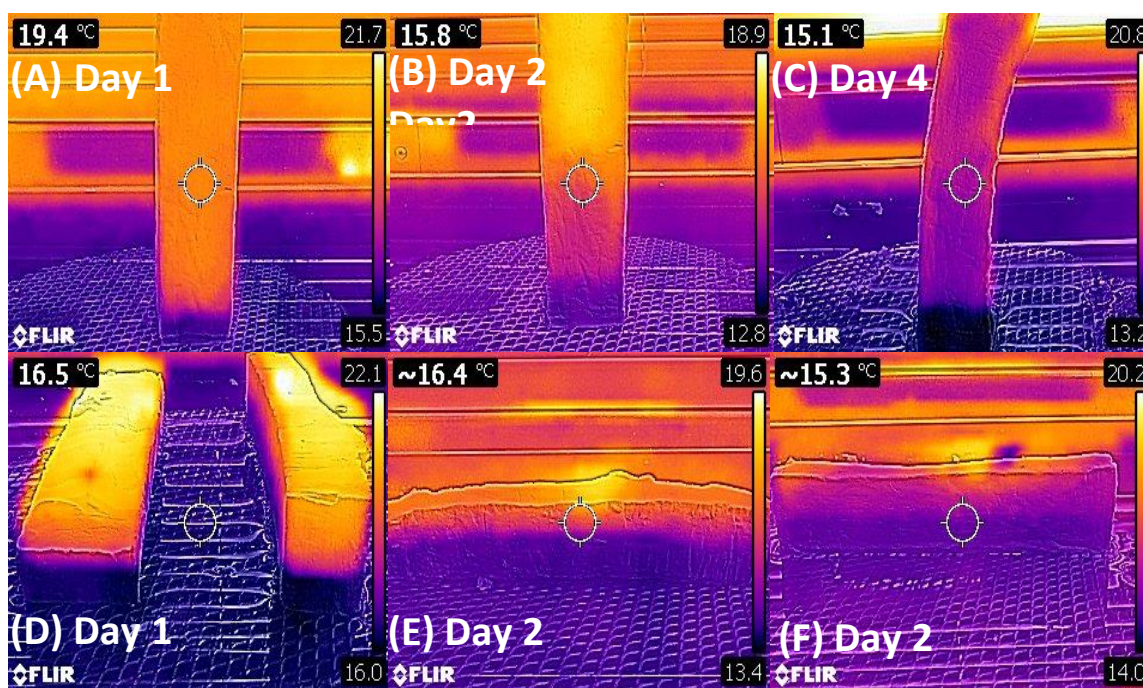


Figure 4.10 Water uptake of clay aerogel composite prisms: (A-C) through the base (Cross-section) , (D) from bottom face and along the lateral side, (E) from bottom face and (F) along the lateral side

Such high values are expected as the predominantly water transport is through the hydrophilic solid content (Clay and PVA) matter in addition to those through the capillaries. Measuring the absorption

coefficient through the base (cross-section) resulted in the lowest absorption coefficient (A) of 0.99 kg m⁻²s^{-1/2} and an apparent moisture diffusivity (*kapp*) of 9.90×10⁻⁰⁵ m² s⁻¹. The water took almost four days to reach the top of the sample (Figure 4.10A, B, and C). This is expected as water has to travel further against gravity, and more importantly water is travelling along the Y-axis (Figure 4.2), and thus has to travel from layer to layer across the open pores. The bottom face (Figure 4.10E) had an absorption coefficient (A) of 1.14 kg m⁻²s^{-1/2} and an apparent moisture diffusivity (*kapp*) of 1.31×10⁻⁰⁴ m² s⁻¹. While across the lateral face the aerogel composite witnessed the highest absorption coefficient and apparent moisture diffusivity of 2.16 kg m⁻²s^{-1/2} and 4.71×10⁻⁰⁴ m² s⁻¹, respectively. The variation can be explained by the anisotropic microstructure (Figure 4.3) of the aerogel, in which the microstructure of lateral face (X-axis, Figure 4.2) will absorb water uninterrupted and continuously from bottom to top through the solid phase and capillaries. Moisture will be able to travel through the open pores of the sample, giving the highest value.

Table 4.3 Liquid water transport properties of clay aerogel composites

	A(kg m ⁻² s ^{-1/2})	<i>kapp</i> (m ² s ⁻¹)
Cross section (Base)	0.99	9.90×10 ⁻⁰⁵
Lateral face	2.16	4.71×10 ⁻⁰⁴
bottom face	1.14	1.31×10 ⁻⁰⁴

4.3.3 Influence of clay-PVA aerogel microstructure on the mechanical properties

The morphology of clay aerogel composites can be tailored by altering the freezing process (i.e. vertical or horizontal freezing) as previously discussed in Section 4.3.1.3. The frozen aerogel sample is characterized with a lamellar structure parallel to the freezing direction (Figure 4.7). Therefore a horizontal frozen sample will have the layers parallel to the load and thus will be able to transfer axial load more effectively from top to bottom acting as columns, resulting in a compressive modulus of

0.48MPa (Figure 4.11). Having the laminar morphology loads aligned perpendicular to an axial-load will transfer loads less effectively from top to bottom due to the deformation of the individual lamellar layers at a micro level, which is expected due to the intrinsic brittleness of the bulk material, resulting in a compressive modulus of 0.16MPa (Figure 4.11), a 67% drop in the compressive modulus.

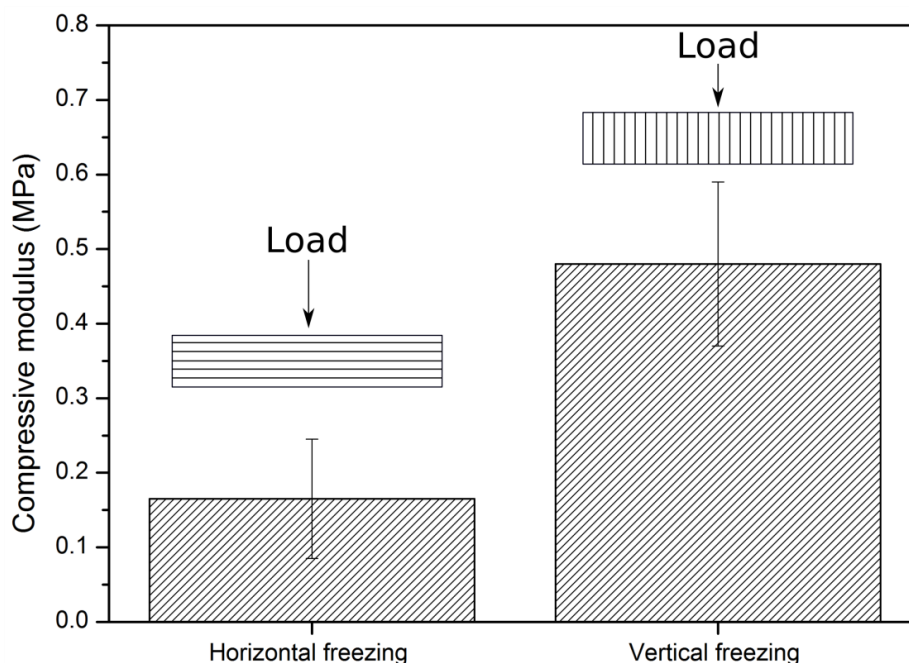


Figure 4.11 Influence of freezing direction on the compressive modulus

4.3.4 Thermal conductivity of clay-PVA aerogels

4.3.4.1 Influence of freezing direction on the thermal conductivity of clay-PVA aerogels

The thermal conductivity of clay aerogel composites is mostly governed by the microstructure. By altering the microstructure, the main mechanism of heat transport through conduction and convection can be altered, and thus influence the thermal conductivity (Figure 4.7). Vertical freezing will orient the aerogel layers parallel to the heat flow. This will allow the convection process of air from the top to bottom of the aerogel with little resistance, and conduction through solid phase will have a more direct route through the aerogel, resulting in a thermal conductivity of 0.039 W/(m.K) in

this study (Figure 4.12). Horizontal freezing will orient the aerogel layers perpendicular to the heat flow, which will restrict the convection of air through the sample, and conduction through the solid phase will be mostly through small struts that connect the layers together resulting in a thermal conductivity of 0.033 W/(m.K) (Figure 4.12).

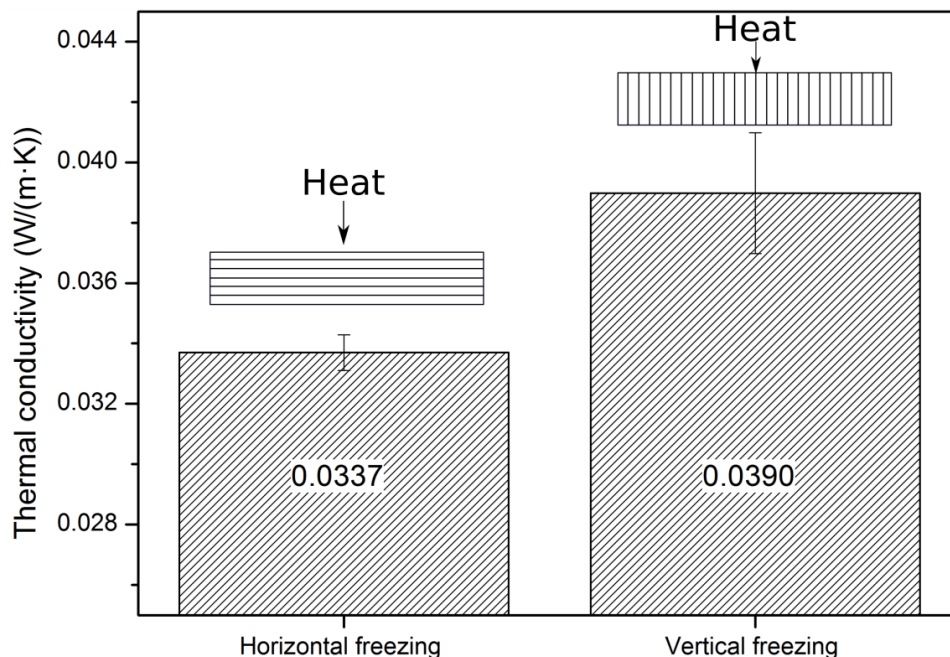


Figure 4.12 Influence of freezing direction on the thermal conductivity

4.3.4.2 Influence of moisture absorption on the thermal conductivity of clay-PVA aerogels

A direct relationship exists between the mass increase the thermal conductivity, showing a drastic effect of moisture change on the thermal conductivity of clay-PVA aerogel composites (Figure 4.13).

The vertical frozen samples were vacuum dried at 80°C for 48 hours to make sure that they are completely dry, and then their thermal conductivity was measured to be 0.038 W/(m.k). Exposing the aerogel composites to 45% RH for 24 hours resulted in a 3.5% increase of thermal conductivity to 0.040 W/(m.k), at 65% RH it increased by 7.5% to 0.042 W/(m.k), at 75% RH by 9.6% to 0.043 W/(m.k), at 85% RH by 13.6% to 0.045 W/(m.k) and at 95% by 30% to 0.053 W/(m.k).

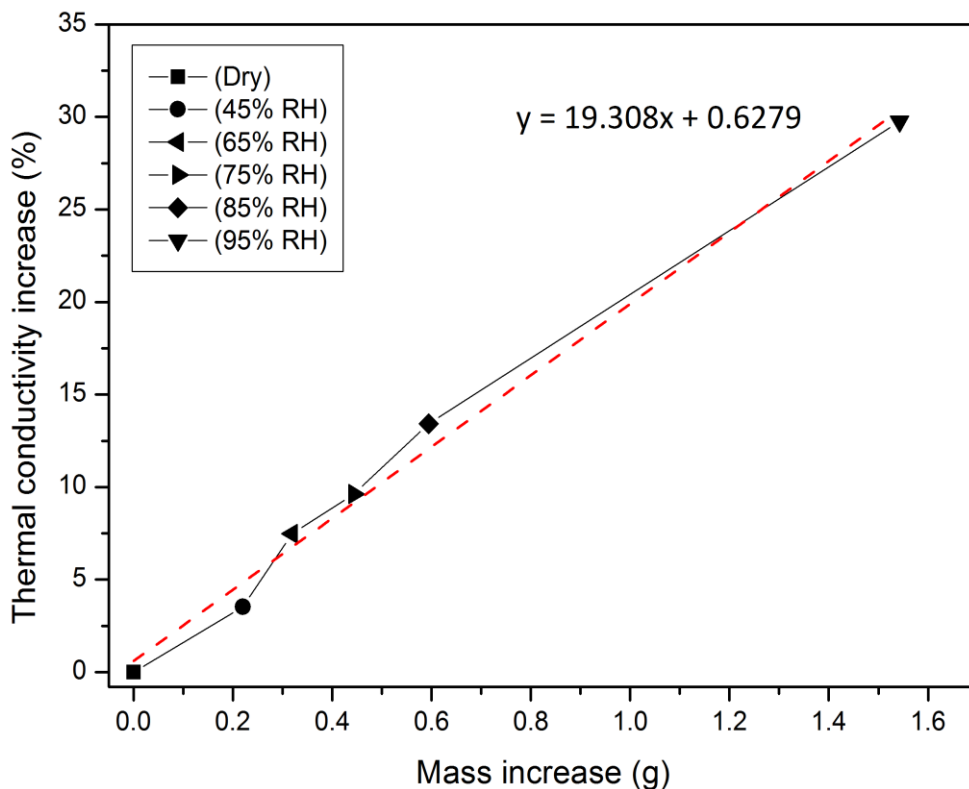


Figure 4.13 Influence of moisture absorption on the thermal conductivity

From the linear equation (Figure 4.13) it can be concluded that for every 0.1 g of moisture absorbed by the aerogel composites the thermal conductivity rises by about 2.5% or by 0.0011 W/(m.K). This is true across all humidity ranges except for the sample exposed at 45%RH resulted in an increase of 1% for every 0.1g. This may be related, as discussed earlier, to the fact that most of the moisture absorbed is only through the capillaries and not through the solid content of the aerogel composite. However, the influence of moisture on the microstructure has to be taken into consideration, especially the damage at high moisture contents in which the lamellar clay aerogel microstructure is disintegrated into a solid structure with a few pores. This may explain the steep increase from 85% RH to 95%RH.

4.4 Interim conclusions

Clay-PVA aerogels were characterized with an anisotropic layered structure that was ordained with the direction of freezing. Depending on the freezing direction the mechanical and physical properties could be altered. Vertical freezing resulted in stronger aerogels with higher thermal conductivities than horizontal freezing that had 67% lower compressive modulus. The clay-PVA aerogel exhibited a 32% increase in their weight at 95% RH in 24 hours with an increase in density from 0.045 to 0.063 g/cm³. 90% of the moisture absorbed at 45%RH was through their capillaries while beyond that the aerogel began to absorb moisture through the hydrophilic solid content being responsible for 94% of the moisture absorbance at 95%RH. The high moisture of clay-PVA aerogels could have a significant influence on the microstructure, transitioning the structuring from a layered morphology to a completely solid structure with almost no pores. The thermal conductivity was also highly affected by moisture and increased from 0.038 W/(m.k) after being vacuum dried to 0.053 W/(m.k), a 30% increase at 95%RH which was a 2.5% for every 0.1 g of moisture absorbed by the aerogel. The aerogel composites had very low vapour resistance factor (u-value) of 1.58 for dry cup arrangement. This was very comparable to air which has a value 1 due to the high porosity of the aerogel composites (85% porosity). The anisotropic morphology had a direct influence on the water absorption coefficient apparent and moisture diffusivity depending on the orientation. The water absorption coefficient (A) and moisture diffusivity (k_{app}) were 2.16 and 4.71×10^{-04} respectively, with the highest across the lateral face which was characterized with a lamellar elongated open structure, allowing uninterrupted water uptake.

Chapter Five: Temperature-induced nature and behaviour of clay-PVA colloidal suspension and its aerogel composites

Abstract

This Chapter investigates effect of the mixing temperature on the structure and performance of clay aerogel colloidal suspensions and their composites. Clay-PVA aerogels were prepared via an environmentally friendly freeze-drying technique. The final aerogel suspensions were subjected to various temperatures, namely room temperature (RT), 60, 70, 80 and 90 °C, in order to better understand the architecture of clay-PVA colloidal suspension and formulation mechanisms of advanced clay aerogel composites, and such develop the optimum processing parameters. This Chapter demonstrates that the mixing temperature had a significant influence on the chemical interaction of the constituents and formulation of bonding/networking of clay aerogel colloidal suspension, and hence the microstructure and performance of the clay aerogel composites; by simply controlling the mixing temperature without altering the composition or adding any additive or increasing the solid content, it was possible to significantly increase the compressive modulus by up to 7 folds without sacrificing any of the physical property of clay aerogel composites.

Highlights:

- Enhancing clay-PVA aerogels by controlling the mixing parameters (i.e. temperature);
- Mechanisms of clay aerogel microstructure and networking architectures;
- Increasing the compressive modulus by 7-folds without any increase in solid content;
- Maintaining low thermal conductivity and low density with a significant increase in strength.

5.1 Introduction

A better understanding of the interaction and behaviour of the clay and polyvinyl alcohol (PVA) particles in water as a colloidal system under varied conditions can yield improved mechanical properties and maintain physical stability of aerogel composites by merely controlling the suspension without any additional additive or change in solid content. The aim of this research is to investigate the influence of treating the colloidal system across a temperature range of 23(RT), 60, 70, 80 and 90°C to evaluate the effect on the clay aerogel suspension systems, formulation mechanisms, physical and mechanical properties of final aerogel composites.

5.2 Experimental work

Temperature induced clay-PVA aerogels were developed as described in Chapter 3, Section 3.2.2. Clay and PVA stock solution were mixed for 24 hours to prepare a formulation of 2.5 wt.% clay and 2 wt.% PVA (Chapter 3, Section 3.2.3.2). The final aerogel precursor is then mixed at room temperature (RT), 60, 70, 80 and 90°C using a hot plate magnetic stirrer for 2 hours (Chapter 3, Section 3.2.2). All mixtures were left to cool down to room temperature prior to freezing, no additives or chemicals were added. The final aerogel suspensions were vertically frozen and finally freeze-dried (Chapter 3, Sections 3.2.1.2 and 3.2.1.3). Testing and characterisation is carried out according to Chapter 3, Section 3.3.

5.3 Results and discussion

5.3.1 Clay-PVA colloidal suspension at elevated temperatures

5.3.1.1 Dynamic rheometry of clay-PVA colloidal suspension

It is witnessed that an increase in temperature resulted in an increase in both the storage modulus (G') (Figure 5.1), which is a measure of the energy stored in the material, and the loss modulus (G'') (Figure 5.1), which is a measure of the energy dissipated or lost per cycle of sinusoidal deformation

[219]. The main reason for this trend may be due to the breakup of thick passive clay particles to a more active and swollen state that fill up the majority volume of a system as illustrated in Figure 5.2.

It has been considered that the entropy gained by counter ions is liberated during swelling [220].

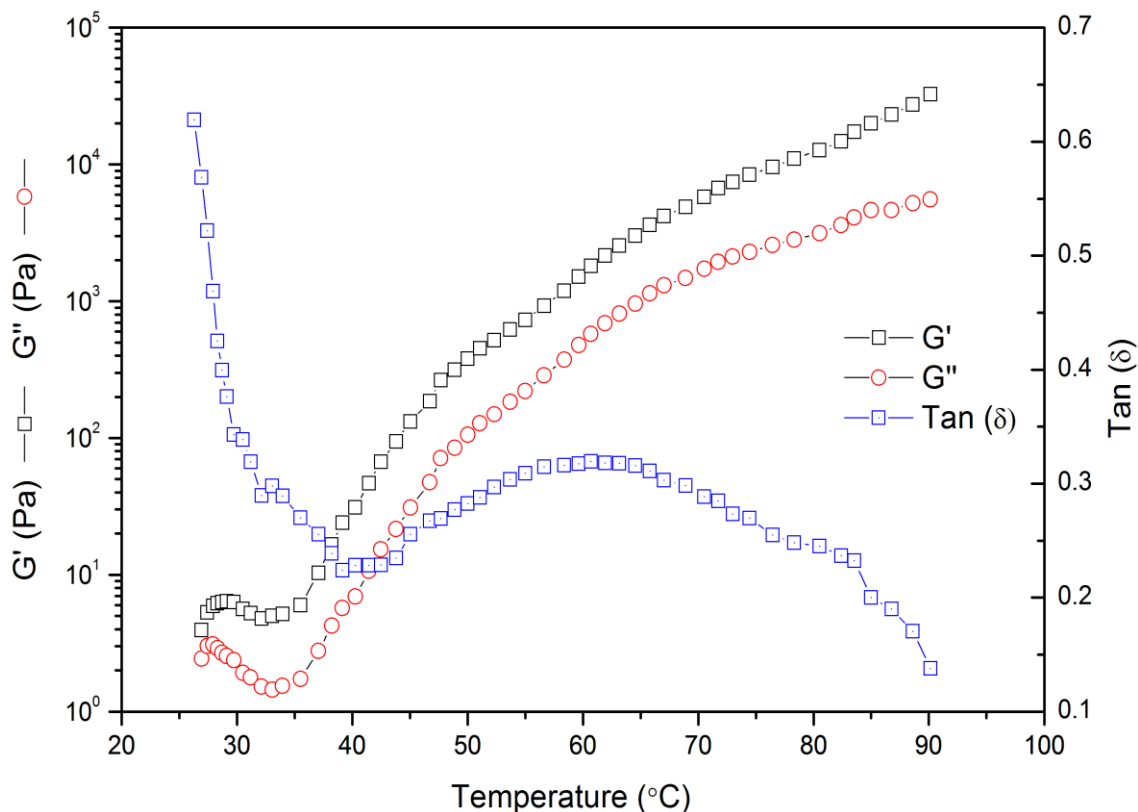


Figure 5.1 Loss and storage modules and their ratio of final aerogel suspension containing 2.5 wt. % Clay and 2 wt. % PVA

The small rise and drop of G' and G'' between room temperature and 33°C may be a result of a phase transition of PVA in which the molecular dimensions are abruptly changed and reversed at a higher critical temperature as discussed in a previous study [221]. Throughout the temperature range a constant phenomenon of $G' > G''$ indicating a highly structured order, in which the ratio of loss modulus to storage modulus ($\tan \delta$) is less than one (Figure 5.1), which suggests that the particles are highly associated and connected due to strong colloidal forces between the clay and PVA as well as Van de Waal forces, and electrostatic forces existed within the clay stacks in itself. It is evident that

Tan δ greatly drops as soon as the temperature begins to increase mainly due to the start of the breaking up of the clay stacks and also the escape of the counter ions which are mostly hydrogen ions (H^+) due to an increase in their energy. This trend continues up to the temperature of 45°C and is supported by the drop in the pH throughout the temperature range (Table 5.1) as a result of higher (H^+) concentration. Tan δ then increases from 45 to 60°C and this may be a result of the aggregation of the PVA chains which occurs at 31°C and then disaggregates above a critical temperature [221]. The aggregation of PVA begins to be reversed from 60°C, and the fluctuation in Tan δ begins to drop to as low as 0.13 at 90°C. The colloid such disintegrates into a more homogeneous connected network where the clay stacks begin to gradually absorb the unabsorbed PVA chains due to an increase in hydrogen bonds as observed through FTIR as discussed in Section 5.3.3.

5.3.1.2 pH of clay-PVA colloidal suspension

The surface charge distributions on clay minerals are anisotropic: the clay faces (bottom and top surfaces) have a negative charge which is pH independent, while the charge on the edges can be either positive or negative depending on pH value. An acidic pH will result in a positive charge on the edges which will promote a face to edge interaction, while an alkaline pH will result in a negative charge on the edges and thus promoting a face to face interaction [222]. Table 5.1 shows that for the temperature range tested, the pH is in the alkaline range and this is favourable for such materials to produce face to face interactions that are responsible for the low thermal conductivity of these materials through the solid phase. It is apparent that as the temperature increased and the counter ions released, the colloids still remained alkaline. The benefit of the increased (H^+) concentration can increase the bonding between the clay and PVA through face to face interaction.

Table 5.1 pH of final aerogel suspensions in relation with temperature (°C)

Temperature (°C)	pH
RT (23)	8.65
60	8.55
70	8.40
80	8.12
90	8.08

5.3.2 Clay-PVA colloidal suspension particle size vs temperature

The treatment with different elevated temperatures resulted in different particle size distributions of aerogel suspension, ranging from 100nm-1000nm (Figure 5.3). The colloidal systems, which were left to cool down to room temperature prior to testing, also show that the effect of the treatment (mixing) temperature was irreversible with respect to a change in temperature.

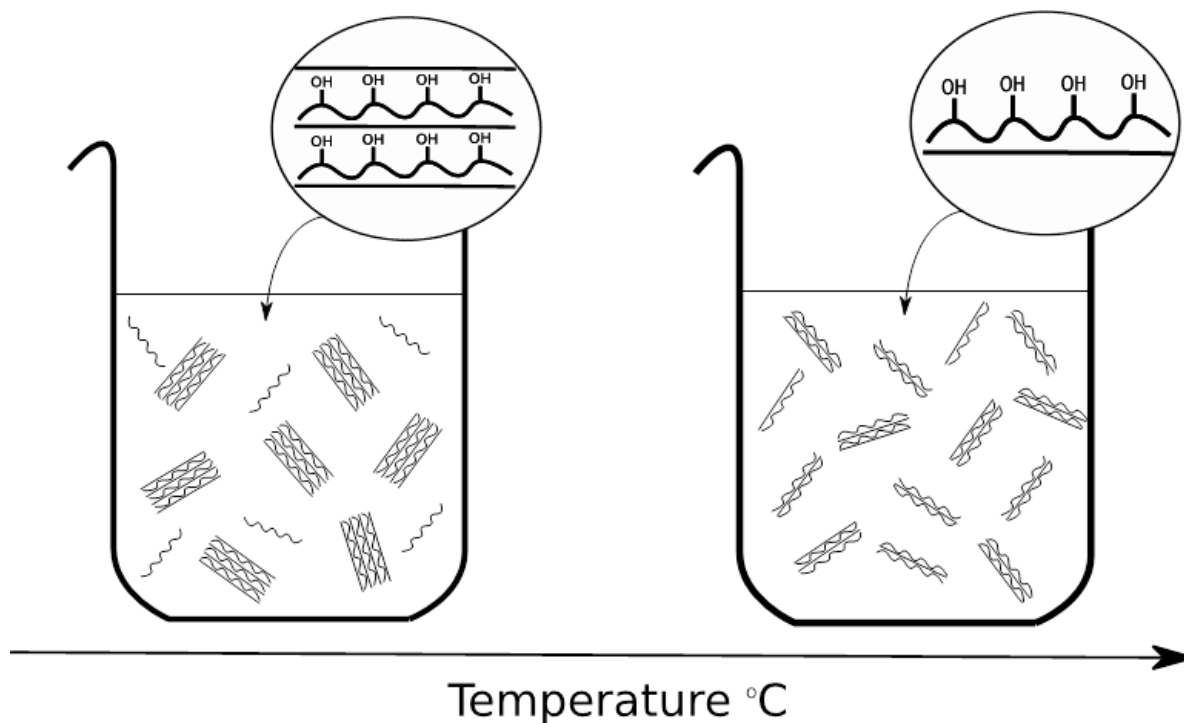


Figure 5.2 Illustration of the clay transition from large to smaller particle stacks or single unit layers

It is found that there is a highly polydispersed colloidal system at room temperature, 60°C and 70°C (Figure 5.3 A, B and C), this may be due to the coagulation of the particles into flocks and the larger particles attract other particles from the sum of the strong colloidal forces, i.e. van der Waals and electrical double bonds which are difficult to control for achieving narrow size distributions. The nanoclay (sodium montmorillonite) stock suspension has an average particle size of 176 ± 1.6 nm, and the PVA stock solution has an average particle size of 247.2 ± 8.7 nm. The final aerogel suspension mixed at room temperature had an average particles size of 499 ± 14 nm, which reflects the amalgamation of the clay and PVA particles. As the temperature increased, the D-values (Particle Size distribution), namely D90, D50, and D10 (Figure 5.3), decreased, showing a higher concentration of smaller particles and hence a smaller average particle sizes (Figure 5.3D and E), by up to 25% at 90°C to 371 nm of aerogel suspension. This is as discussed in the rheology Section (Section 5.3.1.1) mainly due to the breakup of large clay stacks into smaller clay stacks that result in smaller particles with an increase in temperature. It is apparent that a higher packing volume fraction may be obtained with increasing the temperature since the smaller particles occupy the space between the larger particles and such the ice growth during the freezing process will entrap a longer chain of particle and form a more continuous solid structure once the sample is dried. The developed materials will be able to transfer applied stress more efficiently throughout the sample and achieve enhanced mechanical properties (Figure 5.7). This also explains the slight increase in the density of the aerogel (Table 5.2).

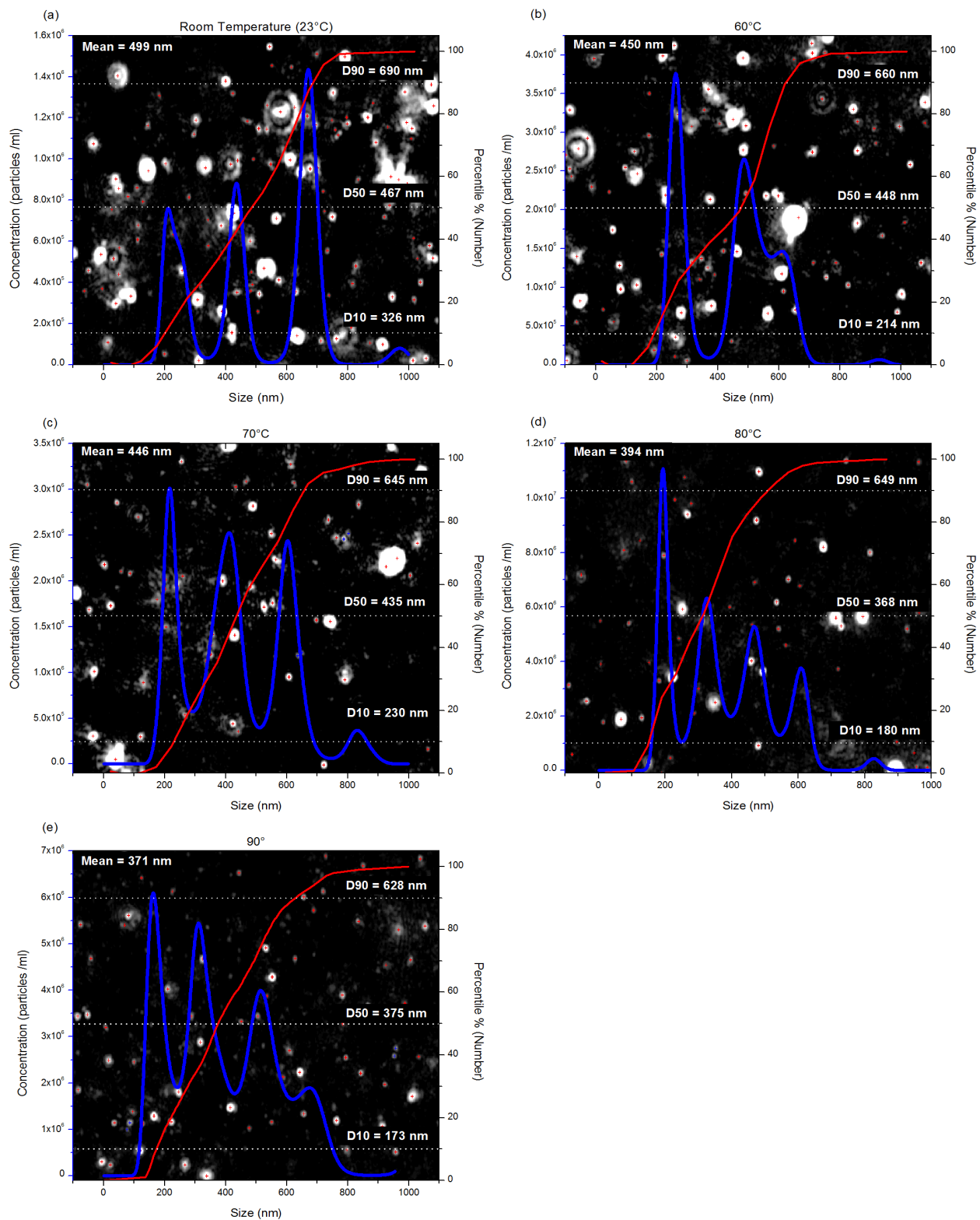


Figure 5.3 Size distribution and concentration of clay aerogel suspensions treated at (A) Room temperature (23°C) (B) 60°C (C) 70°C (D) 80°C (E) 90°C

5.3.3 Functional groups of temperature induced aerogels

The increase in the particle connectivity was confirmed from the FTIR spectra of the clay-PVA aerogel composites (Figure 5.4). The characteristic peaks were consistent for all the aerogel composites at 3316, 2917, 1632, 1424, 1022, and 850 cm^{-1} , which correspond to H-O-H hydrogen bond, C-H stretching, hydroxyl stretching of adsorbed water molecules, CH_3 symmetric deformation, Si-O-Si stretching and the C-H wagging vibrations respectively [39,223,224].

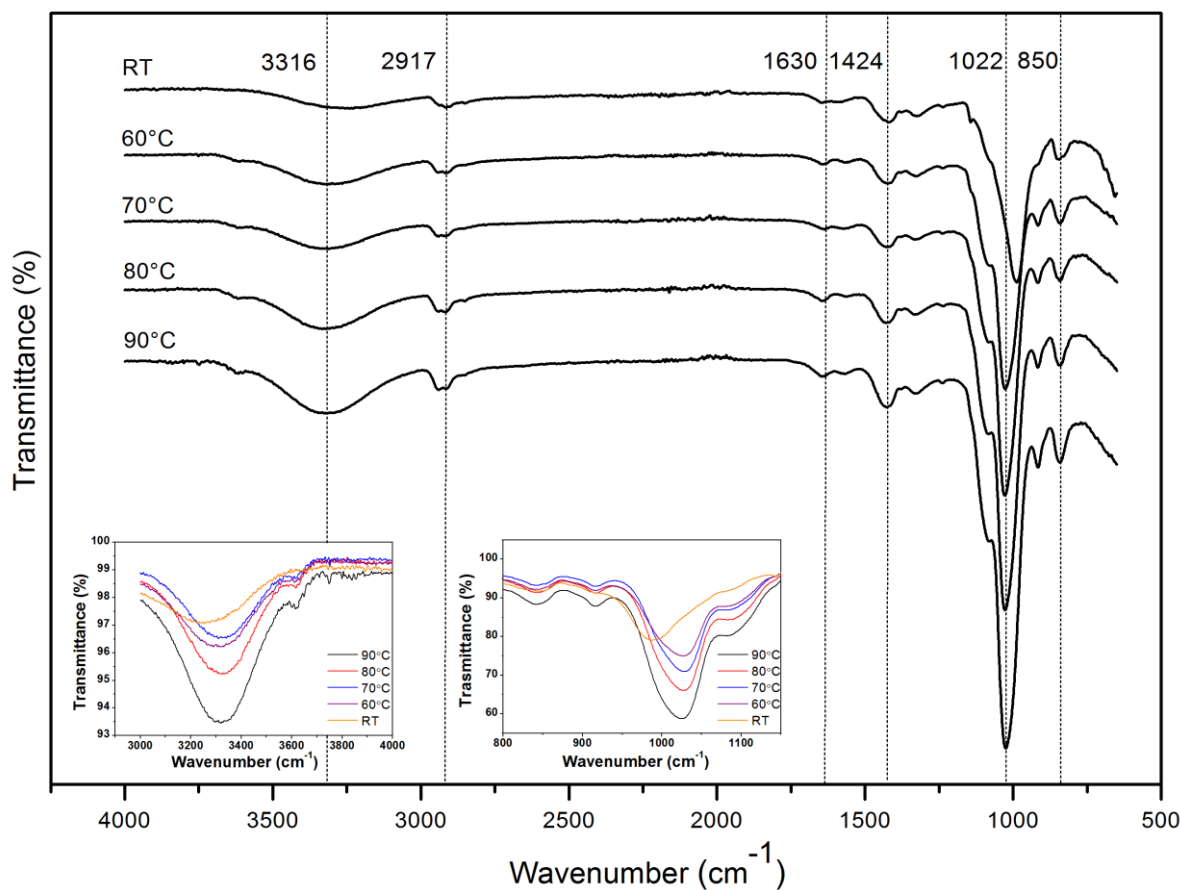


Figure 5.4 FTIR analysis of clay-PVA aerogel composites prepared from different suspensions treated at various temperatures

The most significant change was the transmittance (%) at peaks 3316 cm^{-1} (H-O-H) and 1022 cm^{-1} (Si-O-Si) in which the peaks intensity increased with an increase in the mixing temperature (Figure 5.4 inset). The increase in the hydrogen bond can be attributed to the clay higher absorption of PVA due

to a higher (H+) concentration (Table 5.1) and an increase in the polymer chain flexibility, resulting in an overall stronger aerogel composite, while the increase in the Si-O-Si stretching and the peak shift from 975 to 1022 cm^{-1} may be due to the fact with the swelling medium temperature increasing, the clay layer stacks are transformed from a flocculent mass of stacks to much smaller or single layers with higher PVA absorption.

5.3.4 Morphology of temperature induced aerogels

The final aerogel morphology is a representation of the solid network in a solution or suspension subjected to lyophilisation (freeze-drying), therefore altering the precursor suspension through induced heat will have a direct influence on the final microstructure of the aerogel composite, bearing in mind that the suspensions were left to cool down to room temperature prior to freezing.

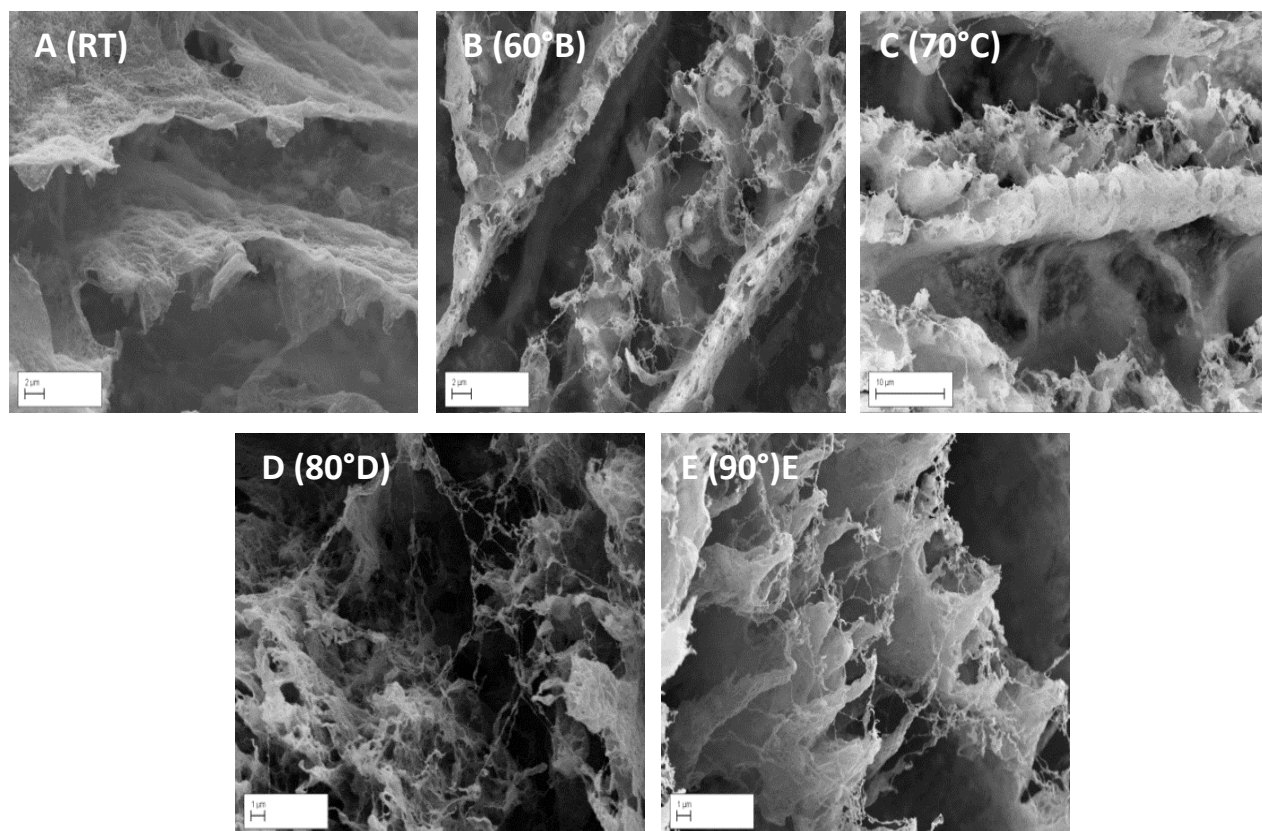


Figure 5.5 Microstructure of clay-PVA aerogels with suspensions treated at various temperatures

It is evident that the aerogel suspension processed at room temperature (RT) had the iconic lamellar “house of cards” structure (Figure 5.5A), while increasing the mixing temperature to 60 and 70°C resulted in the structural transformation to a feather type structure (Figure 5.5B and C), this is similar to a previous report that the clay fragments are compressed in the inter-crystalline boundaries and form slightly thin films branching out from one another, resulting in higher surface roughness than a lamellar architecture would. This type of structure is able to transfer loads more efficiently than a “house of cards” structure due to the higher connectivity and therefore gives rise to an overall stronger aerogel.

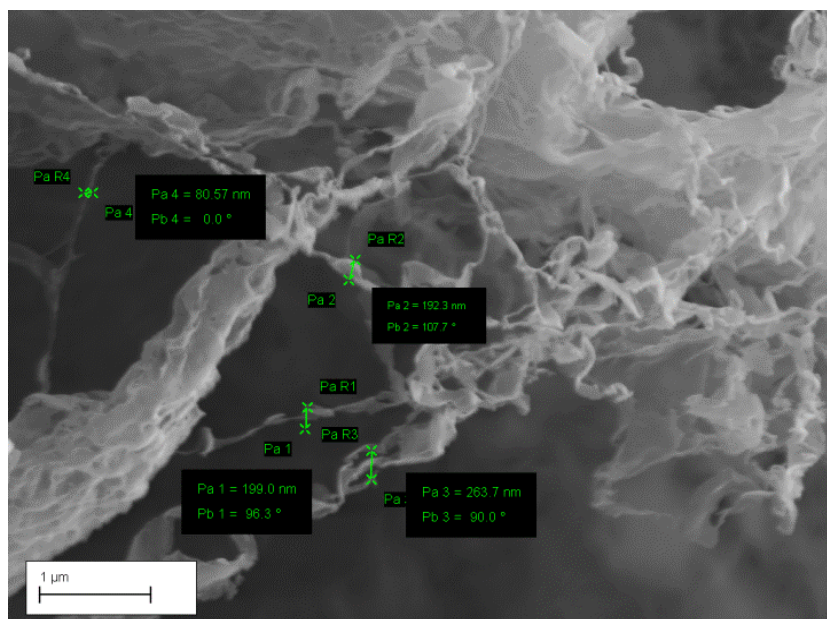


Figure 5.6 Web-like structure of clay-PVA aerogel composites

Further increase in the mixing temperature up to 80 and 90°C resulted in a similar transformation to those at 60 or 70°C (Figure 5.5D and E) with the main difference being the dominant appearance of a web-like phenomena that covers the “house of cards” structure and spans across the layers of the aerogel composite (Figure 5.6). This may be as a result of the reduction in the average particle size and increase in the concentration of particles of well below 200 nm comparable with the particles

size at D10 (180-170) (Figure 5.3) of the colloids mixed at 80 and 90°C. These particles range are resilient to sedimentation due to their small size and thus able to create long thin struts with an average thickness of less than 200 nm (Figure 5.6). An overall entwined structure stabilised by web structure (Figure 5.6D and E) provides a system that can transfer the load highly and efficiently.

5.3.5 Mechanical properties of temperature induced aerogels

It is most interesting that increasing the swelling medium temperature, without altering the compositions of either the clay or PVA, significantly increased the average compressive modulus (Figure 5.7A), up to 7 folds from an initial modulus of 0.48 MPa at room temperature to 3.3 MPa at 90°C, even with a minimal increase in density of about 9% (Figure 5.7 B) which may be a result of a higher particle concentration.

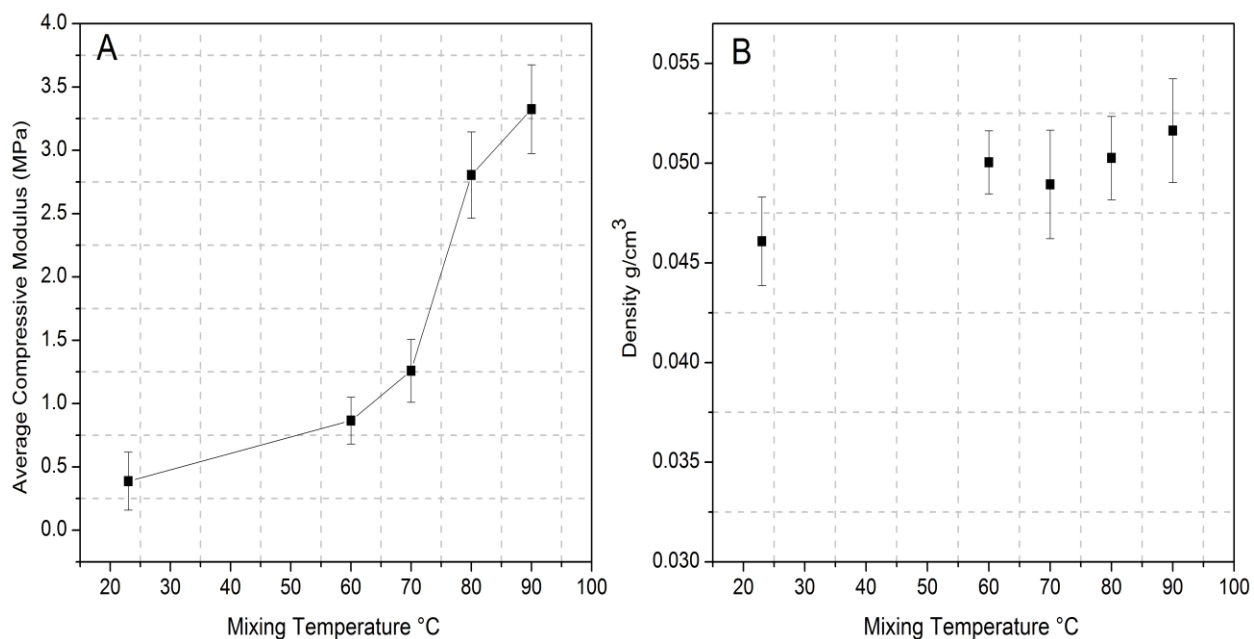


Figure 5.7 Average compressive moduli (A) and density (B) versus mixing temperatures

The increase in strength may be attributed to the increase in the chemical connectivity between the smectic clay sheets and PVA, as well as having a higher concentration of smaller size particle which

can result in a more continuous network structure as discussed in previous Sections. An interesting phenomenon is witnessed in the compressive modulus for samples prepared at 80°C and 90°C, showing an abrupt increase in the compressive modulus by 5 folds compared to that at 70°C, while there is only a 1.5 fold increase from RT to 70°C. This may also be related to the drop in $\tan \delta$ beyond 70°C (Figure 5.1), suggesting a more homogenous connected network as observed through the NanoSight (Figure 5.3), where treating the suspensions at 80 and 90°C produces particle sizes below 400 nm. The final dried structure (Figure 5.5E and D), which presented a web-like structure between the clay structures (Figure 5.6), may also be responsible for a more effective load transfer through the material.

5.3.6 Thermal conductivity of temperature induced aerogels

The microstructure of the aerogel is one of the most decisive parameters when considering thermal conductivity. A high porosity of aerogel means a reduced solid to gas ratio and limits thermal conduction via the solid content. Therefore another decisive factor is density. An increase in density means an increase in the solid content. However, this is only true at a certain extent as a rise in density may also create a more tortuous path for heat to flow through, thus lowering the thermal conductivity. The different mixing temperatures seem to have a slight effect on the thermal conductivity of the aerogel composites. The aerogels prepared at 80 and 90°C reduced the thermal conductivity by 2.5% and 4.8%, respectively compared to that at room temperature, this reduction may be related to the appearance of the web like structures (Figure 5.6), which may allow more paths for the thermal energy to dissipate before traveling through the entire sample despite an increase in density (Table 5.2). The average thermal conductivity of the clay aerogel composites with such structure is 0.042 W/(m.K) (for 2.5 wt. % clay and 2 wt. % PVA), showing that without altering the composition, an increase in modulus can be achieved without sacrificing thermal conductivity.

Table 5.2 Thermal conductivity and density of Clay-PVA aerogels

Mixing temperature (°C)	Thermal conductivity (W/(m.K))	Density (g/cm ³)
RT (23)	0.042	0.046
60	0.042	0.050
70	0.042	0.049
80	0.040	0.050
90	0.041	0.051

5.4 Interim conclusions

Clay aerogel composites and their suspensions prepared at various elevated temperatures ranging from room temperature (RT), 60, 70, 80 to 90°C have been developed. The effect of the colloidal mixing temperature was irreversible even though the suspensions were cooled down to room temperature prior to freezing. An increase in mixing temperature resulted in an increase in the storage modulus (G') with $\tan \delta < 1$, suggesting a highly associated network and an increase concentration in counterions, especially of H^+ . The mixing temperature also had a direct effect on the particle size and concentration (D10, D50, and D90), and hence the microstructure of the aerogel transforming the lamellar structure into a feather type structure, with a dominant web-like structure at 80 and 90°C, allowed an effective load transfer of the aerogel composites. The amount of PVA absorbed could be dependent on the mixing parameters with the transmittance (%) at H-O bonds increasing for the aerogels at higher temperatures compared to that of room temperature. The compressive modulus of aerogel composites was significantly improved by simply treating the initial suspension with elevated temperature. The modulus increased by 7 folds from 0.48 to 3.3 MPa for the aerogel composites prepared from mixing at 90°C. Overall mechanical properties could be significantly improved without sacrificing physical properties such as density and most importantly thermal conductivity.

Chapter Six: Functional clay aerogel composites through hydrophobic modification and architecture of layered clays

Abstract

This Chapter implements hydrophobic modified clay layers with ammonia salts (Organoclay) using ultra-sonication and water as a solvent to develop functional clay-polyvinyl alcohol (PVA) aerogel composites through an environmentally friendly freeze-drying process. Various compositions have been designed aiming at the high effectiveness of reducing moisture absorption while increasing the structural integrity and overall compressive modulus but reducing the thermal conductivity of the aerogel composites. The microstructure systems of the aerogel composites could be tailored to result in multifunctional performance for the targeted applications. The moisture absorption could be reduced by five folds compared to that of normal clay aerogels depending on the exposure relative humidity. While the modulus of the aerogel composites was doubled from an initial modulus of 0.39 to 0.82 MPa, the thermal conductivity was reduced by up 20% reaching values as low as 0.0315 W/(m.k). These aerogel composites could be an effective and efficient thermal insulation material to be implemented in the construction industry.

Highlights:

- Modifying clay aerogel composites through an ion exchange process;
- Using only water as a solvent and an environmentally freeze-drying process;
- An efficient way to overcome high moisture absorbance of clay aerogel composites;
- Maintaining higher structural integrity at high moisture exposure;
- Mechanical properties enhancing in parallel to reducing of thermal conductivity.

6.1 Introduction

Surface modification of clay has been considered vital in improving the practicality and performance of clay/polymer nanocomposites [35]. The modification process may be involved in replacing the clay cations, such as Mg^{2+} , Ca^{2+} , Na^+ , K^+ , and Li^+ , with various organic cations, such as a nitrogen-based quaternary ammonium cation [37]. Alkylammonium salts may cause the interlayer space to expand and convert the initially hydrophilic silicate into hydrophobic organoclay as well as enhance the miscibility of the clay with polymers [38,39]. Organoclay has proven to be an effective tool for treating and filtrating water [41] and more traditionally has been used as a thickening and gelling agent in paints and cosmetics [40]. This study was to develop clay aerogel composites using modified clay (Organoclay) with ammonia salts and polyvinyl alcohol (PVA) through an environmentally friendly freeze-drying process while using only water as a solvent. Various compositions have been designed aiming at the high effectiveness of reducing moisture absorption while increasing the structural integrity of aerogel composites over a long period of exposure to moisture and the overall compressive modulus but reducing the thermal conductivity of the aerogel.

6.2 Experimental work

Organoclay-PVA aerogels were developed as described in Chapter 3, Section 3.2.3. Natural bentonite clay was modified using the surfactant hexadecyltrimethylammonium bromide, and the concentration varied between 0.3, 0.4, 0.5, 0.6, 0.7 and 1 of the CEC of the bentonite montmorillonite. The modified clay was then dispersed into a solution using an ultrasonic processor (Chapter 3, Section 3.2.3.1). The final aerogel precursor suspension was also mixed using using an ultrasonic processor to prepare a formulation of 2.5wt.% clay and 2wt.% PVA (Chapter 3, Section 3.2.3.2). The final aerogel suspension was vertically frozen and finally freeze-dried (Chapter 3, Sections 3.2.1.2 and 3.2.1.3). Samples are coded depending on the cation exchanged, for instance, the sample (0.3CEC) was prepared from

organoclay with 0.3 of the cation exchanged. Testing and characterisation is carried out according to Chapter 3, Section 3.3.

6.3 Results and discussion

6.3.1 Morphology of organoclay-PVA aerogel composites

6.3.1.1 Influence of surfactant on the microstructure of organoclay-PVA aerogels

It is apparent that the morphology of the organoclay-PVA aerogels varies considerably with the compositions, suggesting micro-metric changes in the clay platelets which are associated with both the physical and mechanical properties of the aerogels. At low surfactant concentration (0.3CEC) the morphology exhibited a layered and laminar architecture (Figure 6.1A), very similar and almost identical to that well-known iconic structure of clay aerogels (Chapter 4, Figure 4.4). This is possibly related to the low cation exchange capacity (CEC) (75.2 meq/100g) of the clay used and therefore an overall reduced effectiveness in replacing cations at such low concentration. Increasing the surfactant concentration (0.4 CEC) transitioned the structure into a pillared like structure that forms individual layers that are highly packed together. This may result from the combination of both hydrophilic and hydrophobic clay particles bonding into a more continuous structure (Figure 6.1B) in which part of the individual clay layers that absorbed PVA will swell and the other part, the organoclay-PVA will create a sort of coating around the swelling medium resulting in a pillared structure. A similar pillared structure was witnessed for the surfactant (0.5 CEC), only with a more coarse structure as a result of higher coverage of the hydrophobic particles. Increasing the surfactant concentration (0.6 and 0.7 CEC) transitioned the structure layers into very rough surfaces, which may be related to the fact that the surfactant hydrophobic tails restrict a continuous path of water between the clay layers resulting in areas capable of absorbing water and other areas portioned from water, thus creating a more coarse structure with higher surface area (Figure 6.1D and E).

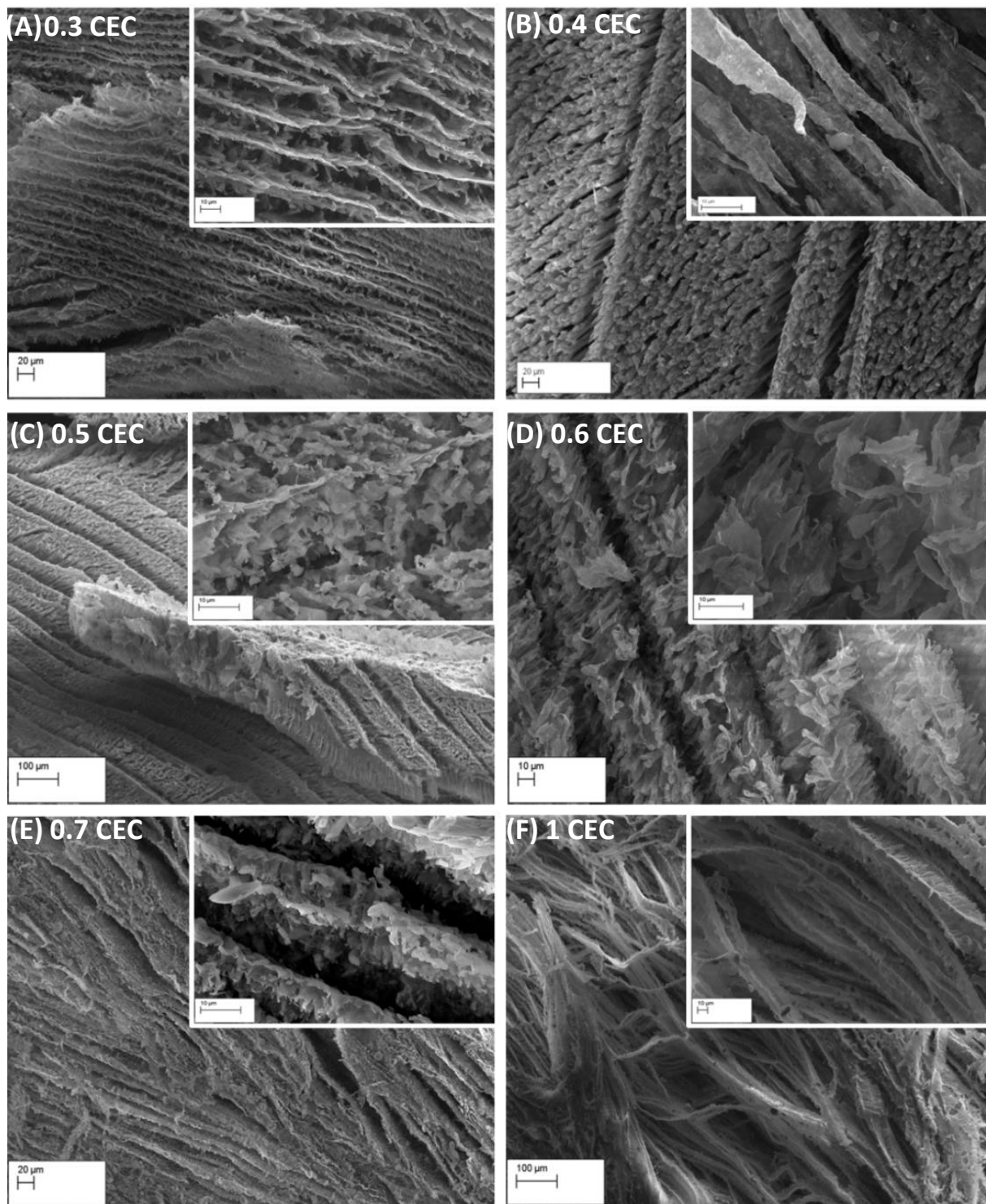


Figure 6.1 SEM results of organoclay-PVA aerogels with different amount of surfactant

Also due to the fact the most of the cations have been exchanged the PVA will have less surface contact with the clay. At higher surfactant concentration (1 CEC), a fibrillary network structure is

observed (Figure 6.1F). This may be due to the increase in the hydrophobicity of the clay particles in which the hydrophobic particles causes a phase separation between the clay and the water, therefore, during the freezing process the ice growth may trap the clay particles along its path, allowing the particles to sediment due to gravity, and align into a lengthy connected formation. Therefore by increasing the surfactant content, the structure of the aerogel can be tailored from a laminar layered structure at 0.3 CEC (Figure 6.1A) to a more coarser and tortuous structure at ≥ 0.4 CEC (Figure 6.1B, C, D, E, and F).

6.3.1.2 Influence of surfactant on the basal spacing of organoclay-PVA aerogels

The basal spacing also changed with the change of cations exchanged, where the diffraction peak corresponding to the basal spacing (d) for the control sample at $2\theta = 7.23$ (Figure 6.2). The angle decreases with increasing the surfactant content (Figure 6.2), resulting in an increase in d -value (Table 6.1) and indicating an intercalated structure. However, the broadness of the diffraction peak may suggest a diverse structure within the layers of single exfoliated clay [27]. Although the aerogel composites of 0.6 and 0.7 CEC did not demonstrate any diffraction peaks corresponding to the basal spacing (d) at $2\theta = 1-10$, which indicates that the structure may be totally exfoliated and the clay be dispersed homogeneously into the polymer matrix. A more realistic statement is the indication of both intercalated and exfoliated structures as the absence of a diffraction peak is not proof of exfoliation, as stated in the previous publication [28]. It is expected that increasing the number of cations exchanged to that of 1 CEC ($\approx 100\%$) would produce a completely exfoliated structure, however a broad diffraction peak does appear at $2\theta = 1.23$, which may be due to the aggregation of the clay layers when water was used as a solvent to prepare the aerogel composites.

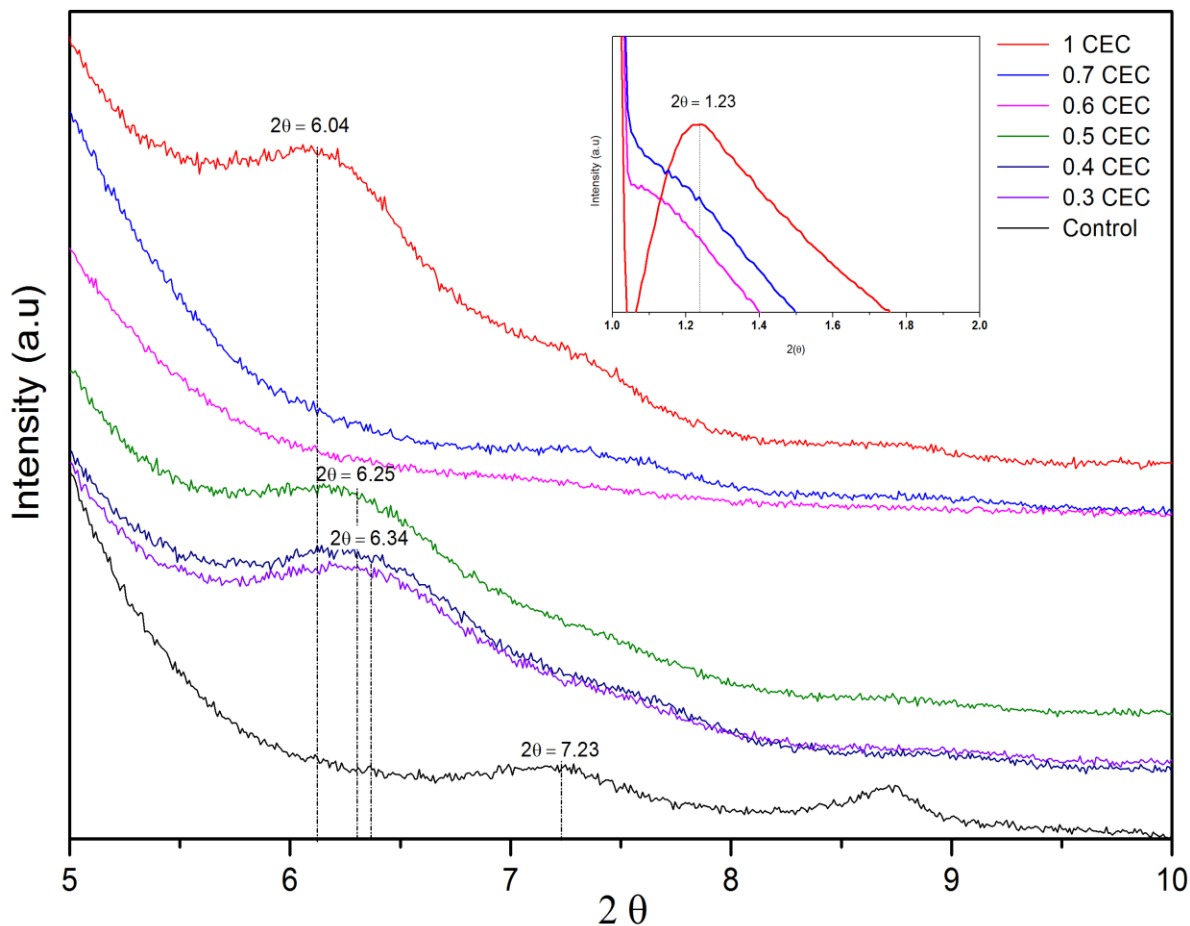


Figure 6.2 XRD spectrums of aerogel composites with different amount of cations exchanged

Table 6.1 d-value of clay aerogel composites with different amounts of cations exchanged

Sample ID	2θ	d-value (nm)
Control	7.23	1.24
0.3 CEC	6.34	1.53
0.4 CEC	6.34	1.53
0.5 CEC	6.25	1.55
0.6 CEC	n/a	n/a
0.7 CEC	n/a	n/a
1 CEC	6.04	1.61

6.3.2 Functional groups of organoclay-PVA aerogels

The FTIR results of the organoclay-aerogel composites reflect bands corresponding to both clay and PVA (Figure 6.3). Unmodified sodium montmorillonite has several characteristic bands; the sharpest

band is located at 3629 cm^{-1} which is associated with the stretching of the hydroxyl groups coordinated to octahedral cations, principally with Al^{3+} cations [237].

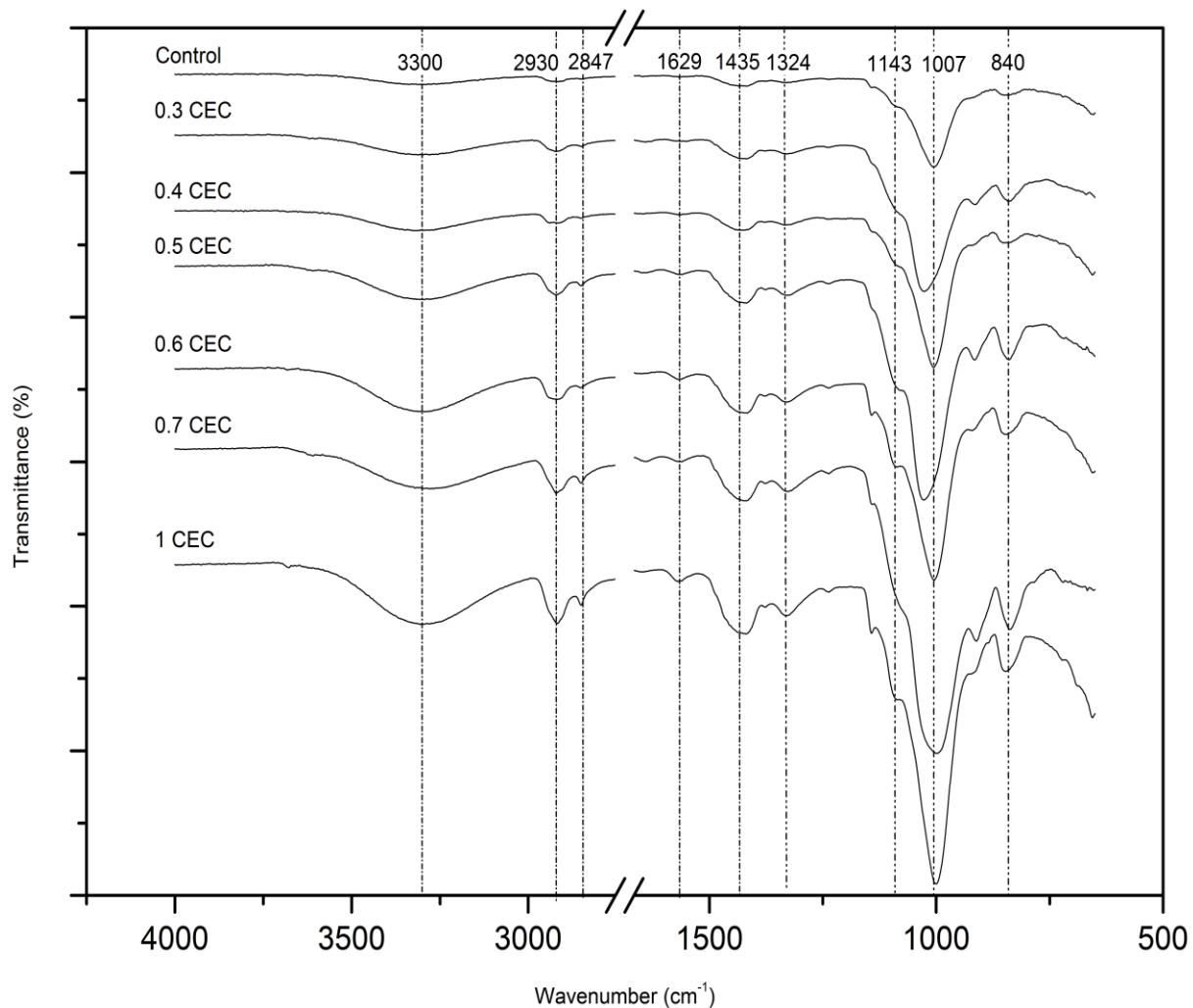


Figure 6.3 FTIR analyses of organoclay-PVA aerogel composites with different amount of surfactant added equivalent to CEC of clay

With the addition of PVA, the band shifts towards 3300 cm^{-1} which is assigned to O-H stretching vibration of hydroxyl group, as hydrogen bonds are formed between the clay and PVA. An increase in intensity was observed as the concentration of the surfactant increased, possibly due to the higher interaction of the PVA with the surfactant. The bands at 2930 cm^{-1} and 2847 cm^{-1} can be associated with CH_2 asymmetric and symmetric stretching respectively, which also witnessed an increase in

intensity as the surfactant concentration increased. This may possibly be due to a change in phase behaviour, a result of the incorporation of the surfactant molecules into the bilayer structure of the clay [225,226]. The band of 1629 cm^{-1} is formed mostly due to the absorbed water, which in fact showed a reduction as the surfactant concentration increased, indicating that the overall water content in the clay aerogel composite is reduced. The band located at 1435 cm^{-1} , which may be associated with the phenyl rings attached to phosphorus atoms [39], and bands 1435 cm^{-1} and 1135 cm^{-1} , which are assigned to C-H in-plane bending vibration [224], increased accordingly with the surfactant concentration, demonstrating higher absorbance of surfactant by the clay. The addition of surfactant also caused a shift in bands between 1116 cm^{-1} and 1007 cm^{-1} , which are produced by the stretching mode of Si-O, out-of-plane and in-plane, respectively [227]. The band at 840 cm^{-1} , which is associated with AlMgOH bending, showed an increase in intensity as a result of exchanging inorganic cations with organic cations [228].

6.3.3 Moisture absorption of organoclay-PVA aerogels

The moisture resistance of the final organoclay-PVA aerogel composites improved considerably, the magnitude of which is dependent on the amount of ammonia salt equivalent to the CEC of clay (Figure 6.4). Increasing the surfactant resulted in the reduction of moisture absorbance (Figure 6.4) due to an increase in surface coverage of the clay silicates with hydrophobic tails. The least moisture absorbed was witnessed at the highest amount of surfactant (1 CEC) with an average of about 40% less moisture absorbance compared to that of the control composites. Even at low concentration (0.3CEC), the aerogel composites were observed to have a significant decrease in the amount of moisture absorbed, by an average of 30%. The transition in the microstructure to a coarser and rough surface at ≥ 0.5 CEC (Figure 6.1) as well as having a more exfoliated structure with the addition of the

surfactant can create a more tortuous path for the moisture to penetrate deep into the sample as the grain boundaries increase and as each layer becomes more branched (Table 6.1) .

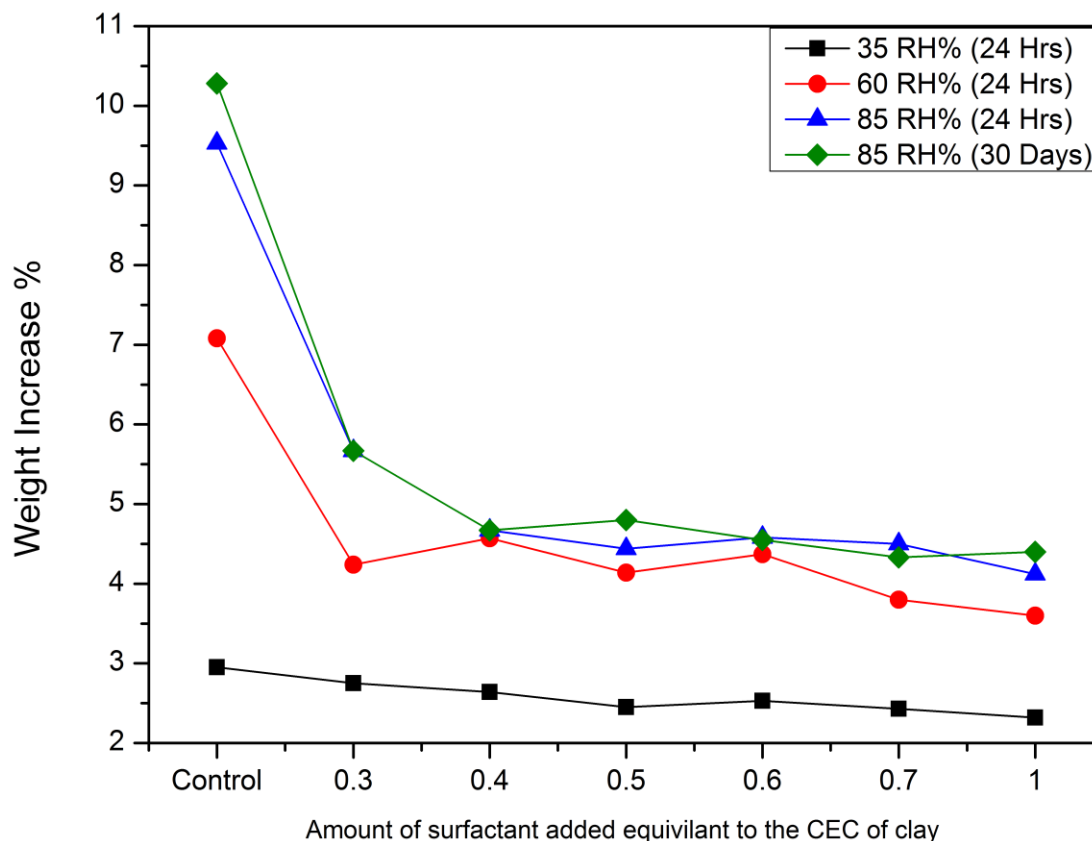


Figure 6.4 Moisture absorption of different organoclay-PVA aerogels at a different set of conditions

The PVA itself may play a significant role in increasing the amount of moisture absorbed due to its hydrophilic nature. The results have also demonstrated that the clay aerogel composites can almost reach an equilibrium state within 24 hours. The long-term moisture absorption (30 days) at 85% RH showed very similar results to that at 85% RH for 24 hours. However, what was significant about the long-term test was the damage, deformation and shrinkage observed for these clay aerogel composites (Figure 6.5). While an overall higher structural integrity of aerogel composites when implementing organoclay was witnessed compared to the control sample, at higher concentration (0.7 and 1 CEC), less structural deformation was observed than that of lower concentration (0.3, 0.4

and 0.5 CEC) (Figure 6.5). Even at higher surfactant concentrations, the aerogel composites became soft, and a reduction in the average compressive modulus by up to 80% was observed (Figure 6.6). This may be due to the PVA breaking down and then disintegration of the structure, as indicated by a colour change to a more brownish state (Figure 6.5, 1CEC).

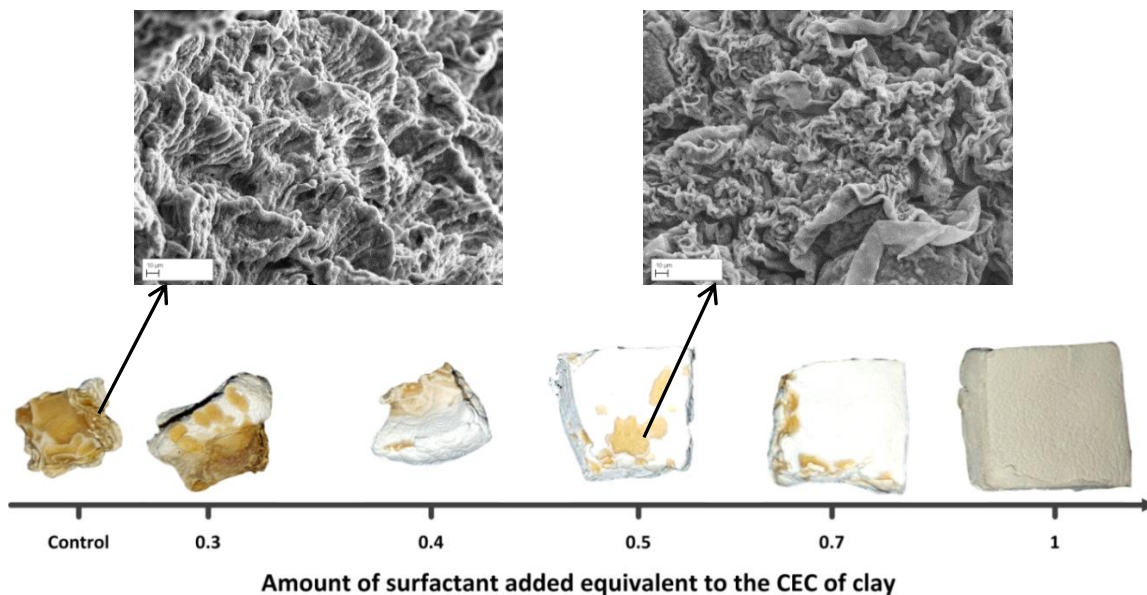


Figure 6.5 Representation of structural damage caused by moisture

6.3.4 Compressive moduli of organoclay-PVA aerogels

The compressive modulus of clay aerogel composites is usually dependant on the solid content; increasing the density will result in an overall stiffer composite. Although the addition of ammonium ions resulted in an increase in density due to an increase in the solid content (Figure 6.7), the increase in the final compressive modulus can also be related to stronger interfacial interactions such as hydrogen bonds created between the modified clay and the PVA during the mixing process where the PVA chains may diffuse into the gallery between the silicates layers and at the edges due to the hydrogen bonds outside of the modified clay layers and between the silicate oxygen and the PVA

hydroxyl groups, as demonstrated through FTIR which showed an increase in intensity across O-H stretching vibration and CH₂ asymmetric and symmetric stretching (Figure 6.3).

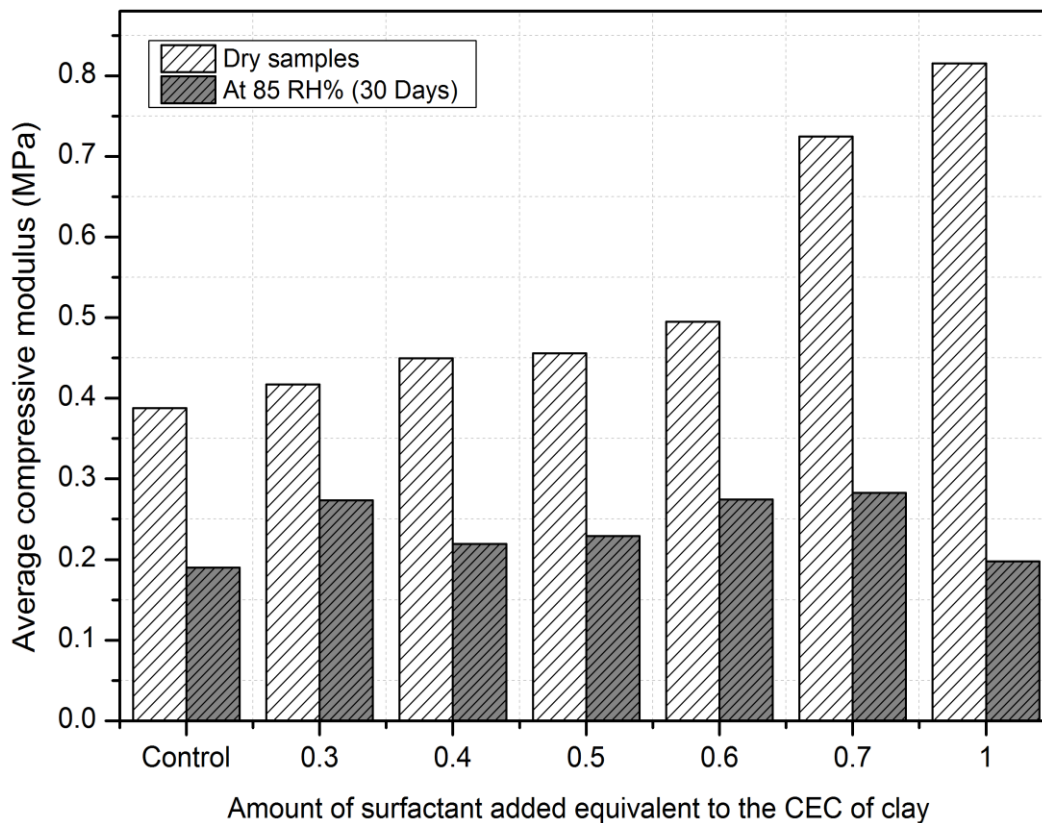


Figure 6.6 Average compressive moduli of organoclay-PVA aerogels

The final organoclay-PVA aerogel composite is capable of bearing higher loads, where at high surfactant content the aerogel composites witnessed a 50% increase in modulus (Figure 6.6) from an initial modulus of 0.39 MPa (Control) to 0.82 MPa (1 CEC). As mentioned, the moisture absorbed by the aerogel composites can significantly hinder the mechanical performance of the clay aerogel composites up to 70% (Figure 6. 6) as it degrades the clay and the PVA due to their hydrophilic nature. What was noticed is that the higher the surfactant concentration, the more significant was the drop in the average compressive modulus after 30 days at 85% relative humidity. This could be explained due to the fact that at low concentration, the aerogel composites had higher structural deformation

which creates a solid continuous structure due to the degradation of both the clay and PVA as they disintegrate and dissolve due to moisture absorbance as witnessed in Figure 6.5, while at higher concentration most of the clay particles are intact and lose strength mostly due to the degradation of PVA which acts as a binding agent between the clay layers, giving the final aerogel composite its strength.

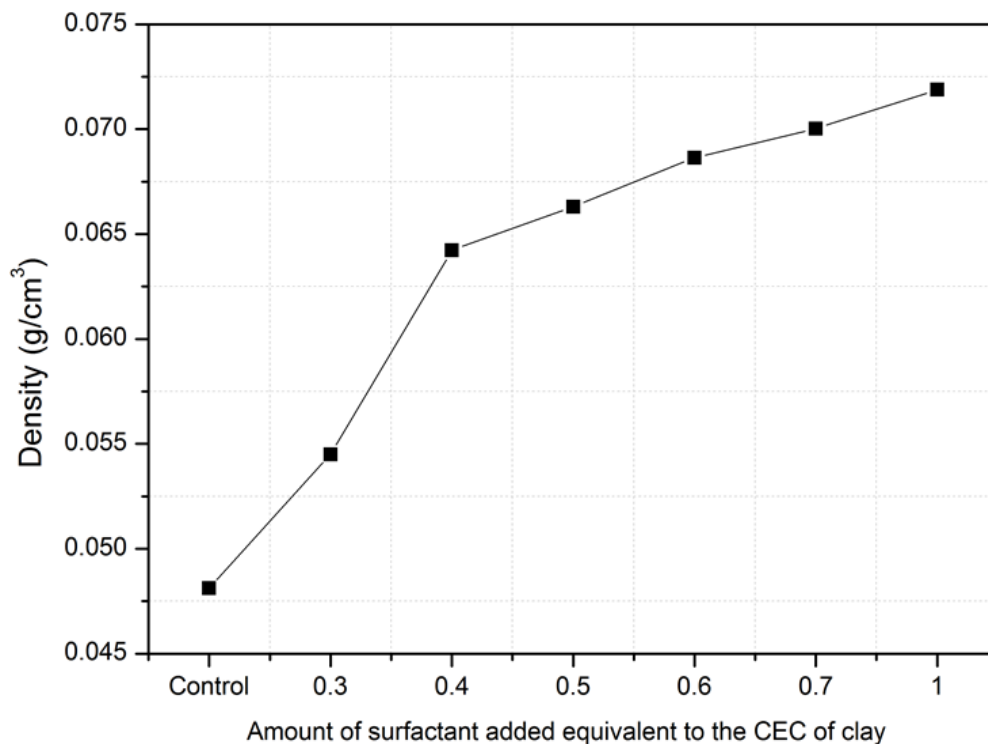


Figure 6.7 Density of organoclay-PVA aerogels versus the amount of surfactant added

6.3.5 Thermal conductivity of organoclay-PVA aerogels

The modification of the smectic clays resulted in a significant decrease up to 25% in its thermal conductivity (Table 6.2), although there is a rise in density with the increase in the amount of surfactant used (Figure 6.7). Therefore it can be said that the thermal conductivity of such materials is less dependent on density and more reliant on the morphology to a certain extent. The better performance is achieved which might be against basic intuition similar to that adding PVA to neat clay

aerogels and increasing the density results in lower thermal conductivity values (Chapter 4, Section 4.3.4). The decrease in thermal conductivity performance of the aerogel composites prepared from organoclay may be related to the change in the morphology of the aerogel composites as afore-discussed, where depending on the amount of surfactant the morphology can transition from a laminar layered structure at (0.3 CEC) to a coarser and rougher surface such as at (0.7 CEC) or to a more connected network at (1 CEC) that results in a more tortuous structure. The tortuous structure can contribute to the reduction of the gaseous thermal conductivity in which the excited gas molecules that are entering the open pore structure of the aerogel collide with the surface of the aerogel and transfer their energy to the surface which is known as the Knudsen effect [229], and as the structure becomes more tortures the probability of this effect increases and thus results in a lower thermal conductivity.

Table 6.2 Thermal conductivity and density of organoclay-PVA aerogels with different amount of surfactants

Sample ID	Density (g/cm ³)	Thermal conductivity (w/(m.K))
Control	0.048	0.0420
0.3 CEC	0.055	0.0357
0.4 CEC	0.064	0.0345
0.5 CEC	0.066	0.0345
0.6 CEC	0.069	0.0340
0.7 CEC	0.070	0.0330
1 CEC	0.072	0.0315

Due to the fact that at low surfactant concentration (0.3 CEC) the morphology was almost unchanged, yet witnessed a 15% drop in thermal conductivity, the lattice parameter and interface density of the organoclay may play an important role in reducing thermal conductivity of the clay particles, because the clay d-value (Interlayer space) increases (Table 6.1) to accommodate the exchanged ammonium ions. The structure is a combination of both intercalated and exfoliated layered silicates as revealed by XRD, this means that a more distorted silicate layer structure of higher mass can have a lower

thermal conductivity across its layers compared to unmodified clay due to an increase in grain boundaries, which can scatter phonons, and such scattering will shorten the vibrations across the materials and therefore result in a lower thermal conductivity.

6.4 Interim conclusions

This Chapter has demonstrated the ability to implement hydrophobic organically modified clays into clay aerogel composites through an environmentally friendly freeze-drying process, using only water as a solvent which is the most desirable solvent from an environmental point of view, especially if commercialisation is to be considered. The implementation of modified clay (organoclay) resulted in improved mechanical and physical properties. The average compressive modulus increased by up to 50% due to improved interfacial bonding between the organoclay and PVA. The morphology was directly influenced by the amount of surfactant, transforming the layered house of cards structure into a fibrillary network with higher surface roughness and connectivity at high surfactant content. The work has also tackled one of the biggest setbacks of clay aerogels which is its high moisture absorption, especially if it is to be implemented into the construction industry as an insulation material. Moisture sorption capacity was effectively reduced by up to 40%, while structural integrity remained even after 30 days at 85% RH. The thermal conductivity of the organoclay-PVA composites reduced by 20% even at low surfactant concentrations due to an increase in d -value (Interlayer space) which created a more tortuous path for heat to flow through. The Chapter demonstrated that a highly efficient and effective process of clay aerogel composites that can be used in the construction industry as insulation material.

Chapter Seven: Functionalising clay aerogel composites with water-soluble isocyanates and organosilanes

Abstract

This Chapter presents crosslinking techniques to develop clay-PVA aerogel composites through an environmentally freeze-drying process using water as a solvent. Two water soluble crosslinkers, namely aliphatic polyisocyanate (Wcro1™) and 3-glycidoxypropyltrimethoxysilane (Wcro2™), were employed and their crosslinking mechanisms were studied. A series of characterisations of the developed clay aerogel composites were carried out. The results showed that the chosen crosslinkers were able to generate substantial crosslinking reactions and hence resulted in changes in microstructures of clay aerogel composites. The crosslinked clay-PVA aerogel witnessed significant improvement in their mechanical and physical properties. The moisture absorbance of the composites was reduced by 27% when the clay aerogel composites were subjected to high humidity (95% RH) while retaining dimensional stability at high moisture exposure. The developed clay-PVA-Wcro1™/Wcro2™ composites have also increased the liquid absorption capacity by 2 and 3 times respectively. The compressive modulus increased by 6 folds from 0.48 to 3.6 MPa and the thermal conductivity was reduced from the 0.042 to 0.039 W/(m.K).

Highlights:

- Organic modification of clay aerogel composites using organosilanes and isocyanates;
- Using only water as a solvent and an environmentally freeze-drying process;
- An effective way to overcome high moisture absorbance of clay aerogel composites;
- Maintaining physical and mechanical integrity at high moisture exposure.

7.1 Introduction

Chemical crosslinking is widely used in material science to modify and enhance the performance of composites by tailoring the nanoscale order of polymers [141,230,231]. Di-functional compounds, such as glutaraldehyde and glyoxal, are the most common reagent used to crosslink PVA by virtue of the reaction of the hydroxyl groups of PVA with aldehydes and the formation of acetal bonds [142]. The effect of crosslinking to enhance the mechanical properties of clay-PVA aerogels has been investigated [60,63,232]. This study explores the crosslinking process as a vital tool to enhance the moisture resistance and at the same time improve the mechanical performance of clay-PVA aerogels. This Chapter explores the crosslinking process as a vital tool to enhance the moisture resistance and at the same time improve the mechanical performance of clay-PVA aerogels. Two crosslinkers have been selected for this research, firstly aliphatic polyisocyanate (Wcro1™) which has been widely used in polyurethane productions and in several different applications such as in paint, hydrogels and adhesives and are important precursors to produce linear and crosslinked polymers, due to its high reactivity of –NCO groups, polyisocyanate can react with –OH or –NH₂ group containing materials [233,234]. Secondly, glycidoxypropyltrimethoxysilane which has been proven effective in many applications, such as proton conducting membranes, corrosion and scratch resistant coatings, mainly due to its crosslinking capacity especially as it can increase the compatibility between the organic and inorganic phases [235,236]. Both crosslinkers can react at room temperature in the presence of an aqueous media making them suitable candidates for the freeze-drying process to prepare aerogels.

7.2 Experimental work

Crosslinked clay-PVA aerogel were developed as described in Chapter 3, Section 3.2.4. Stock clay and PVA solutions are prepared as described in Chapter 3, Section 3.2.1. To prepare the final aerogel dispersion, the required amount of the stock clay and PVA with the crosslinkers are mixed together

using a magnetic stirrer for 24 hours at low shear. A composition of 2.5 wt. % clay and 2 wt. % PVA was used throughout the experimental work. Two crosslinkers were used: Aliphatic polyisocyanate, (Wcro1™) and 3-glycidoxypropyltrimethoxysilane (Wcro2™). The amount of crosslinker is dependent on the amount of PVA (2 wt. %) and therefore 2 wt. % of crosslinker was added to ensure a higher rate of reactions. The final aerogel suspension was vertically frozen and finally freeze-dried (Chapter 3, Sections 3.2.1.2 and 3.2.1.3). Testing and characterisation is carried out according to Chapter 3, Section 3.3.

7.3 Results and discussion

7.3.1 Morphology of crosslinked clay-PVA aerogels

The microstructure of clay aerogels is an important parameter in determining the physical and mechanical properties of the aerogel composites. It is apparent that the clay-PVA aerogel composites produced a layered architecture structure, (lamellar structure) with open pores that are responsible for low thermal conductivity, (Figure 7.2A) as a result of the ice growth between the clay and PVA that pushes the clay and PVA into its grains boundaries. Obstructing this growth results in a significant increase in surface area due to an increase in surface roughness as illustrated in Figure 7.1B and C as a result of an aliphatic polyisocyanate (Wcro1™) and 3-glycidoxypropyltrimethoxysilane (Wcro2™), creating bridges (links) between the polymer chains. In which the bridges may act as a barrier that prevents continuous ice growth; with new ice crystals growing on the other side of the crosslinks and also due to a higher viscosity as a result of the polymer chains being stiffer, can significantly disrupt the alignment of both clay and PVA during the freezing process, as the ice front growth is restricted and no longer moving at a constant rate.

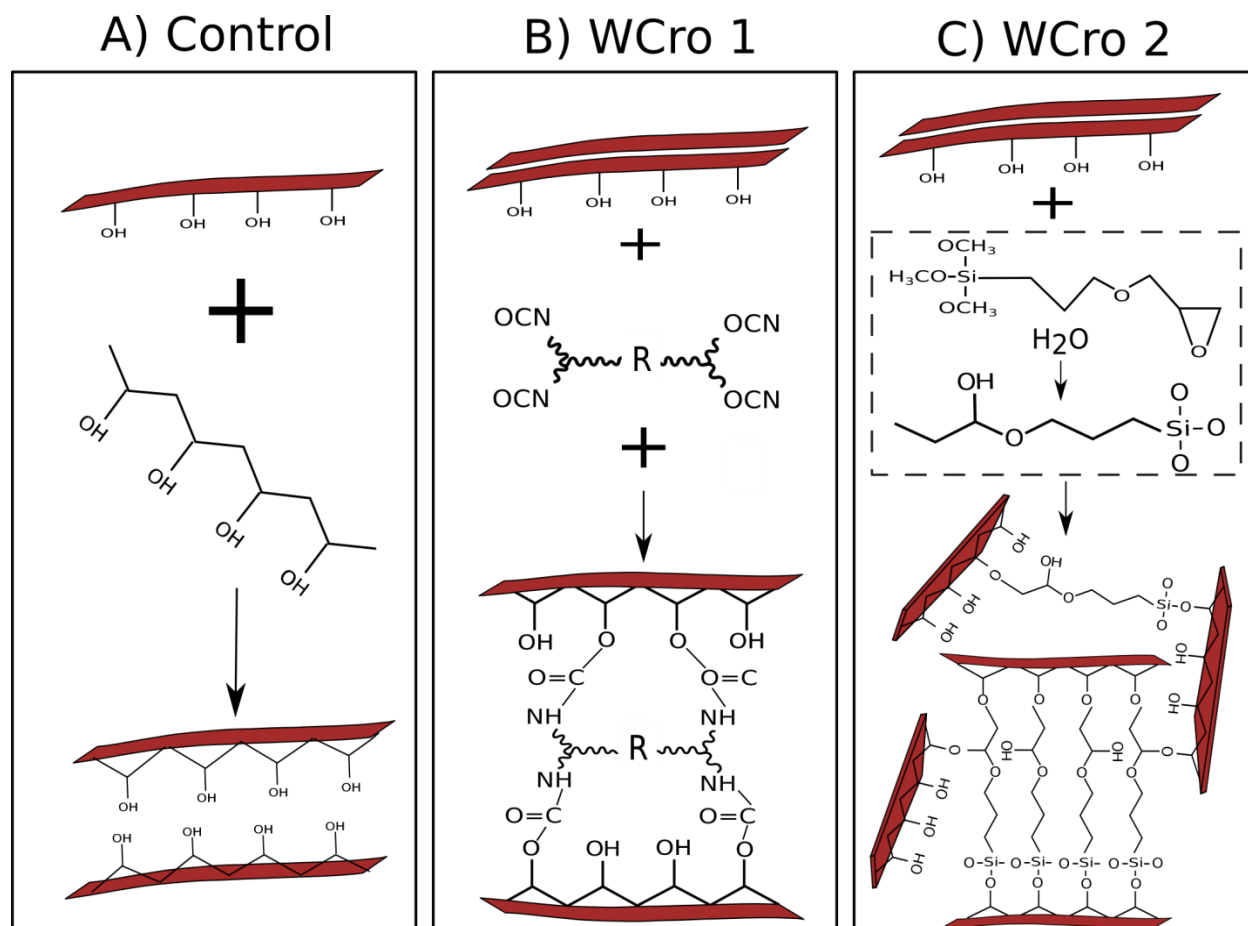


Figure 7.1 Illustration of crosslinking reaction with clay and PVA

The use of aliphatic polyisocyanate (Wcro1™) resulted in a densely layered morphology (Figure 7.2B), the increase in the packing density can be explained by bridges (links) being formed between the PVA chains whereas the clay absorbs the crosslinked polymer chain and the adjacent polymer chain may be absorbed by another clay layer as illustrated in figure 7.1B. Therefore the swelling of the clay will be limited or restricted as the crosslinker creates stronger bonds between the layers. The use of 3-glycidoxypropyltrimethoxysilane (Wcro2™) resulted in a mostly heterogeneous structure (Figure

7.2C) as a result of the alteration in the tridimensional structure as illustrated in Figure 7.1C.

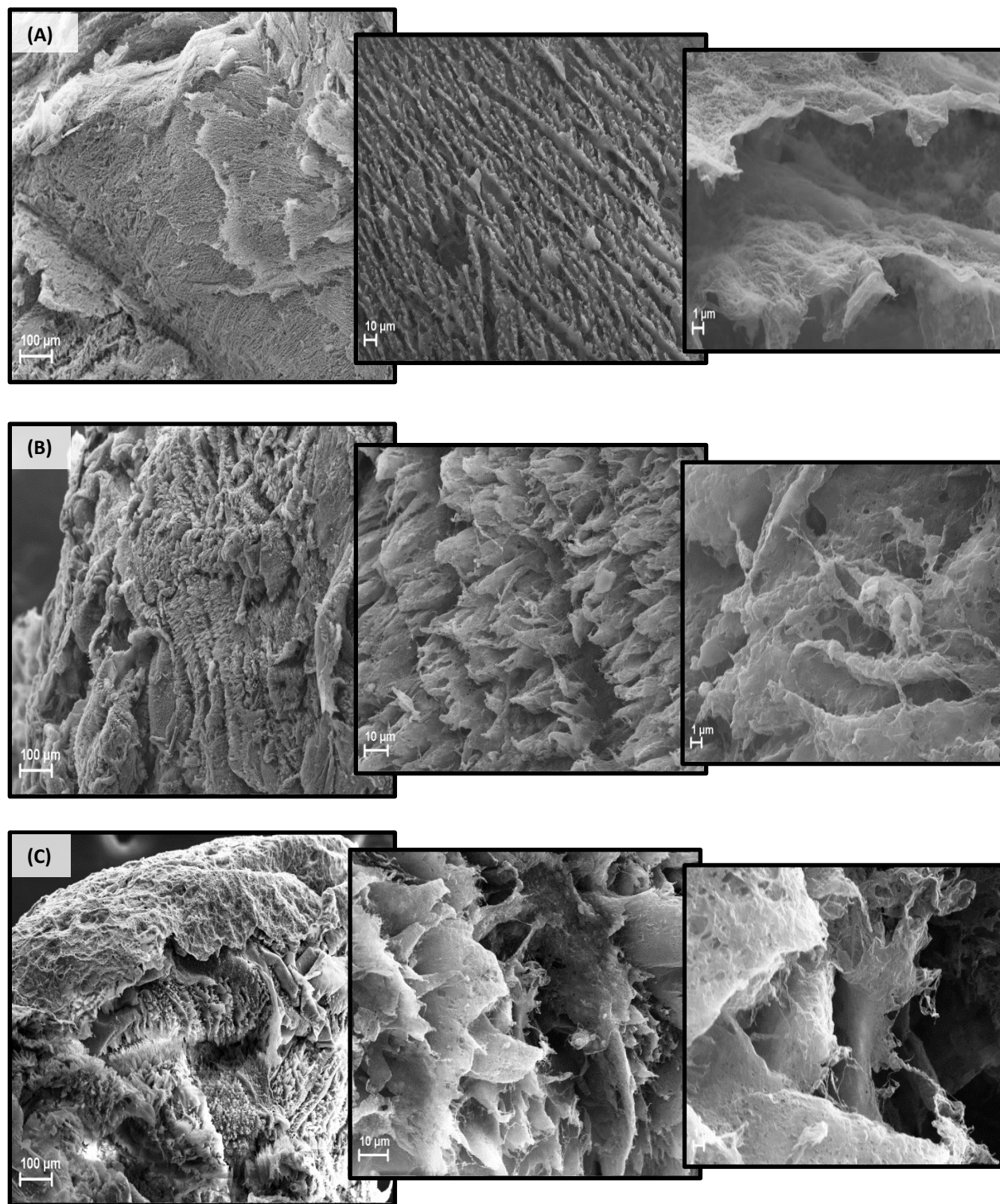


Figure 7.2 (A) Clay-PVA aerogels (B) Clay / (PVA+Wcro1) aerogel (C) Clay / (PVA+Wcro2) aerogel

In which the chain of 3-glycidoxypropyltrimethoxysilane allows for clay and PVA layers to be bonded across different planes through hydrogen bonding, this will, in turn, result in a microstructure that has a multidirectional orientation (Figure 7.2C). The addition of Wcro1™ gives rise to a more consistent texture of the structure than that of Wcro2™ which has a more random structure (Figures 7.2B and C). Clay-PVA- Wcro2™ composites also have a more dense structure with fewer layers visible suggesting lower spacing between layers. This may also explain the rise in density (Table 7.2) and higher compressive modulus of clay-PVA- Wcro1™ than that of clay-PVA-Wcro2™ composites (Figure 7.8) as discussed in Section 7.3.4.

7.3.2 Functional groups of crosslinked clay-PVA aerogels

The FTIR spectrum of the pure PVA and PVA crosslinked with either aliphatic polyisocyanate (Wcro1™), or 3-glycidoxypropyltrimethoxysilane (Wcro2™) is presented in Figure 7.3 A. It can be seen that PVA with the addition of the crosslinkers only resulted in slight changes in the spectrum, as at this stage they have still not been reacted. The strong band at 3292 cm^{-1} is linked to the stretching O–H (Hydroxyl groups) from the intermolecular and intramolecular hydrogen bonds, which are expected to happen among PVA chains due to high hydrophilic forces and between the water molecules [234]. Bands at 2930 and 2862 cm^{-1} , which are main peaks associated with PVA due to C–H alkyl stretching, are not visible in Figure 7.3A as the PVA is in solution before reaction. The broad band observed at 2109 cm^{-1} may indicate the O–H overtone of PVA [250]. The peak at 1633 cm^{-1} is associated with the absorbed water, which is again expected as the PVA is in solution. The peak at 1464 cm^{-1} is as a result of C–H bonds and therefore the strongest band can only be present when the PVA is crosslinked with an aliphatic polyisocyanate (Figures 7.3B and C) which is a hydrocarbon compound [251], which is discussed in more detail in next Section. The peak at 1416 cm^{-1} is associated with C–H wagging vibrations and the band at 1097 cm^{-1} is a result of the C–O stretching vibration of

PVA and thus present in all three solutions [144], alongside with the band at 1722 cm^{-1} which is from the carbonyl group of acetate ion from unhydrolyzed PVA ($\approx 1\%$) as this peak can also be seen in the spectrum of neat aerogel composite (Figure 7.3C) [252]. Figure 7.3B shows the FTIR spectrum of the crosslinked/PVA solutions cured. It would be expected that the band at 3292 cm^{-1} , which associated with O-H bonds, will decrease with the removal of water molecules, but what can also be concluded is that the addition of aliphatic polyisocyanate (wcro1™) or glycidoxypropyltrimethoxysilane (Wcro2™) resulted in a band shift to 3238 cm^{-1} , suggesting that more bridges (links) may have been created between the PVA chains, as O-H interactions are being lost as illustrated in figure 7.1. The cured solutions (Crosslinked) (Figure 7.3B) are also characterised with bands at 2940 and 2840 cm^{-1} which refers to the stretching C-H from alkyl groups. The highest increase in the band was witnessed with the addition (Wcro2™) related to aldehydes compounds in 3-glycidoxypropyltrimethoxysilane in which non-bonded compounds may have gone through condensation during the curing process [250]. The small bands at 1633 cm^{-1} suggests that water molecules may still be bound to the surface however this may be only true for the control in which with the addition of aliphatic polyisocyanate (wcro1™) which is a hydrocarbon compound, the bands at 1633 cm^{-1} , 1464 cm^{-1} , 1242 cm^{-1} can be attributed to amide I, II, and III bands which are induced by the reaction between hydroxyl and isocyanate groups [247,253]. The appearances of amide I, II and III verified the reaction illustrated in Figure 7.1B between $-\text{NCO}$ groups and $-\text{OH}$ groups and thus creating additional covalent bonds between PVA [250]. The use of 3-glycidoxypropyltrimethoxysilane (Wcro2™) resulted in an increase in intensity across the major vibration bands ($1097\text{--}684\text{ cm}^{-1}$). In which the signals at 1097 and 684 cm^{-1} are attributed to asymmetric vibrations of (Si-O-Si); the signals at $952\text{--}953\text{ cm}^{-1}$ are attributed to asymmetric vibrations of (Si-OH); the signals at 755 cm^{-1} are attributed to symmetric stretching vibrations of (Si-O-Si); and the signals at 684 cm^{-1} are attributed

to the bending vibration of (Si-O-Si). The increase in intensity across these bands can be related to polysiloxane (R-Si-O-) reactions of hydrolysis and condensation. Also, absorption peaks in the region from 1250 cm^{-1} can be attributed to silicon-alkyl bonds, indicating a hybrid organic-inorganic structure formation [253,254]. These results are thought to be due to the organotrialkoxysilane sol-gel reactions that have altered the tridimensional structure (Figure 7.1C). The change in pure PVA can restrict the chain mobility of PVA and thus alter the physical properties of the final aerogel composite such as increasing barrier properties and decreasing hydrophilicity. The aerogel composites are associated with major peaks (Figure 7.3C) at 3329, 2929, 1633, 1416, 1016, and 829 cm^{-1} which correspond to H-O-H hydrogen bond, C-H stretching, hydroxyl stretching of adsorbed water molecules, CH_3 symmetric deformation, Si-O-Si stretching and the C-H wagging vibrations, respectively [39,223,224]. The main significant difference in the spectrum of the aerogel composites with the addition of the crosslinkers is the appearance of the bands at 1194, 1097 and 912 cm^{-1} and an increase in intensity at 2929 and 1416 cm^{-1} which are the main crosslinking bands, showing the overall balance of hydrophilic to hydrophobic groups (OH/acetate) is altered [230].

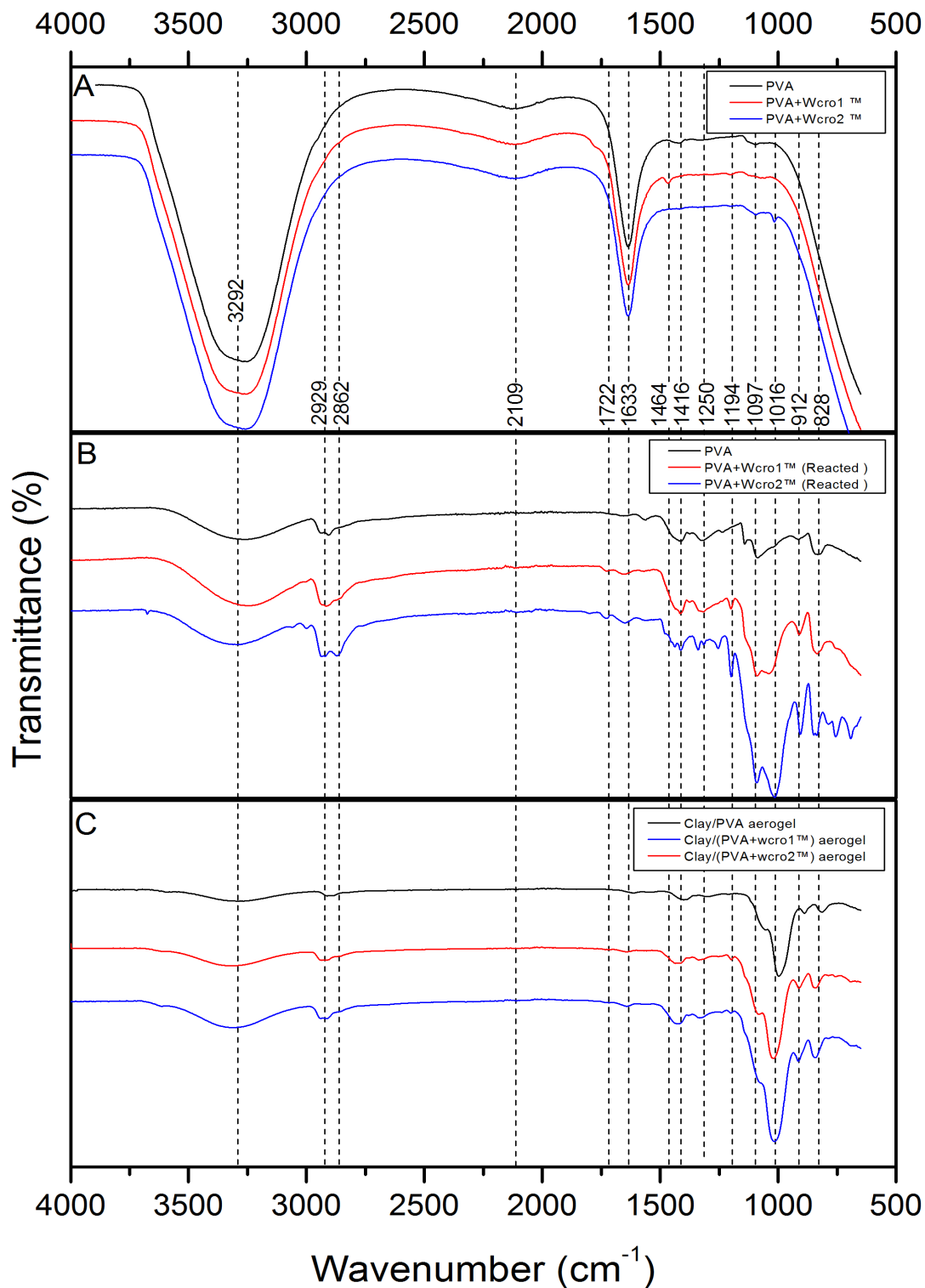


Figure 7.3 FTIR spectrum (A) PVA with/without crosslinks in solution (B) Cured PVA with/without crosslinks and (C) clay-PVA aerogel composite with/without crosslinks

7.3.3 Wettability of crosslinked clay-PVA aerogels

7.3.3.1 Moisture absorption and deformation of crosslinked-PVA clay aerogels

Clay-PVA aerogel composites are expected to absorb moisture due to their hydrophilic nature. The unmodified clay-PVA aerogel composites had the most mass increase as expected across the humidity ranges by up to 27% in 24 hours at 95% RH (Figure 7.4). Both crosslinkers, aliphatic polyisocyanate (Wcro1™) and 3-glycidoxypropyltrimethoxysilane (Wcro2™), gave rise to a substantial improvement in moisture resistance, which is similar for both crosslinkers for all humidity ranges tested (Figure 7.4). Even as the clay was not subjected to any modification, the crosslinked PVA could be absorbed onto the clay surface (Figure 7.1), which in turn protects most of the clay surfaces from moisture attack.

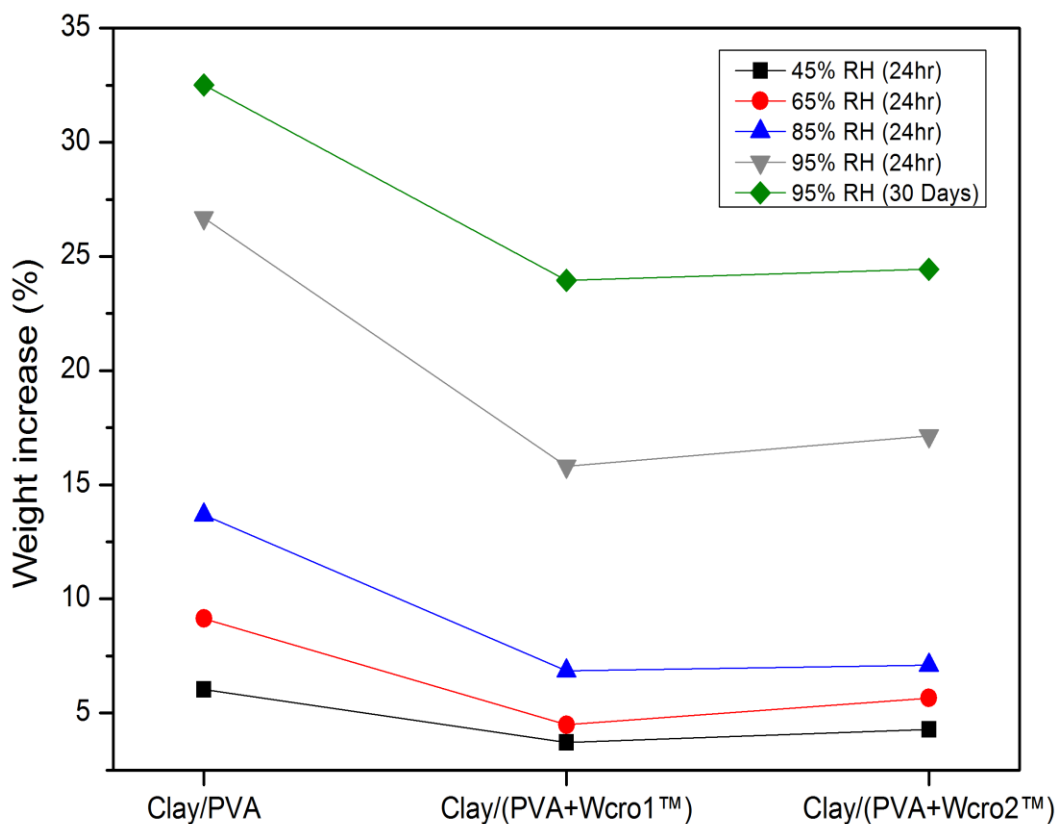


Figure 7.4 Moisture absorption of clay-PVA aerogel composites with/without crosslinks

With the addition of Wcro1™ and Wcro2™, the mass increase was reduced by 16% and 17% respectively, in 24 hours and on average a reduction of 38% compared to the neat clay-PVA aerogel composites, although this was reduced to 27% during the long-term test (30 Days). It must be noted that the hydroxyl groups in the PVA and the clay will eventually absorb moisture, and after the pores are filled with moisture, it will eventually penetrate deep into the solid phase. Alongside from the chemical modification of PVA the reduction in moisture absorbance can also be attributed to the transition of the microstructure from a laminar architecture to a denser coarse microstructure (Figure 7.2) that will increase the barrier properties of the composite and thus reduce the diffusion rate into solid phase by creating a tortuous path for vapor diffusion. The significant outcome from the long-term test is the shrinkage of the composites (Table 7.1), where the control sample shrunk by 60%, while the implantation of crosslinking using Wcro1™ and Wcro2™ resulted in shrinkage of 23 and 30%, respectively. However, after 24 hours, the crosslinked samples did not go through any shrinkage, while the control samples shrunk by 7%, suggesting that the open pores of the crosslinked aerogel composites are only being filled with moisture while only after 30 days the moisture is being absorbed by the solid phase of the cross-linked aerogel, and such the crosslinked aerogel composites had a higher mass increase at 30 days compared to 24 hours.

Table 7.1 Dimensional stability of clay-PVA aerogels with/without crosslinks after 30 days at 95% RH once removed to ambient condition

Sample	Volume shrinkage (%)
Clay-PVA aerogel	63.12
Clay-PVA-Wcro1™ aerogel	22.52
Clay-PVA-Wcro2™ aerogel	29.95

7.3.3.2 Capacity of liquid water absorption of crosslinked aerogels

The liquid sorption capacity has also been determined for possible absorbance application of clay aerogel composites (Figure 7.5). It was found that the neat clay-PVA aerogel composites increased in

mass weight by 330%. The addition of the cross-linkers resulted in higher absorption capabilities, with the implantation of Wcro1™ and Wcro2™ resulting in an increase of 720% and 950% respectively. The fact that the crosslinked aerogel composites absorbed greater amounts of water may be due to much interactive and comprehensive network systems established for clay-PVA Wcro1™/Wcro2™ composites. These open pore microstructure networks are not only able to accommodate more water, but also their integrity remains intact longer due to a slight increase in hydrophobicity (Figure 7.7). It can be seen from the experiments (e.g. Figure 7.5B and C) that with the soaking of the clay-PVA-wcro1™/wcro2™ gave rise more air bubbles compared to that of control sample (surface of water in Figure 7.5A), reflecting more air held in the pores of clay-PVA-Wcro2™/ Wcro2™ composites. It is also showed that for the neat clay aerogels, as soon as they are immersed in water, their structures completely collapse and the layered morphology begins to disintegrate into a complete solid structure with almost no bubbles on the surface of the water. And changes colour from white to brown (Lighter to darker) as soon as immersed in water (Figure 7.5A) suggesting the sample is completely wet.

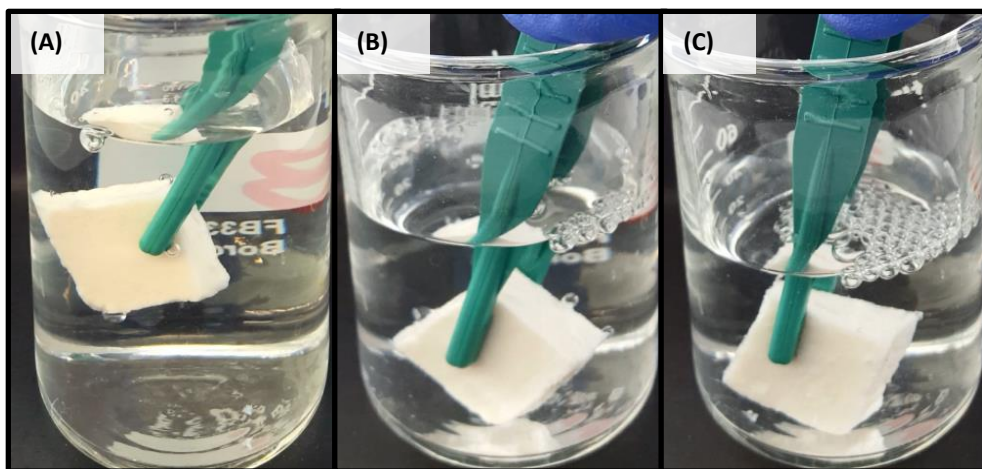


Figure 7.5 Water uptake of clay-PVA aerogels composites (A) Clay-PVA aerogel, (B) Clay-PVA-Wcro1™ aerogel and (C) Clay-PVA-Wcro2™ aerogel

7.3.3.3 Hydrophobicity of crosslinked clay-PVA aerogels

The result of contact angle tests (Figure 7.7) shows that the aerogel composites cannot be defined as hydrophobic materials as water droplets are absorbed by the aerogel composites within 2.5s, showing that these composites require further improvement to overcome the limitation in the wet state. Some improvement using Wcro1™ and Wcro2™ was observed as the crosslinking process decreases the hydrophilic character of PVA.

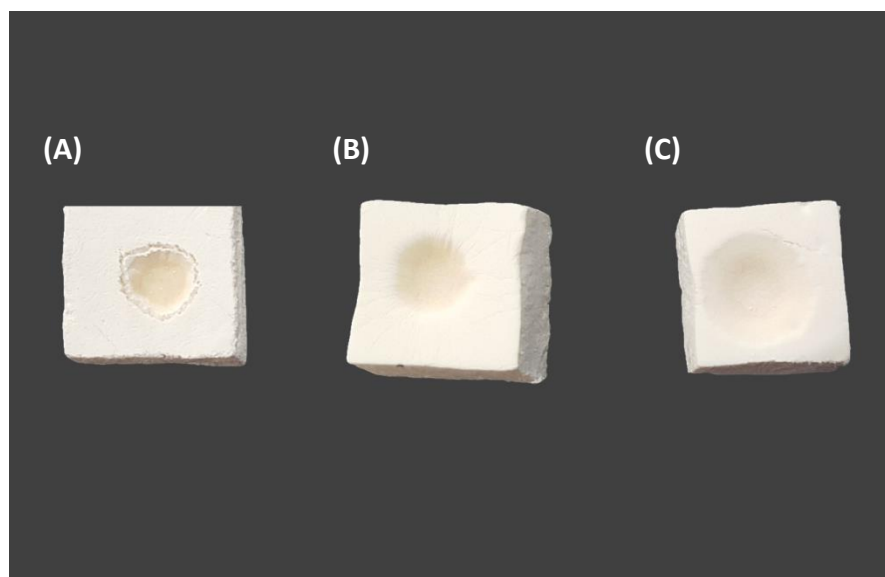


Figure 7.6 Structural damage from water (A) Clay-PVA aerogel, (B) Clay-PVA-Wcro1™ aerogel and (C) Clay-PVA-Wcro2™ aerogel

The initial contact angle of composites ($T=0s$) increased to 85 and 96° using Wcro1™ and Wcro2™ respectively from a contact angle of 70° for the control sample. For both the control samples and the samples that incorporated Wcro1™, the water droplet was completely absorbed by the sample at 0.6s (contact angle=0), while for the composites using Wcro2™, there is an angle of 89° at 0.6s, and it took a further 1.6s for the angle to reach zero (Figure 7.7). What was most significant is that the neat control aerogel composites were damaged and water was immediately absorbed through the solid phase of the sample travelling deep into the aerogel composites leaving a crater like shape

(Figure 7.6A), while for the crosslinked aerogel composites, the water droplet travelled down the pores of the aerogel composites with less structural damage (Figure 7.6B and C). The incorporation of WCro1™ gave rise to the most robust structure with the least damage to the aerogel structure, and slight damage is only observed on the surface of the composites.

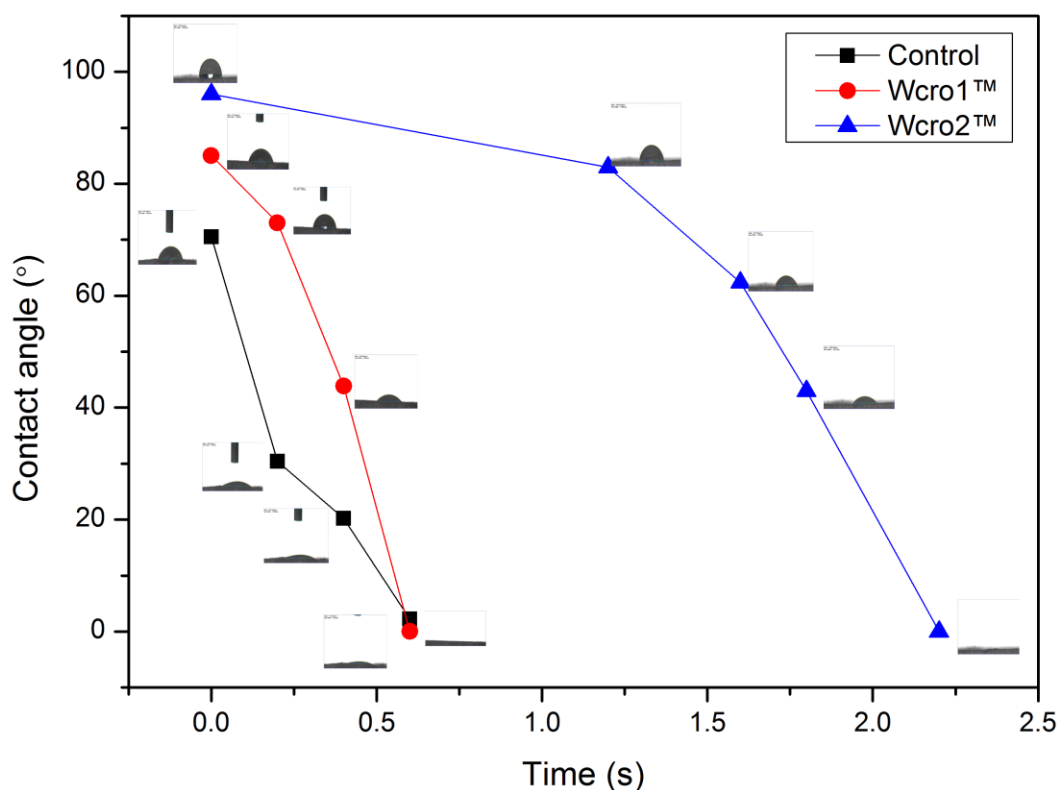


Figure 7.7 Contact angles of clay-PVA aerogel composites with/without crosslinks

7.3.4 Compressive moduli of crosslinked clay-PVA aerogels

The crosslinked aerogel composites witnessed a significant increase in compressive modulus by up to 6 folds from 0.53 to 3.6 MPa when incorporating aliphatic polyisocyanate (Wcro1™) and by 3.5 folds from 0.53 to 2.4 MPa when incorporating 3-glycidoxypropyltrimethoxysilane (Wcro2™) (Figure 7.8). Although the samples witnessed a slight rise in density (Table 7.2) due to the increase in the solid content of the added crosslinkers, the main reason for the significant enhancement to the mechanical properties can be attributed to the crosslinking process (Figure 7.1), where PVA chains are being

linked together. The increase in the stiffness of the PVA limits the range of motions which in turn results in a more rigid and stiff composite and restrains the movement associated with new covalent bonds (Figure 7.3).

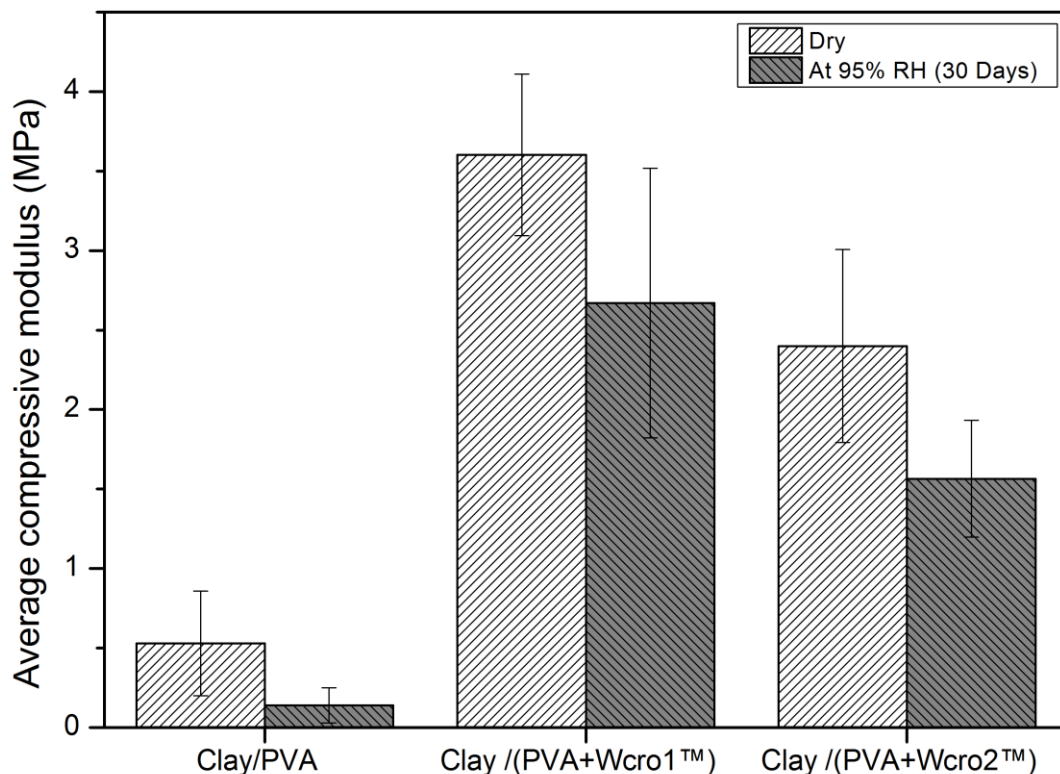


Figure 7.8 Average compressive moduli of clay-PVA aerogels with/without crosslinks

The same concentration was used with both crosslinkers. Therefore, it can be suggested that aliphatic polyisocyanate (Wcro1™) is more effective in creating bridges between the PVA chains. The enhancement can also be related to the morphology of the aerogel composite (Figure 7.2 B and C) in which the highly packed layers are able to transfer the load more efficiently through the material, resulting in higher compressive moduli. The compressive modulus of the control aerogel dropped by 73% from 0.53 to 0.14 MPa after being exposed to 95% RH for 30 days, while the compressive modulus of the crosslinked aerogels dropped by 26% and 38% for Wcro1™ and Wcro2™ respectively due to the fact that less moisture is being absorbed by the aerogel composites, and thus limiting

structural damage caused by the reduction of possible chain conformation and restraining the movement associated with these new covalent bonds.

Table 7.2 Density of clay-PVA aerogels with/without crosslinks

Sample	Density (g/cm ³)
Clay-PVA aerogel	0.048
Clay-PVA-Wcro1™ aerogel	0.079
Clay-PVA-Wcro2™ aerogel	0.071

7.3.5 Thermal conductivity of crosslinked clay-PVA aerogels

The thermal conductivity of the aerogel composites are highly dependent on the microstructure and only influenced by the density above a certain limit at which the heat transfer by conduction through the solid phase becomes the dominate mode of heat transport through the aerogel as the porosity is sacrificed.

Table 7.3 Thermal conductivity of clay-PVA aerogels with/without crosslinks

Sample	Thermal Conductivity (W/(m.K))
Clay-PVA aerogel	0.042
Clay-PVA+Wcro1™ aerogel	0.039
Clay-PVA+Wcro2™ aerogel	0.041

For instance, the neat clay-PVA aerogel had a density of 0.048 g/cm³ with a thermal conductivity of 0.042 W/(m.K) (Table 7.3), while with the addition of the crosslinkers (wcro1™ and wcro2™), the thermal conductivity was reduced to 0.039 and 0.041 W/(m.K) even with a higher density of 0.079 and 0.071 g/cm³, respectively. The reduction of the thermal conductivity can be related to the microstructure (Figure 7.2), where the increase in surface roughness and the transition to a coarser structure create a longer path for heat to pass through. Therefore, more heat is being dissipated. The nanostructure system can be another factor. Due to the fact the crosslinkers can increase the crystallite size by 10% and increases the crystallinity by 15% that results in an increase in grain

boundaries. This generates an increase in the mean free path of phonons and therefore lowers the overall thermal conductivity of the composites.

7.4 Interim conclusions

This Chapter has demonstrated that crosslinking reaction was a vital parameter for preparing clay-PVA aerogel composites through an environmentally freeze-drying process while using only water as a solvent. The crosslinked aerogels exhibited a significant increase in the compressive moduli due to the change in microstructure which exhibited higher connectivity between the laminar structures. The implantation of aliphatic polyisocyanate (Wcro1™) and 3-glycidoxypropyltrimethoxysilane (Wcro2™) resulted in a compressive modulus of 3.6 and 2.4 MPa respectively compared to 0.48 MPa of the neat clay-PVA aerogel. The crosslinked clay-PVA composites also exhibited significant improvement in their moisture resistance, reducing the moisture absorbed by 27% while retaining dimensional stability. The crosslinked aerogels doubled or tripled liquid absorption capacity while maintained structural integrity when submerged in water. Despite the fact that the crosslinkers resulted in an increase in density the thermal conductivity was slightly enhanced due to a more tortuous path for heat to flow through. Overall the use of crosslinkers was an effective development for preparing clay-PVA aerogel composites, with aliphatic polyisocyanate (Wcro1™) showing the highest promise in terms of mechanical and physical properties.

Chapter Eight: Hydrophobic clay aerogel composites through the implantation of environmentally friendly water repellent agents

Abstract

This Chapter reports the preparation of hydrophobic clay aerogel composites using an environmentally friendly freeze-drying process and using only water as a solvent. This was achieved by using three water dispersible repellent components, a combination of melamine resins with paraffin waxes (WDisRep1™), C6-Fluoroalkyl acrylate (WDisRep3™) and C2-C4 Fluorochemical (WDisRep4™). Microstructure, wettability, moisture resistance, mechanical properties and thermal conductivity of the developed clay aerogel composites were fully characterized to understand working mechanisms and determine the correlations of various processing parameters and performance. The final clay aerogel composites exhibited superior mechanical and physical properties in which the composites moisture absorbance was reduced by up to 40%, while maintaining excellent dimensional stability. The aerogel composites achieved a contact angle of 140° with a 93% reduction in water absorption. The composites achieved a compressive modulus as high as 3.2 MPa, while maintaining low thermal conductivity at 0.038 W/(m.K).

Highlights:

- Water repellents polymers to prepare clay-PVA aerogel composites;
- Using only water as a solvent and an environmentally freeze-drying process;
- Achieving 3.2 MPa compressive modulus with minimal increase in density;
- Highly water repellent and hydrophobic (contact angle=140°) clay-PVA composites.

8.1 Introduction

High moisture content can lead to a 50% rise in thermal conductivity for every 1 (v/v%) as well as significant loss in mechanical strengths and in long moisture exposures cases or direct content to water will result in the degradation of the composite and render the material ineffective and useless [7,8]. The wettability of a solid surface is influenced mainly either by a chemical component or the geometric component of the solid surface or a combination of both [237]. Liquid repellency is crucial in many industries and applications [238,239]. The main chemical approach in decreasing the wettability of solids has been through the use of coatings of fluorinated compounds with low surface energy while the main geometric factor has been by the formation of fractal or rough surface structures [240]. In order to effectively and efficiently use clay aerogel composites as an insulation material in the construction industry, its wettability has to be addressed. This Chapter demonstrates the production of hydrophobic clay-PVA aerogels through an environmentally friendly freeze-drying process through the implementation of soluble water repellent components.

8.2 Experimental work

Water repellent clay-PVA aerogel were developed as described in Chapter 3, Section 3.2.4. Stock clay and PVA solutions are prepared as described in Chapter 3, Section 3.2.1. To prepare the final aerogel dispersion, the required amount of the stock solutions of clay and PVA with the water repellent are mixed together using a magnetic stirrer for 24 hours at low shear. A composition of 2.5 wt. % clay and 2 wt. % PVA was used throughout the experimental work. Three water repellent were used: WDisRep1™ a combination of melamine resins with paraffin waxes, WDisRep3™ -C6-Fluoroalkyl acrylate and WDisRep4™-C2-C4 Fluorochemical at a loading of 1 wt.%. The final aerogel suspension was vertically frozen and finally freeze-dried (Chapter 3, Sections 3.2.1.2 and 3.2.1.3). Testing and characterisation is carried out according to Chapter 3, Section 3.3.

8.3 Results and discussion

8.3.1 Morphology of water repellent clay-PVA aerogels

The morphology aerogel is a representation of ice crystals once dried and is a highly important factor in influencing and controlling both the mechanical and physical properties of the aerogel. The iconic lamellar “house of cards structure” (Figure 8.1A) of clay-PVA aerogels is a replica of the ice crystals once dried as a result of the intergrowth of ice crystals being propagated radially and resulting in long open pores. The addition of melamine resins with paraffin waxes (WDisRep1™) completely distorted the structure, as if the structure collapsed on itself (Figure 8.1B). This can be attributed to (I) the melamine resin, as this thermoset resin may build up a strong 3-dimensional network once cured and merge all the lamellar layers together causing shrinkage once hardened, (II) the phase change of paraffin wax from solid to liquid during the freeze-drying process, which could distort the structure. This can be seen from the image where the layers entangles together with small openings although some layers can still be witnessed (Figure 8.1B inset). The addition of polymers with fluoroalkyl (Rf) groups (WDisRep3™ and WDisRep4™) can have different aggregation structures depending on the chain lengths [241]. The addition of C6- Fluoroalkyl acrylate (WDisRep3™) resulted in a highly coarse laminar structure (Figure 8.1C) with higher interconnectivity as braces/struts (Figure 8.1C inset) being created in between the layers which can be explained by the nature of the semicrystalline tight hexagonal packing (with a diameter of 0.5nm) of the C6-Fluoroalkyl acrylate that can agglomerate into struts/braces between the layered architecture, that would result in an overall more rigid structure, while the addition of the shorter C2-C4-Fluoroalkyl acrylate (WDisRep4™) resulted in thick layers that have highly rough surfaces (Figure 8.1D) and thin struts between the layers. This, which may be due to as a result of the transition of the packing order of the Fluoroalkyl acrylate from a uniform tight lamellar structure at longer chains to a more loose amorphous structure that would

stack on top of each other creating a flat structure, this may result in an aerogel with thicker layers. Due while due to the fact the WDisRep4™ contains a range of Fluoroalkyl acrylate of different lengths, the struts can be explained the same as those for with WDisRep3™.

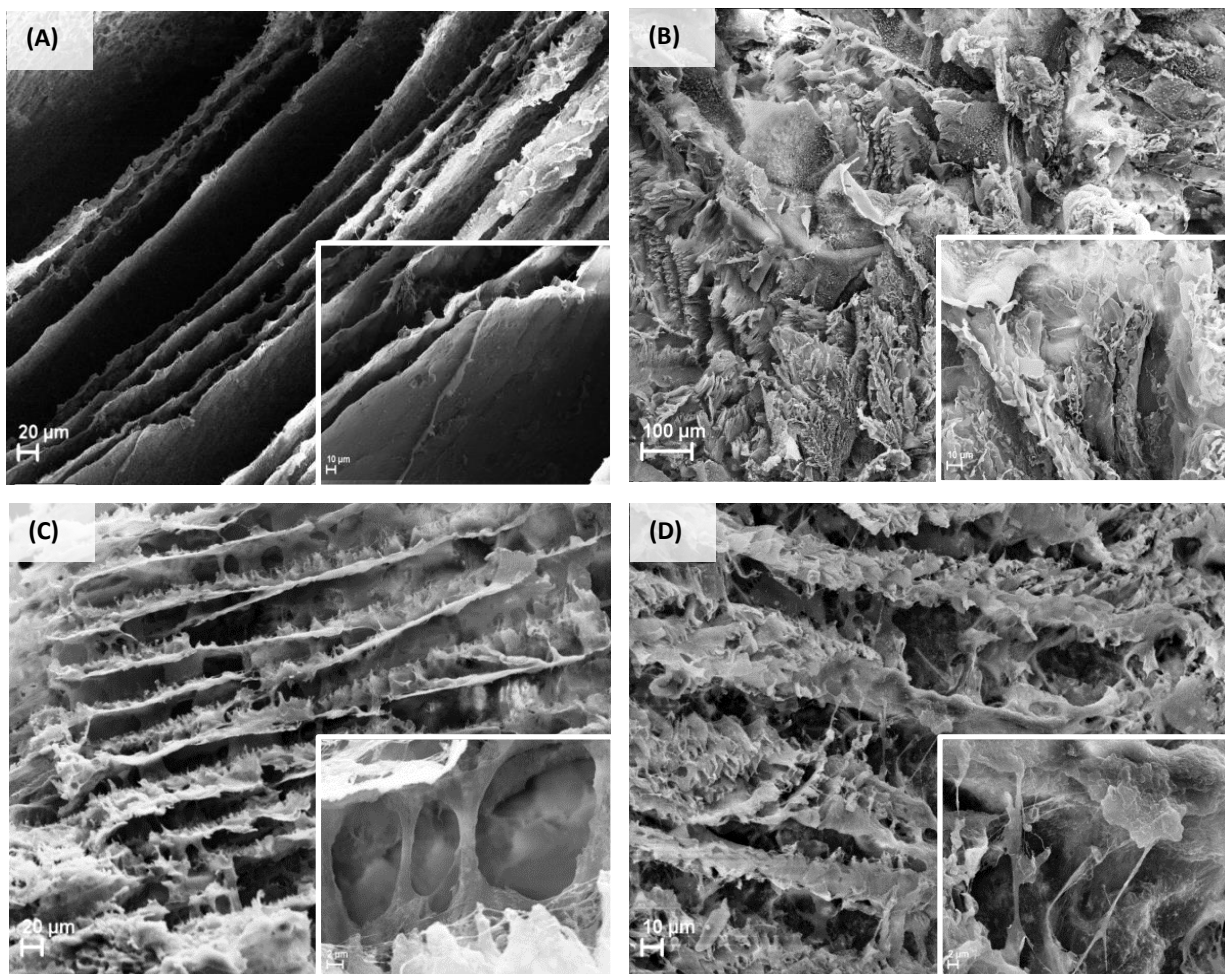


Figure 8.1 SEM results of aerogel composites: (A) Clay-PVA, (B) Clay-PVA-WDisRep1™, (C) Clay-PVA-WDisRep3™ aerogel and (D) Clay-PVA-WDisRep4™

8.3.2 Functional groups of water repellent clay-PVA aerogels

The FTIR spectrum of the water repellent components and the aerogel composites with the incorporation of the components are presented in Figure 8.2. WDisRep3™ and WDisRep3™ are fluorochemical (Fluorocarbon) based repellents, containing fluoroalkyl acrylates copolymers with perfluoroalkyl (R_f) groups of C6 and a mixture of C2-C4, respectively. WDisRep4™ is combination

melamine resins with paraffin waxes. All the components are dispersed in water, and therefore in their liquid state, they are characterised with an intense band at 3320 cm^{-1} (Figure 8.2) that diminishes as the samples are dried indicating the elimination of water molecules bonded to the surface of OH groups [242]. The O-H band (3320 cm^{-1}) is also present in the aerogel composites, and the intensity is also decreased as the samples are dried due to the elimination of water molecules but in the composites the O-H stretching can also be assigned to the vibration of hydroxyl groups as hydrogen bonds (H-O-H) are formed between the clay and PVA [223]. The peaks at 2920 and 2850 cm^{-1} which are assigned to the C-H stretching and CH_2 stretching vibrations, respectively are present in all the repellent components in solution state [243]. These bands witness a sharp increase in intensity once cured (Dried) which is also the case for the aerogel composite suggesting that -OH bonds are being replaced by non-polar bonds such as C-H which can contribute to a more hydrophobic material. At band 2272 cm^{-1} a small peak is presented only in WDisRep4™ indicating a -CNO group [244]. The peaks intensity at 1772 cm^{-1} which represent the C=O stretching of acrylate groups increased as curing took place in both the liquid and composite [245] and expected that they are present in both the fluorocarbon repellents but not WDisRep1™ (a combination melamine resins with paraffin waxes). Strong peaks at 1640 cm^{-1} represent C=C stretching of acrylic and methacrylic double bond which seems to completely disappear as the samples are cured suggesting the grafting of the polymers into a hydrophobic state [246]. This peak can also be associated with water which would also be a reasonable statement as it disappears with drying as bound water molecules are being repelled. The peaks at 1550 and 1450 cm^{-1} are attributed to the -OH and Si-C bonds, respectively [247,248].

Chapter Eight: Hydrophobic clay aerogel composites through the implantation of environmentally friendly water repellent agents

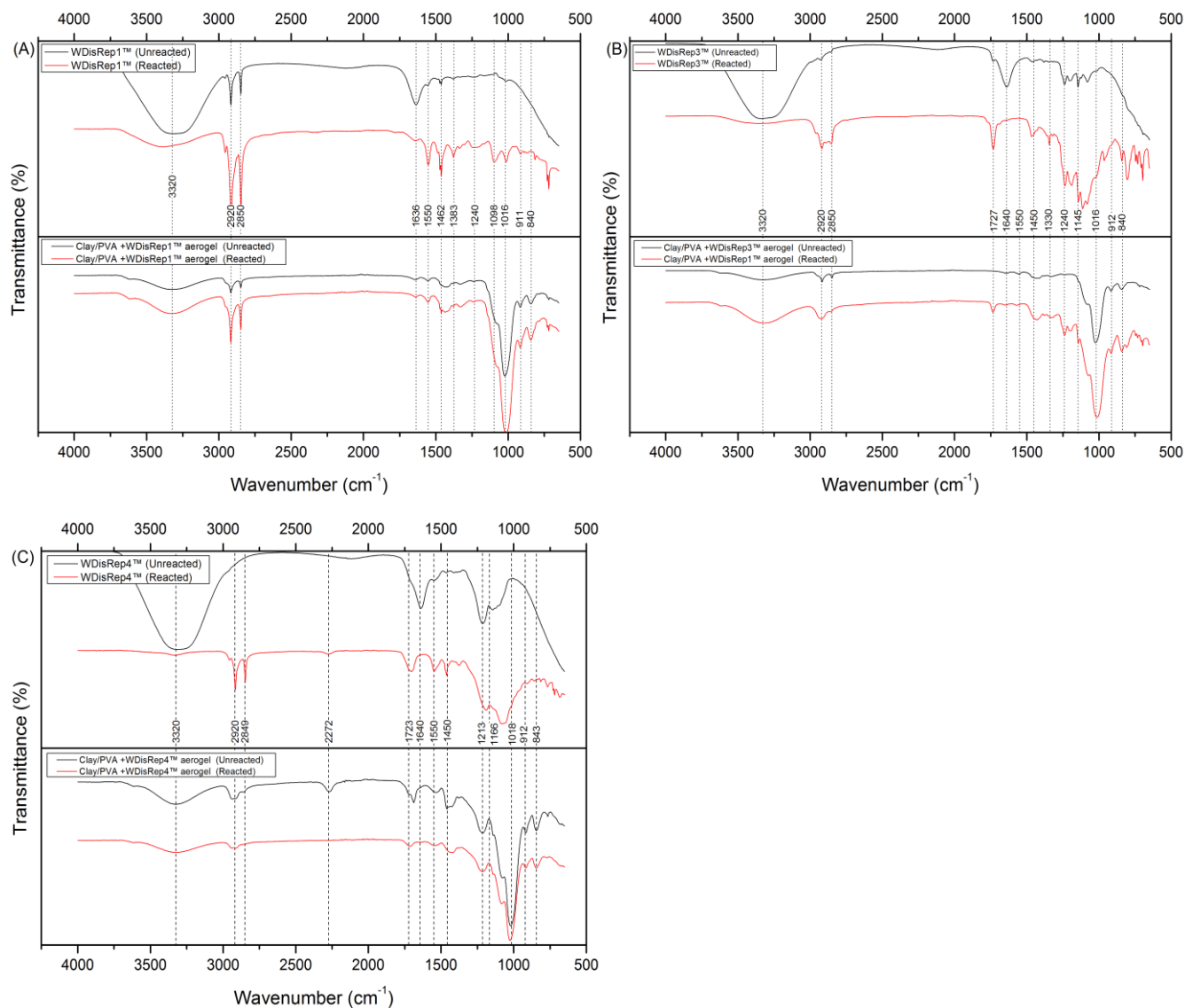


Figure 8.2 FTIR spectrum of water repellents and their aerogel composites: (A) WDiRep1™, (B) WDiRep3™ and (C) WDiRep4™

The main region of significant difference between the different aerogels is between 1400 and 1000 cm^{-1} (Table 8.1) which significantly attributes to hydrophobic components, thus responsible for the improvement in water the repellency [249]. The peak at 1383 cm^{-1} is caused by C–C bonds while the peaks at 1240 and 1213 cm^{-1} reflect the presence of acetylated group [250]. Peaks at 1166 and 1145 cm^{-1} originate from the C–F symmetric stretching and C–O–C stretching vibrations, respectively [251]. The bands at 1016 cm^{-1} and 840 cm^{-1} are produced by the stretching mode of Si–O, out-of-plane and

the stretching vibration of the $-CH_2$ functional group [227]. These adsorption peaks can be observed in both the spectra of the aerogels composites and in the water repellent and suggests on overall substitutions of hydroxyl groups with acetyl groups and thus improve the hydrophobicity of the material.

Table 8.1 Major functional groups of hydrophobic clay aerogel composites

Major functional group	Clay-PVA	Clay-PVA-WDisRep1™	Clay-PVA-WDisRep3™	Clay-PVA-WDisRep4™
O-H	3320	3320	3320	3320
C-H	2929	2920	2916	2916
CH ₂	2862	2850	2850	2850
-CNO	-	-	-	2272
C=O	-	-	1727	1727
C=C	-	1640	1640	1640
-OH	-	1550	1550	1550
Si-C	-	1450	1450	1450
C-H	1416	-	-	-
C-C	-	1383	-	-
CH	-	-	1330	-
C-H	-	1240	1240	-
C-H	-	-	-	1213
C-F	-	-	-	1166
C-O-C	-	-	1145	-
CH	-	1098	-	-
Si-O	1016	1016	1016	1016
C=C-H ₂	-	-	-	-
CH ₂	912	911	912	912
-CH ₂	840	840	840	840

8.3.3 Wettability of water repellent clay-PVA aerogels

8.3.3.1 Moisture absorption of water repellent clay-PVA aerogels

It would be expected that the unmodified clay aerogels will witness the highest weight increase by up to 27% (Figure 8.3) due to their hydrophilic nature and high tendency to absorb moisture. All three water repellent components implemented in the aerogel composites showed significant enhancement in reducing the moisture absorbance of the clay aerogel composites across the humidity ranges (Figure 8.3). C6-Fluoroalkyl acrylate (WDisRep3™) displayed the most promising results having reduced the weight increase by 50% followed by C2-C4 Fluorochemical (WDisRep4™)

which resulted in a 36% drop and finally the combination of melamine resins with paraffin waxes (WDisRep1™) resulted in a 33% drop in weight increase at 95% RH at 24 hours.

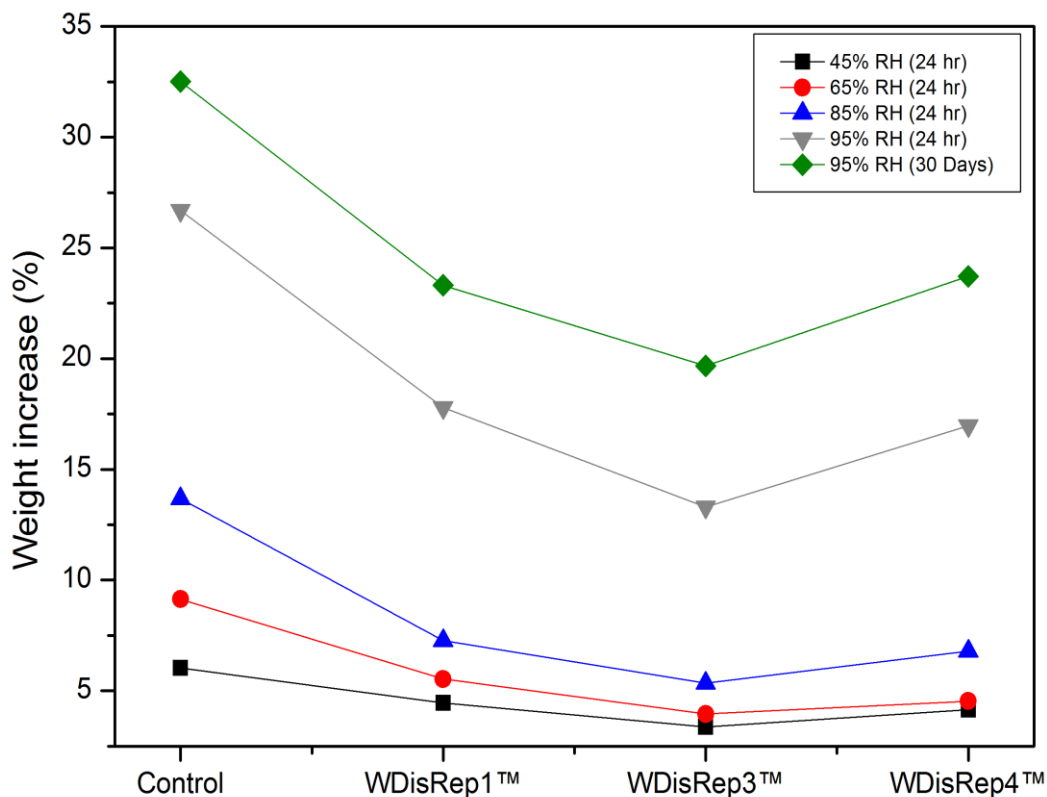


Figure 8.3 Moisture absorption of clay-PVA aerogels with/without water repellent components

During the long-term test (30 days) at 95% RH, the modified aerogels maintained effectiveness in resisting moisture (Figure 8.3) with C6-Fluoroalkyl acrylate (WDisRep3™) being also the most effective by dropping the weight increase by 40% compared to the control sample. The significance about the long-term test is the dimension stability (shrinkage) which can be severely compromised when moisture penetrates and is being absorbed by the solid phase of the aerogel. The dimensional stability of the aerogel composites after being exposed at 95% RH for 30 days is summarised in Table 8.2. The neat clay-PVA aerogels shrank by 63% leaving the composite completely destroyed and ineffective as an insulation material as the microstructure is completely destroyed. The addition of the water-repellent components significantly influenced the dimensional stability of the composites

at high moisture absorbance whereby implementing WDisRep1™, WDisRep3™, and WDisRep4™ the samples shrank by 18.28%, 13.08% and 20.54%, respectively an average improvement of 78% in dimensional stability with C6-Fluoroalkyl acrylate WDisRep3™ having the lowest shrinkage percentage of only 13.08%.

Table 8.2 Dimensional stability of clay-PVA aerogels with/without water repellent components

Sample	Volume Shrinkage (%)
Clay-PVA aerogel	63.12%
Clay-PVA-WDisRep1™ aerogel	18.28%
Clay-PVA-WDisRep3™ aerogel	13.08%
Clay-PVA-WDisRep4™ aerogel	20.54%

8.3.3.2 Water absorption of water repellent clay-PVA aerogels

The water immersion test (Figure 8.4) showed that the neat clay-PVA aerogels weight increased by 330% (Table 8.3), what is also observed is the immediate change in colour of the aerogel from white to brown as the composite begins to disintegrate when in contact in water (Figure 8.4A). The modified aerogels absorbed 90% less water (Table 8.3) as a result of their hydrophobic nature (Table 8.4). In Figure 8.4B, C, and D a gloss on the surface of the composite can be seen as a result of the aerogel repelling the water and thus creating a thin layer of air between the sample, and no air bubbles escaping to the surface was witnessed during the experiment suggesting that pores of the aerogel are not being filled with water, therefore, it can be suggested that the weight increase is a result of water being attached to the surfaces of the aerogels and that water was not absorbed by the solid phase of the aerogel.

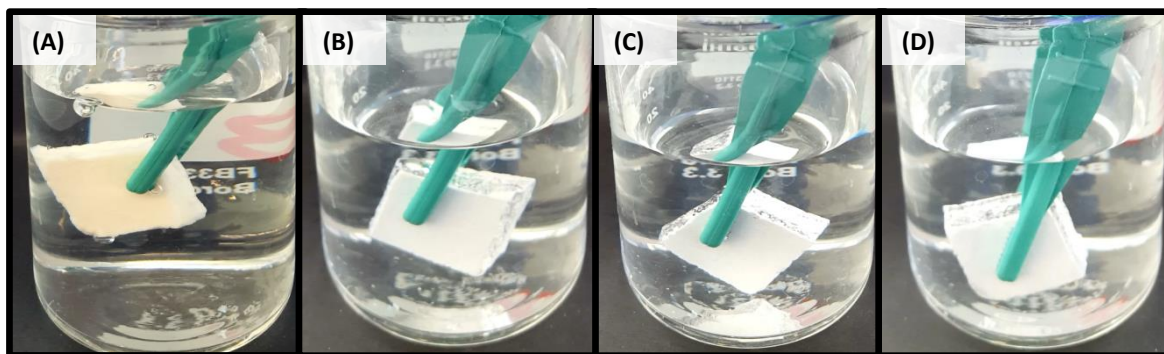


Figure 8.4 Water uptake of aerogels composites: (A) Clay-PVA, (B) Clay-PVA-WDisRep1™, (C) Clay-PVA-WDisRep3™ and (D) Clay-PVA-WDisRep4™

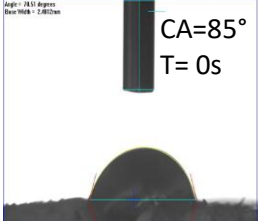
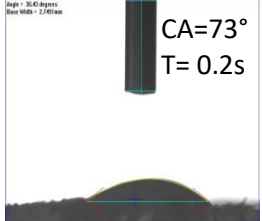
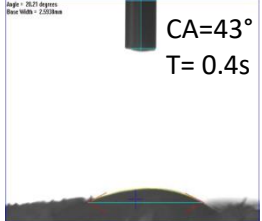
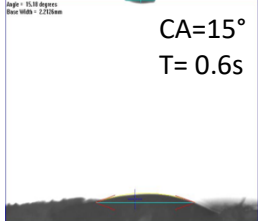
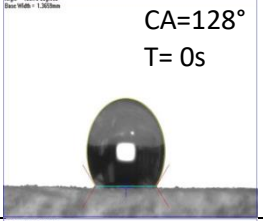
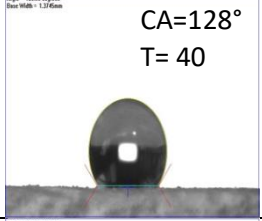
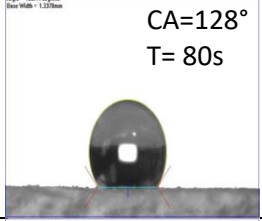
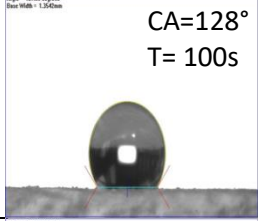
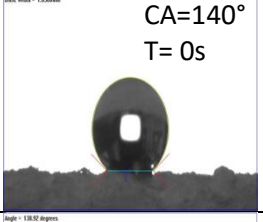
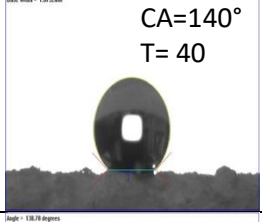
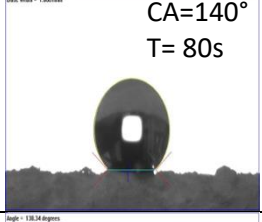
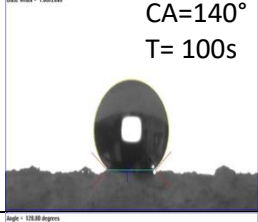
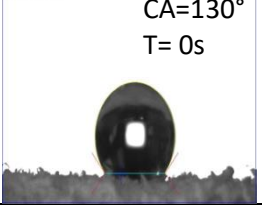
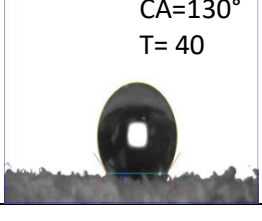
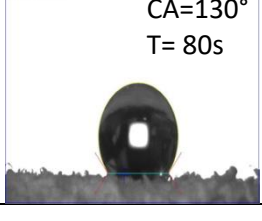
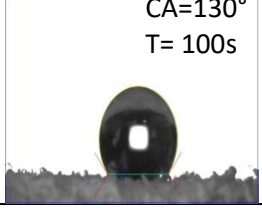
Table 8. 3 Water absorption of clay aerogel composite with/without water repellents

Sample	Weight increase (%)
Clay-PVA aerogel	329.18%
Clay-PVA-WDisRep1™ aerogel	54.76%
Clay-PVA-WDisRep3™ aerogel	21.24%
Clay-PVA-WDisRep4™ aerogel	25.20%

8.3.3.3 Hydrophobicity of water repellent clay-PVA aerogels

The contact angle showed significant improvement (Table 8.4) with the addition of the water repellent agents. The neat clay aerogel (Hydrophilic) within 0.6s absorbed the water droplet completely. The addition of WDisRep1™, WDisRep3™ and WDisRep4™ resulted in contact angles of 128°, 140° and 130° respectively and are stable for more than two minutes. The implementation of the water-repellent components resulted in –OH bonds being replaced by non-polar bonds such as C-H ($1400-1000\text{cm}^{-1}$) while being absent in the control clay-PVA aerogel (Table 8.1) leading to a highly hydrophilic material. As WDisRep3™ created additional bands between $1400-1000\text{cm}^{-1}$ with higher intensities (Figure 8.2B) and thus had the highest proportion of -OH bonds replaced by non-polar bonds, it would be expected that it would have the highest contact angle as it's the most hydrophobic.

Table 8.4 Contact angle of clay-PVA aerogel composite with/without water repellent

Control	 <p>CA=85° T= 0s</p>	 <p>CA=73° T= 0.2s</p>	 <p>CA=43° T= 0.4s</p>	 <p>CA=15° T= 0.6s</p>
WDisRep1™	 <p>CA=128° T= 0s</p>	 <p>CA=128° T= 40</p>	 <p>CA=128° T= 80s</p>	 <p>CA=128° T= 100s</p>
WDisRep3™	 <p>CA=140° T= 0s</p>	 <p>CA=140° T= 40</p>	 <p>CA=140° T= 80s</p>	 <p>CA=140° T= 100s</p>
WDisRep4™	 <p>CA=130° T= 0s</p>	 <p>CA=130° T= 40</p>	 <p>CA=130° T= 80s</p>	 <p>CA=130° T= 100s</p>

8.4.4 Compressive modulus of water repellent clay-PVA aerogels

The implementation of the water repellent agents (polymeric components) into the aerogel composites resulted in significant improvements to the average compressive moduli as polymeric components come in a wide range of strengths (Figure 8.5). The neat clay-PVA aerogels had an average compressive modulus of 0.48 MPa while with the addition of WDisRep1™, WDisRep3™, and WDisRep4™ increased the compressive modulus to 2.6, 3.3 and 1.2 Mpa, respectively. The highest performance was recorded for the WDisRep3™ as a result of the transition of the layered architecture into a more connected system with struts being formed in between the layered structures (Figure 8.1 C).

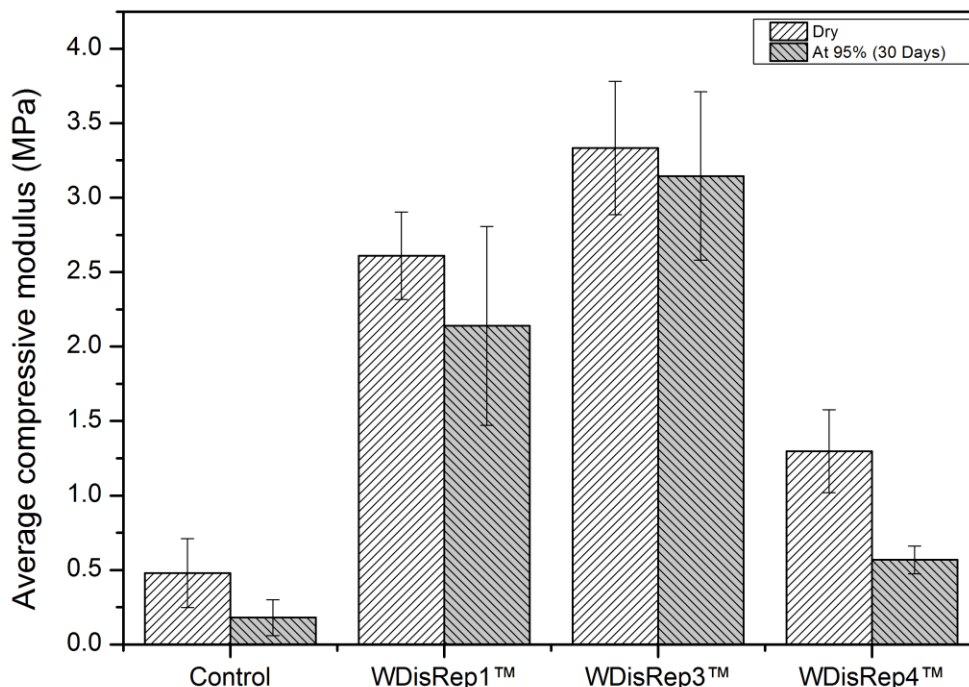


Figure 8.5 Average compressive moduli of clay-PVA aerogels with/without water repellents

The second highest performance was recorded with the incorporation of WDisRep1™ which increased the modulus to 2.6 MPa which can be related to the lack of open pores in the microstructure (Figure 8.1B) and therefore the load is easily transferred through the material. The lowest compressive modulus was reported for WDisRep4™ with a 1.2 MPa average compressive modulus which is still a 60% increase compared to the neat clay-PVA aerogels, the increase in the compressive modulus can be attributed to the increase in layer thickness as more polymer chains are absorbed on the clay surface and the thin struts being formed between the layers (Figure 8.1D). After 30 days at 95% RH, the lowest drop in compressive modulus by only 6% from 3.3 to 3.1 MPa was recorded for clay-PVA-WDisRep3™ aerogel which is also the sample that absorbed the least amount of moisture during the 30 days (Figure 8.3). Although WdisRep1™ and WDisRep4™ absorbed almost the same amount of moisture the latter had a 50% drop in its compressive modulus compared to a 23% drop for WdisRep1™ which might be related to the fact that the incorporation of WdisRep1™

resulted in a more dense and packed structure which can prevent moisture to penetrate deep into the sample compared to the open pores structure clay-PVA-WDisRep4™ aerogel where the moisture would be able to cover a higher surface area.

8.4.5 Thermal Conductivity of water repellent clay-PVA aerogels

The addition of polymeric components to the neat clay-PVA aerogels would result in an increase in density due to the addition of the solid content (Table 8.5). It would be expected especially with most foam-like materials that the thermal conductivity and the density of a material have a proportional relationship in which lowering the density of the material would result in a lower thermal conductivity, however, this is only true to a certain extent.

Table 8.5 Thermal conductivity and density of clay-PVA aerogels with/ without water repellent

Sample	Thermal Conductivity	Density (g/cm ³)
Clay-PVA aerogel	0.042	0.048
Clay –PVA-WDisRep1™ aerogel	0.043	0.126
Clay-PVA-WDisRep3™ aerogel	0.038	0.109
Clay-PVA-WDisRep4™ aerogel	0.039	0.089

In clay aerogel composites the microstructure is the most influential factor in determining the thermal conductivity, for instance, the neat clay-PVA aerogel had a thermal conductivity of 0.042 W/(m.K) with a density of 0.55 g/cm³ while the implementation of WDisRep3™ and WDisRep4™ resulted in an increase in density by 50% and 44%, yet a lower thermal conductivity of 0.038 and 0.039 W/(m.K) was obtained, respectively (Table 8.5). The increase in effectiveness of the thermal conductivity can be related to an increase in the solid connectivity between the layers (Figure 8.1) which would create a more tortuous path for heat to pass through the whole material and therefore more heat would be dissipated with the exception of WDisRep1™ (Figure 8.1C and D) which created a more compact solid structure that allows for easy transfer of heat and a result had the highest

thermal conductivity. More importantly it can also be related to increased hydrophobicity and moisture resistance of the samples, as they would absorb less moisture and water from the condensation of the fox 200 cold plate (0° C).

8.4 Interim conclusions

The hydrophobic clay-PVA aerogel composites have been developed through an environmentally freeze-drying process using only water as a solvent through the implementation of environmentally friendly water soluble water repellent components. All components, namely WDisRep1™, WDisRep3™ and WDisRep4™, resulted in superior mechanical properties reaching values of 2.6, 3.4 and 1.3 Mpa, respectively. The hydrophobic clay-PVA aerogels displayed excellent moisture resistance properties in which they absorbed less moisture by more than 40% while maintaining excellent dimensional stability and mechanical properties after 30 days at 95% RH. The composites also achieved significant contact angles of 140° and absorbed on average 300% less water than the control clay aerogel composite, classifying the developed clay aerogel composites as hydrophobic. Low thermal conductivity could still be achieved even with the increase in density and change in physical properties, reaching values of 0.038 W/(m.K) due to less moisture absorption and the change in the microstructure with the addition of the polymeric components. Overall the ideal candidate to prepare hydrophobic clay/PVA aerogel composite in order for them to be implemented in the construction industry as an insulation material is C6-Fluoroalkyl acrylate (WDisRep3™), as it had the lowest weight increases in the moisture and the water absorption, as well as achieving the highest contact angles. It also recorded the highest compressive modulus and lowest thermal conductivity.

Chapter Nine: Optimisation of highly functional hydrophobic clay aerogel composites for the construction industry

Abstract

This Chapter further investigates the effect of the combined loadings of the most effective water repellent (WR) from Chapter 8 and crosslinkers used in Chapter 7 on the mechanical and physical properties of clay aerogel composites. It was concluded that at 2 wt.% of C6- Fluoroalkyl acrylate (WDisRep3™) a contact angle of 140° with a compressive modulus of 3.5 MPa with a tolerable density of 0.11 g/cm³ was achieved. However, (WR) samples shrank by 28% after a long-term water absorption. Therefore a hybrid solution using either crosslinker, aliphatic polyisocyanate (Wcro1™) or 3-glycidoxypropyltrimethoxysilane (Wcro2™) and C6-Fluoroalkyl acrylate (WDisRep3™) to prepare clay-PVA aerogel composites has been developed. Through this approach, the moisture absorption of the developed clay aerogel composites could be reduced by 60% and contact angles was as high as 145° with only 6% shrinkage after 30 days in water. An acceptable density of 0.1 g/cm³ was maintained with a thermal conductivity of 0.039 W/(m.K) and a compressive modulus of 8 MPa. The optimum ratio to provide the best density to performance ratio of clay-PVA aerogel composites has been reported as 1 wt.% aliphatic polyisocyanate and 2 wt.% C6-Fluoroalkyl acrylate.

Highlights:

- Hybrid solution using crosslinkers and water repellent to develop the optimum clay aerogel composites:
- Using only water as a suspension solution and an environmentally freeze-drying process:
- Highly water repellent and hydrophobic clay-PVA composites developed;
- Optimum formulation of crosslinkers to water repellent for the best density to performance ratio.

9.1 Introduction

The durability and performance of all building insulation especially porous materials are highly affected by the moisture content and sorption properties [218]. One of the major setbacks associated with clay aerogel composites is their tendency to absorb a high amount of moisture due to their hydrophilic nature [198]. High absorption will not only result in an increase in thermal conductivity by 50% for every 1 (v/v%) absorbed as with other porous materials, but also disintegrate the composite as a whole causing significant shrinkage and even collapse of the microstructure. This renders the aerogel completely ineffective as an insulation material [7,8]. In previous Chapters, the effect of the incorporations of either a crosslinker or water repellent polymers into the aerogel composites has been investigated. This Chapter implements a hybrid solution of implementing both crosslinker and the optimised water repellent polymers to develop highly functional and durable hydrophobic clay aerogel composites.

9.2 Experimental work

Crosslinked water repellent aerogel production were developed as described in Chapter 3, Section 3.2.6. Stock solutions of clay and PVA are prepared as described in Chapter 3, Section 3.2.1. To prepare the final aerogel dispersion, the required amount of the stock solution of clay and PVA with the water repellent and crosslinker are mixed together using a magnetic stirrer for 24 hours at low shear. The amount of C6-Fluoroalkyl acrylate (WDisRep3™) was varied between 0.3, 0.5, 0.8, 1, 1.2, 1.5, and 2 wt. % for one set of experiment. The second set the water repellent component was the combination of C6-Fluoroalkyl acrylate, (WDisRep3™) with either crosslinking agents Aliphatic polyisocyanate (Wcro1™) or 3-glycidoxypropyltrimethoxysilane (Wcro2™) with a ratio between the crosslinker and the water repellent of 0.5:0.5, 1:1, 2:1 and 1:2 wt.%. The sample codes as referred to in the main body are presented in Chapter 3, Section, 3.2.6, Table 3.5. The final aerogel suspension

was vertically frozen and finally freeze-dried (Chapter 3, Sections 3.2.1.2 and 3.2.1.3). Testing and characterisation is carried out according to Chapter 3, Section 3.3.

9.3 Results and discussion

9.3.1 Wettability of crosslinked water repellent aerogels

9.3.1.1 Moisture absorption of crosslinked water repellent aerogels

It has been established that clay aerogel composites are highly hydrophilic by nature due to their water-soluble components and high porosity. It is evidenced that the weight of the neat clay aerogels without any additives can increase by 30% at 95% RH, 14% at 85% RH, 9% at 65% RH, 6% at 45% RH and by 33% after the cycle test (Figure 9.1). The moisture absorbance also varies with the different concentrations of C6-Fluoroalkyl acrylate (WDisRep3™), but showed effectiveness in reducing the moisture absorbance even at low concentrations (Figure 9.1A). Across the humidity ranges tested the addition of 0.3 wt.% resulted in an average drop of 9.5%, 0.5 wt.% resulted in a 20% drop, 0.8 wt.% resulted in a 25% drop, 1 wt.% resulted in a 36% drop, 1.2 wt.% resulted in a 40% drop, 1.5 resulted in a 43% drop and finally the addition of 2 wt.% resulted in a 48% drop in the weight increase. The increase in content was limited to 2% as it reached a density of 0.11g/cm³, which is proximate to the limit of the preferred density range of insulation materials in the construction industry. The mechanism of water/moisture repellency C6-Fluoroalkyl acrylate may be associated with its low surface tension, which is derived from the perfluoroalkyl (R_f) groups. These groups are responsible for the water repellency. Also the reduction in the moisture absorbance across all the humidity ranges can be related to the change in morphology (Table 9.1) where the addition of C6-Fluoroalkyl acrylate transitioned the structure from a laminar layer architecture to a denser coarse structure with higher connectivity, that can create a more tortuous path for moisture to penetrate deep into the sample. A significant conclusion can be drawn from the cycle test (Figure 9.1A) in which the control sample

weight increased by 33% regardless of the fact that the cycle test ends at 65% RH which resulted in a 9% increase, while the samples which incorporated WDisRep3™ their weight increase regressed to the weight increase that the samples witnessed at 65%RH (\pm Deviation), for instance, sample 1.0WR weight increased by 17% and 6.4% at 95% RH and 65% RH, respectively and after the cycle test the weight increase was recorded at 6.3%. Therefore, it can be suggested that the neat clay-PVA aerogel absorbed most of the moisture through the solid hydrophilic content, creating strong hydrogen bonds with the aerogel, while for the samples with C6-Fluoroalkyl acrylate, most of the moisture is absorbed through the capillaries pores allowing moisture to diffuse from areas of high moisture content to regions with lower moisture content as the humidity conditions are altered.

The influence and effect of solely Wcro1™ or Wcro2™ have been previously investigated (Chapter 8). Incorporating either isocyanates or organosilanes (Wcro1™/Wcro2™) compounds with C6-Fluoroalkyl acrylate (WDisRep3™) resulted in significant reduction of the moisture absorption (Figure 9.1B and C), mainly due to the crosslinking increasing the barrier properties and decreasing the overall hydrophilicity by the reduction of the hydroxyl groups. The reduction in moisture sorption can also be related to the change in the morphology (Table 9.2 and 9.3). Across all the humidity ranges the composition of samples CR1/WR0.5:0.5 and CR2/WR0.5:0.5 resulted in a weight increase by 23% and 26% respectively. At such low concentration, the results are comparable to the neat aerogel. However, the samples CR1/WR1:1 and CR2/WR1:1 resulted in a 38% and 42% reduction, respectively. The samples CR1/WR1:2 and CR2/WR1:2 resulted in a significant decrease of 59% and 60% respectively. The samples CR1/WR2:1 and CR2/WR2:1 resulted in a drop of 54% and 56% respectively. Both CR1/WR and CR2/WR samples witnessed lower weight increases after the cyclic test, and the weight increase fluctuated back to what the samples absorbed at 65% RH and as discussed earlier this suggests that most of the moisture is absorbed through the capillaries.

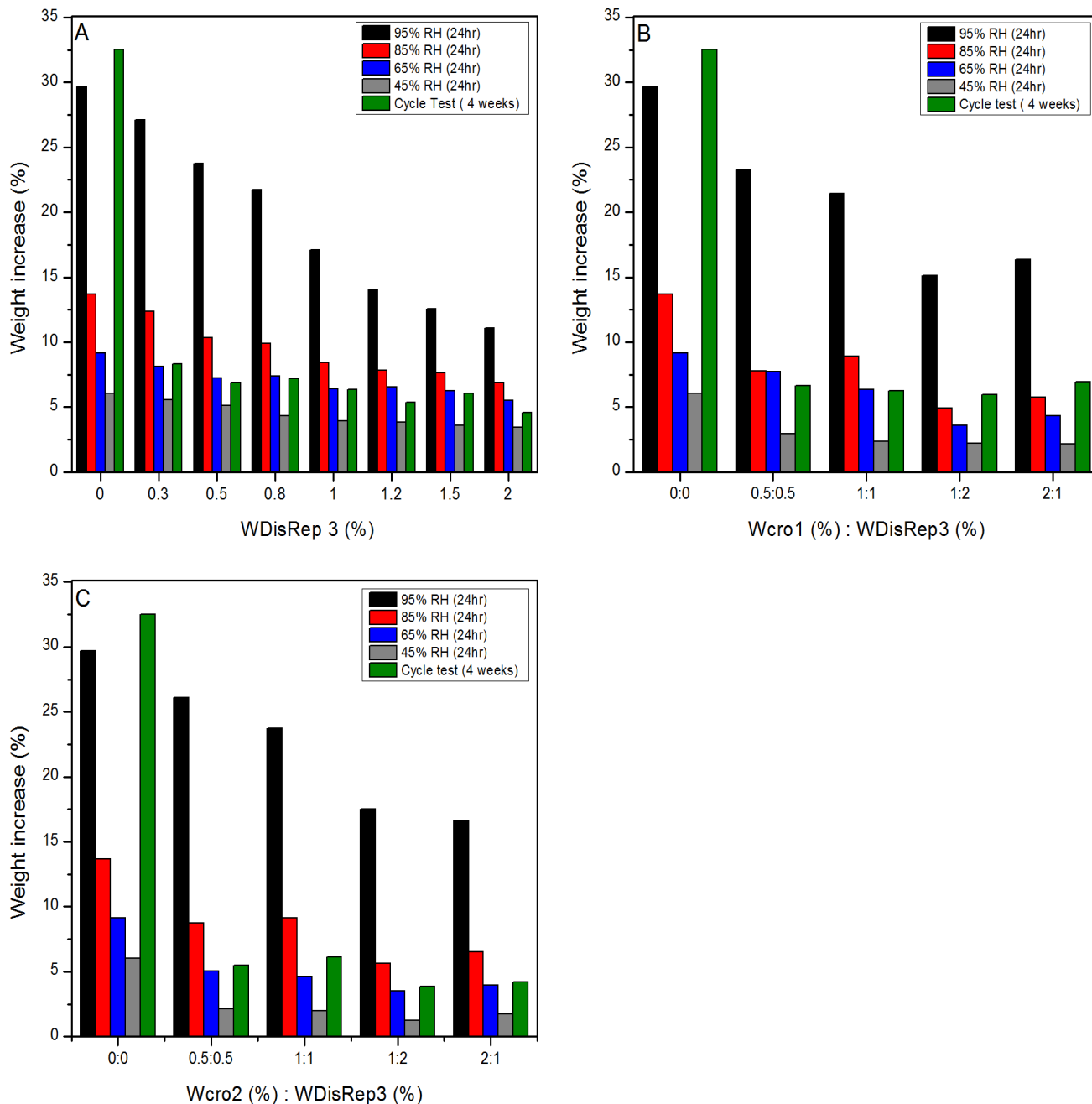


Figure 9.1 Aerogel exposure to varying moisture condition: Weigh change with (A) varying loading of WDisRep3™, (B) varying ratios of Wcro1™ to WDisRep3™ and (C) varying ratios of Wcro2™ to WDisRep3™

9.3.1.2 Long-term water absorption of crosslinked water repellent aerogels

The long-term water absorption of clay aerogel composites (Figure 9.2) is crucial to understand their long-term efficiency and durability when used in construction, especially building construction.

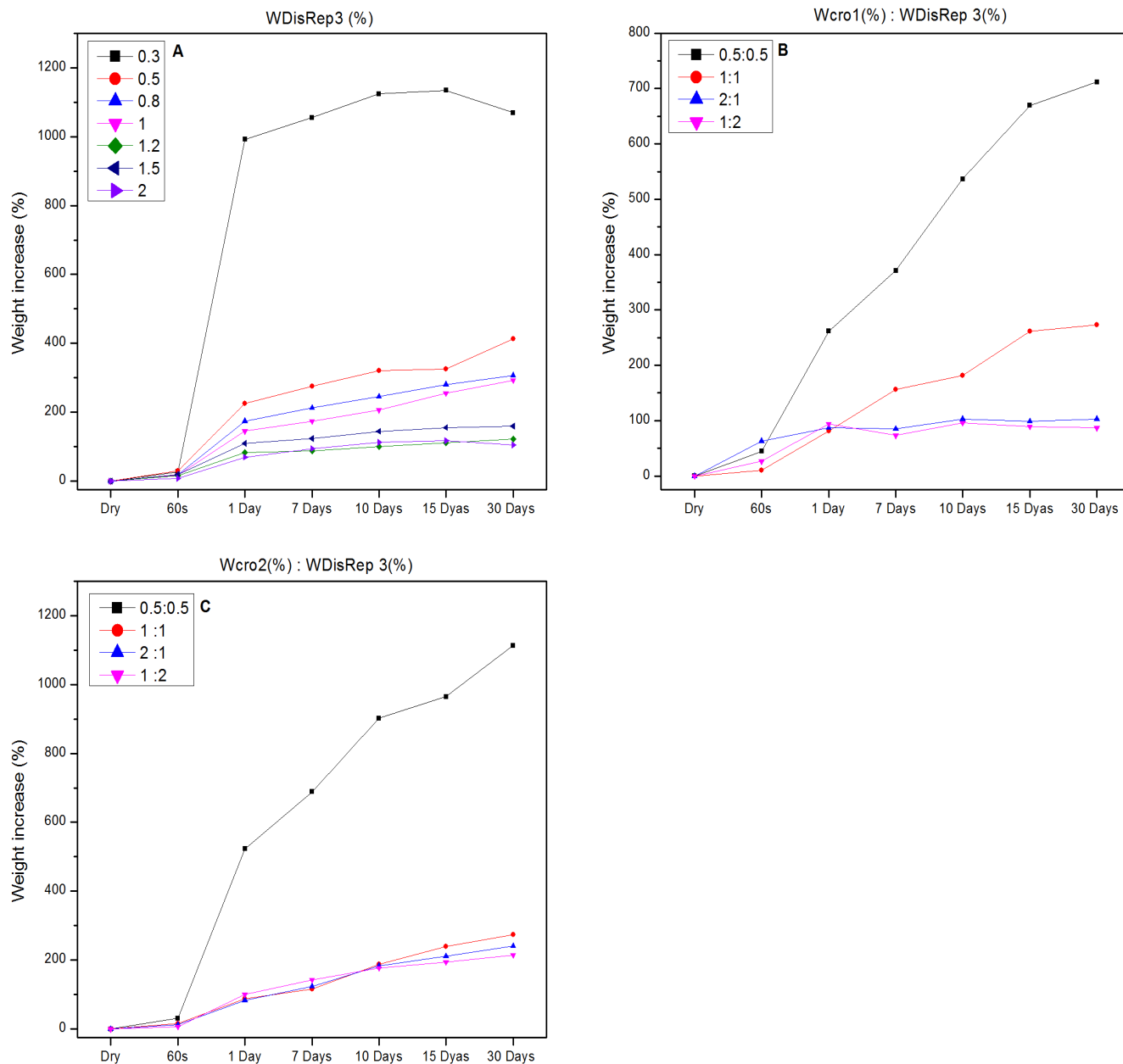


Figure 9.2 Water sorption of aerogels: Weight change with (A) varying loading of WDisRep3™, (B) varying ratios of Wcro1™ to WDisRep3™ and (C) varying ratios of Wcro2™ to WDisRep3™.

It should be noted that the neat clay aerogel samples weight could not be recorded over a long period of immersion in water due to the poor dimensional stability. As soon as it contacted with water it begins to disintegrate as a result of its high hydrophilicity (Figure 9.3) where the water droplet was absorbed entirely. Samples with the incorporation of WDisRep3™ (WR) (Figure 9.2A) witnessed about

10% of their weight increase within the first 60s and this is considered that at this point this is mostly due to water bonded to the surface of the aerogels, for reference the control clay aerogels witnessed about 400% increase in weight within 60s. The weight sample 0.3WR, which has low C6-Fluoroalkyl acrylate content, increased by more than 1000% at 30 days. This aerogel composite may be classified as hydrophilic as it has a contact angle $\leq 90^\circ$. It should be noted that the reduction in the weight increase (Figure 9.2A) at 30 days for sample 0.3WR may be due to the sample disintegrating in water. The weight increase due to water absorption is significantly reduced as the loadings of repellents are increased (Figure 9.2A) due to an overall rise in hydrophobicity (Figure 9.3A). The sample 2.0WR recorded a contact angle of 140° , which in turn reflects the 90% drop in the weight increase at 30 days from 1000% to 105%. Even at very low concentrations WDisRep3™ showed effectiveness in reducing the water absorbed; where it was reduced from 1134% to 413% for sample 0.5WR as a result of a significant increase in hydrophobicity with a contact angle of 128° . This is a substantial increase from the control sample (0° contact angle) and sample 0.3WR (80° contact angle). The addition of either isocyanates or organosilanes (Wcro1™/Wcro2™) compounds to the neat aerogels played a significant role in reducing the moisture absorbed (Chapter 8, Section 8.3.3.1) due to the reduction of the hydroxyl groups, however due to the nature of the aerogel high porosity the water penetrated the sample with minimal structural damage and thus did not influence the contact angle as previously reported (Chapter 7, Section 7.3.3.3).

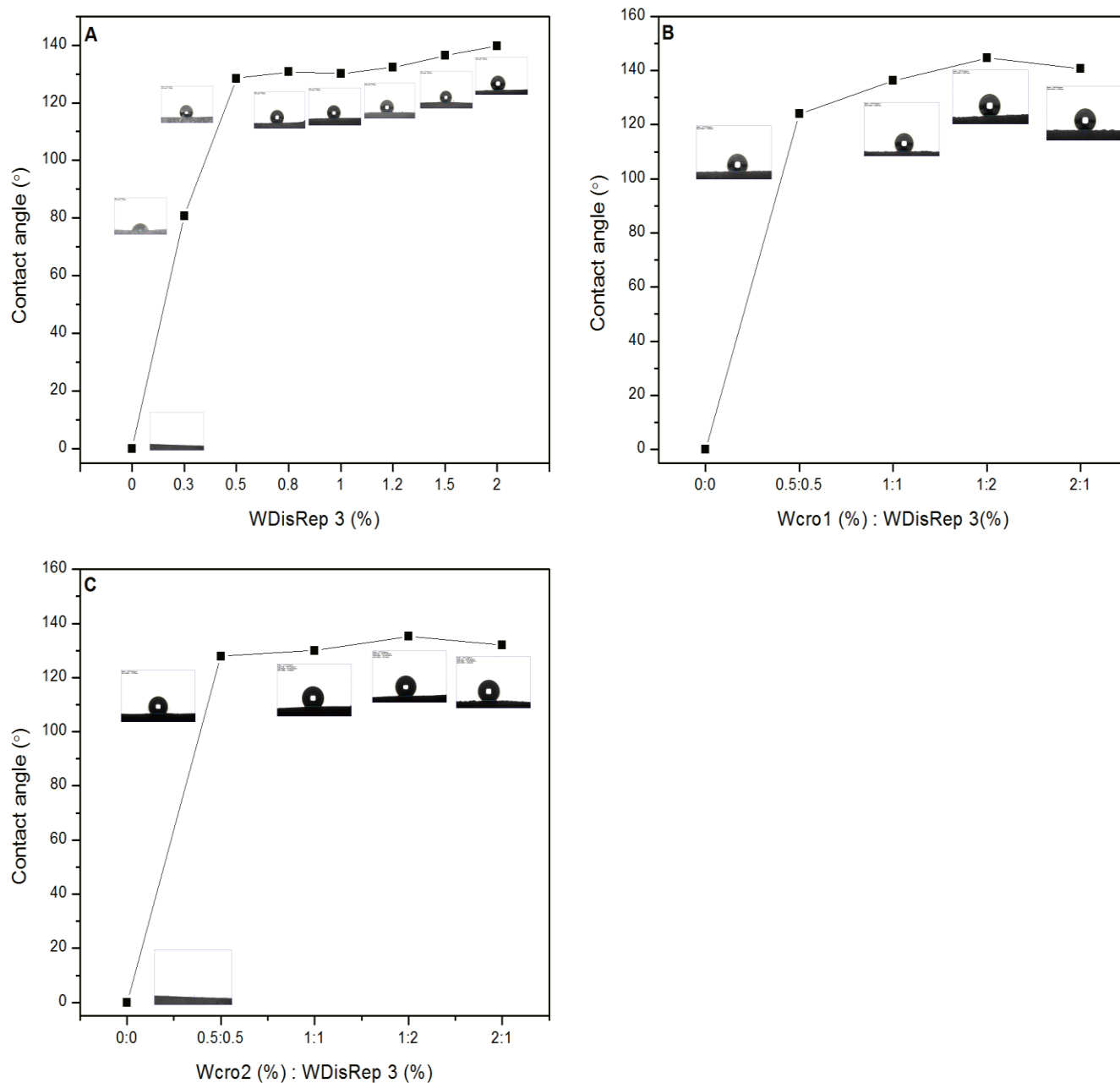


Figure 9.3 Contact angle of aerogel with (A) varying loading of WDisRep 3™, (B) varying ratios of WCro1™ to WDisRep3 and (C) varying ratios of WCro2™ to WDisRep3

Therefore combining the crosslinkers with WDisRep3™ can increase the overall hydrophobicity and moisture resistivity of the aerogels. Samples CR1/WR0.5:0.5 and CR2/WR0.5:0.5 witnessed the highest weigh increase by 712 and 1113 %, respectively, even though they had a contact angle of $\approx 120^\circ$. It can be confirmed that WDisRep3™ is responsible for the hydrophobicity as sample 0.5WR

having a contact angle of 128°. However, the overall moisture resistivity across the all humidity ranges for samples CR1/WR0.5:0.5 and CR2/WR0.5:0.5 is reduced by 5% compared to sample 0.5WR. Samples CR1/WR1:1 and CR2/WR1:1 witnessed almost the same weight increase by 275% and 273% respectively, with a contact angle of 130°. These results are comparable with sample 1.0WR, again suggesting that WDisRep3™ is solely responsible for the hydrophobicity of the samples. Both samples CR1/WR1:2 and CR2/WR1:2 witnessed the highest contact angles of 145° and 135°, and lowest weight increase of 87 and 215% respectively, at 30 days. The sample with the incorporation of Wcro1™, absorbed 20% less than the sample WR2.0. The sample CR1/WR1:2 only, from 10 days onward to day 30 witnessed only a 4.5% standard deviation in the weight increase (Figure 9.2B), suggesting that the sample is saturated and the absorption through the solid phase is minimised. Increasing the content of the crosslinker either for samples CR1/WR2:1, or CR2/WR2:1 resulted in overall higher water absorption by 102 and 240% with contact angles of 141 and 132°, respectively. Demonstrating that increasing the content of WDisRep3™ is more effective to reduce water absorption than the addition of crosslinkers, especially due to the nature of the aerogel layered morphology, which allows for water to easily penetrate through the sample.

9.3.1.3 Dimensional stability of crosslinked water repellent aerogels

More importantly is the structural integrity after immersion for 30 days. As the dimensional stability (Figure 9.5) is crucial in determining the durability of the aerogel. The shrinkage of an insulation material will create thermal bridges and will, in turn, result in a total increase in the overall thermal conductivity of the building envelope. The control sample shrank by more than 98% (Figure 9.5) due to the disintegration and dissolving of the hydrophilic content. Due to the control sample breaking up into smaller pieces in water, the sample 0.3WR might be used as a more reliable measurement for comparison and had 92% shrinkage (Figure 9.5).

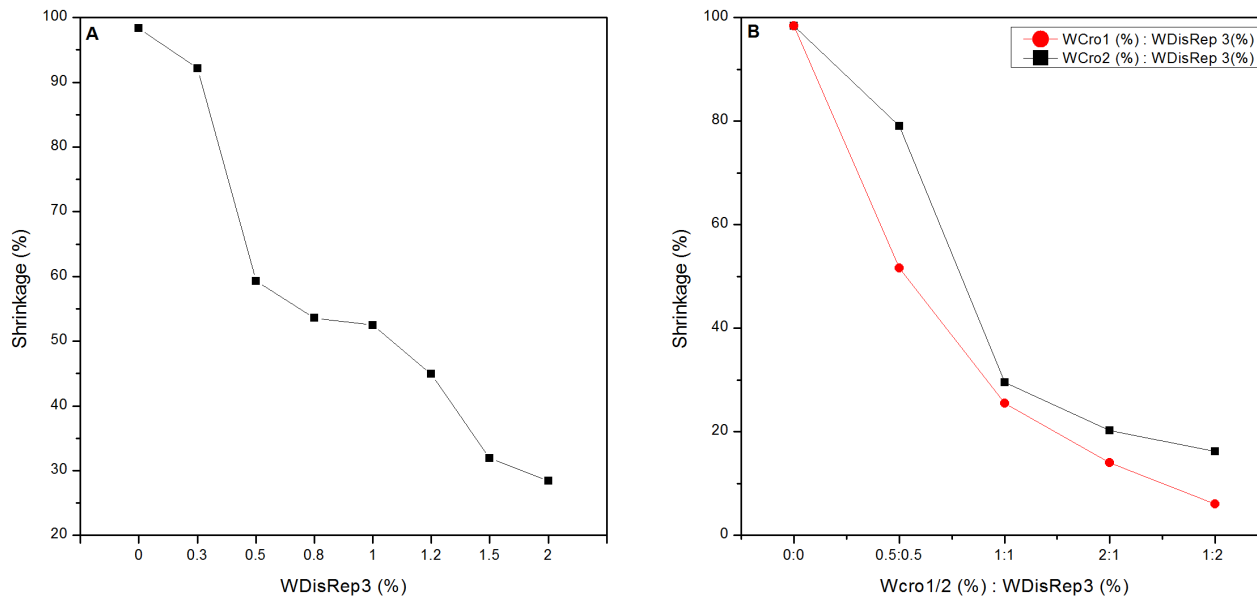


Figure 9.4 Shrinkage of aerogels after 30 days of water absorption: (A) varying loadings of WDisRep3™ and (B) varying ratios of Wcro1™/Wcro2™ to WDisRep3™

The higher the hydrophobicity of the aerogels the less shrinkage the composite will experience as the hydrophilic components (Clay and PVA) will have less water or moisture bonded to them which will cause the sample morphology to collapse on itself as seen in Table 9.1. Sample 2.0WR shrank by 28% a 70% enhancement in the dimensional stability of aerogel composites at 30 days (Figure 9.4A). The combination of crosslinker and the water repellent, such as CR1/WR01:2 and CR2/WR01:2, resulted in significant dimensional stability; the materials shrank by only 6 and 16 %, respectively. The lowest shrinkage for sample CR1/WR01:2 (Figure 9.4B) can be considered marginal for a 30-day test. It can also be seen from Table 9.3 that it had the best structural integrity where the morphology integrity is unchanged from its dry state and after being exposed to water. It can be concluded in terms of wettability that the combination of aliphatic polyisocyanate (Wcro1™) with C6-Fluoroalkyl acrylate (WDisRep3™) results in better performance in both moisture/water absorption and structural integrity.



Figure 9.5 Shrinkage of the sample after 30 days in water: Sample CR1/WR1:2 shrunken by 6 % (Left) and Sample 0.3WR shrunken by 92% (Right)

9.3.2 Compressive modulus of crosslinked water repellent aerogels

The compressive modulus of aerogel composites or foam-like materials is usually related to the density. Therefore it would be expected that increasing the content of WDisRep3™ will result in an increase in density (Figure 9.6). Part of the increase in the moduli (Figure 9.6) can be related to the increase in density, but more importantly the increase in moduli is mostly consequence of the change in morphology (Tables 9.1, 9.2 and 9.3), in which the layered architecture of the control aerogel (Table 9.1) transitioned into a more interconnected with higher connectivity between the layers of aerogel composites that is capable of transferring load more effectively and efficiently. The control clay aerogel recorded a compressive modulus of 0.38 MPa, while sample 2.0WR recorded a modulus of 3.5 MPa, a significant 8 fold increase with an increase in density from 0.048 to 0.11 g/cm³. More important is the drop in the compressive modulus after cyclic test which only witnessed an 8.5% drop to that of 3.2 MPa, this is a significant enhancement compared to the control samples which

witnessed an 80% drop in modulus. Even at low concentrations of WDisrep3™, such as sample 0.3WR had a 3 fold increase on the compressive modulus and only dropped by 22% after the cycle test.

The combination of either the crosslinker with the water repellent resulted in a significant increase in the compressive modulus (Figure 9.6B and C). Sample CR1/WR2:1 recorded a significant compressive modulus of 8 MPa, a 21 fold increase from the control sample with an increase in density to 0.084 g/cm³. It is worth to note that although a 75% increase in density, it remains under 0.1g/cm³ which is the preferred density for insulation materials. Overall sample with the code CR1/WR had a better performance in which their compressive moduli witnessed almost no change (\pm deviation). This is expected as they absorbed the least moisture (Figure 9.1B) and exhibited the highest hydrophobicity (Figure 9.3B) and structural integrity (Table 9.2). Samples CR2/WR recorded an increase in compressive modulus up to 6.2 MPa. Interestingly an increase is also witnessed in the compressive modulus after the cyclic test, which can be explained by the change in morphology (Table 9.3) where the layered morphology was more vulnerable to damage when in contact with water. Samples CR1/WR0.5:0.5 and CR2/WR0.5:0.5 which both have a total additive content of 1 wt.% recorded a compressive modulus of 3.2 and 3.6 MPa respectively, while sample 1.0WR recorded a modulus of 2.2 MPa showing that the crosslinking is a more effective means of increasing the compressive moduli than adding C6-Fluoroalkyl acrylate which is a polymeric based water repellent. Sample 2.0WR had a density of 0.11 g/cm³ while samples CR1/WR2:1 and CR2/WR2:1 recorded a density of 0.097 and 0.11 g/cm³ respectively, showing that the crosslinking has a less dominant effect on the density of the aerogel. Samples CR1/WR2:1 and CR2/WR1:2 had a density of 0.084 and 0.078 g/cm³ respectively, showing that the concentration of WDisRep3™ is dominant in influencing the density.

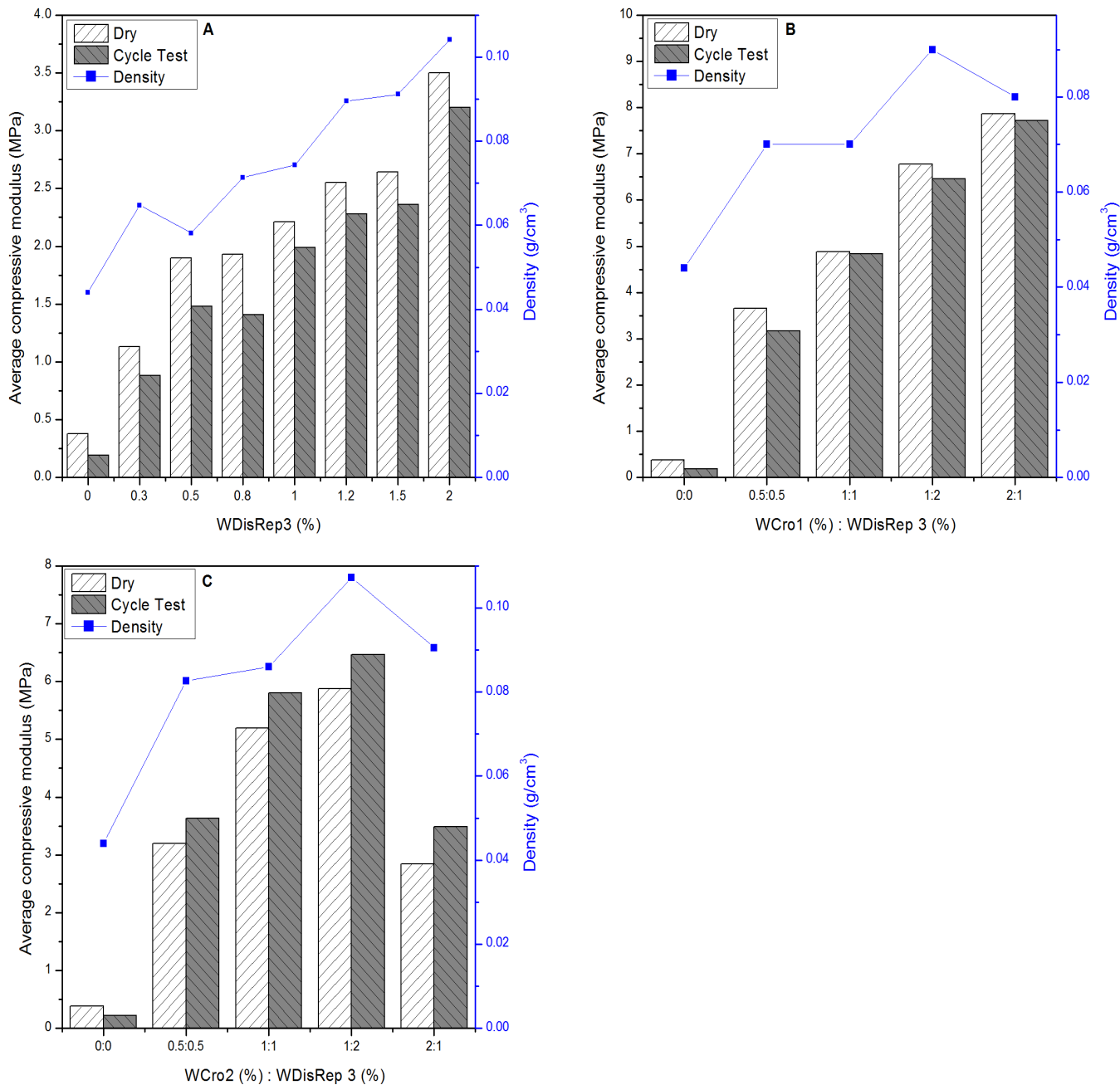


Figure 9.6 Compressive moduli of aerogel composites (A) with varying loading of WDisRep3™, (B) varying ratios of WCro1™ to WDisRep3™ and (C) varying ratios of WCro2™ to WDisRep3™

9.3.3 Morphology crosslinked water repellent aerogels

The effect of the different concentrations of WDisRep3™ can be seen in Table 9.1 for both the dry state and wet state. The control aerogel composites are characterised with a layered architecture in

the dry state, which is completely destroyed as soon as the surface of the aerogel is exposed to water and thus completely diminishing the aerogel properties. Sample 0.5WR resulted in a denser structure, which is completely distorted and all the layers collapsed to form a solid microstructure when in contact with water. Increasing the content of WDisRep3™ to 1 wt. % created a structure that is a highly coarse, with higher interconnectivity between layers and even though that the concentration of WDisrep3™ accounts for 20% of the solid content (5.5 wt.%), the structure still witnessed water damage. At 1.5 wt.% the WDiRep3™ water repellent begins to take effectiveness in protecting the layered microstructure from water damage. Increasing the content to 2 wt.% resulted in a highly coarse laminar structure with higher interconnectivity braces/struts created in between the layers with almost no change or damage to the morphology after exposure to water. The influence of aliphatic polyisocyanate (Wcro1™) and C6-Fluoroalkyl acrylate (WDisRep3™) on the aerogel morphology can be seen in Table 9.2. Sample CR1/WR0.5:0.5 gave rise a layered morphology that is completely distorted into a solid structure with most of the pores disappear after exposure to water. Sample CR1/WR1:1 gave rise to a morphology with increased surface roughness that exhibited very minor structural damage, where the layers slightly fuse together (Edges of the image). Sample CR1/WR1:2 gave rise to a layered morphology with increased connectivity with struts or braces being formed between the layers, and water had no influence on the morphology in any respect. Sample CR1/WR2:1 had an increase in connectivity and witnessed a complete structural collapse.

Table 9.1 Microstructures of control and WR samples before and after exposure to water

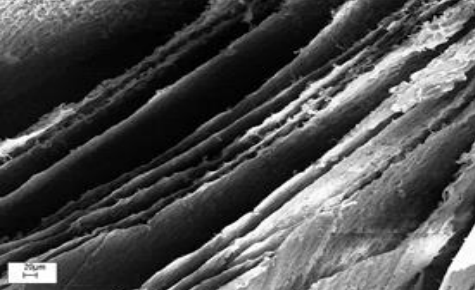
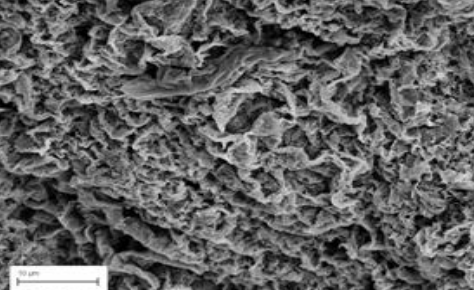
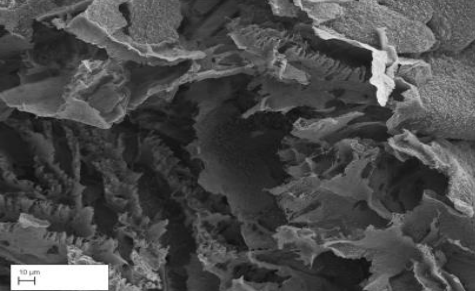
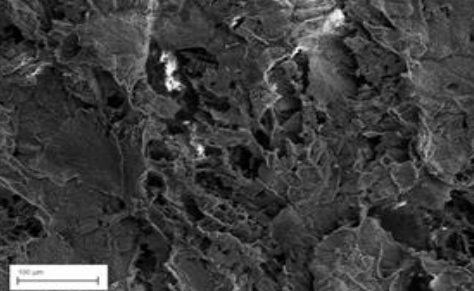
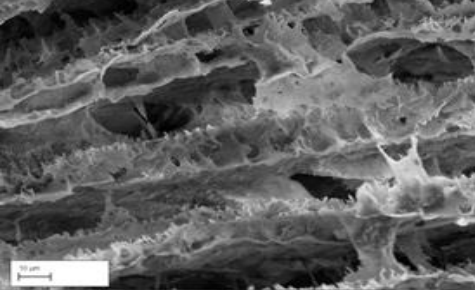
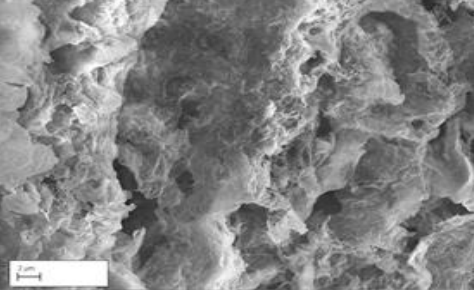
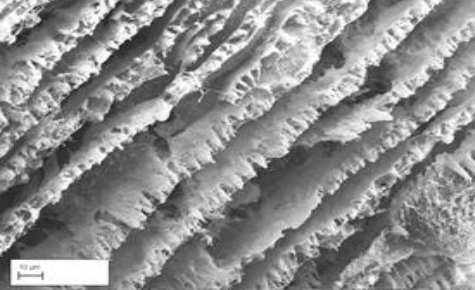
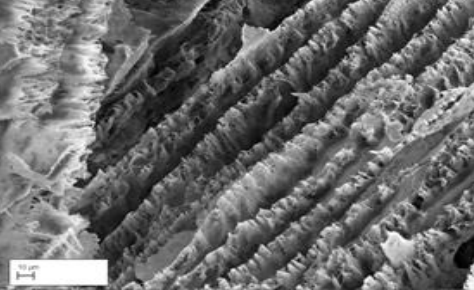
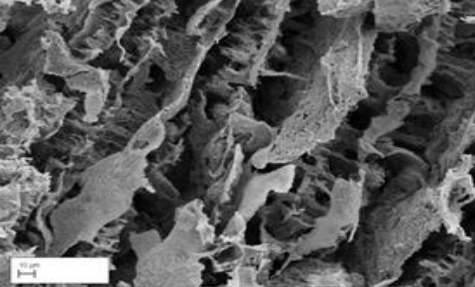
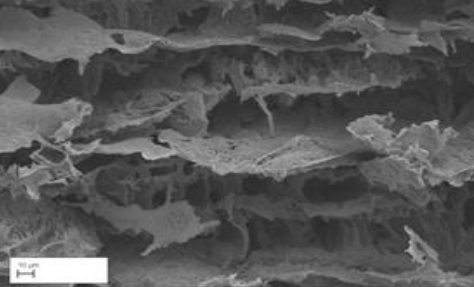
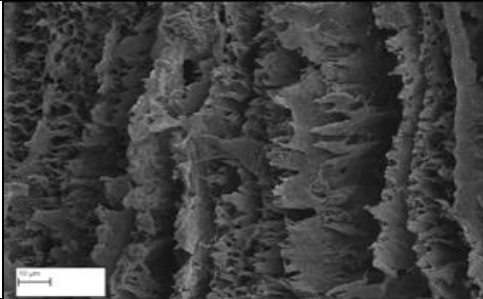
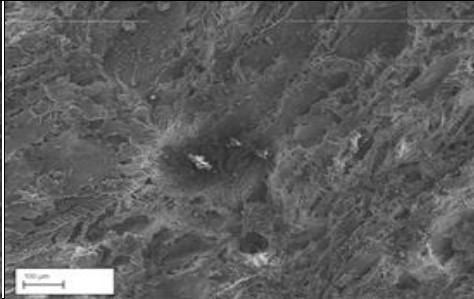
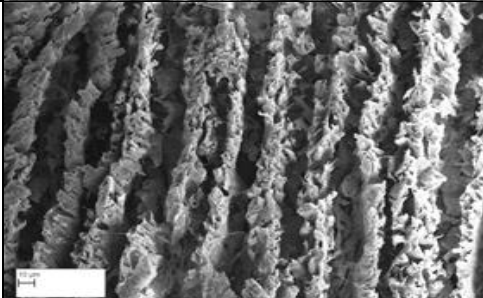
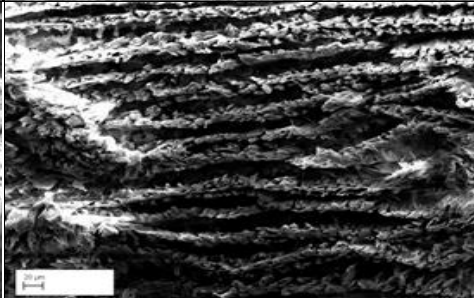
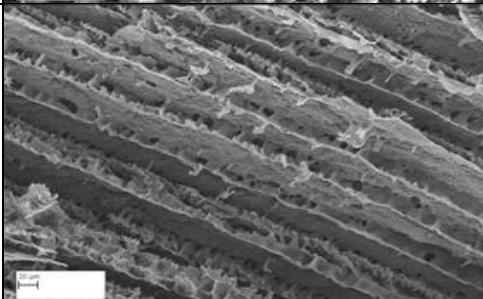
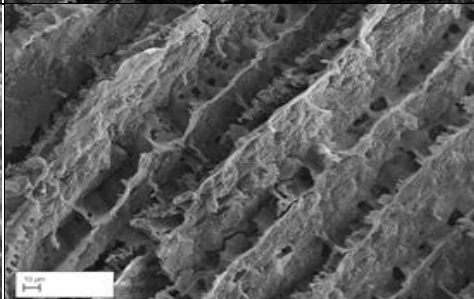
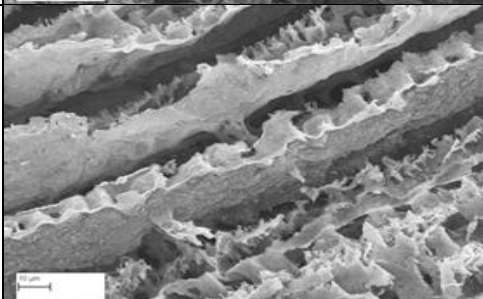
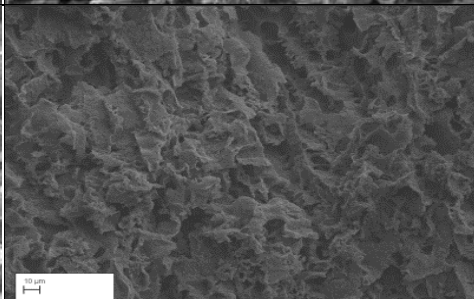
Sample	Dry	Wet
Control		
0.5 wt.% WDisRep3™		
1 wt.% WDisRep3™		
1.5 wt.% WDisRep3™		
2 wt.% WDisRep3™		

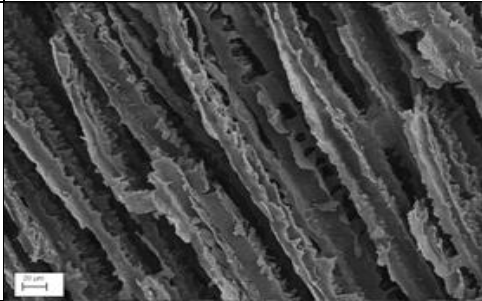
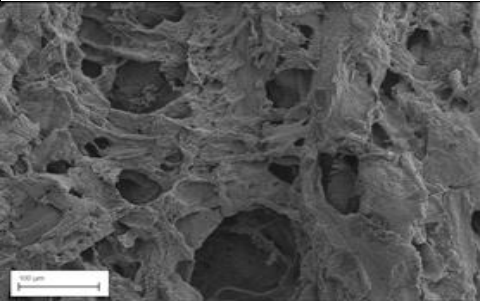
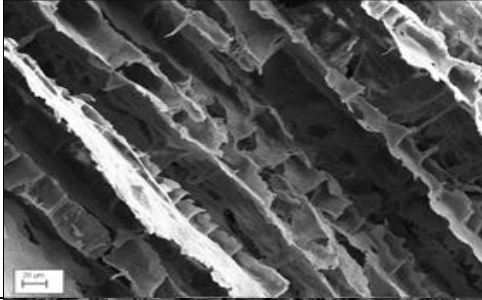
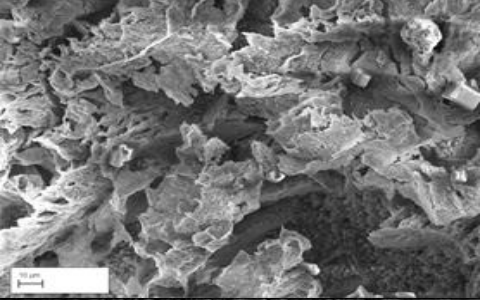
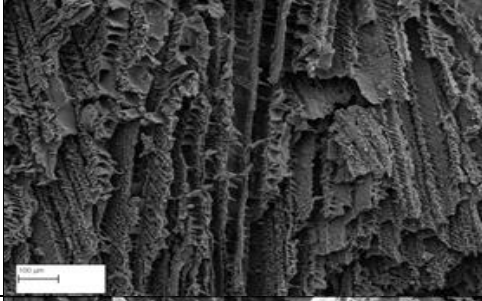
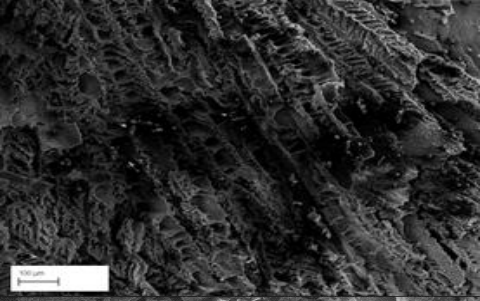
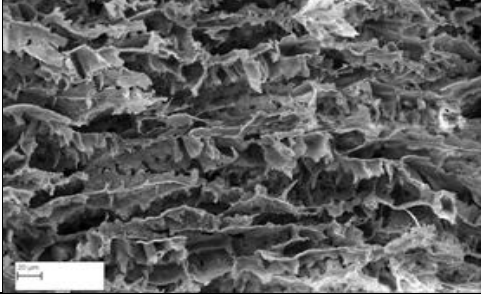
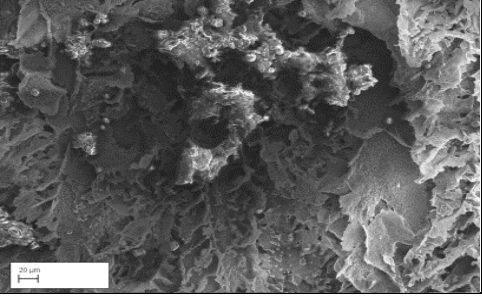
Table 9.2 Microstructures of CR1/WR samples before and after exposure to water

(Wcro1™ : WDisRep3™)	Dry	Wet
0.5 : 0.5		
1 : 1		
1 : 2		
2 : 1		

The influence of the combination 3-glycidoxypropyltrimethoxysilane (Wcro2™) with C6-Fluoroalkyl acrylate on the aerogel morphology can be seen in Table 9.3. Sample CR1/WR0.5:0.5 had a layered morphology with higher surface roughness compared to the control aerogel. The structure begins to fuse and merge together, leading to few voids after exposure to water. Sample CR2/WR1:1 resulted in a layered morphology with higher connectivity, with the layers being still visible but more distorted

as a result of shrinkage after being exposed to water. Sample CR2/WR1:2 had a highly packed layered architecture with a higher surface area due to an increase in surface roughness, the water damage seems to be limited (Dark area in the SEM image), which is expected due to the high water repellent content.

Table 9.3 Microstructures of CR2/WR samples before and after exposure to water

(Wcro2™ : WDisRep3™)	Dry	Wet
0.5 : 0.5		
1 : 1		
1 : 2		
2 : 1		

Reducing the water repellent and increasing the crosslinker to that of sample CR2/WR2:1 resulted in densely layered morphology, and even though the sample had a contact angle of 132°, the damage to the microstructure is evident. Overall neither glycidoxypropyltrimethoxysilane(Wcro2™) nor Aliphatic polyisocyanate (Wcro1™) significantly contribute to the structural integrity and dimensional stability, but C6-Fluoroalkyl acrylate (WDisRep3™) is the main contributor if added by more than 1 wt.%.

9.3.4 Thermal Conductivity of crosslinked water repellent aerogels

The combination of crosslinkers and WDisRep3™, which showed the lowest wettability and highest mechanical properties, had their thermal conductivity W/(m.K) measured after being exposed to different humidity condition (Figure 9.7). Thermal conductivity and moisture have a proportional relationship. Limiting the absorption of insulation materials is critical to ensure the effectiveness of its insulating properties. Neat clay-PVA aerogels absorbed high moisture and thus had 30% rise in the thermal conductivity from 0.042 to 0.055 W/(m.K) (Figure 9.7), this may be due to the high conductivity of moisture and the fact that the neat aerogel sample shrank by more than 40% at 95% RH. The overall reduction in the thermal conductivity of samples CR1/WR and CR2/WR is mainly related to two reasons: Firstly it can be related to the transition of the microstructure from a laminar architecture (Table 9.2 and 9.3) to a more coarse and interconnected, that may have created a longer and more difficult paths for heat to be transferred through aerogel as it may cause heat to dissipate as the surface area of aerogel is increased; Secondly can be related to their low wettability and low moisture absorption and thus during testing the samples would absorb less moisture from the condensation of the cold plate (0°) of the FOX 200. The lowest thermal conductivity at 95% RH was for sample CR1/WR1:2 at 0.045 a W/(m.K) a 15% increase from 0.039 W/(m.K) recording a 16% weight increase at 95% RH. The CR1/WR and CR2/WR samples overall had a 15% lower thermal

conductivity compared to the control sample due to lower moisture contents as well as higher structure integrity when exposed to high humidity.

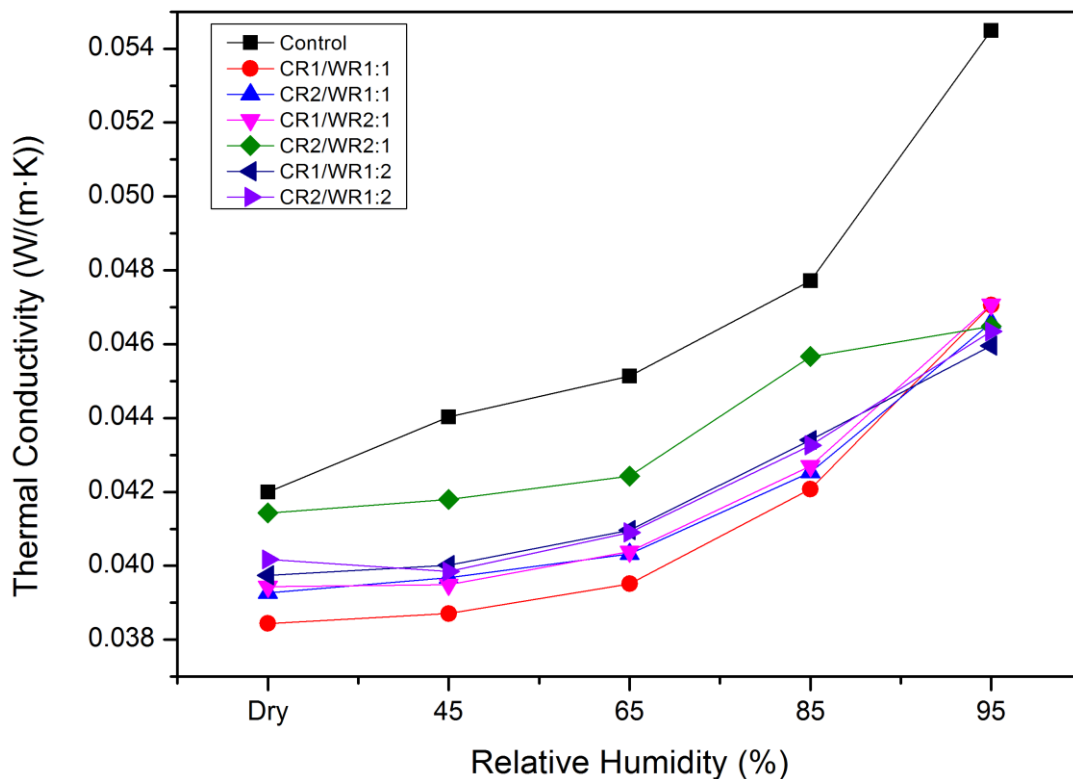


Figure 9.7 Thermal conductivity of crosslinked water repellent aerogels composites vs relative humidity

9.3.5 Flammability of crosslinked/water repellent aerogels

The flammability of clay aerogel composites with the incorporation of WDisRep3™ is presented in Table 9.4. The PVA in the control aerogel sample acts as the main fuel and source of ignition. The clay in the control aerogel will reduce the overall flammability due to its inorganic nature and provides heat and mass transport barriers, with large surface/volume ratio, also clay provides tortuous pathways for the oxygen and volatile decomposition products during burning, thus reducing the burning rate. Most polymers are highly flammable due to hydrocarbons, which contain many bonds with large potential energy. Once ignited these bonds rapidly breakup and release all the energy in the form of heat. Therefore, it is expected that as the content of WDisRep3™ is increased so does the

Chapter Nine: Optimization of highly functional hydrophobic clay aerogel composites for the construction industry

flammability of the composites from a total time after flame of 2s at 0 wt.% to 5s at 2wt.%. However, even with this increase in both t_1 and t_2 , the classification remains V-0 as described in Chapter 3, Section 3.3.1.5.

Table 9.4 UL94 test for WR samples

Sample ID	Average time after flame 1	Average time after flame 2	Classification
Control	2	0	V-0
0.8%	2.25	0	V-0
1.0%	4.6	2.2	V-0
1.2%	3.3	1.6	V-0
1.5%	2	0	V-0
2.0%	4	1	V-0

Table 9.5 shows the flammability data of clay aerogel composites that are incorporated both aliphatic polyisocyanate (Wcro1™) and C6-Fluoroalkyl acrylate (WDisRep3™). Isocyanates are a family of highly reactive and relatively low molecular weight aromatic and aliphatic compounds that are highly flammable. Therefore, by increasing the content of aliphatic polyisocyanate (Wcro1™), the average time after flame is increased. Sample CR1/WR2:1 witnessed the highest average after flame time due to the highest content of Wcro1™.



Figure 9.8 (A) Samples CR1-WR 0.5:2 after UL94 test (B) Cross-section of burned aerogels

Even at low concentrations (0.5 wt. %), t_1 increased by more than 200%. All the samples with an aliphatic polyisocyanate (Wcro1™) were classified with V-1, except for sample CR1/WR2:1 which was

classified as V-0 (Table 9.5 and Figure 9.8). Although stated previously that an increase in the polymeric component Fluoroalkyl acrylate (WDisRep3™) resulted in an increase in the average time after flame. It has a positive influence on the flammability when aliphatic polyisocyanate (Wcro1™) is incorporated. CR1/WR 0.5:1 and CR1/WR 0.5:2 had a t_1 of 14.00 and 6.38, respectively shows that by increasing the polymeric content the flammability can be reduced. The same is witnessed in samples CR1/WR 1:2 and CR1/WR 2:1. It should also be noted that only the outside of the samples is burned (2 mm) while the inner aerogel remained intact (Figure 9.8B).

Table 9.5 UL94 test for CR1-WR samples

Sample ID	Average time after flame 1	Average time after flame 2	Classification
CR1/WR 0.5:1	14.00	0	V-1
CR1/WR 0.5:0.5	17.17	0	V-1
CR1/WR 1:1	14.00	0	V-1
CR1/WR 1:2	14.63	7.75	V-1
CR1/WR 2:1	20.33	7	V-1
CR1/WR 0.5:2	6.38	0	V-0

9.4 Interim conclusions

An effective approach, the combination C6-Fluoroalkyl acrylate (WDisRep3™) with either Aliphatic polyisocyanate, (Wcro1™) or 3-glycidoxypropyltrimethoxysilane (Wcro2™), have been developed to enhance clay-PVA aerogel composites as high-performance, hydrophobic insulation materials. A direct relationship between the content of C6- Fluoroalkyl acrylate (WDisRep 3™) and the wettability was deduced. The ideal content of WDisRep3™ was found to be 2% which provided the best density to performance ratio. The sample with 2 wt.% WDisRep3™ absorbed on average 50% less moisture than the neat aerogels across all the humidity conditions, and absorbed 90% less water, with a contact angle of 140° and shrunk by 28%, a 70% improvement from the neat aerogel which shrunk by more than 90%. This also resulted in an increase in compressive moduli from 0.5 to 3.5MPa. With

the combination of Aliphatic polyisocyanate, (Wcro1™) or 3-glycidoxypropyltrimethoxysilane (Wcro2™) with C6-Fluoroalkyl acrylate (WDisRep3™), mostly C6-Fluoroalkyl acrylates was responsible for the low wettability of the aerogel composites. However, the combination of the crosslinkers resulted in higher structural integrity and dimensional stability of the aerogel composites. Samples CR1/WR01:2 and CR2/ WR01:2 shrank by only 6 and 16 % respectively after 30 days immersion in water and had a significant increase in modulus to up to 8 MPa. Increasing the polymeric component of WDisRep3™ resulted in an increase in the total duration of time after flame time. However, all WR samples were classified with V-0. Samples CR1/WR that had isocyanates compounds incorporated (Aliphatic polyisocyanate) almost doubled the average duration of time after flame time. Only sample CR1/WR 0.5:2 was classified with V-0. Clay-PVA aerogels are highly hydrophilic and are prone to absorb moisture and water, causing reduction in compressive modulus, increase in the thermal conductivity and irreversible structural degradation. This part of research demonstrated that these critical issues associated with clay aerogels can be effectively overcome and addressed.

Chapter Ten: Final appraisal and future work

10.1 Summary of the research

Silica aerogels and its composites have been well established in the scientific and industrial communities. However, with the current mandate for green products and environmentally friendly processes, clay aerogel composites possess an attractive potential as a replacement or alternative to silica aerogel composites. This is especially true if aerogels are to become a replacement for currently petroleum-based insulation materials. Throughout this thesis montmorillonite clay, an abundant and natural material and polyvinyl alcohols (PVA), a biodegradable polymer were used through an environmentally freeze-drying process to develop clay aerogel composites. The study implements novel formulations and processing technologies to functionalize clay aerogel composites and such explore their potentials for design and application. This thesis investigates and develops clay aerogel composites through a holistic and systematic approach, and both qualitative and quantitative characterisations are carried out extensively, the results interpreted to generate a better understanding of mechanisms of formulation, structure architecting and resulting performance of functionalized clay aerogel composites.

10.2 Major conclusions

The major contributions to the scientific community from thesis can be summarized as the following eight conclusive statements:

- (1) The most suitable raw material to prepare clay aerogels are clay minerals with a 2:1 structure due to their swelling abilities, high cation exchange capacity, high aspect ratios and large surface areas. The correlation of various natural and synthetic polymers with the bulk properties of aerogel composites has been established. Polyvinyl alcohol, polyimide,

polyethylene, pectin natural, rubber natural fibres, lignin, chitin cellulose, casein and carbon nanotubes all had a positive impact on the compressive modulus of clay aerogel composites. However, the most successful attempts were through the use of water-soluble polymers, especially polyvinyl alcohol (PVA), due to an ideal hydrogen bonding mechanism in which the hydrogen on the polymer was perfectly spaced to match the oxygen in the lattice of clay, resulting in clay-PVA aerogel composites capable of having a compressive modulus of 13 MPa and an apparent density of 0.12 g/cm³. Other techniques were proven effective in increasing the compressive modulus, such as glass fibre laminating and dip-coating. However, these approaches usually come at the expense of an increase in thermal conductivity .

(2) Many factors could influence the physical properties of clay aerogel composites, such as the microstructure, which could be altered by inducing air bubbles into the aerogel structure. Air bubbles could reduce the thermal conductivity by 22%. Choosing the correct molecular weight of the polymer could lead to not only an enhance in mechanical properties, but can also result in a reduction in thermal conductivity. Overall the clay aerogel composites had low flammability mainly due to their intrinsic properties of the inorganic clay. The literature tends to shift the focus of the high hydrophilicity of clay aerogel composites to their advantage by using them as absorbent material. This is valid only if they are intended for that application, however as an insulation material liquid absorption can be problematic.

(3) The microstructure of clay-PVA aerogel composites have been thoroughly investigated and characterised using SEM and 3D scanning techniques. Factors influencing the morphology, such as freezing direction and moisture absorption, were studied. Change in morphology could influence the bulk physical and mechanical properties of the aerogel composites. The

water resistivity and water uptake of clay aerogel composites were also investigated. The aerogel composite as an anisotropic layered architecture structure, in which the properties are related to the orientation. The layers were structured along the direction of freezing (vertical or horizontal). Having the layer parallel to the axial load could result in a 4 fold increase in the compressive modulus compared to that the layers that were orientated perpendicular to the load, while the thermal conductivity could be reduced from 0.039 to 0.033 W.(m.K) by structuring the aerogel layers perpendicular to the heat flow. The water uptake is dependent on the orientation which is expected due to the anisotropic nature of the microstructure. While having the highest absorption coefficient across the lateral face of the aerogel composite, moisture absorption had not only a structural influence on the morphology but also had a direct relationship with the thermal conductivity. For every 0.1 g of moisture absorbed the thermal conductivity increased by 2.5%. Reaching values of 0.053 W/(m.K) at high humidity exposures (95 RH%).

- (4) The processing parameters were investigated, namely varying the mixing temperature between room temperature (RT), 60, 70, 80 and 90°C. The mechanism of changing properties and their correlation with the final clay suspension to heat and its influence on the bulk properties has been investigated. The main effect was on the particle size distribution as a result of the breakup of large clay stacks into smaller clay stacks with an increase in temperature, reducing the average particle size from 500 nm at room temperature to 371 nm at 90°C. The size of the particles had a direct influence on the aerogel composite morphology, mainly creating web-like structures between the layers acting as nano-reinforcements, and hence resulting in higher connectivity. This also translated to a 7 fold increase in the compressive modulus with minimum increase in density, well below the 0.1 g/cm³, the

preferred density for construction insulation materials. The functional groups also showed an increase in O-H bands as the temperature increased. Overall this method provides a practical way to increase the strength of clay-PVA aerogel composites without any additional additives.

(5) Organoclay was prepared using Hexadecyltrimethylammonium bromide $\geq 98\%$ through an ion exchange process. The amount of cation exchange varied between 0.3, 0.4, 0.5, 0.6, 0.7 and 1 of the cation exchange capacity (CEC) of bentonite montmorillonite. The organoclay-PVA colloidal suspension was dispersed in water using ultrasonic technologies to prepare aerogel composites through an environmental freezing-process while using only water as a solvent. The impact of organoclay on the final aerogel composite was evaluated. The functionalisation of the aerogel composite was determined through FTIR. With increasing the amount of surfactant, the mechanical properties were increased due to the higher interaction between the organoclay and PVA, achieving a compressive modulus of 0.85 MPa a 50% increase from 0.48 MPa. More significant was the overall reduction in the moisture absorption by up to 40%, while structural integrity remained even after 30 days at high moisture exposure. By increasing the d-spacing, the thermal conductivity can be reduced to as low as 0.031 W/(m.K). This development provides an approach to tailor the aerogel composites with enhanced mechanical and physical properties to be used as an effective insulation material in the construction industry.

(6) Two water-soluble crosslinkers, namely aliphatic polyisocyanate (Wcro1™), and 3-glycidoxypropyltrimethoxysilane (Wcro2™) were investigated. The proposed chemical interaction and mechanisms of the crosslinkers were established and described through the interpretation of aerogel functional groups. The mechanism of crosslinking was responsible

for an increase in compressive modulus by more than 6 folds from 0.48 MPa to 3.6MPa. Although the crosslinked aerogels did not witness hydrophobic behaviour with only a slight increase in the time it took the aerogel to absorb the water droplet. However, the crosslinked clay-PVA composites exhibited significant improvement in their moisture resistance, reducing the moisture absorbed by 27% at 95% RH while retaining dimensional stability. The dimensional integrity in water also results in higher water absorption of the crosslinked aerogel composite by 950%. The crosslinking could create an increase in the grain boundaries which generates an increase in the free path of phonons and therefore lowers the overall thermal conductivity of the composite.

(7) Three water-soluble water repellents were incorporated into the final aerogel formulations, namely C6-Fluoroalkyl acrylate (WDisRep3™), C2-C4 Fluorochemical (WDisRep4™) and a combination of melamine resins with paraffin waxes (WDisRep1™). The addition of the water replants had a direct influence on the mechanical properties due mainly to the addition of the polymeric competent contributing to the increased modulus. However, the change in morphology played a vital role, for instance, C6-Fluoroalkyl acrylate (WDisRep3™) created large struts between the aerogel layers, resulting in an overall more effective transfer of load through the aerogel. The overall hydrophobicity (Contact angle) was significantly increased from 0° to 140°, due to the water repellency properties of the aerogel composites. The overall water absorbed could be reduced from 330% to as low as 21%. The thermal conductivity was reduced due to a more tortuous path created by the addition of C6-Fluoroalkyl acrylate (WDisRep3™) to 0.038 W/(m.K). This was also associated with the fact that less moisture was absorbed while maintaining excellent dimensional stability and mechanical properties after 30 days at 95% relative humidity.

(8) The mechanism and knowledge of implementing a hybrid solution of crosslinkers with the best performing water repellent (C6-Fluoroalkyl acrylate (WDisRep3™) to generate highly functional aerogel composites were developed. Different loadings of C6- Fluoroalkyl acrylate were further investigated to establish a correlation between the loadings and the properties. Various different formulations using different ratios of crosslinkers to WDisRep3™ were investigated to generate the optimum design mixes. Even at a low concentration of WDisRep3™ (0.3 wt.%), the aerogel composites had a significant increase on the hydrophobicity (80°). However, it was concluded 2 wt.% of WDisRep3™ provided the best density to performance ratio. Aliphatic polyisocyanate, (Wcro1) showed higher compatibility with C6- Fluoroalkyl acrylate (WDisRep3™) than 3-glycidoxypropyltrimethoxysilane (Wcro2). The optimum formulation was found to be with the addition of 1 wt.% Aliphatic polyisocyanate, (Wcro1) and 2 wt.% C6- Fluoroalkyl acrylate (WDisRep3™). This resulted in highly functional hydrophobic clay aerogel composites. The moisture absorption was reduced by more than 60% across all humidity ranges. The wettability significantly improved with a contact angle of 145 °, while the water absorption was reduced by 92% with an overall 6% shrinkage after 30 days of water absorption.

10.3 Future work

This thesis has demonstrated significant knowledge and contributions to the scientific community. However, in order for clay aerogel composites to be exploited in its full capacity in the construction industry as an insulation material the following suggestions have been made:

(1) A UL94 V-0 was carried out to determine the flammability of the aerogel composite. This test is mostly designed for pure polymers rather than composites. Therefore more specialised

tests have to be carried out to evaluate in more detail the flammability of the composites, especially with the addition of different additives. A cone calorimeter can provide more insights on the ignition time, mass loss, and heat release rate. Measurement and characterisation of the combustion products are necessary to understand any associated problems with toxic fire products, that can lead to environmental contamination and health hazards.

- (2) Although this thesis proposes several approaches to reduce the thermal conductivity of clay-PVA aerogel composites. The current thermal conductivity is comparable to petroleum-based insulation materials and is higher than traditional silica aerogels. In order to fully exploit clay aerogel composites, their thermal conductivity can be further reduced by using phase changing materials, that are capable of absorbing heat. Another approach may be through replacing the air in the pores with gases that have a lower thermal conductivity such as argon gas.
- (3) This thesis has demonstrated that clay aerogel composites are highly influenced by the processing parameters. Therefore it is suggested that large-scale processing parameters have to be investigated. A test house (demo pilot) could be fitted with an internal wall insulation of clay aerogel. The house would be monitored and its performance compared to conventional insulation material. This will aid demonstrate and explore the feasibility of using clay aerogel composites as an insulation material in the construction industry.
- (4) Life cycle analysis (LCA) could be carried out to establish the true impact of the raw materials and additives used to prepare aerogel composites along with the impact of large-scale /lab scale production process. A comparative study between conventional insulation material and

clay aerogel composites can then be established. This will show the true potential environmental benefits of using clay aerogel composites.

References

- [1] Al-Homoud DMS. Performance characteristics and practical applications of common building thermal insulation materials. *Build Environ* 2005;40(3):353-366.
- [2] D'Agostino D, Zacà I, Baglivo C, Congedo PM. Economic and Thermal Evaluation of Different Uses of an Existing Structure in a Warm Climate. *Energies* 2017;10(5):658.
- [3] Gurav JL, Jung I, Park H, Kang ES, Nadargi DY. Silica aerogel: synthesis and applications. *Journal of Nanomaterials* 2010;2010:23.
- [4] Jelle BP. Traditional, state-of-the-art and future thermal building insulation materials and solutions—Properties, requirements and possibilities. *Energy Build* 2011;43(10):2549-2563.
- [5] Zhou X, Zheng F, Li H, Lu C. An environment-friendly thermal insulation material from cotton stalk fibers. *Energy and Buildings* 2010;42(7):1070-1074.
- [6] Stevens ES. *Green plastics: an introduction to the new science of biodegradable plastics*. 2002.
- [7] Karamanos A, Papadopoulos A, Anastasellos D. Heat transfer phenomena in fibrous insulating materials. 2004:1-12.
- [8] Pakkala TA, Lahdensivu J. Long-term water absorption tests for frost insulation materials taking into account frost attack. *Case Studies in Construction Materials* 2014;1:40-45.
- [9] Du A, Zhou B, Zhang Z, Shen J. A special material or a new state of matter: a review and reconsideration of the aerogel. *Materials* 2013;6(3):941-968.
- [10] Lu H, Luo H, Leventis N. *Aerogel handbook*. 2011.
- [11] de Fátima Júlio M, Ilharco LM. Superhydrophobic hybrid aerogel powders from waterglass with distinctive applications. *Microporous and Mesoporous Materials* 2014;199:29-39.
- [12] Wu W, Wang K, Zhan M. Preparation and performance of polyimide-reinforced clay aerogel composites. *Ind Eng Chem Res* 2012;51(39):12821-12826.
- [13] Cuce E, Cuce PM, Wood CJ, Riffat SB. Toward aerogel based thermal superinsulation in buildings: A comprehensive review. *Renewable and Sustainable Energy Reviews* 2014;34:273-299.
- [14] Wang Y, Gawryla MD, Schiraldi DA. Effects of freezing conditions on the morphology and mechanical properties of clay and polymer/clay aerogels. *J Appl Polym Sci* 2013;129(3):1637-1641.
- [15] Wang Y. *Processing, structure and properties of layered films and clay aerogel composites*. 2012.
- [16] Liu A, Berglund LA. Clay nanopaper composites of nacre-like structure based on montmorillonite and cellulose nanofibers—Improvements due to chitosan addition. *Carbohydr Polym* 2012;87(1):53-60.

- [17] Madejová J. FTIR techniques in clay mineral studies. *Vibrational spectroscopy* 2003;31(1):1-10.
- [18] Bujdák J, Rode BM. The effect of clay structure on peptide bond formation catalysis. *Journal of Molecular Catalysis A: Chemical* 1999;144(1):129-136.
- [19] Pethrick RA. *Polymer–Clay Nanocomposites*, Edited by TJ Pinnavaia and GW Beall John Wiley & Sons Ltd, Chichester, UK, 2000 0-471-6300-9 pp xi 345, price£ 125.00. *Polym Int* 2002;51(5):464-464.
- [20] Gawryla MD, Liu L, Grunlan JC, Schiraldi DA. pH Tailoring Electrical and Mechanical Behavior of Polymer–Clay–Nanotube Aerogels. *Macromolecular rapid communications* 2009;30(19):1669-1673.
- [21] Wang Y, Alhassan S, Yang V, Schiraldi D. Polyether-block-amide copolymer/clay films prepared via a freeze-drying method. *Composites Part B: Engineering* 2013;45(1):625-630.
- [22] Bandi S, Schiraldi DA. Glass transition behavior of clay aerogel/poly (vinyl alcohol) composites. *Macromolecules* 2006;39(19):6537-6545.
- [23] Schmandt-Besserat D. The earliest uses of clay in Syria. *Expedition* 1977;19(3):28.
- [24] Rytwo G. Clay minerals as an ancient nanotechnology: historical uses of clay organic interactions, and future possible perspectives. *Macla* 2008;9:15-17.
- [25] Guggenheim S, Martin R. Definition of clay and clay mineral: joint report of the AIPEA nomenclature and CMS nomenclature committees. *Clays Clay Miner* 1995;43(2):255-256.
- [26] Bergaya F, Lagaly G. Chapter 1 General Introduction: Clays, Clay Minerals, and Clay Science. *Developments in Clay Science* 2006;1:1-18.
- [27] Robertson R. *Fuller's earth: a history of calcium montmorillonite*. 1986.
- [28] Weiss A. A secret of Chinese porcelain manufacture. *Angewandte Chemie International Edition* 1963;2(12):697-703.
- [29] Carretero MI. Clay minerals and their beneficial effects upon human health. A review. *Appl Clay Sci* 2002;21(3-4):155-163.
- [30] Ayadi AJ, Soro J, Kamoun A, Baklouti S, Sfax R, Thomas A. Study of clay's mineralogy effect on rheological behavior of ceramic suspensions using an experimental design. *Int.J.Res.Rev.Applied Sci* 2013;14:374-384.
- [31] Theng BKG. Formation and properties of clay-polymer complexes. 2012;4.
- [32] Brigatti MF, Galan E, Theng BKG. Chapter 2 Structures and Mineralogy of Clay Minerals. *Developments in Clay Science* 2006;1:19-86.
- [33] Pinnavaia TJ, Beall GW. *Polymer-clay nanocomposites*. 2000.

- [34] Sarier N, Onder E, Ersoy S. The modification of Na-montmorillonite by salts of fatty acids: An easy intercalation process. *Colloids and Surfaces A: Physicochemical and Engineering Aspects* 2010;371(1):40-49.
- [35] Liu P. Polymer modified clay minerals: A review. *Appl Clay Sci* 2007;38(1):64-76.
- [36] Bergaya F, Lagaly G. Surface modification of clay minerals. *Applied Clay Science* 2001;19(1):1-3.
- [37] Healy B. Surface modified clays: An innovative technology for groundwater remediation. *Ground Water Management* 1993;15:61-71.
- [38] Gorrasi G, Tortora M, Vittoria V, Kaempfer D, Mülhaupt R. Transport properties of organic vapors in nanocomposites of organophilic layered silicate and syndiotactic polypropylene. *Polymer* 2003;44(13):3679-3685.
- [39] Patel HA, Somani RS, Bajaj HC, Jasra RV. Preparation and characterization of phosphonium montmorillonite with enhanced thermal stability. *Appl Clay Sci* 2007;35(3):194-200.
- [40] Hedley C, Yuan G, Theng B. Thermal analysis of montmorillonites modified with quaternary phosphonium and ammonium surfactants. *Appl Clay Sci* 2007;35(3):180-188.
- [41] Beall GW. The use of organo-clays in water treatment. *Appl Clay Sci* 2003;24(1-2):11-20.
- [42] Gelfer M, Avila-orta C, Liu L, Yang L, Chu B, Hsiao BS, Song HH, Si M, Rafailovich M, Tsou AH. Manipulating the microstructure and rheology in polymer-organoclay composites. *Polymer Engineering & Science* 2002;42(9):1841-1851.
- [43] McLauchlin AR, Thomas NL. Preparation and thermal characterisation of poly (lactic acid) nanocomposites prepared from organoclays based on an amphoteric surfactant. *Polym Degrad Stab* 2009;94(5):868-872.
- [44] Zhang L, Wan C, Zhang Y. Investigation on morphology and mechanical properties of polyamide 6/maleated ethylene-propylene-diene rubber/organoclay composites. *Polymer Engineering & Science* 2009;49(2):209-216.
- [45] Nakazawa H, Yamada H, Fujita T, Ito Y. Texture control of clay-aerogel through the crystallization process of ice. *Clay Science* 1987;6(6):269-276.
- [46] Somlai LS, Bandi SA, Schiraldi DA, Mathias LJ. Facile processing of clays into organically-modified aerogels. *AIChE J* 2006;52(3):1162-1168.
- [47] Gawryla MD, van den Berg O, Weder C, Schiraldi DA. Clay aerogel/cellulose whisker nanocomposites: a nanoscale wattle and daub. *Journal of Materials Chemistry* 2009;19(15):2118-2124.
- [48] Iannicelli J, Mn N. Relation of viscosity of kaolin-water suspensions to montmorillonite content of certain Georgia clays. 2013:347.

- [49] Johnson J, Schiraldi D. Improving the mechanical properties of clay/polymer aerogels by a simple dip-coating procedure. *J Appl Polym Sci* 2012;126(6):2004-2009.
- [50] Gawryla MD. *Low Density Materials through Freeze-Drying: Clay Aerogels and Beyond....* 2009.
- [51] Matsumoto M, Saito S, Ohmine I. Molecular dynamics simulation of the ice nucleation and growth process leading to water freezing. *Nature* 2002;416(6879):409-413.
- [52] Hussain F, Hojjati M, Okamoto M, Gorga RE. Review article: polymer-matrix nanocomposites, processing, manufacturing, and application: an overview. *J Composite Mater* 2006;40(17):1511-1575.
- [53] Viggiano RP, Schiraldi DA. Fabrication and mechanical characterization of lignin-based aerogels. *Green Materials* 2014;2(3):153-158.
- [54] Schiraldi DA, Bandi SA, Gawryla MD. PROGRESS IN CLAY AEROGEL/POLYMER COMPOSITE MATERIALS. *Polymer Preprints* 2006;47(2):313.
- [55] Zhou Y, Fu S, Pu Y, Pan S, Ragauskas AJ. Preparation of aligned porous chitin nanowhisker foams by directional freeze-casting technique. *Carbohydr Polym* 2014;112:277-283.
- [56] de Morais Teixeira E, Corrêa AC, Manzoli A, de Lima Leite F, de Oliveira CR, Mattoso LHC. Cellulose nanofibers from white and naturally colored cotton fibers. *Cellulose* 2010;17(3):595-606.
- [57] Premkumar T, Mezzenga R, Geckeler KE. Carbon nanotubes in the liquid phase: addressing the issue of dispersion. *Small* 2012;8(9):1299-1313.
- [58] Chen H, Chiou B, Wang Y, Schiraldi DA. Biodegradable pectin/clay aerogels. *ACS applied materials & interfaces* 2013;5(5):1715-1721.
- [59] Pojanavaraphan T, Schiraldi DA, Magaraphan R. Mechanical, rheological, and swelling behavior of natural rubber/montmorillonite aerogels prepared by freeze-drying. *Appl Clay Sci* 2010;50(2):271-279.
- [60] Chen H, Hollinger E, Wang Y, Schiraldi DA. Facile fabrication of poly (vinyl alcohol) gels and derivative aerogels. *Polymer* 2014;55(1):380-384.
- [61] Kobayashi Y, Saito T, Isogai A. Aerogels with 3D Ordered Nanofiber Skeletons of Liquid-Crystalline Nanocellulose Derivatives as Tough and Transparent Insulators. *Angewandte Chemie* 2014;126(39):10562-10565.
- [62] Finlay K, Gawryla MD, Schiraldi DA. Biologically based fiber-reinforced/clay aerogel composites. *Ind Eng Chem Res* 2008;47(3):615-619.
- [63] Chen H, Liu B, Huang W, Wang J, Zeng G, Wu W, Schiraldi DA. Fabrication and Properties of Irradiation-Cross-Linked Poly (vinyl alcohol)/Clay Aerogel Composites. *ACS applied materials & interfaces* 2014;6(18):16227-16236.

- [64] Zani A, Dellasega D, Russo V, Passoni M. Ultra-low density carbon foams produced by pulsed laser deposition. *Carbon* 2013;56:358-365.
- [65] Viggiano RP, Gawryla MD, Schiraldi DA. Foam-like polymer/clay aerogels which incorporate air bubbles. *J Appl Polym Sci* 2014;131(3).
- [66] Horne DS. Casein structure, self-assembly and gelation. *Current Opinion in Colloid & Interface Science* 2002;7(5–6):456-461.
- [67] Fan Q, Ma J, Xu Q, Zhang J, Simion D, Carmen G, Guo C. Animal-derived natural products review: Focus on novel modifications and applications. *Colloids and Surfaces B: Biointerfaces* 2015;128:181-190.
- [68] Sarode AR, Sawale PD, Khedkar CD, Kalyankar SD, Pawshe RD. Casein and Caseinate: Methods of Manufacture. 2016:676-682.
- [69] Ridout MJ, Paananen A, Mamode A, Linder MB, Wilde PJ. Interaction of transglutaminase with adsorbed and spread films of β -casein and κ -casein. *Colloids and Surfaces B: Biointerfaces* 2015;128:254-260.
- [70] Pojanavaraphan T, Magaraphan R, Chiou B, Schiraldi DA. Development of biodegradable foamlike materials based on casein and sodium montmorillonite clay. *Biomacromolecules* 2010;11(10):2640-2646.
- [71] Ghosh A, Ali MA, Dias GJ. Effect of cross-linking on microstructure and physical performance of casein protein. *Biomacromolecules* 2009;10(7):1681-1688.
- [72] Gerrard JA. Protein–protein crosslinking in food: methods, consequences, applications. *Trends Food Sci Technol* 2002;13(12):391-399.
- [73] Wang Y, Schiraldi DA. Foam-like materials produced from milk and sodium montmorillonite clay using a freeze-drying process. *Green Materials* 2013;1(1):11-15.
- [74] O'Connell JE, de Kruif CG. β -Casein micelles; cross-linking with transglutaminase. *Colloids Surf Physicochem Eng Aspects* 2003;216(1–3):75-81.
- [75] Bönisch MP, Heidebach TC, Kulozik U. Influence of transglutaminase protein cross-linking on the rennet coagulation of casein. *Food Hydrocoll* 2008;22(2):288-297.
- [76] Schorsch C, Carrie H, Norton IT. Cross-linking casein micelles by a microbial transglutaminase: influence of cross-links in acid-induced gelation. *Int Dairy J* 2000;10(8):529-539.
- [77] Tingaut P, Eyholzer C, Zimmermann T. Functional polymer nanocomposite materials from microfibrillated cellulose. 2011.
- [78] Klemm D, Heublein B, Fink H, Bohn A. Cellulose: fascinating biopolymer and sustainable raw material. *Angewandte Chemie International Edition* 2005;44(22):3358-3393.

- [79] Innerlohinger J, Weber HK, Kraft G. Aerocellulose: Aerogels and Aerogel-like Materials made from Cellulose. 2006;244(1):126-135.
- [80] Donius AE, Liu A, Berglund LA, Wegst UG. Superior mechanical performance of highly porous, anisotropic nanocellulose–montmorillonite aerogels prepared by freeze casting. *Journal of the mechanical behavior of biomedical materials* 2014;37:88-99.
- [81] Dash R, Li Y, Ragauskas AJ. Cellulose nanowhisker foams by freeze casting. *Carbohydr Polym* 2012;88(2):789-792.
- [82] Saha MC, Mahfuz H, Chakravarty UK, Uddin M, Kabir ME, Jeelani S. Effect of density, microstructure, and strain rate on compression behavior of polymeric foams. *Materials Science and Engineering: A* 2005;406(1–2):328-336.
- [83] Chen W, Yu H, Li Q, Liu Y, Li J. Ultralight and highly flexible aerogels with long cellulose I nanofibers. *Soft matter* 2011;7(21):10360-10368.
- [84] Hostler S, Abramson A, Gawryla M, Bandi S, Schiraldi D. Thermal conductivity of a clay-based aerogel. *Int J Heat Mass Transfer* 2009;52(3):665-669.
- [85] Ahmadzadeh S, Keramat J, Nasirpour A, Hamdami N, Behzad T, Aranda L, Vilasi M, Desobry S. Structural and mechanical properties of clay nanocomposite foams based on cellulose for the food-packaging industry. *J Appl Polym Sci* 2015.
- [86] Malcolm PS. *Polymer chemistry: an introduction*. Oxford University Press, New York 1999:87-91.
- [87] Rinaudo M. Chitin and chitosan: Properties and applications. *Progress in Polymer Science* 2006;31(7):603-632.
- [88] Ravi Kumar MNV. A review of chitin and chitosan applications. *React Funct Polym* 2000;46(1):1-27.
- [89] Sing M, Johnson III J, Schiraldi DA. REINFORCEMENT OF CLAY AEROGELS VIA INCORPORATION OF A POLYMER DERIVED FROM CHITIN. *Polymer Preprints* 2010;51(1):655.
- [90] Beppu MM, Santana CC. PAA influence on chitosan membrane calcification. *Materials Science and Engineering: C* 2003;23(5):651-658.
- [91] El Kadib A, Bousmina M. Chitosan Bio-Based Organic–Inorganic Hybrid Aerogel Microspheres. *Chemistry-A European Journal* 2012;18(27):8264-8277.
- [92] Stewart D. Lignin as a base material for materials applications: Chemistry, application and economics. *Industrial Crops and Products* 2008;27(2):202-207.
- [93] Ghaffar SH, Fan M. Lignin in straw and its applications as an adhesive. *Int J Adhes Adhes* 2014;48:92-101.

- [94] Thielemans W, Can E, Morye S, Wool R. Novel applications of lignin in composite materials. *J Appl Polym Sci* 2002;83(2):323-331.
- [95] Grishechko LI, Amaral-Labat G, Szczurek A, Fierro V, Kuznetsov BN, Pizzi A, Celzard A. New tannin–lignin aerogels. *Industrial Crops and Products* 2013;41:347-355.
- [96] Chen F, Li J. Synthesis and structural characteristics of organic aerogels with different content of lignin. 2010;113:1837-1840.
- [97] Oliviero M, Verdolotti L, Nedi I, Docimo F, Di Maio E, Iannace S. Effect of two kinds of lignins, alkaline lignin and sodium lignosulfonate, on the foamability of thermoplastic zein-based bionanocomposites. *Journal of Cellular Plastics* 2012;48(6):516-525.
- [98] Oliviero M, Verdolotti L, Di Maio E, Aurilia M, Iannace S. Effect of supramolecular structures on thermoplastic zein–lignin bionanocomposites. *J Agric Food Chem* 2011;59(18):10062-10070.
- [99] Chen Q, Huang W, Chen P, Peng C, Xie H, Zhao ZK, Sohail M, Bao M. Synthesis of Lignin-Derived Bisphenols Catalyzed by Lignosulfonic Acid in Water for Polycarbonate Synthesis. *ChemCatChem* 2015;7(7):1083-1089.
- [100] Bitinis N, Verdejo R, Cassagnau P, Lopez-Manchado MA. Structure and properties of polylactide/natural rubber blends. *Mater Chem Phys* 2011;129(3):823-831.
- [101] Murakami S, Senoo K, Toki S, Kohjiya S. Structural development of natural rubber during uniaxial stretching by in situ wide angle X-ray diffraction using a synchrotron radiation. *Polymer* 2002;43(7):2117-2120.
- [102] Jia Q, Wu Y, Wang Y, Lu M, Zhang L. Enhanced interfacial interaction of rubber/clay nanocomposites by a novel two-step method. *Composites Sci Technol* 2008;68(3–4):1050-1056.
- [103] Tangboriboonrat P, Lerthittrakul C. Morphology of natural rubber latex particles prevulcanised by sulphur and peroxide systems. *Colloid Polym Sci* 2002;280(12):1097-1103.
- [104] Bandi S, Bell M, Schiraldi DA. Temperature-responsive clay aerogel-polymer composites. *Macromolecules* 2005;38(22):9216-9220.
- [105] Valadares LF, Leite CAP, Galembeck F. Preparation of natural rubber–montmorillonite nanocomposite in aqueous medium: evidence for polymer–platelet adhesion. *Polymer* 2006;47(2):672-678.
- [106] Ceylan D, Okay O. Macroporous polyisobutylene gels: a novel tough organogel with superfast responsiveness. *Macromolecules* 2007;40(24):8742-8749.
- [107] Dogu S, Okay O. Tough organogels based on polyisobutylene with aligned porous structures. *Polymer* 2008;49(21):4626-4634.

- [108] Oztoprak Z, Hekimoglu T, Karakutuk I, Tuncaboylu DC, Okay O. Porous rubber cryogels: effect of the gel preparation temperature. *Polymer bulletin* 2014;71(8):1983-1999.
- [109] Pojanavaraphan T, Liu L, Ceylan D, Okay O, Magaraphan R, Schiraldi DA. Solution cross-linked natural rubber (NR)/clay aerogel composites. *Macromolecules* 2011;44(4):923-931.
- [110] Durmaz S, Fank S, Okay O. Swelling and mechanical properties of solution-crosslinked poly (isobutylene) gels. *Macromolecular Chemistry and Physics* 2002;203(4):663-672.
- [111] Shi L, Gunasekaran S. Preparation of pectin–ZnO nanocomposite. *Nanoscale research letters* 2008;3(12):491-495.
- [112] Mangiacapra P, Gorrasi G, Sorrentino A, Vittoria V. Biodegradable nanocomposites obtained by ball milling of pectin and montmorillonites. *Carbohydr Polym* 2006;64(4):516-523.
- [113] Vartiainen J, Tammelin T, Pere J, Tapper U, Harlin A. Biohybrid barrier films from fluidized pectin and nanoclay. *Carbohydr Polym* 2010;82(3):989-996.
- [114] Munarin F, Tanzi MC, Petrini P. Advances in biomedical applications of pectin gels. *Int J Biol Macromol* 2012;51(4):681-689.
- [115] Alhassan SM, Qutubuddin S, Schiraldi D. Influence of electrolyte and polymer loadings on mechanical properties of clay aerogels. *Langmuir* 2010;26(14):12198-12202.
- [116] Ahmadian-Alam L, Haddadi-Asl V, Roghani-Mamaqani H, Hatami L, Salami-Kalajahi M. Use of clay-anchored reactive modifier for the synthesis of poly (styrene-co-butyl acrylate)/clay nanocomposite via in situ AGET ATRP. *Journal of Polymer Research* 2012;19(1):1-12.
- [117] Nicolau A, Nucci AM, Martini EM, Samios D. Electrical impedance spectroscopy of epoxy systems II: Molar fraction variation, resistivity, capacitance and relaxation processes of 1, 4-butanediol diglycidyl ether/succinic anhydride and triethylamine as initiator. *European polymer journal* 2007;43(6):2708-2717.
- [118] Azeez AA, Rhee KY, Park SJ, Hui D. Epoxy clay nanocomposites – processing, properties and applications: A review. *Composites Part B: Engineering* 2013;45(1):308-320.
- [119] Arndt EM, Gawryla MD, Schiraldi DA. Elastic, low density epoxy/clay aerogel composites. *Journal of Materials Chemistry* 2007;17(33):3525-3529.
- [120] Mohan T, Kumar MR, Velmurugan R. Thermal, mechanical and vibration characteristics of epoxy-clay nanocomposites. *J Mater Sci* 2006;41(18):5915-5925.
- [121] Kornmann X, Lindberg H, Berglund LA. Synthesis of epoxy–clay nanocomposites. Influence of the nature of the curing agent on structure. *Polymer* 2001;42(10):4493-4499.

- [122] Breunig M, Hozsa C, Lungwitz U, Watanabe K, Umeda I, Kato H, Goepferich A. Mechanistic investigation of poly(ethylene imine)-based siRNA delivery: Disulfide bonds boost intracellular release of the cargo. *J Controlled Release* 2008;130(1):57-63.
- [123] Mann S. *Biom mineralization: principles and concepts in bioinorganic materials chemistry*. 2001;5.
- [124] Chen Z, Deng M, Chen Y, He G, Wu M, Wang J. Preparation and performance of cellulose acetate/polyethyleneimine blend microfiltration membranes and their applications. *J Membr Sci* 2004;235(1–2):73-86.
- [125] Wang S, Hu Y, Tang Y, Wang Z, Chen Z, Fan W. Preparation of polyethylene–clay nanocomposites directly from Na montmorillonite by a melt intercalation method. *J Appl Polym Sci* 2003;89(9):2583-2585.
- [126] Jankowski P, Ogończyk D, Lisowski W, Garstecki P. Polyethyleneimine coating renders polycarbonate resistant to organic solvents. *Lab on a Chip* 2012;12(14):2580-2584.
- [127] Johnson III JR, Spikowski J, Schiraldi DA. Mineralization of clay/polymer aerogels: a bioinspired approach to composite reinforcement. *ACS applied materials & interfaces* 2009;1(6):1305-1309.
- [128] Yano K, Usuki A, Okada A, Kurauchi T, Kamigaito O. Synthesis and properties of polyimide–clay hybrid. *Journal of Polymer Science Part A: Polymer Chemistry* 1993;31(10):2493-2498.
- [129] Mittal KL. *Polyimides: synthesis, characterization, and applications*. 2013;1.
- [130] Olad A. *Polymer/clay nanocomposites. Advances in diverse industrial applications of nanocomposites* 2011:113-138.
- [131] Kivılcım N, Seçkin T, Köytepe S. Porous pyridine based polyimide–silica nanocomposites with low dielectric constant. *Journal of Porous Materials* 2013;20(4):709-718.
- [132] Jang J, Lee DK. Plasticizer effect on the melting and crystallization behavior of polyvinyl alcohol. *Polymer* 2003;44(26):8139-8146.
- [133] Baker MI, Walsh SP, Schwartz Z, Boyan BD. A review of polyvinyl alcohol and its uses in cartilage and orthopedic applications. *Journal of Biomedical Materials Research Part B: Applied Biomaterials* 2012;100(5):1451-1457.
- [134] Roohani M, Habibi Y, Belgacem NM, Ebrahim G, Karimi AN, Dufresne A. Cellulose whiskers reinforced polyvinyl alcohol copolymers nanocomposites. *European Polymer Journal* 2008;44(8):2489-2498.
- [135] DeMerlis C, Schoneker D. Review of the oral toxicity of polyvinyl alcohol (PVA). *Food and Chemical Toxicology* 2003;41(3):319-326.
- [136] Karimi A, Daud W, Ashri WM. *Materials, preparation, and characterization of PVA/MMT nanocomposite hydrogels: A review. Polymer Composites* 2015.

- [137] Sinha Ray S, Okamoto M. Polymer/layered silicate nanocomposites: a review from preparation to processing. *Progress in Polymer Science* 2003;28(11):1539-1641.
- [138] Podsiadlo P, Kaushik AK, Arruda EM, Waas AM, Shim BS, Xu J, Nandivada H, Pumphlin BG, Lahann J, Ramamoorthy A, Kotov NA. Ultrastrong and stiff layered polymer nanocomposites. *Science* 2007;318(5847):80-83.
- [139] Lamison K, Gawryla MD, Schiraldi DA. The effect of molecular weight on poly (vinyl alcohol)/clay aerogel composite properties. *Polym.Prepr* 2007;48(1):974-975.
- [140] Bandi SA. HIGH PERFORMANCE BLENDS AND COMPOSITES: PART (I) CLAY AEROGEL/POLYMER COMPOSITES PART (II) MECHANISTIC INVESTIGATION OF COLOR GENERATION IN PET/MXD6 BARRIER BLENDS. 2006.
- [141] Gohil J, Bhattacharya A, Ray P. Studies on the crosslinking of poly (vinyl alcohol). *Journal of polymer research* 2006;13(2):161-169.
- [142] Zhang Y, Zhu PC, Edgren D. Crosslinking reaction of poly (vinyl alcohol) with glyoxal. *Journal of polymer research* 2010;17(5):725-730.
- [143] Sereikaitė J, Bassus D, Bobnis R, Dienys G, Bumelienė Z, Bumelis V. Divinyl sulfone as a crosslinking reagent for oligomeric proteins. *Russian Journal of Bioorganic Chemistry* 2003;29(3):227-230.
- [144] Dufresne A, Reche L, Marchessault RH, Lacroix M. Gamma-ray crosslinking of poly(3-hydroxyoctanoate-co-undecenoate). *Int J Biol Macromol* 2001;29(2):73-82.
- [145] Saheb DN, Jog J. Natural fiber polymer composites: a review. *Adv Polym Technol* 1999;18(4):351-363.
- [146] Kalia S, Kaith B, Kaur I. Pretreatments of natural fibers and their application as reinforcing material in polymer composites—a review. *Polymer Engineering & Science* 2009;49(7):1253-1272.
- [147] Faruk O, Bledzki AK, Fink H, Sain M. Biocomposites reinforced with natural fibers: 2000–2010. *Progress in Polymer Science* 2012;37(11):1552-1596.
- [148] Wahit MU, Akos NI, Laftah WA. Influence of natural fibers on the mechanical properties and biodegradation of poly (lactic acid) and poly (ϵ -caprolactone) composites: A review. *Polymer Composites* 2012;33(7):1045-1053.
- [149] Faruk O, Bledzki AK, Fink H, Sain M. Progress report on natural fiber reinforced composites. *Macromolecular Materials and Engineering* 2014;299(1):9-26.
- [150] Finlay KA, Gawryla MD, Schiraldi DA. Effects of Fiber Reinforcement on Clay Aerogel Composites. *Materials* 2015;8(8):5440-5451.
- [151] Popov VN. Carbon nanotubes: properties and application. *Materials Science and Engineering: R: Reports* 2004;43(3):61-102.

- [152] Zhang W, Phang IY, Liu T. Growth of carbon nanotubes on clay: unique nanostructured filler for high-performance polymer nanocomposites. *ADVANCED MATERIALS-DEERFIELD BEACH THEN WEINHEIM* 2006;18(1):73.
- [153] Thostenson ET, Ren Z, Chou T. Advances in the science and technology of carbon nanotubes and their composites: a review. *Composites Sci Technol* 2001;61(13):1899-1912.
- [154] Ashrafi B, Guan J, Mirjalili V, Zhang Y, Chun L, Hubert P, Simard B, Kingston CT, Bourne O, Johnston A. Enhancement of mechanical performance of epoxy/carbon fiber laminate composites using single-walled carbon nanotubes. *Composites Sci Technol* 2011;71(13):1569-1578.
- [155] Ajayan PM, Zhou OZ. Applications of carbon nanotubes. 2001:391-425.
- [156] Wang D, Chen L. Temperature and pH-responsive single-walled carbon nanotube dispersions. *Nano letters* 2007;7(6):1480-1484.
- [157] Liu L, Grunlan JC. Clay assisted dispersion of carbon nanotubes in conductive epoxy nanocomposites. *Advanced Functional Materials* 2007;17(14):2343-2348.
- [158] Barrau S, Demont P, Perez E, Peigney A, Laurent C, Lacabanne C. Effect of palmitic acid on the electrical conductivity of carbon nanotubes-epoxy resin composites. *Macromolecules* 2003;36(26):9678-9680.
- [159] Al-Biloushi M, Wang Y, Schiraldi DA. Characterization of polymer/clay aerogel based glass fiber laminates. *Polymer Preprints* 2011;52(1):261.
- [160] Wang Y, Al-Biloushi M, Schiraldi DA. Polymer/clay aerogel-based glass fabric laminates. *J Appl Polym Sci* 2012;124(4):2945-2953.
- [161] Ebert H. Functional materials for energy-efficient buildings. 2015;98:08001.
- [162] Soleimani Dorcheh A, Abbasi MH. Silica aerogel; synthesis, properties and characterization. *J Mater Process Technol* 2008;199(1-3):10-26.
- [163] Progelhof R, Throne J, Ruetsch R. Methods for predicting the thermal conductivity of composite systems: a review. *Polymer Engineering & Science* 1976;16(9):615-625.
- [164] Gong L, Kyriakides S, Jang W-. Compressive response of open-cell foams. Part I: Morphology and elastic properties. *Int J Solids Structures* 2005;42(5-6):1355-1379.
- [165] García-Ochoa F, Santos VE, Casas JA, Gómez E. Xanthan gum: production, recovery, and properties. *Biotechnol Adv* 2000;18(7):549-579.
- [166] Pancholi K, Stride E, Edirisinghe M. Dynamics of bubble formation in highly viscous liquids. *Langmuir* 2008;24(8):4388-4393.

- [167] Oh S, Klein SP, Shah D. Effect of micellar life-time on the bubble dynamics in sodium dodecyl sulfate solutions. *AIChE J* 1992;38(1):149-152.
- [168] Koski A, Yim K, Shivkumar S. Effect of molecular weight on fibrous PVA produced by electrospinning. *Mater Lett* 2004;58(3-4):493-497.
- [169] Nicholls JR, Lawson KJ, Johnstone A, Rickerby DS. Methods to reduce the thermal conductivity of EB-PVD TBCs. *Surface and Coatings Technology* 2002;151-152:383-391.
- [170] Takahashi S, Goldberg HA, Feeney CA, Karim DP, Farrell M, O'Leary K, Paul DR. Gas barrier properties of butyl rubber/vermiculite nanocomposite coatings. *Polymer* 2006;47(9):3083-3093.
- [171] James F, Shackelford F, Alexander W. *Materials science and engineering handbook*. CRC Press, LLC 2001.
- [172] Schartel B, Bartholmai M, Knoll U. Some comments on the use of cone calorimeter data. *Polym Degrad Stab* 2005;88(3):540-547.
- [173] Schartel B, Hull TR. Development of fire-retarded materials—Interpretation of cone calorimeter data. *Fire Mater* 2007;31(5):327-354.
- [174] Babrauskas V. Development of the cone calorimeter—a bench-scale heat release rate apparatus based on oxygen consumption. *Fire Mater* 1984;8(2):81-95.
- [175] Babrauskas V. The cone calorimeter. 2016:952-980.
- [176] Arora S, Kumar M, Kumar M. Thermal and flammability studies of poly(vinyl alcohol) composites filled with sodium hydroxide. *J Appl Polym Sci* 2013;127(5):3877-3884.
- [177] Wang L, Sánchez-Soto M, MasPOCH ML. Polymer/clay aerogel composites with flame retardant agents: Mechanical, thermal and fire behavior. *Mater Des* 2013;52:609-614.
- [178] Lu S, Hamerton I. Recent developments in the chemistry of halogen-free flame retardant polymers. *Progress in Polymer Science* 2002;27(8):1661-1712.
- [179] Chen H, Wang Y, Sánchez-Soto M, Schiraldi DA. Low flammability, foam-like materials based on ammonium alginate and sodium montmorillonite clay. *Polymer* 2012;53(25):5825-5831.
- [180] Hirschler MM. Flame retardants and heat release: review of data on individual polymers. *Fire Mater* 2015;39(3):232-258.
- [181] Alarie Y. Toxicity of fire smoke. *Crit Rev Toxicol* 2002;32(4):259-289.
- [182] Cheng Y, Lu L, Zhang W, Shi J, Cao Y. Reinforced low density alginate-based aerogels: Preparation, hydrophobic modification and characterization. *Carbohydr Polym* 2012;88(3):1093-1099.

- [183] Smidsrød O, Skjåk-Bræk G. Alginate as immobilization matrix for cells. *Trends Biotechnol* 1990;8:71-78.
- [184] Pawar SN, Edgar KJ. Alginate derivatization: A review of chemistry, properties and applications. *Biomaterials* 2012;33(11):3279-3305.
- [185] Zhang J, Ji Q, Shen X, Xia Y, Tan L, Kong Q. Pyrolysis products and thermal degradation mechanism of intrinsically flame-retardant calcium alginate fibre. *Polym Degrad Stab* 2011;96(5):936-942.
- [186] Broido A. A simple, sensitive graphical method of treating thermogravimetric analysis data. *Journal of Polymer Science Part A-2: Polymer Physics* 1969;7(10):1761-1773.
- [187] Tian Y, Li Y, Xu X, Jin Z. Starch retrogradation studied by thermogravimetric analysis (TGA). *Carbohydr Polym* 2011;84(3):1165-1168.
- [188] Haines PJ. *Thermal methods of analysis: principles, applications and problems*. 2012.
- [189] Nishizaki H, Yoshida K, Wang J. Comparative study of various methods for thermogravimetric analysis of polystyrene degradation. *J Appl Polym Sci* 1980;25(12):2869-2877.
- [190] Prime RB, Bair HE, Vyazovkin S, Gallagher PK, Riga A. *Thermogravimetric analysis (TGA). Thermal analysis of polymers: Fundamentals and applications* 2009:241-317.
- [191] Wang S, Hu Y, Song L, Wang Z, Chen Z, Fan W. Preparation and thermal properties of ABS/montmorillonite nanocomposite. *Polym Degrad Stab* 2002;77(3):423-426.
- [192] Wu J. Structural, thermal, and electrical characterization of layered nanocomposites derived from sodium-montmorillonite and polyethers. *Chemistry of materials* 1993;5(6):835; 835-838; 838.
- [193] Lin H, Singh M. 26th Annual Conference on Composites, Advanced Ceramics, Materials, and Structures: AB: January 13-18, 2002, Cocoa Beach, Florida. 2002;1.
- [194] Ghosh M. *Polyimides: fundamentals and applications*. 1996.
- [195] Piscitelli F, Posocco P, Toth R, Fermiglia M, Priol S, Mensitieri G, Lavorgna M. Sodium montmorillonite silylation: Unexpected effect of the aminosilane chain length. *J Colloid Interface Sci* 2010;351(1):108-115.
- [196] Fitaroni LB, de Lima JA, Cruz SA, Waldman WR. Thermal stability of polypropylene–montmorillonite clay nanocomposites: Limitation of the thermogravimetric analysis. *Polym Degrad Stab* 2015;111:102-108.
- [197] Wang L, Schiraldi DA, Sánchez-Soto M. Foamlike Xanthan Gum/Clay Aerogel Composites and Tailoring Properties by Blending with Agar. *Ind Eng Chem Res* 2014;53(18):7680-7687.
- [198] Gawryla MD, Schiraldi DA. Novel absorbent materials created via ice templating. *Macromolecular Materials and Engineering* 2009;294(9):570-574.

- [199] Schiraldi DA, Gawryla MD, Alhassan S. Clay aerogel composite materials. 2011;63:147-151.
- [200] Adebajo MO, Frost RL, Kloprogge JT, Carmody O, Kokot S. Porous materials for oil spill cleanup: a review of synthesis and absorbing properties. *Journal of Porous materials* 2003;10(3):159-170.
- [201] Xue Z, Wang S, Lin L, Chen L, Liu M, Feng L, Jiang L. A novel superhydrophilic and underwater superoleophobic hydrogel-coated mesh for oil/water separation. *Adv Mater* 2011;23(37):4270-4273.
- [202] Crespy D, Rossi RM. Temperature-responsive polymers with LCST in the physiological range and their applications in textiles. *Polym Int* 2007;56(12):1461-1468.
- [203] Gontard N, Guilbert S, CUQ J. Water and glycerol as plasticizers affect mechanical and water vapor barrier properties of an edible wheat gluten film. *J Food Sci* 1993;58(1):206-211.
- [204] Haraguchi K, Takehisa T, Fan S. Effects of clay content on the properties of nanocomposite hydrogels composed of poly (N-isopropylacrylamide) and clay. *Macromolecules* 2002;35(27):10162-10171.
- [205] Kubota K, Fujishige S, Ando I. Single-chain transition of poly (N-isopropylacrylamide) in water. *J Phys Chem* 1990;94(12):5154-5158.
- [206] Schiraldi DA, Gawryla MD, Bandi SA. Absorbent compositions with clay aerogels and methods for forming absorbent compositions 2008.
- [207] Tro NJ. *Introductory Chemistry Essentials: Books a la Carte Edition*. 2014.
- [208] Xi Y, Mallavarapu M, Naidu R. Preparation, characterization of surfactants modified clay minerals and nitrate adsorption. *Applied Clay Science* 2010;48(1):92-96.
- [209] ASTM Committee D-20 on Plastics. Section D20. 70.01. Standard Test Methods for Density and Specific Gravity (Relative Density) of Plastics by Displacement. 1991.
- [210] Underwriters' Laboratories. Standard for Tests for Flammability of Plastic Materials for Parts in Devices and Appliances. 1978.
- [211] BS EN ISO 604:2003: Plastics. Determination of compressive properties. 2003.
- [212] Bragg WH, Bragg WL. The Reflection of X-rays by Crystals. *Proceedings of the Royal Society of London A: Mathematical, Physical and Engineering Sciences* 1913;88(605):428-438.
- [213] Wilson MA, Hoff WD, Hall C. Water movement in porous building materials—XIII. Absorption into a two-layer composite. *Building and Environment* 1995;30(2):209-219.
- [214] ASTM D. 5229/D 5229M-92. Standard test method for moisture absorption properties and equilibrium conditioning of polymer matrix composite materials. 2014.

- [215] BS EN ISO 12572:2001: Hygrothermal performance of building materials and products. Determination of water vapour transmission properties. 2001.
- [216] BS 5250:2011: Code of practice for control of condensation in buildings. 2011.
- [217] Abdou A, Budaiwi I. The variation of thermal conductivity of fibrous insulation materials under different levels of moisture content. *Constr Build Mater* 2013;43:533-544.
- [218] Jerman M, Černý R. Effect of moisture content on heat and moisture transport and storage properties of thermal insulation materials. *Energy Build* 2012;53:39-46.
- [219] Ferry JD. *Viscoelastic properties of polymers*. 1980.
- [220] Hansen EL, Hemmen H, Fonseca DdM, Coutant C, Knudsen K, Plivelic T, Bonn D, Fossum JO. Swelling transition of a clay induced by heating. *Scientific reports* 2012;2.
- [221] Fujishige S, Kubota K, Ando I. Phase transition of aqueous solutions of poly (N-isopropylacrylamide) and poly (N-isopropylmethacrylamide). *J Phys Chem* 1989;93(8):3311-3313.
- [222] Arroyo F, Carrique F, Jiménez-Olivares M, Delgado A. Rheological and electrokinetic properties of sodium montmorillonite suspensions: II. Low-frequency dielectric dispersion. *J Colloid Interface Sci* 2000;229(1):118-122.
- [223] Khanna P, Singh N, Charan S, Subbarao V, Gokhale R, Mulik U. Synthesis and characterization of Ag/PVA nanocomposite by chemical reduction method. *Mater Chem Phys* 2005;93(1):117-121.
- [224] Balachandranb V. FT-IR, FT-Raman, DFT structure, vibrational frequency analysis and Mulliken charges of 2-chlorophenylisothiocyanate. *Indian J Pure Appl Phys* 2012;50(1):19-25.
- [225] Pietralik Z, Krzysztoń R, Kida W, Andrzejewska W, Kozak M. Structure and conformational dynamics of DMPC/dicationic surfactant and DMPC/dicationic surfactant/DNA systems. *International journal of molecular sciences* 2013;14(4):7642-7659.
- [226] Majhi PR, Blume A. Temperature-induced micelle-vesicle transitions in DMPC-SDS and DMPC-DTAB mixtures studied by calorimetry and dynamic light scattering. *The Journal of Physical Chemistry B* 2002;106(41):10753-10763.
- [227] Tadokoro H. Infrared studies of polyvinyl alcohol by deuteration of its OH groups. *Bull Chem Soc Jpn* 1959;32(11):1252-1257.
- [228] Kumpulainen S, Kiviranta L. Mineralogical and chemical characterization of various bentonite and smectite-rich clay materials. *Posiva Working Report* 2010;52.
- [229] Boday DJ. *Silica aerogel-polymer nanocomposites and new nanoparticle syntheses*. 2009.

- [230] Mansur HS, Sadahira CM, Souza AN, Mansur AAP. FTIR spectroscopy characterization of poly (vinyl alcohol) hydrogel with different hydrolysis degree and chemically crosslinked with glutaraldehyde. *Materials Science and Engineering: C* 2008;28(4):539-548.
- [231] Shang K, Ye D, Kang A, Wang Y, Liao W, Xu S, Wang Y. Robust and fire retardant borate-crosslinked poly (vinyl alcohol)/montmorillonite aerogel via melt-crosslink. *Polymer* 2017.
- [232] Chen H, Zhao Y, Shen P, Wang J, Huang W, Schiraldi DA. Effects of Molecular Weight upon Irradiation-Cross-Linked Poly (vinyl alcohol)/Clay Aerogel Properties. *ACS applied materials & interfaces* 2015;7(36):20208-20214.
- [233] Castella N, Grishchuk S, Karger-Kocsis J, Unik M. Hybrid resins from polyisocyanate, epoxy resin and water glass: chemistry, structure and properties. *J Mater Sci* 2010;45(7):1734-1743.
- [234] Ren W, Wu R, Guo P, Zhu J, Li H, Xu S, Wang J. Preparation and characterization of covalently bonded PVA/Laponite/HAPI nanocomposite multilayer freestanding films by layer-by-layer assembly. *Journal of Polymer Science Part B: Polymer Physics* 2015;53(8):545-551.
- [235] Shajesh P, Smitha S, Aravind P, Warriar K. Effect of 3-glycidoxypropyltrimethoxysilane precursor on the properties of ambient pressure dried silica aerogels. *J Sol Gel Sci Technol* 2009;50(3):353-358.
- [236] Metroke TL, Kachurina O, Knobbe ET. Spectroscopic and corrosion resistance characterization of GLYMO-TEOS Ormosil coatings for aluminum alloy corrosion inhibition. *Progress in Organic Coatings* 2002;44(4):295-305.
- [237] Anderson W. Wettability literature survey-part 2: Wettability measurement. *J Pet Technol* 1986;38(11):1,246-1,262.
- [238] Onda T, Shibuichi S, Satoh N, Tsujii K. Super-water-repellent fractal surfaces. *Langmuir* 1996;12(9):2125-2127.
- [239] Feng L, Li S, Li H, Zhai J, Song Y, Jiang L, Zhu D. Super-hydrophobic surface of aligned polyacrylonitrile nanofibers. *Angewandte Chemie* 2002;114(7):1269-1271.
- [240] Yan H, Kurogi K, Mayama H, Tsujii K. Environmentally Stable Super Water-Repellent Poly (alkylpyrrole) Films. *Angewandte Chemie International Edition* 2005;44(22):3453-3456.
- [241] Honda K, Morita M, Otsuka H, Takahara A. Molecular aggregation structure and surface properties of poly (fluoroalkyl acrylate) thin films. *Macromolecules* 2005;38(13):5699-5705.
- [242] Baraton M, Uvarova IV. Functional gradient materials and surface layers prepared by fine particles technology. 2012;16.
- [243] Granville AM, Boyes SG, Akgun B, Foster MD, Brittain WJ. Synthesis and characterization of stimuli-responsive semifluorinated polymer brushes prepared by atom transfer radical polymerization. *Macromolecules* 2004;37(8):2790-2796.

- [244] Antonucci J, Stansbury J. prepolymer polyol,[PFP], used in the synthesis of [PFMA). Progress in Biomedical Polymers 2013:121.
- [245] Belaidi O, Bouchaour T, Maschke U. Molecular structure and vibrational spectra of 2-ethylhexyl acrylate by density functional theory calculations. Organic Chemistry International 2013;2013.
- [246] Wang Q, Zhang Q, Zhan X, Chen F. Structure and surface properties of polyacrylates with short fluorocarbon side chain: role of the main chain and spacer group. Journal of Polymer Science Part A: Polymer Chemistry 2010;48(12):2584-2593.
- [247] Štandeker S, Novak Z, Knez Ž. Adsorption of toxic organic compounds from water with hydrophobic silica aerogels. J Colloid Interface Sci 2007;310(2):362-368.
- [248] Mahadik DB, Rao AV, Rao AP, Wagh PB, Ingale SV, Gupta SC. Effect of concentration of trimethylchlorosilane (TMCS) and hexamethyldisilazane (HMDZ) silylating agents on surface free energy of silica aerogels. J Colloid Interface Sci 2011;356(1):298-302.
- [249] Kumar V, Pulpytel J, Giudetti G, Rauscher H, Rossi F, Arefi-Khonsari F. Amphiphilic Copolymer Coatings via Plasma Polymerisation Process: Switching and Anti-Biofouling Characteristics. Plasma Processes and Polymers 2011;8(5):373-385.
- [250] Feng L, Zhao W, Zheng J, Frisco S, Song P, Li X. The shape-stabilized phase change materials composed of polyethylene glycol and various mesoporous matrices (AC, SBA-15 and MCM-41). Solar Energy Mater Solar Cells 2011;95(12):3550-3556.
- [251] Ren Q, Zhao T. Synthesis and application of modified vegetable oils in water-repellent finishing of cotton fabrics. Carbohydr Polym 2010;80(2):381-386.



Contents lists available at ScienceDirect

Composites Part B

journal homepage: www.elsevier.com/locate/compositesb



Review article

Enhancing mechanical properties of clay aerogel composites: An overview



Omar Abo Madyan ^{a, b}, Mizi Fan ^{a, b, *}, Luciano Feo ^c, David Hui ^d

^a College of Material Engineering, Fujian Agriculture and Forestry University, Fuzhou 350002, China

^b Civil Engineering, College of Engineering, Design and Physical Sciences, Brunel University, UB8 3PH, United Kingdom

^c Department of Civil Engineering, Università degli Studi di Salerno, Fisciano, Italy

^d Department of Mechanical Engineering, University of New Orleans, Lake Front, New Orleans, LA 70138, USA

ARTICLE INFO

Article history:

Received 26 April 2016

Accepted 27 April 2016

Available online 6 May 2016

Keywords:

Clay aerogel

B. Microstructures

B. Mechanical property

C. Micro-mechanics

ABSTRACT

While aerogel is a new classification of materials and considered most promising candidate for the advanced thermal insulation, clay aerogel shows significant potentials as it is natural, non-toxic, biodegradable and biocompatible material. To date most aerogels are produced through a supercritical drying process and most reviewed aerogels are silica based aerogels, nevertheless, more environmentally friendly aerogels have been attempted through the use of clays through an environmentally freeze-drying process. This paper presents a comprehensive overview of developing robust clay aerogels, including enhancing clay aerogel with various natural and synthetic polymers, and the reinforcement of clay–polymer aerogel with carbon nanotubes, natural fibres, glass fibre lamination and dip coatings. The results show that many factors could contribute to the classification of clay aerogels, including processing parameters and methodologies, raw materials as well as minor additives. One of the most significant setbacks regarding clay aerogels is their mechanical properties and in the past several years significant efforts have been spent on the improvement. The most successful method demonstrated so far was the incorporation of a water-soluble polymer and reinforcing aerogel composites with fibrous materials to achieve various levels of enhancements of clay-aerogels. This review shall provide a much useful concise database for the development, production and potential utilisation of clay aerogel for various industrial sectors.

© 2016 Elsevier Ltd. All rights reserved.

Contents

1. Introduction	315
2. Mechanical strength of clay aerogels composites	315
3. Enhancing mechanical strength of clay aerogel through natural polymers	316
3.1. Casein reinforced clay aerogel	316
3.2. Cellulose reinforced clay aerogel	317
3.3. Chitin reinforced clay aerogel	318
3.4. Lignin reinforced clay aerogel	318
3.5. Natural rubber reinforced clay aerogel	319
3.6. Pectin reinforced clay aerogel	321
4. Enhancing mechanical strength of clay aerogel through synthetic polymers	321
4.1. Epoxy reinforced clay aerogel	321
4.2. Polyethylene imine reinforced clay aerogel	322
4.3. Polyimide reinforced clay aerogel	322
4.4. Polyvinyl alcohol reinforced clay aerogel	323

* Corresponding author. Civil Engineering, College of Engineering, Design and Physical Sciences, Brunel University, UB8 3PH, United Kingdom.
E-mail address: mizi.fan@brunel.ac.uk (M. Fan).



Physical properties of clay aerogel composites: An overview



Omar Abo Madyan ^{a, b}, Mizi Fan ^{a, b, *}, Luciano Feo ^c, David Hui ^d

^a College of Material Engineering, Fujian Agriculture and Forestry University, Fuzhou 350002, China

^b Civil Engineering, College of Engineering, Design and Physical Sciences, Brunel University, UB8 3PH, United Kingdom

^c Department of Civil Engineering, Università degli Studi di Salerno, Fisciano, Italy

^d Department of Mechanical Engineering, University of New Orleans, Lake Front, New Orleans, LA 70138, USA

ARTICLE INFO

Article history:

Received 2 June 2016

Accepted 12 June 2016

Available online 14 July 2016

ABSTRACT

A prior study conducted by the authors had investigated the mechanical enhancement of clay aerogel composites; this paper is an extension to the previous study and focuses on the physical properties of clay aerogel composites. Different physical properties of clay aerogel composites, including thermal conductivity, fire resistance, thermal stability and water absorption, and how they are influenced by the microstructure, processing parameters and composition have been discussed. The results show that the addition of Poly (vinyl alcohol) of different molecular weights as well as controlling the processing parameters to create an open cell structure could effectively lower the thermal conductivity. The fire performance could be enhanced with the addition of fire retardant additives without altering the aerogel structure, and with the correct polymer and modification, the clay aerogels could act as excellent liquid absorbents. Clay aerogel is a relatively new class of aerogels, the accumulated database presented here should serve as most useful information in order to realize the full potentials of clay aerogels in many different applications.

© 2016 Elsevier Ltd. All rights reserved.

1. Introduction

Aerogels, which were first introduced in 1931 [1], are usually defined as an ultralight with a density of between 0.004 and 0.100 g/cm³ and highly porous materials composed of up to 99.98% air [2]. They are prepared by replacing the liquid within a precursor gel with air through a supercritical drying technique [3]. The process requires fairly high temperature and pressure to transform the entrapped liquid into a supercritical fluid, leaving behind a porous nanostructured network with minimal shrinkage to the original volume of the gel [4–6]. The distinctive chemical and physical properties of aerogels, such as their high specific surface area (500–1200 m²/g), high porosity (80–99.8%), low density (\approx 0.003 g/cm³) and low thermal conductivity values (0.01–0.02 W/mk) [7,8], have gained them much attention in many industrial sectors, among them thermal and acoustic insulation and a catalyst support in the drug industry are considered most potential [9,10]. The fact that most aerogel production consumes high amounts of energy, which can be considered as a drawback

especially when large scale production is considered, as well as safety concerns regarding the high temperature and pressure [11]; has driven research focus on producing new types of aerogels at reduced costs and better performance to ease commercialization. Clay aerogels are an emerging class of aerogels and were first reported by Mackenzie and Call [3], and are prepared through an environmentally freeze-drying process using inexpensive and harmless materials which makes them more desirable in terms of sustainability and environmental concerns [12,13]. The process for producing clay aerogels involves freeze-drying an aqueous clay suspension, which transforms the clay particles into a lamellar (House of cards) structure with a layer thickness of 1–4 μ m and distances between layers of 20–100 μ m resulting in ultra-low densities (0.05–0.1 g/cm³) [14,15]. The layered clay aerogel structure yields unique properties which are desirable in many applications, including the construction sector as an insulation material and in pharmaceutical industries as a catalyst [16,17]. One of the setbacks regarding clay aerogels is their poor mechanical strengths, however, it has been reported that incorporating a reinforcing medium, such as polymers or other additives, is able to increase the mechanical strength comparable to that of petroleum based foamed materials [18,19], with reduced permeability and flammability [20,21].

* Corresponding author. Civil Engineering, College of Engineering, Design and Physical Sciences, Brunel University, UB8 3PH, United Kingdom.
E-mail address: mizi.fan@brunel.ac.uk (M. Fan).



Research paper

Functional clay aerogel composites through hydrophobic modification and architecture of layered clays



Omar Abo Madyan, Mizi Fan *, Zhaohui Huang

Civil Engineering, College of Engineering, Design and Physical Sciences, Brunel University UB8 3PH, United Kingdom

ARTICLE INFO

Article history:

Received 27 September 2016

Received in revised form 9 January 2017

Accepted 10 January 2017

Available online 20 February 2017

Keywords:

Clay/PVA aerogel

Cation exchange

Moisture absorption

Microstructure

Compressive modulus

Thermal conductivity

ABSTRACT

This paper implements hydrophobic modified clay layers with ammonia salts (Organoclay) using ultra-sonication and water as a solvent to develop functional clay/Poly vinyl alcohol (PVA) aerogel composites through an environmentally friendly freeze drying process. Various compositions have been designed aiming at the high effectiveness of reducing moisture absorption while increasing the structural integrity and overall compressive modulus but reducing the thermal conductivity of the aerogel composites. The results showed significant enhancement to both physical and mechanical properties of the aerogel composites. The microstructure systems of the aerogel composites could be tailored to result in multifunctional performance for the targeted applications. The moisture absorption could be reduced five folds compared to that of normal clay aerogels depending on the exposure relative humidity. While the modulus of the aerogel composites was doubled from an initial modulus of 0.39 to 0.82 MPa, the thermal conductivity was reduced by up 20% reaching values as low as 0.0315 w/mk. These aerogel composites could be an effective and efficient thermal insulation material to be implemented in the construction industry.

© 2017 Elsevier B.V. All rights reserved.

1. Introduction

Aerogels are highly porous low density materials produced by replacing a liquid in a gel with a gas usually through a supercritical extraction technique (Fricke and Tillotson, 1997). They are now considered as one of the most promising insulation materials in the construction sector due to their remarkable low thermal conductivity and specific acoustics properties. However, the cost of aerogels still remains higher than that of currently available insulation materials in the market (Cuce et al., 2014), which has led intensive research, aiming at producing new classes of aerogels (Gurav et al., 2010).

Smectic clays have been widely used to prepare nanocomposites as a result of their swelling ability, high cation exchange capacity, and their ability to be physically and chemically modified for different applications (Tiwari et al., 2008). Smectic clays can be converted into foamed like materials (Call, 1953) through an environmental freeze-drying process using inexpensive and harmless materials (Pojanavaraphan et al., 2010a). The net clay aerogels composites possess ultra-low bulk densities in the range of 0.03–0.015 g/cm³ (Schiraldi et al., 2011) and are usually characterised with a layered “house of cards” structure, leading to extraordinary physical and chemical properties, such as low thermal conductivity (0.02–0.05 w/mk) (Gawryla et al., 2009a; Arndt et al.,

2007). One of the major setbacks of clay aerogels is their poor mechanical strength, especially if it is to be implemented in the construction industry as an insulation material, although many attempts have been reported to reinforce the clay aerogel using natural or synthetic polymers and fibers (Finlay et al., 2015; Gawryla et al., 2009b; Wang and Schiraldi, 2013; Pojanavaraphan et al., 2010b; Schiraldi et al., 2011). Another major challenge that can significantly hinder the performance and effectiveness of the aerogel composite is their lack of moisture resistance, which may be related to the water soluble polymers and hydrophilic sodium montmorillonite (Na⁺-MMT) used in the process. Even the dried structure may absorb moisture which can cause the clay and polymers to decompose and lose their mechanical properties (Gawryla and Schiraldi, 2009). It is also reported that the k-value (thermal conductivity) of hydrophilic porous materials can increase by more than 50% for every 1 (v/v%) of moisture absorbed (Karamanos et al., 2004).

Surface modification of clay has been considered vital in improving the practicality and performance of clay/polymer nanocomposites (Liu, 2007). The modification process may be involved in replacing the clay cations, such as Mg²⁺, Ca²⁺, Na⁺, k⁺, and Li⁺, with various organic cations, such as a nitrogen based quaternary ammonium cation (Healy, 1993). Alkyl ammonium salts may cause the interlayer space to expand and convert the initially hydrophilic silicate into hydrophobic organoclay as well as enhance the miscibility of the clay with polymers (Gorrası et al., 2003; Patel et al., 2007). Organoclay has proven to be an effective tool for treating and filtrating water (Beall, 2003) and more

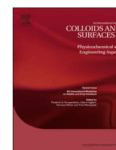
* Corresponding author at: Civil Engineering, College of Engineering, Design and Physical Sciences, Brunel University UB8 3PH, United Kingdom.

E-mail address: mizi.fan@brunel.ac.uk (M. Fan).



Contents lists available at ScienceDirect

Colloids and Surfaces A

journal homepage: www.elsevier.com/locate/colsurfa

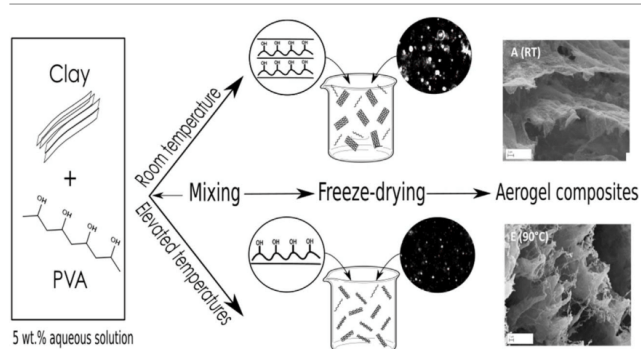
Temperature induced nature and behaviour of clay-PVA colloidal suspension and its aerogel composites

Omar Abo Madyan^{a,b}, Mizi Fan^{a,b,*}^a College of Material Engineering, Fujian Agriculture and Forestry University, Fuzhou, 350002, China^b Civil Engineering, College of Engineering, Design and Physical Sciences, Brunel University, UB8 3PH, United Kingdom

HIGHLIGHTS

- Enhancing clay-PVA aerogels by controlling the mixing parameters (I.e. temperature).
- Maintaining low thermal conductivity and low density with significant increase in strength.
- Increasing the compressive modulus by 7-folds without any increase in solid content.

GRAPHICAL ABSTRACT



ARTICLE INFO

Keywords:

Temperature induced
Colloidal suspension
Clay-PVA aerogel
Compressive modulus
Thermal conductivity
High performance

ABSTRACT

The present paper investigates the mixing temperature on the structure and performance of clay aerogel colloidal suspensions and their composites. Clay-polymer aerogels were prepared via an environmentally friendly freeze-drying technique and clay aerogel suspensions were subjected to various temperatures, namely room temperature (RT), 60, 70, 80 and 90 °C, in order to better understand the architecturing of clay colloidal suspension and formulation mechanisms of advanced clay aerogel composites, and such develop the optimum processing parameters. This research demonstrated that the mixing temperature had a significant influence on the chemical interaction of the constituents and formulation of bonding/networking of clay aerogel colloidal suspension, and hence the microstructure and performance of the clay aerogel composites; by simply controlling the mixing temperature without altering the composition or adding any additive or increasing the solid content, it was possible to significantly increase the compressive modulus by up to 7 folds without sacrificing any of the physical property of clay aerogel composites.

* Corresponding author at: HWLL245, Brunel University, UB8 3PH, United Kingdom.
E-mail address: mizi.fan@brunel.ac.uk (M. Fan).

<http://dx.doi.org/10.1016/j.colsurfa.2017.06.041>

Received 3 May 2017; Accepted 15 June 2017

Available online 16 June 2017

0927-7757/ © 2017 Elsevier B.V. All rights reserved.



ELSEVIER

Contents lists available at ScienceDirect

Applied Clay Science

journal homepage: www.elsevier.com/locate/clay

Research Paper

Organic functionalization of clay aerogel and its composites through in-situ crosslinking

Omar Abo Madyan^{a,b}, Mizi Fan^{a,b,*}^a College of Materials Engineering, Fujian Agriculture and Forestry University, PR China^b College of Engineering, Design and Physical Sciences, Brunel University London, United Kingdom

ARTICLE INFO

Keywords:

Clay/PVA aerogel
Organic modification
Organosilane
Isocyanate compressive modulus
Moisture absorption

ABSTRACT

Clay aerogel composites have great potential for a wide range of applications; however, their high moisture absorbance and inferior mechanical properties have to be addressed. This paper presents crosslinking techniques to develop clay/PVA aerogel composites through an environmentally freeze-drying process using water as a solvent. Water soluble isocyanate and organosilane compounds, namely aliphatic polyisocyanate (Wcro1™) and 3-glycidoxypropyltrimethoxysilane (Wcro2™) were employed and their crosslinking mechanisms were studied. The results of the aerogels characterizations showed that the chosen crosslinkers were able to generate substantial crosslinking reactions. The crosslinked clay/PVA aerogel gave rise to significant improvements in their mechanical and physical properties. The moisture absorbance of the composites was reduced by 27%, while retaining dimensional stability. The developed functionalized clay/PVA aerogels also increased the liquid absorption capacity by 3 times, the compressive modulus increased by 6 folds from 0.48 to 3.6 MPa and the thermal conductivity reduced from the 0.043 to 0.039 W/mK.

1. Introduction

Clay aerogels are a relatively new class of aerogels and have recently gained much attention in the world of material science. Clay aerogels are considered the end product of an environmentally friendly process in which a clay or a clay/polymer dispersion is rapidly frozen to formulate the solid structure followed by freeze-drying (lyophilization) to evaporate the ice (Nakazawa et al., 1987; Liu et al., 2017). The process is able to create the distinctive lamellar “house of cards” structure which is responsible for unique physical characteristics, such as low density ($< 0.1 \text{ g/cm}^3$) and high porosity (void fraction to 85–95%) (Johnson III et al., 2009; Sehaqui et al., 2011). Neat clay aerogels are highly fragile and require the incorporation of a fibril or polymeric component as a reinforcement in order to enhance their mechanical and other specific properties for their intended applications (Bandi et al., 2005; Pojanavaraphan et al., 2010; Chen et al., 2013; Chen et al., 2014a; Alhwaige et al., 2016; Madyan et al., 2016b), such as super insulation, packing, absorbent and catalytic materials (Pojanavaraphan et al., 2011; Grisechko et al., 2013). The most effective and suitable reinforcement processes have been soluble (hydrophilic) polymers with polyvinyl alcohol (PVA) in preparing clay aerogel composites (Bandi and Schiraldi, 2006; Madyan et al., 2016a), as its low toxicity, biocompatibility, water solubility, good mechanical

properties and most importantly can create an ideal hydrogen bond mechanism, where the the hydrogen on the polymer is perfectly spaced to match the oxygen in the lattice of the clay (Podsiadlo et al., 2007). Clay aerogels and its composites are mostly produced through water based processes utilizing hydrophilic clay and soluble polymers. Water is the most desirable solvent (Gutiérrez et al., 2008), especially with the mandate of the utilization of advanced materials based on natural, non-toxic, abundant, biodegradable and biocompatible materials. It can be expected that the dried structure of clay aerogels will in turn absorb water due to the nature of the hydrophilic components which can cause the final aerogel structure to disintegrate (Madyan et al., 2017), leading to the loss of mechanical and physical integrity and rendering it unusable in many applications, such as an insulation material. Moisture can significantly reduce the capacity of thermal insulation, as water has a thermal conductivity value 10 to 20 times higher than most insulation materials (Choi, 1995), each 1 (v/v %) of moisture absorbed could lead to an increase in the thermal conductivity by $> 50\%$ (Karamanos et al., 2004). Moisture can also create an ideal environment to boost mold and mildew growth, causing physical damage to the material and creating a bio-hazard (Al-Homoud, 2005).

Chemical cross-linking is widely used in material science to modify and enhance the performance of composites by tailoring the nanoscale order of polymers (Gohil et al., 2006; Mansur et al., 2008; Shang et al.,

* Corresponding author at: College of Engineering, Design and Physical Sciences, Brunel University London, United Kingdom.
E-mail address: mizi.fan@brunel.ac.uk (M. Fan).

<https://doi.org/10.1016/j.day.2018.11.017>

Received 7 June 2018; Received in revised form 15 November 2018; Accepted 22 November 2018

Available online 13 December 2018

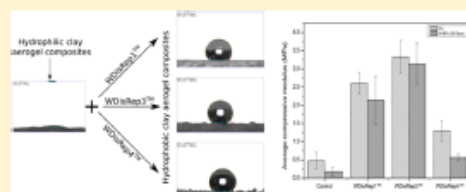
0169-1317/© 2018 Published by Elsevier B.V.

Hydrophobic Clay Aerogel Composites through the Implantation of Environmentally Friendly Water-Repellent Agents

 Omar Abo Madyan¹ and Mizi Fan*

Civil Engineering, College of Engineering, Design and Physical Sciences, Brunel University, London UB8 3PH, United Kingdom

ABSTRACT: Clay aerogel composites have high potential to be used in the construction industry as an insulation material; however, their hydrophilic nature may result in an amount of moisture absorption that could significantly hinder both physical and mechanical properties. This study develops hydrophobic clay aerogel composites using an environmentally friendly freeze-drying process. This was achieved by using three water dispersible repellent components: WDisRep1, WDisRep3, and WDisRep4. Microstructure, wettability, moisture resistance, mechanical properties, and thermal conductivity of the developed clay aerogel composites were fully characterized to understand working mechanisms and performance. The composites exhibited superior mechanical and physical properties in which the composites' moisture absorbance was reduced by up to 40%, while maintaining excellent dimensional stability. The aerogel composites achieved a contact angle of 140° with a 93% reduction in water absorption. The composites achieved a compressive modulus as high as 3.2 MPa while maintaining low thermal conductivity at 0.038 W/(m K).


 Downloaded via BRUNEL UNIV LONDON on January 3, 2019 at 19:22:54 (UTC).
 See <https://pubs.acs.org/sharingguidelines> for options on how to legitimately share published articles.

1. INTRODUCTION

Aerogels are classified as low density and highly porous materials comprised of an interconnected three-dimensional solid network structure, with >90% being occupied with air. The most common synthesis of aerogels, first introduced by Kistler in 1931,^{1,2} involves replacing the pore liquid of a gel with a gas/air through supercritical drying techniques.³ Silica aerogels are the most commonly investigated and are attractive for many industrial sectors due to their unique properties, such as high specific surface area (500–1200 m²/g), high porosity (80–99.8%), low density (0.3–0.05 g/cm³), and low thermal conductivity values (0.01–0.02 W/(m K)).^{4,5}

The mandate for cost reduction and the utilization of abundant, natural, and nontoxic materials to prepare functional materials have driven research to formulate new categories of aerogels for effective and efficient implementation in many different applications.^{6,7} Clay aerogel is one of these developments, a relatively new type of aerogel introduced in 1987.⁸ Clay aerogel is prepared through an environmentally friendly freeze-drying process, in which a clay and/or polymer suspension is frozen and then the ice is sublimed, leaving behind a dry solid network with properties similar to those of foamed polymers.^{8,9} Clay aerogels are characterized with a unique lamellar “house of cards” structure which is responsible for their unique properties, such as low density (<0.1 g/cm³), high porosity, and low thermal conductivity values (0.02–0.05 W/(m K)).¹⁰ Neat clay aerogels have relatively weak mechanical properties and require reinforcements to be implemented as an insulation material.¹¹ Some attempts have been reported through the incorporation of either a polymeric or fibrous components to reinforce the clay aerogel.^{12–15} PVA has been the most suitable and reviewed component to prepare

clay aerogel composite due to its solubility (hydrophilic), good mechanical properties, and nontoxicity, thus making it a highly suitable component.^{16,17} However, the hydrophilic nature of the incorporated components makes the final dry structure inclined to absorb a high amount of moisture, which can limit various applications, such as an insulation material.¹⁸ Every 1% (v/v) increase in moisture content can lead to a 7% rise in thermal conductivity as well as significant loss in mechanical strength. A long duration of moisture exposure or direct contact to liquid water will result in the degradation of the composite and render the material ineffective and useless.¹⁸

The wettability of a solid surface is mainly influenced either by a chemical component or a geometric component of the solid surface or a combination of both.¹⁹ The main chemical approach in decreasing the wettability of solids has been through the use of coatings of fluorinated compounds with low surface energy, while the main geometric factor has been by the formation of fractal or rough surface structures.²⁰ This paper presents the hydrophobic clay/PVA aerogels through the implementation of soluble water-repellent components by using an environmentally friendly freeze-drying process.

2. EXPERIMENTAL SECTION

2.1. Materials. Hydrophilic nanoclay bentonite (montmorillonite, ≤25 μm) and poly(vinyl alcohol) (PVA) (98–99% hydrolyzed) with a molecular weight of 89000–150000 were purchased from Sigma-Aldrich. Three water dispersible repellents, namely WDisRep1 (a combination of melamine resins with paraffin waxes, solid content

Received: October 16, 2018

Revised: November 16, 2018

Published: December 10, 2018